

A Genome-Wide RNAi Screen for Modifiers of Polyglutamine-Induced Neurotoxicity in *Drosophila*



Doctoral Thesis

In partial fulfilment of the requirements for the degree
"Doctor rerum naturalium (Dr. rer. nat.)"
in the Molecular Medicine Study Programme at the
Georg-August University Göttingen

submitted by

Hannes Voßfeldt

born in

Zerbst/Anhalt, Germany

Göttingen, January 2012

FÜR MEINE FAMILIE
-
IM GEDENKEN AN NADINE
DU FEHLST.

...

IT MATTERS NOT HOW STRAIT THE GATE,
HOW CHARGED WITH PUNISHMENTS THE SCROLL,
I AM THE MASTER OF MY FATE:
I AM THE CAPTAIN OF MY SOUL.

...

Invictus – William Ernest Henley

Members of the Thesis Committee:

Supervisor

Prof. Dr. med. Jörg B. Schulz
Head of Department of Neurology
University Medical Centre
RWTH Aachen University
Pauwelsstrasse 30
52074 Aachen

Second member of the Thesis Committee

Prof. Dr. rer. nat. Ernst A. Wimmer
Head of Department of Developmental Biology
Johann Friedrich Blumenbach Institute of Zoology and Anthropology
Georg-August University Göttingen
Justus-von-Liebig-Weg 11
37077 Göttingen

Third member of the Thesis Committee

Dr. rer. nat. Till Marquardt
Research Group Developmental Neurobiology
European Neuroscience Institute Göttingen
Grisebachstrasse 5
37077 Göttingen

Date of Disputation: 2 April 2012

Affidavit

I hereby declare that my doctoral thesis entitled “A Genome-Wide RNAi Screen for Modifiers of Polyglutamine-Induced Neurotoxicity in *Drosophila*” has been written independently with no other sources and aids than quoted.

Göttingen, January 2012

Hannes Voßfeldt

List of Publications

Parts of this work have already been published with authorisation of Prof. Jörg B. Schulz, Head of the Department of Neurology, University Medical Centre of the RWTH Aachen University, on behalf of the thesis committee.

- Poster “A genome-wide screen for modifiers of Ataxin-3-induced neurotoxicity in *Drosophila melanogaster*”, Regional *Drosophila* Meeting 2009, Münster/Germany
(28 August 2009)
- Talk “A genome-wide screen for modifiers of ATXN3-induced neurotoxicity in *Drosophila melanogaster*”, PhD Retreat Molecular Medicine, Göttingen/Germany
(17 June 2010)
- Talk “A genome-wide RNAi screen for modifiers of polyglutamine-induced neurotoxicity in *Drosophila*”, ScieTalk 2011, Göttingen/Germany
(8 June 2011)
- Poster “A genome-wide screen for modifiers of polyglutamine-induced neurotoxicity in *Drosophila melanogaster*”, 23rd Biennial Meeting of ISN-ESN 2011, Athens/Greece
(30 August 2011)
- Paper Voßfeldt H, Butzlaff M, Prüßing K, Ní Chárthaigh R-A, Karsten P, et al. (2012) Large-Scale Screen for Modifiers of Ataxin-3-Derived Polyglutamine-Induced Toxicity in *Drosophila*. PLoS ONE 7(11): e47452. doi:10.1371/journal.pone.0047452

Acknowledgements

The work for this PhD thesis was conducted at the Department of Neurodegeneration and Restorative Research, University Medicine Göttingen (Germany) and the Department of Neurology, University Medical Centre of the RWTH Aachen University, Aachen (Germany), both headed by Prof. Dr. Jörg B. Schulz. I would like to thank Prof. Schulz for giving me the opportunity to produce my thesis in his department and for being my supervisor, furthermore for his intellectual input, constructive criticism and his helpfulness.

I would like to thank the members of my thesis committee, Prof. Ernst A. Wimmer and Dr. Till Marquardt, for their intellectual and professional support and for accompanying the process of my promotion.

I am deeply indebted to Dr. Aaron Voigt for being my advisor throughout the course of my PhD work, for being a great source of ideas and inspiration, for his intellectual and practical support and for his dedication and efforts in the past years.

I owe special thanks to my dear colleagues at the Department of Neurology of the UK Aachen, above all my lab mates Dr. Malte Butzlaff, Dr. Peter Karsten, Sabine Hamm, Anne Lankes, Katja Prüßing, Jane Patricia Tögel, Kavita Kaur, Róisín-Ana Ní Chárthaigh, Li Zhang, Xia Pan, Antje Hofmeister and Marion Roller for invaluable help, support and not least their friendship. I thank Natalie Burdick-Reinhardt and Isabel Möhring for their immense helpfulness and their pleasant company. I thank the people at the Department of Neurology for creating a friendly and enjoyable working and interpersonal atmosphere.

I am indebted to Daniela Otten (Department of Biochemistry, Prof. Lüscher, UK Aachen) for technical support, ideas and discussion and to Fabian Hosp (MDC for Molecular Medicine Berlin, Prof. Selbach) for mass spectrometry experiments, ideas and discussion. I thank Dipl.-Ing. Manfred Bovi (Department of Pathology, UK Aachen) for recording the scanning electron micrographs.

I am thankful for the financing of this project by the Competence Network Degenerative Dementias (KNDD).

Table of Contents

List of Figures	X
List of Tables	XI
List of Abbreviations	XII
1 Abstract	1
1 Zusammenfassung	2
2 Introduction	3
2.1 Overview: proteopathies and polyglutamine diseases	3
2.2 Pathogenic mechanisms of polyglutamine diseases	6
2.2.1 Cytotoxicity of polyglutamine structures	6
2.2.2 Molecular pathways to polyglutamine disease.....	10
2.3 Examples of polyglutamine diseases	13
2.3.1 Huntington’s Disease (HD)	13
2.3.2 Spinocerebellar ataxias.....	14
2.3.2.1 Spinocerebellar ataxia type 1 (SCA1)	15
2.3.2.2 Spinocerebellar ataxia type 2 (SCA2)	16
2.3.2.3 Spinocerebellar ataxia type 3 (SCA3)/Machado-Joseph disease (MJD)	18
2.4 <i>Drosophila melanogaster</i> as an animal model in research	21
2.4.1 The UAS/GAL4 expression system.....	21
2.4.2 RNA interference (RNAi).....	22
2.4.3 Rough eye phenotype (REP)	24
2.4.4 <i>Drosophila</i> models of polyglutamine disease	24
2.4.5 Previously implemented modifier studies	26
3 Aim of the Study	27

4 Material and Methods	28
4.1 Chemicals, reagents and equipment	28
4.2 Fly experiments.....	32
4.2.1 Transgenic flies and housing conditions	32
4.2.2 Mating procedures.....	33
4.2.3 Evaluation of rough eye phenotype modification.....	34
4.2.4 Documentation of eye phenotypes.....	35
4.2.5 Dissection and staining of eye imaginal discs	35
4.2.6 Longevity analysis.....	35
4.2.7 Protein collection from fly heads	36
4.2.8 Immunoblotting.....	36
4.2.9 Filter Retardation Assay	37
4.2.10 Histological and immunohistochemical staining of paraffin sections	38
4.2.11 Immunohistochemical staining of cryo sections	39
4.2.12 Semi-thin tangential sectioning of fly heads and photoreceptor quantification	39
4.3 Cell culture experiments.....	40
4.3.1 Cell culture conditions and media	40
4.3.2 Generation of stable shRNA-expressing cells.....	40
4.3.3 Plasmid transfection	41
4.3.4 Protein collection from cell culture and immunoblotting.....	41
4.3.5 Cytochemistry.....	42
5 Results	43
5.1 Characterisation of a SCA3 fly model for the modifier screen	43
5.1.1 Phenotypes of the disease model flies	43
5.1.2 Assessment of SCA3tr-Q78 protein expression and effects in the eye.....	45
5.1.3 Evaluation of photoreceptor integrity	48

5.2 Modifier screen for polyQ-induced neurotoxicity	49
5.2.1 Screen for unspecific RNAi effects in control flies.....	50
5.2.2 Primary screen for polyglutamine modifiers	50
5.2.3 Specificity of RNAi effects for SCA3tr-Q78-induced neurotoxicity.....	55
5.2.4 Evaluation of gene silencing by RNAi lines	56
5.3 Impact of modifiers on polyQ toxicity and aggregation	57
5.3.1 Evaluation of tissue integrity of <i>SCA3tr-Q78</i> -shRNA-coexpressing flies	57
5.3.2 Filter retardation analysis of RNAi influence on polyQ aggregates.....	58
5.3.3 RNAi effects on polyQ inclusions <i>in situ</i>	60
5.4 Summary of RNAi screen results	61
5.5 Analysis of the effect of <i>TRMT2A</i> silencing on polyQ toxicity in <i>Drosophila</i>	62
5.5.1 Impact of <i>TRMT2A</i> silencing on polyglutamine-induced REPs	62
5.5.2 Evaluation of photoreceptor integrity of polyQ flies with <i>TRMT2A</i> knockdown	64
5.5.3 Assessment of adult-onset polyQ fly longevity.....	65
5.5.4 Influence of <i>CG3808</i> downregulation on aggregate formation in <i>Drosophila</i>	66
5.6 Impact of <i>TRMT2A</i> knockdown on polyQ toxicity in a mammalian system	68
5.6.1 Generation of stable <i>TRMT2A</i> knockdown HEK cells.....	69
5.6.2 Transfection of stable <i>TRMT2A</i> knockdown cells with polyQ constructs.....	70
5.6.3 Investigation of aggregation in polyQ-transfected knockdown cells.....	72
5.7 Attempts on revelation of the molecular mechanism of <i>TRMT2A</i> knockdown on polyQ proteins	73
6 Discussion.....	75
6.1 Characterisation of the utilised polyQ <i>Drosophila</i> model	75
6.2 Modifiers of Ataxin-3-induced REP in <i>Drosophila</i>	77
6.2.1 Comparison to related polyQ modifier screens.....	78
6.2.2 Chaperones as polyQ misfolding and aggregation modifiers.....	80

6.2.3 Components of the UPS in polyQ pathogenesis.....	81
6.2.4 PolyQ-induced neurotoxicity modifiers involved in transcriptional regulation	82
6.2.5 Nuclear transport proteins are modifiers of polyQ toxicity	83
6.2.6 Further remarks on polyQ toxicity modifiers and the RNAi screen.....	83
6.3 Aggregation in <i>SCA3tr-Q78</i> -shRNA-coexpressing flies	84
6.4 The role of TRMT2A in polyQ pathogenesis	85
7 Summary and Concluding Remarks	88
8 Bibliography	89
Curriculum Vitae.....	104
Private Danksagungen.....	106
Appendix.....	107
I Additonal eye phenotypes	107
II RNAi lines modifying <i>SCA3tr-Q78</i> -induced REP	108
III Fly lines used for verification of RNAi.....	135
IV List of screened RNAi lines obtained from the VDRC as human orthologue sublibrary	138

List of Figures

Figure 1.	Exemplary overview of proteopathies and the respective disease subcategories.	4
Figure 2.	Model of conformational change, oligomerisation and aggregation as underlying pathogenic mechanism for polyQ diseases.	8
Figure 3.	Pathogenic processes during the development of polyQ diseases.	12
Figure 4.	Model of the UAS/GAL4 expression system.	22
Figure 5.	Mechanism of RNAi with shRNA.	23
Figure 6.	Phenotypes induced by GMR-mediated expression of different transgenes.	45
Figure 7.	Biochemical detection of SCA3tr-Q78 protein levels and aggregation together with verification of SCA3tr-Q78 expression, aggregation and induced cell death in larval imaginal discs.	46
Figure 8.	Histological and immunohistochemical analysis of utilised fly models.	48
Figure 9.	Photoreceptors in semi-thin sections of SCA3 disease models.	49
Figure 10.	Flow chart of the implemented screen to identify modifiers of SCA3-induced toxicity including subsequent analysis of primary screen candidates.	50
Figure 11.	Modification of the SCA3tr-Q78-induced phenotype by enhancing and suppressing candidate RNAi lines.	51
Figure 12.	Summary of the SCA3tr-Q78 modifier screen and overview of modifier categories.	56
Figure 13.	Influence of selected shRNAs on tissue integrity of SCA3tr-Q78 fly head sections.	58
Figure 14.	Analysis of SDS-insoluble SCA3tr-Q78 aggregate load with shRNA modifiers.	59
Figure 15.	Influence of RNAi on microscopically detectable Ataxin-3 inclusions <i>in situ</i> .	61
Figure 16.	Rescue of polyQ-induced REP by shRNA against CG3808.	63
Figure 17.	Evaluation of photoreceptor integrity in polyQ flies with CG3808 RNAi.	64
Figure 18.	Adult-onset model of SCA3tr-Q78 in <i>Drosophila</i> and extension of polyQ fly life time by CG3808 RNAi.	66
Figure 19.	Overview of anti-aggregation effects of CG3808 RNAi in different polyQ models and settings.	67
Figure 20.	Stable shRNA-mediated silencing of TRMT2A expression after viral transduction of HEK293 cells.	70
Figure 21.	Aggregation properties of normal and expanded Huntingtin in control and TRMT2A knockdown HEK cells.	71
Figure 22.	Impact of TRMT2A knockdown on different SDS-insoluble Huntingtin aggregates.	72
Figure 23.	Overlap between screens for genetic modifiers of polyQ-induced neurotoxicity or aggregation.	80
Figure 24.	Putative mechanistic explanation of polyQ toxicity amelioration by TRMT2A knockdown.	86

List of Tables

Table 1.	Overview of polyglutamine diseases.	5
Table 2.	Chemicals and reagents.	28
Table 3.	Equipment.	30
Table 4.	Software and online resources.	31
Table 5.	Utilised <i>Drosophila melanogaster</i> strains.	32
Table 6.	Stocks utilised for screening approaches.	34
Table 7.	Antibodies utilised for <i>Drosophila</i> head and cell lysate immunoblotting and for immunohistochemical stainings.	37
Table 8.	Lentiviral clones and non-target strain utilised for <i>TRMT2A</i> silencing experiments in HEK293 cells.	40
Table 9.	List of candidates with viable progeny modifying Ataxin-3-induced REP in <i>Drosophila</i> .	52

List of Abbreviations

Abbreviation	Denotation
ADCA	Autosomal dominant cerebellar ataxia
Ago2	Argonaute2
ALS	Amyotrophic lateral sclerosis
AO	Acridine orange
ATXN	Ataxin
BDNF	Brain -derived neurotrophic factor
CACNA1 _A	Calcium channel, voltage-dependent, P/Q type, alpha 1A subunit
CAA	Cytosine-adenine-adenine (trinucleotide coding for glutamine)
CAG	Cytosine-adenine-guanine (trinucleotide coding for glutamine)
cAMP	Cyclic adenosine monophosphate
CAT	Cytosine-adenine-thymine (trinucleotide coding for valine)
CG	Protein-coding gene (in <i>Drosophila melanogaster</i>)
CNS	Central nervous system
CBP	CREB-binding protein
CREB	cAMP responsive element-binding protein
DRPLA	Dentatorubral-pallidoluysian atrophy
dsRNA	Double-stranded RNA
eGFP	Enhanced green fluorescent protein
EP	Enhancer/promoter
FTD	Frontotemporal dementia
FRA	Filter retardation assay
GABA	γ -amino butyric acid
GMR	<i>glass</i> multiple reporter
HA	Haemagglutinin
HAP1	Huntingtin-associated protein 1
HAT	Histone acetyltransferase
HD	Huntington's disease
HDAC	Histone deacetylase

HDJ1	Human DnaJ protein 1
HEAT	<u>H</u> untingtin, <u>E</u> F3, PP2 <u>A</u> , <u>T</u> OR1
HEK	Human embryonic kidney cells
HIP1	Huntingtin-interacting protein 1
HRP	Horseradish peroxidase
HSP	Heat shock protein
HTS	High-throughput screen
HTT/Htt	Huntingtin
IR	Inverted repeats
kDa	Kilodalton
Lys	Lysine
MF	Morphogenetic furrow
MJD	Machado-Joseph disease
miRNA	MicroRNA
MOI	Multiplicity of infection
mRNA	Messenger RNA
MSN	Medium spiny neuron
NII	Neuronal intranuclear inclusion
ORF	Open reading frame
polyQ	Polyglutamine
RBM17	RNA-binding motif protein 17
REP	Rough eye phenotype
RISC	RNA-induced silencing complex
RLC	RISC loading complex
RNAi	RNA interference
SBMA	Spinal bulbar muscular atrophy
SCA	Spinocerebellar ataxia
SEM	Scanning electron microscopy
shRNA	Short hairpin RNA
siRNA	Small interfering RNA
Sp1	Specificity protein 1
TBP	TATA box-binding protein
TDP-43	TAR DNA-binding protein 43

TPR2	Tetratricopeptide repeat protein 2
TRMT2A	tRNA methyltransferase homologue 2A
tRNA	Transfer RNA
UAS	Upstream activation sequence
UIM	Ubiquitin-interacting motif
UPS	Ubiquitin-proteasomal system
VDRC	Vienna <i>Drosophila</i> RNAi Centre
WT	Wild type

1 Abstract

Spinocerebellar ataxia type 3 (SCA3) or Machado-Joseph disease (MJD) belongs to the group of polyglutamine (polyQ) neurodegenerative diseases and is the most prevalent autosomal dominant cerebellar ataxia worldwide. A highly variable polyglutamine tract is thought to confer toxicity upon the otherwise unrelated proteins causing polyQ diseases. Apart from the polyQ extension, the physiological function and cellular context of these proteins and their interaction partners appear to be crucial for the specific pathogenesis and course of the disorders. In order to elucidate the molecular disease mechanisms triggered by trinucleotide repeats, we intended to identify genetic interactors enhancing or suppressing polyQ toxicity.

Therefore, expression of a human Ataxin-3-derived polyQ transgene was targeted to the *Drosophila* compound eye. The resulting photoreceptor degeneration induced a rough eye phenotype (REP) in adult flies. Eye-specific silencing of distinct genes (fly genes with a human orthologue, ca. 7,500 genes) by RNAi was utilised to identify genetic interactors of the REP. Changes in the observed REP are likely to originate from the knockdown of the RNAi target. Thus, silenced candidate genes are capable of modifying polyQ-induced neurotoxicity.

The gene products that were discovered in this manner represent various biological pathways and molecular functions. Secondary investigations were conducted with a set of candidate genes to gain more insight into the mode and quality of the interactions and revealed novel modifier genes involved for example in tRNA methylation or sphingolipid metabolism. These results are likely to shed further light on the molecular pathogenesis of MJD and other polyQ disorders together with the role of Ataxin-3 and its modulator proteins in this process.

1 Zusammenfassung

Die Spinozerebelläre Ataxie Typ 3 (SCA3) oder Machado-Joseph-Krankheit (MJD) gehört zur Gruppe der neurodegenerativen Polyglutaminerkrankungen (PolyQ-Erkrankungen) und ist die häufigste autosomal-dominante zerebelläre Ataxie weltweit. Ein in der Länge hochvariabler Polyglutaminabschnitt ist vermutlich die Ursache für die Toxizität der ansonsten nicht verwandten Proteine, welche die PolyQ-Erkrankungen verursachen. Abgesehen von dem verlängerten Polyglutaminbereich scheinen die physiologische Funktion und der zelluläre Kontext dieser Proteine und ihrer Interaktionspartner entscheidend für die spezifische Pathogenese und den Krankheitsverlauf zu sein. Diese Arbeit soll dazu beitragen, genetische Interaktoren zu identifizieren, welche die PolyQ-Toxizität verstärken oder vermindern, um somit die molekularen Krankheitsmechanismen zu entschlüsseln, die durch die Trinukleotid-Wiederholungen ausgelöst werden.

Dafür wurde ein humanes, von Ataxin-3 abgeleitetes Transgen in den Facettenaugen von *Drosophila* exprimiert. Die daraus resultierende Degeneration der Photorezeptoren induziert einen Raue-Augen-Phänotyp (Rough Eye Phenotype, REP) in adulten Fliegen. Um genetische Modifikatoren des REP zu identifizieren, wurde die Expression bestimmter Gene (Fliegengene mit einem humanen Ortholog, insgesamt ca. 7.500) augenspezifisch per RNAi vermindert. Mögliche Veränderungen im beobachteten REP sind dann höchstwahrscheinlich auf den RNAi-vermittelten Knockdown der Genexpression zurückzuführen. Damit wären die stummgeschalteten Kandidatengene zur Modifizierung der PolyQ-induzierten Neurotoxizität fähig.

Die auf diese Weise identifizierten Genprodukte sind in verschiedene biologische Prozesse involviert und stehen stellvertretend für unterschiedlichste molekulare Funktionen. Für eine Auswahl von Kandidatengenen wurden zusätzliche Untersuchungen angestellt, um die Art und das Ausmaß der Interaktionen zu bestimmen. Dabei wurden neue Modifikatorogene analysiert, welche z. B. in die Methylierung von tRNA oder den Sphingolipid-Metabolismus involviert sind. Diese Ergebnisse können neue Erkenntnisse bei der Aufklärung der Pathogenese der MJD und anderer PolyQ-Erkrankungen hervorbringen und gleichzeitig zum Verständnis der Rolle von Ataxin-3 und seinen Modulatorproteinen beitragen.

2 Introduction

Neurodegenerative diseases affecting and impairing the central nervous system are on the rise throughout the world. Senescence being the main risk factor for these diseases, the number of age-related disorders is rising dramatically especially in industrial countries where life expectancy advances. Concomitantly, more and more inherited diseases of the nervous system can be precisely diagnosed and investigated, revealing underlying mechanisms and connections, but also posing new questions. In contrast to the scientific progress in this field as well as to the increasing burden of neurodegenerative diseases both to society and individuals stands the lack of efficient therapeutical options, let alone of a cure for the vast majority of these devastating and mostly fatal disorders.

2.1 Overview: proteopathies and polyglutamine diseases

Proteopathies are disorders in which abnormal accumulation of specific proteins represents the pathological hallmark of the respective diseases. Therefore it can be suggested that the altered proteins might cause the corresponding medical condition [5]. Nowadays, more than 40 groups of proteopathies are known, occurring through the mutation and putative misfolding of various proteins like hemoglobin, rhodopsin, fibrinogen, tau or amyloid β peptide [6]. In tissues affected by a proteopathy, aggregates of the respective mutated protein can be detected. It is generally believed that these accumulations play a role in the pathogenesis, although it is not clear whether they are the actual toxic species.

Trinucleotide repeat disorders, also called triplet repeat expansion disorders, make up an own heterogeneous group in the entity of proteopathies. They are characterized by the expansion of a tract of trinucleotide repeats within the particular disease gene. Healthy individuals bear a distinct repeat range in the normal allele and only upon elongation of this nucleotide stretch above a certain threshold the gene product is rendered toxic [7-9]. The trinucleotide disorders can be grouped into two categories: the polyglutamine diseases and the non-polyglutamine diseases, the latter being caused by genes exhibiting repeats different from the CAG (coding for glutamine) triplets characteristic for polyglutamine diseases (**Figure 1**).

The group of polyglutamine (polyQ) diseases comprises nine heritable neurodegenerative disorders, including Huntington's disease (HD), spinal bulbar muscular atrophy (SBMA) and six

spinocerebellar ataxias (SCA). All nine arise from a gain-of-function mutation in their respective disease genes, resulting from an autosomal dominant (except for the X-linked SMBA) expansion of polyglutamine repeats [9-11]. Therefore they are also entitled polyglutamine expansion disorders (**Table 1**).

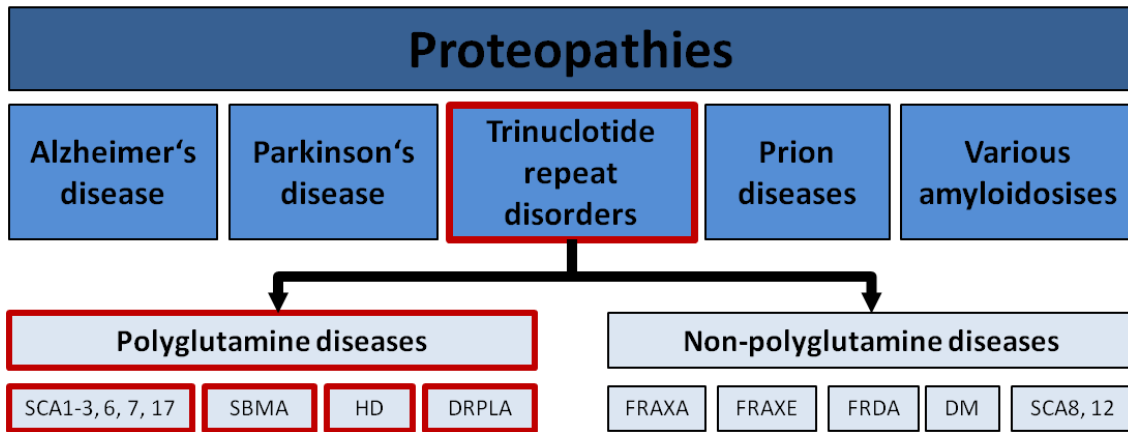


Figure 1. Exemplary overview of proteopathies and the respective disease subcategories.

The entity of trinucleotide disorders is a subgroup of proteopathies together with other neurodegenerative diseases and comprises the polyglutamine and non-polyglutamine diseases. The members of the polyQ disease family are depicted entirely (see also **Table 1**), the listing of the other disease groups is not intended to be exhaustive.

SCA, spinocerebellar ataxia; SBMA, spinal bulbar muscular atrophy; HD, Huntington's disease; DRPLA, dentatorubral-pallidoluysian atrophy; FRAXA, fragile X syndrome, FRAXE, fragile XE syndrome; FRDA, Friedreich ataxia; DM, myotonic dystrophy

Although the principle genetic basis of polyglutamine diseases has been known for 20 years, the molecular pathogenesis remains elusive and therapeutic approaches are merely aimed at the symptoms rather than the cause of the disorders [2].

Polyglutamine diseases have a remarkable genotype-phenotype correlation with most of the diseases emanating from an expansion above a threshold of 40 CAG repeats (**Table 1**). This origin of the disorders is regardless of the predicted functions of the causative genes or the surrounding amino acids of the polyQ stretch. The age of onset is inversely correlated to the length of the polyglutamine tract, whereas the severity increases with the number of trinucleotide repeats [12, 13].

Apart from the polyQ tract, the gene products share no homology to each other, suggesting a common pathogenic mechanism leading to the development of disease. Furthermore, the specificity for affecting certain brain regions in the diverse polyQ diseases cannot be explained by differential expression patterns of the disease genes. With regard to similar toxicity of heterogeneous proteins in different cellular and spatial settings, there is overwhelming

need for insights into polyQ protein-interacting genes in order to decipher the molecular processes leading to neurotoxicity.

Table 1. Overview of polyglutamine diseases.

Disease	Gene product	Inheritance	Normal repeat length	Expanded repeat length	Distinguishing clinical features¹
HD	Huntingtin	AD	6-34	36-121	Chorea, dystonia, cognitive deficits, psychiatric problems
SCA1 (ADCA)	Ataxin-1	AD	6-44	39-82	Pyramidal signs, peripheral neuropathy
SCA2 (ADCA)	Ataxin-2	AD	15-24	32-200	Slow saccadic eye movements, peripheral neuropathy, decreased deep tendon reflexes, dementia
SCA3 (ADCA)	Ataxin-3	AD	13-36	61-84	Pyramidal and extrapyramidal signs, lid retraction, nystagmus, decreased saccade velocity, amyotrophy, fasciculations, sensory loss
SCA6 (ADCA)	CACNA1 _A	AD	4-19	10-33	Sometimes episodic ataxia, very slow progression
SCA7 (ADCA)	Ataxin-7	AD	4-35	37-306	Visual loss with retinopathy
SCA17 (ADCA)	TBP	AD	25-42	47-63	Mental deterioration, occasional chorea, dystonia, myoclonus, epilepsy
DRPLA (ADCA)	Atrophin	AD	7-34	49-88	Chorea, seizures, dementia, myoclonus
SBMA	Androgen receptor	XR	9-36	38-62	Motor weakness, swallowing difficulties, gynecomastia, decreased fertility

¹ all ADCAs have gait ataxia.

ADCA, autosomal-dominant cerebellar ataxia; AD, autosomal-dominant; XR, X-linked recessive; HD, Huntington's disease; SCA, spinocerebellar ataxia; DRPLA, dentatorubral-pallidoluysian atrophy; SBMA, spinal bulbar muscular atrophy; CACNA1_A, Calcium channel, voltage-dependent, P/Q type, alpha 1A subunit; TBP, TATA box-binding protein [8, 14]

2.2 Pathogenic mechanisms of polyglutamine diseases

Despite the revelation of the connection with polyQ tract expansion within the respective proteins, the molecular mechanisms resulting in polyQ diseases are still under debate. It has been widely believed that aggregation of polyglutamine proteins, namely inclusions bodies, is the causative agent [15], nevertheless, research over the years has diversified this opinion [16] and has put focus on different species and structures of polyQ proteins (**Figure 2**). Additionally, it is crucial for the understanding of the disorders and for the development of therapeutical approaches to identify the very molecular pathways and cellular context by which toxicity of the proteins eventually leads to neuronal death.

2.2.1 Cytotoxicity of polyglutamine structures

Polyglutamine monomers

The conformational change of the molecular structure of native polyglutamine proteins into β -sheet-rich monomeric proteins is an essential step in the toxification of these gene products [17, 18]. Due to the obstacles that arise while trying to observe the structure of these β -strands in the actual disease protein, most of the studies with this focus have been conducted utilising artificial proteins [19-21]. Numerous investigations proposed cylindrical, hairpin and intramolecular β -sheet models, however it is not clear which of these might be the predominant form in affected cells. It has been shown that polyQ monomers are cytotoxic in cultured cells [22]. Despite these findings it remains elusive whether toxicity is conferred directly by the monomers themselves or if the transition into oligomers is responsible for the cytotoxicity. It is noteworthy that the monomer-oligomer transition propagates rapidly throughout the cell and can also take place in the reverse direction [23].

Polyglutamine oligomers

Oligomers of disease proteins have been proposed as the toxic species leading to cell death in a variety of neurodegenerative disorders, including Alzheimer's disease [24]. There are several lines of evidence for oligomeric intermolecular structures of expanded polyglutamine proteins. For instance an anti-parallel β -sheet structure with intermolecular hydrogen bonds called "polar zipper" [25], a parallel β -sheet conformation [18] or a cylindrical assembly designated "nanotube" [20], all analysed *in vitro*, have been described. Nevertheless, the predominance of any one of these species in living cells could not be verified. Studies investigating the formation of expanded polyQ oligomers out of monomers revealed a bidirectional transition of these species and the predominant cytotoxic potential of the oligomer fraction towards neuronal cells [23, 26, 27]. Furthermore, polyQ oligomers are more toxic than inclusion bodies [26] and heat shock proteins 40 and 70 (HSP40/70) are capable of ameliorating the deleterious effects of expanded polyQ proteins without influencing the formation of inclusions [28-30]. In a mouse model of SBMA, the presence of oligomers exhibited a close correlation to disease symptoms [31]. From these findings and other studies concerning polyQ oligomers [32-35], a pivotal role of these structures in polyQ pathogenesis can be deduced (toxic oligomer hypothesis). Some reports even favour a common toxic structure hypothesis [33, 36] based upon the cross-reactivity of antibodies against A β oligomers with other amyloidogenic proteins (like α -synuclein and polyglutamine proteins). Accordingly, amyloidogenic proteins causing neurodegenerative diseases would share a common toxic structure regardless of their amino acid sequence. However, these findings have not yet been verified in tissue of polyQ disease patients.

Polyglutamine inclusions

The formation of intranuclear inclusion bodies composed of expanded polyQ proteins has for a long time been considered to be the toxic event underlying the pathogenesis of the respective disorders [37-41]. Apart from the polyQ gene products themselves, a variety of other proteins like ubiquitin and heat shock proteins have been shown to be present in nuclear inclusions. Deprivation of these proteins from other cell compartments may result in dysfunction of neuronal cells [37, 42] concomitantly with disruption of axonal transport and nuclear function [43]. Despite these findings, results of more recent studies have established a rather cell-protective role of polyQ inclusion bodies. In addition to the lacking

correlation between inclusion body formation on the one hand and cellular imbalance and death on the other [44, 45], polyQ inclusion bodies proved to be beneficial in rat striatal neurons exposed to mutant Huntingtin (Htt) [46]. Furthermore, cells with inclusions survived significantly longer than those with soluble oligomers [23]. Although this hypothesis is not yet fully verified *in vivo*, formation of polyQ inclusions appears to mitigate detrimental effects of the mutated proteins rather than being the initial molecular step of polyQ disease emergence.

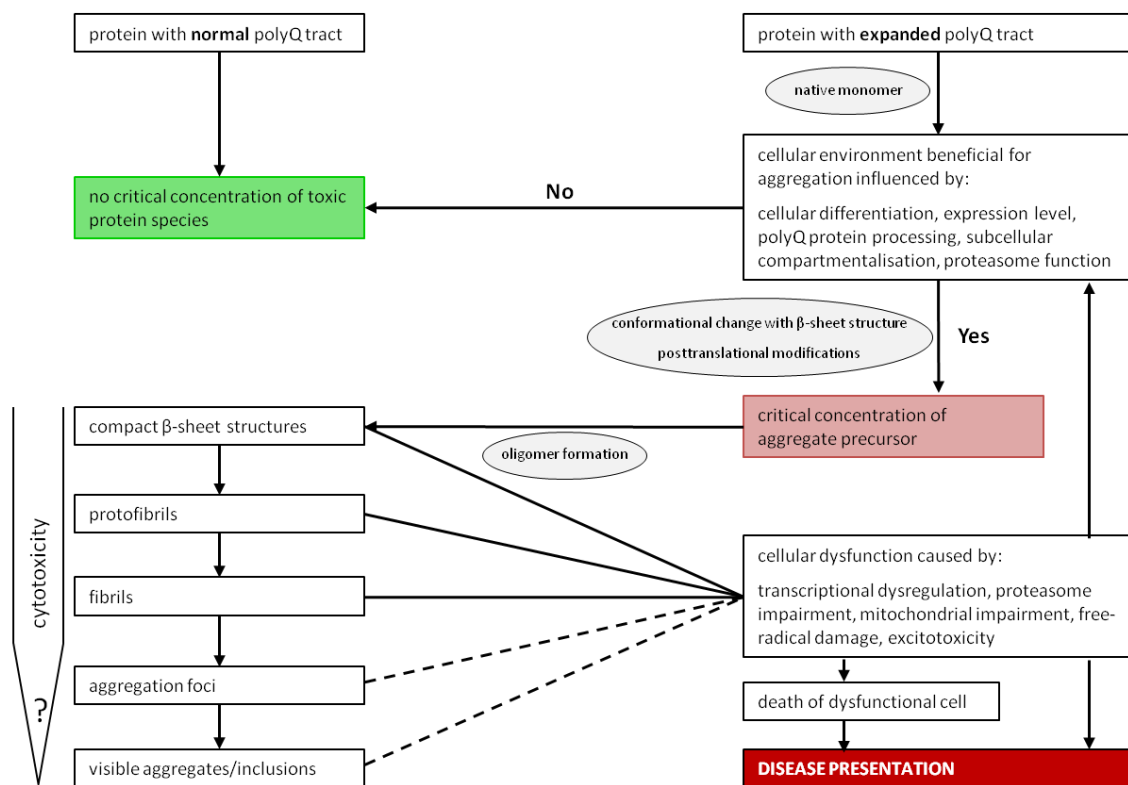


Figure 2. Model of conformational change, oligomerisation and aggregation as underlying pathogenic mechanism for polyQ diseases.

PolyQ pathogenesis requires an expanded polyQ tract in the disease protein and a cellular environment promoting the accumulation of conformationally altered polyQ monomers. Cytotoxic effects are exerted in the course of oligomerisation of aggregate precursors and the formation of different aggregation states and species with varying impact on cellular dysfunction. Subsequent cellular impairment renders the environment even more aggregation-prone. Eventually, the toxic effects exceed the cell's coping capability and lead to death of the dysfunctional cell and to disease onset.

Adapted from [1, 2].

Influence of residues adjacent to the polyglutamine tract

Although the expansion of the polyQ stretch in disease proteins is the molecular basis of cytotoxicity and pathogenicity in polyQ diseases, it does not explain the selectivity for distinct neuronal populations and tissues in the respective disorders. The different disease proteins exhibit a widespread distribution throughout the central nervous system (CNS) and are not confined to the especially vulnerable cell types. For instance, Huntington's disease mainly affects striatal GABAergic medium spiny neurons (MSNs) [47] whereas Ataxin-1 in SCA1 is most detrimental in Purkinje cells of the cerebellum [48]. In contrast, toxicity of Ataxin-3 in SCA3 affects a wide range of cell types in pons, substantia nigra, thalamus and diverse brain stem nuclei [49, 50]. An explanation for this discrepancy may be found in the disease protein portions apart from the polyQ stretch. Mutation in the CAG tract may also alter the protein-protein interactions of the non-polyQ parts of the protein. The association of mutated Htt for instance is more tightly with Htt-associated protein 1 (HAP1) and less strong with Htt-interacting protein 1 (HIP1) compared to wild-type Htt [51]. The modified interaction properties lead to the disruption of axonal transport of brain-derived neurotrophic factor (BDNF) and disturbances of clathrin-mediated endocytosis respectively. The correlation of Ataxin-1 mutation and Purkinje cell demise probably arises from a complex the disease protein forms with the neurotoxic RNA-binding motif protein 17 (RBM17). RBM17 is highly expressed in Purkinje cells and opposes another interactor of Ataxin-1, the neuroprotective Capicua [52]. Mutation of Ataxin-1 shifts the interaction balance towards a stronger association with RBM17 and results in cerebellar cell loss [53, 54].

Posttranslational modifications of amino acid residues outside the polyQ stretch have a remarkable impact on the toxicity of the disease proteins by influencing protein-protein interactions as well as by determining processing of the respective gene products. For example, phosphorylation of distinct amino acids of Htt, Ataxin-1 and the androgen receptor (AR) alters the affinity properties to ligands [55] and is capable of either reducing [56, 57] or increasing [58] the formation of inclusion bodies and toxicity.

Ubiquitination of polyQ-containing proteins subjects them to degradation by the ubiquitin-proteasomal system (UPS) and therefore represents a toxicity-ameliorating mechanism. On the contrary, the competing sumoylation renders the proteins more stable and promotes cell death via aberrant transcription and an increase in the amount of toxic oligomers [59, 60]. Selective expression of cofactors influencing posttranslational

modifications of polyQ proteins adds to the specificity of toxicity to certain cell populations [61].

According to the toxic fragment hypothesis, proteolytical processing of polyQ proteins is the initial step in rendering them toxic, leading to an increase in aggregation and to nuclear translocation [62]. Htt, Ataxin-3 and AR have all been described to be susceptible to cleavage by caspases at specific amino acid sites [31, 63-65]. Mutation or phosphorylation of these sites is sufficient to decrease inclusion body formation as a result of reduced proteolytical cleavage and hence toxicity [66, 67].

2.2.2 Molecular pathways to polyglutamine disease

Transcriptional dysregulation

The nuclear translocation and accumulation of expanded and proteolytically processed polyQ proteins suggests hampering of regular transcription in neuronal cells via altered interactions with transcriptional factors and cofactors. Several nuclear transcriptional regulators like CREB-binding protein (CBP), TAFII130, Sp1 and p53 have been shown to interact with polyQ proteins and are recruited to nuclear inclusions [40, 68, 69]. Microarray-based experiments with HD and DRPL mouse models exhibited similar alterations in gene expression [70]. Due to the pivotal role of histone acetylation for gene transcription, aberrant interactions of mutant polyQ proteins with histone acetyltransferases (HAT) influence gene expression as shown for Htt and CBP [71]. HAT activators have also been proposed as a therapeutic strategy in neurodegenerative diseases [72], the same applies to inhibitors of histone deacetylases (HDAC) [73, 74]. For the latter, improvements of polyQ-induced phenotypes in mouse and *Drosophila* models could be shown [75, 76]. Remarkably, the SCA3 causative protein, Ataxin-3, is a transcriptional repressor in its native state, involved in chromatin binding and histone deacetylation via HDAC3. Mutated Ataxin-3 loses its repressor function, leading to increased histone acetylation in cultured cells and the brains of SCA3 patients [77].

Impairment of the ubiquitin-proteasomal system (UPS)

The ubiquitin-proteasomal system is responsible for clearance and degradation of defective, aged and misfolded proteins in the cell. As polyQ inclusion bodies are ubiquitin-positive and components of the proteasome are recruited to these accumulations, studies suggest an impairment of proper UPS function in polyQ disease as a trigger for neuronal

cell death [78, 79]. This hypothesis is supported by the fact that cells with inclusion bodies exhibit decreased UPS activity [80]. Accordingly, mice and patients with polyQ disease present with global dysfunction of the UPS [81]. There is evidence that eukaryotic proteasomes are not capable of properly degrading polyQ sequences of the respective proteins, subsequently leading to proteasomal blockage [82]. Moreover, aberrant forms of ubiquitin have been shown to enhance aggregation [83].

In contrast, no malfunction of the UPS has been described for mouse models of HD and SCA7 [84-86]. Additionally, the reasoning of proteasomal component sequestration leading to increased cell death contradicts the rather non-pathogenic role of polyQ inclusion bodies.

It is noteworthy that the causative protein for SCA3, Ataxin-3, is the first deubiquitinating enzyme known whose catalytic activity is modulated by ubiquitination itself, enhancing its activity in cleaving Lysin63 linkages in ubiquitin chains [87] and thereby also modulating protein quality control via the UPS *per se*.

Impairment of mitochondrial function

Especially in Huntington's disease, evidence for an involvement of mitochondrial dysfunction during disease pathogenesis is established [88, 89]. Reports show signs of impairment of mitochondrial function such as decreased glucose metabolism and mitochondrial complex activity in HD patients [90] as well as lower membrane potentials in HD mice and patients compared to controls [91]. Transcriptional repression of PGC-1 α (a transcriptional coactivator of genes involved in energy metabolism) by mutant Huntingtin results in dysregulation of mitochondrial function and eventually in neuronal cell death [92]. These findings render mitochondrial impairment a side effect of transcriptional derangement in polyQ diseases. Huntingtin has also been implicated in the fission-fusion balance of mitochondria. Here, mutant Htt promotes mitochondrial fragmentation *in vitro* and *in vivo*, preceding the onset of Huntingtin aggregates and neurological deficits. In consequence, defects in anterograde and retrograde mitochondrial transport lead to neuronal cell death [93]. Antioxidants such as coenzyme Q10 and mitochondrial stability enhancers proved to be beneficial for the motor functions of HD mice [94-96], however, positive effects for other polyQ diseases cannot be deduced from these results.

Impairment of axonal transport

Huntingtin seems to play a role in axonal transport as a lack of normal protein levels in *Drosophila* neurons disrupts this process crucial for mobility of mitochondria, mRNA and proteins and thus survival of the neurons [97, 98]. Furthermore, polyQ length correlates with inhibition of anterograde and retrograde axonal transport by mutant Htt and AR [97-99]. In addition, expanded polyQ proteins and the resulting aggregates or inclusion bodies themselves are capable of blocking axonal transport in disease models, triggering neurotoxicity [100-102].

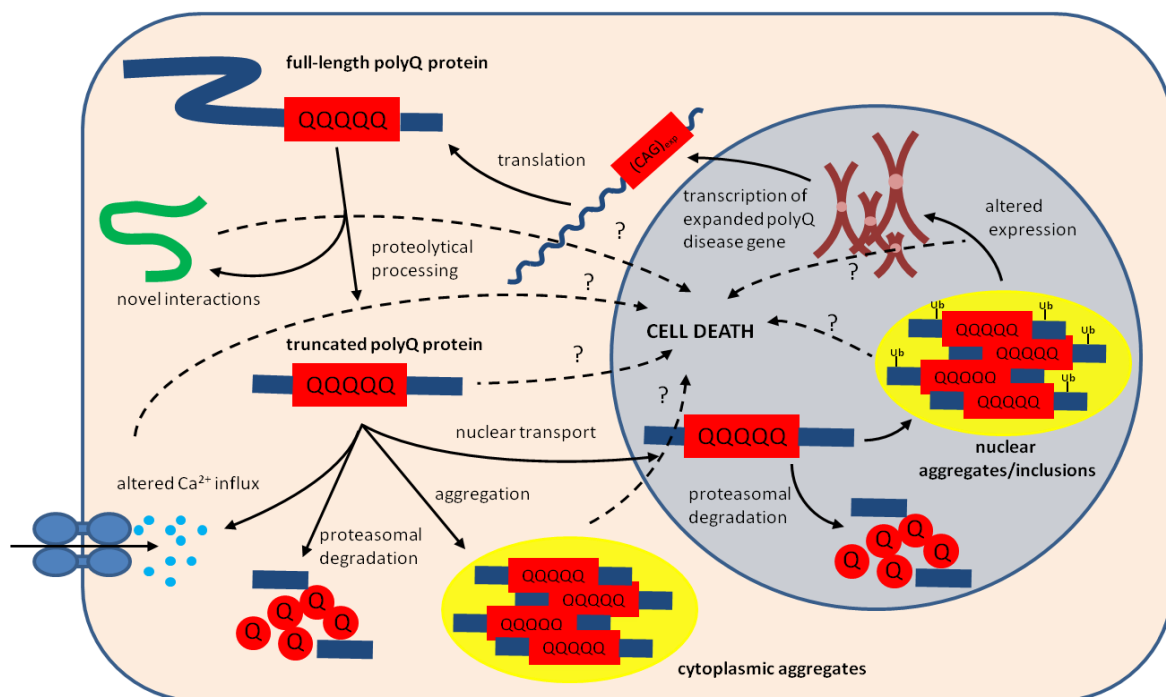


Figure 3. Pathogenic processes during the development of polyQ diseases.

Disease genes with an expanded CAG trinucleotide tract are transcribed and the mRNA is translated into a full-length protein with an elongated polyQ stretch. The mutant full-length protein itself already adopts novel interactions with other proteins and is furthermore proteolytically cleaved to a truncated form. These processed polyQ protein may alter ion transport into the cell and are prone to aggregation, thereby forming cytoplasmic aggregates and intranuclear inclusions upon transport into the nucleus. Toxic truncated polyQ proteins are a target for proteasomal degradation (intranuclear inclusions are ubiquitinated) and retained in a native conformation by chaperones if possible (not depicted). The alterations or impairment of the processes above are all presumptively capable of resulting in cellular dysfunction and eventually cell death.

Impairment of mitochondrial function and axonal transport are not shown.

Adapted from [4].

2.3 Examples of polyglutamine diseases

2.3.1 Huntington's Disease (HD)

Epidemiology and clinical features

Huntington's disease is the most common polyQ disease with a prevalence of 4-10 cases per 100,000 people in the Western world and many more at risk. The mean age of onset of HD is 40 years [47]. Clinically, extrapyramidal motor signs like chorea (usually the first motor symptom in adults), bradykinesia and dystonia together with features like progressive motor dysfunction, cognitive decline and psychiatric disturbance hint to the diagnosis Huntington's disease. Caudate and cortex are the brain regions most affected by atrophy diagnosed via neuroimaging. Additionally, the caudate and also the putamen present atrophy in neuropathology [103]. GABAergic medium-sized spiny striatal neurons are the cells most vulnerable to the detrimental effects of mutated Huntingtin [104, 105]. Secondary to the loss of striatopallidal projection fibres is atrophy of the globus pallidus, together with common cerebral cortical cell loss. Death occurs inevitably 10-20 years after emergence of the disease. Patients usually deacease from bulbar dysfunction and complications like pneumonia or heart failure [47, 106].

Molecular genetics and pathology

The molecularpathological hallmark of Huntington's disease is an expansion of a highly variable and unstable CAG repeat tract at the N-terminus (exon 1) of the disease gene *huntingtin* (*HTT*) [47, 107]. The gene itself is located on the short arm of chromosome 4 at position 16.3 [107]. The repetitive trinucleotide stretch within *HTT* has a length of 6-34 repeats in the normal population. After crossing a threshold repeat length of about 36, the overlong polyQ tract of the translated gene product renders the protein toxic, with a reduced penetrance in counts of 36-39 [108]. The longest ever reported repeat length amounts to about 250 glutamines [109].

The age of onset of HD is inversely correlated with the polyQ tract length. A juvenile form of HD originates from a glutamine repeat count of 70 and more. The gene product Huntingtin is a very large protein with a molecular weight of 348 kDa and can be detected in several tissues, but especially in the brain, from early embryogenesis on [110-112]. Huntingtin has been proposed to act as a scaffolding protein due to its multiple HEAT

repeats [113] and the large number of interacting proteins revealed in a yeast two-hybrid screen [114]. The protein seems to be crucial during embryogenesis as mice lacking the functional gene are lethal [115]. Furthermore, Htt has an influence on the expression of brain-derived neurotrophic factor (BDNF) via unknown mechanisms [116]. Several studies suggest an association of Huntingtin with vesicles and microtubules, indicating a role in cytoskeletal anchoring and transport of mitochondria [93, 117, 118].

2.3.2 Spinocerebellar ataxias

The spinocerebellar ataxias and the more complex dentatorubral-pallidoluysian atrophy belong to the group of autosomal-dominant cerebellar ataxias (ADCAs) which one to three among 100,000 Europeans suffer from. Among these disorders there are seven polyQ diseases (SCA1-3, SCA6-7, SCA17, DRPLA), the most frequent of which will be addressed here [14, 119]. When using the term SCAs in the following text, it will refer only to these seven polyQ-related ones, leaving out the other 25 spinocerebellar ataxias and certain episodic ataxias unless pointed out otherwise. The group of spinocerebellar ataxias (SCAs) is a growing entity of disorders sharing many clinical and pathological features. Neurodegeneration in these disorders mainly affects the cerebellum and its afferent and efferent connections. Due to this classification, dentatorubral-pallidoluysian atrophy (DRPLA) can also be grouped into this disease category, although not being an actual SCA [4]. The disambiguation of the single spinocerebellar ataxias from each other is almost impossible if only the clinical manifestation and neuroimaging are being considered. Juvenile occurrence of SCAs has been observed, as well as late-onset forms; nevertheless the typical manifestation is in middle-aged patients. After disease onset, the SCAs progress to premature death after 10-20 years. Differential severity and age of onset can be explained by the highly variable number of expanded glutamine repeats, leading to a more severe disease course at high repeat numbers and being inversely correlated with the age at disease initiation. In this context and like in other polyQ diseases, the phenomenon known as anticipation plays an important role. This term describes the increase in CAG repeat number in successive generations, rendering the disorder more severe in the descendants of an affected, specifically male individual [120-122].

Statements about the epidemiology of SCAs are rather hard to make due to only few and mostly regionally restricted data on prevalence and incidence. The heterogeneous

presentation of the diseases also leads to significant variations in ethnic and continental populations which are even more enhanced by founder effects (reviewed in [4]).

2.3.2.1 Spinocerebellar ataxia type 1 (SCA1)

The disease gene for spinocerebellar ataxia type 1, namely Ataxin-1, was the first ataxia gene to be discovered with an unstable trinucleotide repeat stretch in the line of various other genes responsible for SCAs [123]. SCA1 is ranked third in prevalence among the polyQ ataxia subtypes. The disease makes up for 6-8 % of the worldwide ADCA cases and is the most common SCA in South Africa and Italy [119, 124, 125].

Clinical features

SCA1 usually presents when the individual affected is in his or her forties, although juvenile and late onset forms have been reported. Clinical signs for SCA1 are highly variable which makes the disease hard to distinguish from the other spinocerebellar ataxias [126]. Symptoms include ataxia of the gait and stance, spasticity together with dysarthria, oculomotor abnormalities and pyramidal signs [127]. Differentiation of SCA1 from the other SCAs is possible by investigating central motor pathways with motor-evoked potentials in which the conduction time is remarkably longer than in SCA2, SCA3 and SCA6 [128].

Molecular genetics and pathology

Spinocerebellar ataxia type 1 is caused by an abnormal CAG trinucleotide repeat expansion in the open reading frame (ORF) of the *ATXN1* gene located on the short arm of chromosome 6. It is expressed in a variety of different tissues [129], however, the exact functions of the gene product Ataxin-1 at its nuclear localisation are not known. No phenotypes resembling those of SCA1 patients have been found in *ATXN1* knockout mice, speaking against a loss-of-function of the protein as disease origin [130]. Normal alleles bear a repeat number of 6-44 CAGs. In the range of 36 to 44 CAG repeats are considered non-pathogenic if they are interrupted by one to three CAT trinucleotides [129, 131]. Alleles carrying 36-38 CAG repeats without CAT interruptions, called mutable normal or intermediate alleles, are unlikely to be symptomatic but have a high chance to elongate during inheritance to progeny. There are reports of seldom reduced penetrance of

expanded CAG repeat alleles with CAT interruption [131], nevertheless, full penetrance and pathogenicity of *ATXN1* starts with uninterrupted 39 CAG repeats [132]. As in all polyQ diseases, anticipation and the rule of a longer, uninterrupted CAG repeat stretch causing a more severe course of the disease and an earlier age of onset apply [133, 134].

Like in the other polyQ diseases, the elongated polyQ stretch in Ataxin-1 is believed to confer abnormal folding properties onto the protein, rendering it prone to self-aggregation and accumulation in nuclear inclusion bodies (NIs). In these insoluble aggregates components of the protein degradation machinery such as chaperones or heat shock proteins (HSPs) and proteasomal constituents together with ubiquitin have been detected. These findings suggest the aggregates to be interfering with the cell's protein clearance mechanisms, consequently leading to SCA1 pathogenesis [135-138]. Studies furthermore proved the dependency of Ataxin-1 on phosphorylation and interaction with various proteins for aggregation and toxicity [58, 139].

Pathologically, SCA1 is characterised by atrophy of the brain stem and the cerebellum, where demise of especially Purkinje cells is observed [48].

2.3.2.2 Spinocerebellar ataxia type 2 (SCA2)

SCA2 is the second most prevalent autosomal dominant ataxia worldwide (15 % of all ADCA families). There is a particularly higher number of cases in Italy [125], India [140] and especially Cuba (Holguín province) [141-143].

Clinical features

The clinical manifestations of SCA2 differ from those of other SCAs insofar as that deep tendon reflexes present decreased and that there is saccadic slowing which is the most outstanding symptom in comparison to the resembling disorders SCA1 and 3 [144]. Patients show pyramidal findings and sometimes parkinsonism [145]. Other symptoms include cerebellar dysfunction in all SCA2 patients and peripheral neuropathy with varying frequency [146, 147]. SCA2 may also present as pure familial parkinsonism without cerebellar signs which is responsive to L-dopa treatment, but only affects a few patients with a smaller number of CAG repeats [148]. Disease onset is usually in the fourth life decade, afterwards progressing for approximately 10 to 15 years until premature death [149].

Molecular genetics and pathology

The underlying cause for SCA2 is the instability of the CAG trinucleotide tract in the gene *ATXN2* coding for Ataxin-2. *ATXN2* alleles containing 31 or fewer CAG repeats are considered non-pathological. Repeat numbers exceeding this threshold are causative for SCA2, with 32 and 33 CAG repeats resulting in late onset SCA2 after the age of 50 years. The expanded CAG allele may be interrupted by a CAA trinucleotide, increasing the meiotic stability of the repeat [150], although not influencing the pathogenicity since it codes for glutamine as well [151-153].

The protein has a cytoplasmic localization in normal as well as in SCA2 brains where it associates with Golgi membranes [154]. There is no difference in the expression pattern of SCA2-affected and non-affected individuals, additionally, aggregates of Ataxin-2 exhibit neither ubiquitination nor nuclear translocation [155].

The interaction of Ataxin-2 with the RNA-recognition motif-containing Ataxin-2 binding protein 1 implies an involvement of Ataxin-2 in mRNA translation or transport [156]. Despite this, Ataxin-2-deficient mice do not show marked neurodegeneration, however, they present with decreased fertility, obesity and altered hippocampal plasticity [157, 158]. Recent studies presented evidence for an association of intermediate-length polyQ expansions (27-33Q) in Ataxin-2 with amyotrophic lateral sclerosis (ALS). This influence is thought to be mediated by the RNA-dependent interaction of Ataxin-2 with one of the putative ALS causative proteins, namely TDP-43 [159].

Neuropathologically, SCA2 post-mortem brains show a significant reduction of cerebellar Purkinje and granule cells, whereas other cerebellar nuclei are greatly spared. Furthermore, the inferior olive and the pontocerebellar nuclei in the brain stem together with the substantia nigra show neuronal loss. Spinal cords are demyelinated in the posterior columns and degenerated thalamic and reticulotegmental nuclei of the pons have been reported, but not all of these findings were consistent in all patients [160-163]. One study also revealed involvement of the cerebral cortex, presenting with gyral atrophy especially in the frontotemporal lobes and atrophic as well as gliotic white matter [160].

2.3.2.3 Spinocerebellar ataxia type 3 (SCA3)/Machado-Joseph disease (MJD)

SCA3 is the most frequent among the SCA subtypes in most populations, comprising about 21 % of the worldwide cases of autosomal-dominant cerebellar ataxias, however, there are considerable regional variations of prevalence [14, 119]. SCA3 is also known as Machado-Joseph disease (MJD) after a family of Azorean immigrants to the US in which the disease was first diagnosed [164]. A similar founder effect is believed to have resulted in the high prevalence of SCA3 cases for example in Brazil.

Clinical features

SCA3 has one of the most heterogeneous clinical phenotypes of all cerebellar ataxias [165]. It includes progressive cerebellar ataxia and pyramidal signs associated to a variable degree with a dystonic-rigid extrapyramidal syndrome or peripheral neuropathy [166-168]. These symptoms may or may not be accompanied by progressive external ophthalmoplegia, pseudoexophthalmus due to lid retraction [167], familial parkinsonism [169] and restless-legs syndrome [170, 171]. A rather specific sign of SCA3 is impaired temperature discrimination in limbs, trunk and face [172]. Based on the phenotypic variability arising from the combination of different clinical signs in family members, SCA3 has been classified into several subtypes, illustrating the extreme clinical heterogeneity [173, 174].

- ◇ **Type I disease** (13 % of patients, dystonic-rigid form): early age of onset combined with spasticity, rigidity, bradykinesia and often little ataxia, presumably caused by a longer disease-associated repeat allele (mean 80).
- ◇ **Type II disease** (57 %, ataxia with pyramidal signs): presents with ataxia and upper motor neurons signs, also spastic paraplegia is possible. This disease type correlates to a wide range of intermediate length disease-causing repeat alleles (mean 76).
- ◇ **Type III disease** (30 %, with peripheral amyotrophy): has the latest age of onset with ataxia and peripheral neuropathy, linked to shorter disease-causing repeat alleles (mean 73) [175].

Comparable to the heterogeneity of symptoms is the variability in age of onset of SCA3 which is commonly between the second and the fifth life decade with a mean of 37 years

[165]. Again, there is inverse correlation of age of symptom onset and length of the CAG repeat in the disease gene. Due to the multitude of debilitating clinical symptoms, SCA3 patients are increasingly dependent on external help as the disease progresses. After onset of brain stem signs like facial atrophy and dysphagia, eventually death occurs from pulmonary complications and cachexia from six to 29 years after onset (recent studies show a 21-year mean survival time) [176, 177].

Molecular genetics and pathology

The disease gene responsible for Machado-Joseph disease when mutated, *ATXN3* (also called *MJD1*), was mapped to the long arm of chromosome 14 [178]. The CAG trinucleotide repeat coding for polyglutamine is located in exon 10 of the gene [178, 179]. Fifty-six alternative splicing variants for *ATXN3* have been described, of which at least 20 are translated into different protein isoforms [180]. Non-pathogenic alleles with variations of the CAG repeat in normal individuals can range from 12 to 43 repeats [175, 181-185]. A bimodal pattern of distribution of the normal allele frequency with peaks at 14 and 21-23 repeats has been shown for SCA3 patients [186, 187]. Furthermore, different nucleotides flanking the CAG sequence seem to correlate with specific repeat numbers and hence influence the stability of the polyQ stretch [187, 188]. CAG repeat numbers expanded above the normal length in pathogenic alleles are the cause of Machado-Joseph disease [145, 172, 178, 181-185, 189]. Trinucleotide repeat numbers ranging from 52 to 86 have been found in SCA3 patients. Alleles with seldom intermediate repeat numbers of 45 to 51 CAGs may exhibit reduced penetrance. As in other polyQ diseases, somatic and gametic instability is common in alleles with a prolonged CAG tract. This may result in spermatozoa having larger repeat counts than somatic cells and in cerebellar tissues with shorter repeat tracts than other brain regions [190, 191]. Anticipation has been described for SCA3, preferentially via paternal transmission [182, 192, 193].

The wild-type gene product Ataxin-3 encoded by *ATXN3* is a highly conserved and ubiquitously expressed 42 kDa protein [194]. It is predominantly located in the cytoplasm but also capable of nuclear shuttling [194]. Ataxin-3 has been found to be a deubiquitinating protease [195-200] via a globular amino-terminal Josephin domain [201] and three ubiquitin-interacting motifs (UIMs) contained in the flexible carboxy-terminal tail [202]. The UIMs flank the polyQ tract, however, it is not known whether or how pathological expansion influences the enzymatic activity of the protein. As already

mentioned, ubiquitination of Ataxin-3 regulates its ubiquitin chain-editing function [87]. The Josephin domain has also been shown to interact with the Huntingtin-associated protein 1 (HAP1) [203], together with the polyQ domain it determines stability and aggregation of Ataxin-3 [204-208]. Overall findings propose a role of Ataxin-3 in cellular protein quality control, supported by suppression of polyQ-induced neurodegeneration in *Drosophila* [209], the regulation of aggresome formation [210], protein degradation and enzymatic activity [211].

Most data suggest a toxification mechanism for Ataxin-3 with an expanded polyQ tract, rendering it prone to misfolding and aggregation [212]. As for other polyQ proteins, this process has been experimentally proven by various studies *in vitro* as well as *in vivo* [78, 213-219]. There is no difference in the expression patterns of the normal and the mutated form of Ataxin-3 in brains and unaffected tissue of SCA3 patients [78].

In contrast to the predominantly cytoplasmic distribution of the native protein, mutated Ataxin-3 tends to accumulate in the nucleus of affected neurons, forming neuronal intranuclear inclusions (NIIs) in various brain regions [78]. NIIs can also be accompanied by axonal inclusions [220] and appear ubiquitinated and in association with heat shock proteins (HSP70 and 90, HDJ-2) and proteasomal subunits (20S proteasome core, 11S and 19S regulatory caps of 26S proteasome) [79, 221, 222]. It is currently under heavy debate whether these inclusion bodies are the actual pathogenic species of mutated Ataxin-3 and other polyQ proteins or, on the contrary, merely are a safe storage for misfolded proteins to shield the cell from their toxicity [212, 223].

In accordance with the toxic fragment hypothesis, cleavage of Ataxin-3 to form shorter, polyQ-containing polypeptides seems to greatly enhance pathogenesis compared to the full-length protein, as has been shown in transgenic mice and flies. Moreover, these cleavage fragments appear to be the accumulating species in affected cells, which eventually undergo apoptosis [62, 65, 209, 219, 224, 225]. There are also alternative approaches to explain the aetiology of the disease apart from aggregation, including frameshifting during translation leading to deleterious polyalanine tracts [226], and RNA toxicity [227].

2.4 *Drosophila melanogaster* as an animal model in research

The fruit fly *Drosophila melanogaster* has been proven to constitute an excellent model organism for scientific research for more than a century now (reviewed in [228]). Since roughly 75 % of the known disease-associated genes in humans also have orthologues in flies (annotated genome with roughly 16,000 protein-coding genes [229]), it might be reasonable to draw conclusions from investigations on molecular mechanisms in the fly to those in humans. *Drosophila melanogaster* was one of the first multicellular organisms whose genome has been sequenced completely and the corresponding genetic knowledge is well-established. Creation of transgenic animals allows for the modelling of human diseases by expressing toxic gene products. Besides these rationales, *Drosophila* also conjoins additional advantageous properties especially for high-throughput approaches. Due to the fast replication cycle and the high number of offspring, experiments can be conducted within short time periods with a reasonable number of individuals, allowing for drug and genetic modifier screening [230]. Although being an invertebrate organism, experimental findings are gained from an *in vivo* situation and conclusions about molecular mechanisms in higher animals can be drawn without raising ethical issues. Last but not least, several powerful genetic tools have been introduced in the past years in order to render research with the fruit fly even more feasible, precise and easy to handle. Some of these tools and a number of respective models and studies for polyQ disease are reviewed below.

2.4.1 The UAS/GAL4 expression system

The bipartite UAS/GAL4 ectopic expression system is frequently used in *Drosophila* as a means of overexpression of transgenes [231-233]. It makes use of the yeast transcriptional activator GAL4. Enhancer trap constructs (designed to facilitate GAL4 expression) were randomly inserted into the fly genome. If the insertion took place in the vicinity of an endogenous gene, GAL4 expression might mimic the expression pattern of this particular gene. To date there are plenty of so-called GAL4 driver lines available, mediating GAL4 expression in virtually every tissue at different time points throughout fly development. The gene of interest is introduced into a different fly line and put under the control of a GAL4 target, the upstream activation sequences (UAS). Upon crossbreeding of

these two fly lines, both moieties of the system are conjoined. GAL4 is produced under the control of the endogenous enhancer and able to bind to the UAS flanking the previously silent transgene of interest. Thus, expression of the gene of interest is enabled and directed in a spatiotemporal manner in the offspring (**Figure 4**). This renders the UAS/GAL4 system a valuable tool in fly genetics, although caution has to be taken since high GAL4 expression levels can have detrimental effects during development [234].

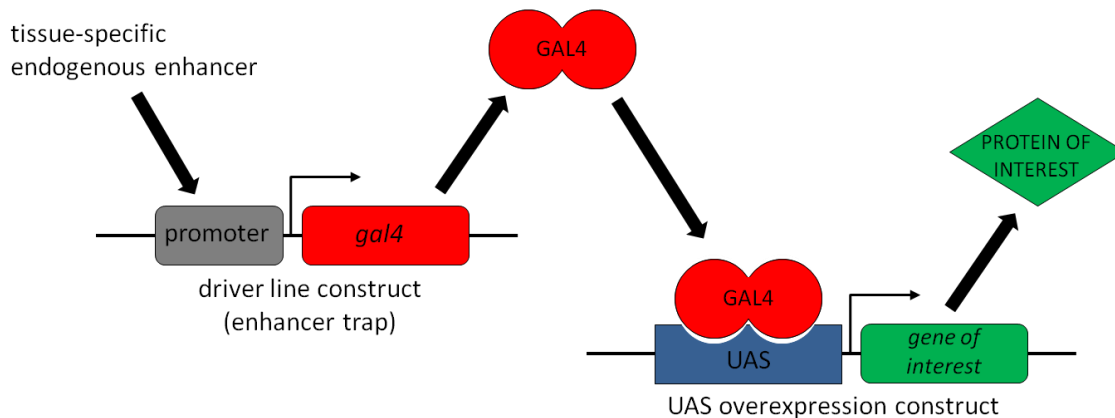


Figure 4. Model of the UAS/GAL4 expression system.

A tissue-specific endogenous enhancer binds to the promoter (grey) of the enhancer trap construct, thereby enabling *gal4* expression (red) in the driver fly line. Association of GAL4 with the upstream activation sequence (UAS) of the fly line transgenic for the gene of interest activates expression (green). The bipartite nature of the system allows for tissue specificity and temporal restriction of activation of the gene of interest.

2.4.2 RNA interference (RNAi)

The gene silencing effect induced by double stranded RNA (dsRNA) termed RNA interference (RNAi) was fully established after experiments in *Caenorhabditis elegans* in 1998 [235]. It was the final step in a series of fundamental findings in plants [236, 237] as well as animals [238, 239]. Originally an endogenous mechanism involved in translational repression [240], development [241] and defence against parasitic genes [242], RNAi quickly evolved to be a powerful technique in scientific research, e.g. in mimicking knockout experiments without the extensive work effort of creating classical knockout animals. The effectors of RNAi are diverse small interfering RNAs (siRNAs) categorised according to their origin, biogenesis, mode of action and size [243, 244]. The source of siRNAs used in this work are transgenes coding for short hairpin RNAs (shRNAs). These transgenes consist of 100-400 base pairs present as an inverted repeat (IR) separated by miscellaneous nucleotides. Following expression of the IR, it will form a short hairpin RNA

(shRNA) which is exported from the nucleus to the cytoplasm. The shRNA is bound and cleaved by the ribonuclease protein Dicer-2, resulting in a double stranded structure without loop and RNA tails [245]. This small interfering RNA (siRNA) is then bound and translocated to the RNA-induced silencing complex (RISC) by the RISC loading complex (RLC) protein R2D2 which additionally discriminates between guide and passenger strands of the siRNA [246, 247]. The RLC recruits Argonaute2 (Ago2) and transfers the dsRNA to it, resulting in decay of the passenger strand by this endonuclease [248]. Subsequent to the release of the passenger strand and disassembly of R2D2, the active RISC is formed. The complex is capable of recognising and binding the messenger RNA (mRNA) target by base pairing with the guide strand. Eventually, this leads to cleavage of the mRNA and effectively to silencing of gene expression (**Figure 5**) [249].

Based upon this mechanism, Dietzl *et al.* were the first to establish a *Drosophila* RNAi library covering ~90 % of the entire fly genome. It utilises the conditional UAS/GAL4 expression system for induction of shRNAs under UAS control, leading to RNAi for the respective gene upon crossbreeding with a GAL4 driver line [250].

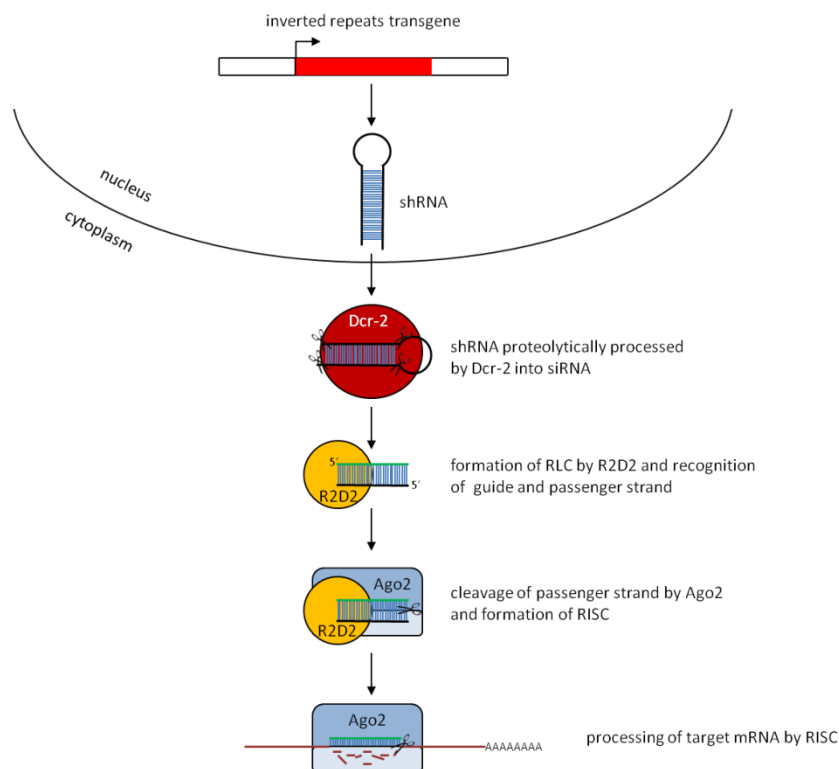


Figure 5. Mechanism of RNAi with shRNA.

The inverted repeats of the shRNA transgene are transcribed and the RNA is assembled into an shRNA. Following export from the nucleus, the shRNA is processed into double-stranded siRNA by Dcr-2. R2D2 forms the RLC together with the siRNA and discriminates the guide and the passenger strand, the latter is degraded upon binding of the RLC to Ago2. The guide strand and Ago2 form the RISC, eventually binding to and cleaving the target mRNA. Partially adapted from Dan Cojocari, Dept. of Medical Biophysics, University of Toronto, 2010.

2.4.3 Rough eye phenotype (REP)

The *Drosophila* compound eye is a highly ordered structure made up of about 800 single unit eyes termed ommatidia. Each ommatidium consists of eight photoreceptor cells arranged in an asymmetric trapezoid pattern accompanied by cone and pigment cells [251]. Cellular dysfunction and cell death as well as perturbation of crucial developmental pathways during compound eye formation lead to disturbances in this exact lattice and a so-called rough eye phenotype (REP). Consequently, a REP can be induced by the overexpression of toxic gene products. Expression of a disease gene can be targeted to postmitotic cells, including photoreceptor neurons, of the compound eye with the driver line *glass* multiple reporter (GMR)-GAL4 in combination with the UAS [252]. *Glass* expression starts at day one of larval stage L3 in all cells posterior of the morphogenetic furrow of the eye disc [253] as well as in a minor population of cells in the brain. The severity of the REP is directly correlated to the loss of underlying photoreceptor neurons reflected by vacant, interstitial or fused ommatidia and disordered sensory bristles. Since the fly compound eye is a neuronal structure easily accessible by light microscopy, the REP is an easy readout to assess changes in the decline of photoreceptor neurons caused by eye-specific expression of neurotoxic proteins. Thus, changes in REP have been successfully used in genetic screens set to identify modifiers of neurodegenerative disorders [28, 136, 254-256]. However, neurodegeneration in the fly eye cannot completely mimic the complex processes leading to disease in the human brain.

2.4.4 *Drosophila* models of polyglutamine disease

Disease models for polyQ disorders in *Drosophila* mostly involve overexpression of the common pathogenic feature of the causative proteins, concentrating on the expanded polyQ tract itself. Several fly lines have been introduced containing proteins entirely composed of normal or mutated polyQ stretches of different length (20Q, 22Q, 108Q, 127Q; [28, 257]). The expanded polyQ peptides in these models were sufficient to cause neurotoxicity despite the absence of their disease gene context. Additionally, studies have shown that a pure polyQ domain is much more toxic than a polyQ domain flanked by even relatively small protein sequences [258]. The detrimental intrinsic cytotoxic effects could be modified by genetic factors or modulations of the polyQ tract alone. These pure polyQ

approaches naturally neglect disease gene-specific characteristics and do not explain cell type specificity of distinct polyQ diseases. However, the previous work utilising such polyQ peptides revealed valuable novel insights into disease mechanisms.

The utilisation of truncated disease gene models is a feasible approach to study polyQ toxicity since it is assumed that causative proteins are also cleaved and thus truncated *in vivo* prior to oligomerisation and noxious effects. Several fly models for polyQ diseases are described. These models rely on expression of polyQ repeats either embedded in the C-terminal region of the human Ataxin-3/MJD protein (SCA3tr-Q27, SCA3tr-Q78; [219]), in an N-terminal truncated fragment of human Htt (Q2, Q75, Q120, Q128; [259, 260]) or exon 1 of Htt only (Q93; [75]). The distinction between the pathologies of polyQ diseases is more apparent at the level of truncated polyQ proteins. For instance, expression of the viral antiapoptotic protein p35 mitigated the REP in the *SCA3tr-Q78* model, but failed to do so in Htt-trQ120 [219, 259]. Most of these truncated disease gene models exhibit progressive protein aggregation, forming nuclear inclusions in neurons, and late-stage neurodegeneration. On the contrary, flies with a normal number of repeats show a diffuse and cytoplasmic protein distribution and no overt neurotoxicity.

Expression of human versions of the full length polyQ proteins in *Drosophila* is an approach to investigate the pathogenic potential of elongated polyQ tracts in their native protein context. Studies show that high levels of wild-type full length Ataxin-1 (Q30) exert disturbances in eye morphology and expansion of the polyQ tract (Q82) leads to detrimental effects and a rough eye phenotype that can be modified by genetic interactors [136]. Investigations on Huntington's disease involve generation of a fly line with a full-length Huntingtin containing 128Q [261], presenting a neurodegenerative eye phenotype due to demise of photoreceptor neurons. Similar approaches have been described for the androgen receptor in SBMA [262] and for full-length Ataxin-3 with polyQ expansion of 84 repeats in SCA3 [209]. In the latter model, flies showed severe and adult-onset neural degeneration when expression of the toxic disease protein was restricted to the compound eye or the nervous system, which was not observed for the wild-type protein. The full-length mutated protein is more selectively toxic to the nervous system compared to the truncated isoform and accumulated in ubiquitinated inclusions. Coexpression of wild-type full-length Ataxin-3 on the contrary is able to ameliorate the detrimental effects of the toxic variant even in models of SCA1 and HD.

2.4.5 Previously implemented modifier studies

Several studies were conducted in order to reveal genes that modify the cytotoxicity and deleterious consequences of polyQ expansion in the diverse causative disease proteins. As already mentioned above, the baculovirus antiapoptotic gene *p35* suppressed truncated mutant Ataxin-3-dependent degeneration in the eye, as does the human heat shock protein HSP70 [30, 219]. Kazemi-Esfarjani *et al.* published results of one of the first large scale modifier screens in flies expressing prolonged polyQ peptides only [28]. They utilised a set of 7,000 P-element insertions for crossbreeding with the disease flies and assessed the offspring for suppression or enhancement of the polyQ-induced rough eye phenotype. Out of a number of potential candidates they presented two chaperone-related gene products, dHDJ1 (equivalent to human HSP40/HDJ1) and dTPR2 (equivalent to human TPR2) as potent genetic suppressors of polyQ toxicity. Fernandez-Funez *et al.* utilised a fly model based on full-length Ataxin-1 Q82 expression for two screens with 1,500 lethal P-elements and 3,000 EP insertions respectively, also evaluating the change of REP in the F1 generation [136]. They identified 18 genes that, if altered in expression, enhanced or suppressed Ataxin-1 toxicity. Among these genes were some coding for ubiquitin-related proteins, chaperones, RNA-binding molecules and transcription factors. Bilen *et al.* described the crucial involvement of microRNAs (miRNAs) pathways in the modulation of polyQ toxicity induced by Ataxin-3 after screens in *Drosophila* and human cells [263]. The same group conducted a genome-wide EP element-based screen for modifiers of Ataxin-3-induced neurodegeneration in *Drosophila* [256]. They identified 25 modifiers representing 18 genes that are mainly involved in biological processes affecting protein misfolding and ubiquitin-related pathways. Among others, this experiment was designed as a genetic high-throughput screen based on the misexpression of endogenous genes [264]. Despite their general feasibility, these screening strategies create artificial expressions states potentially masking the native influence of the respective gene product. Furthermore, they are mostly confined to a small portion of the genome.

These disadvantages can be overcome by mimicking classical knockout experiments with the help of RNA interference-mediated gene silencing. This powerful technique has been successfully implemented into high-throughput screening for modifiers of Huntingtin aggregation in yeast [265] and *Drosophila* cells [266]. Genome-wide studies utilising RNAi revealed regulators of polyQ and Huntingtin aggregation in *C. elegans* [267] and *Drosophila* [268] respectively.

3 Aim of the Study

The comprehensive understanding of molecular mechanisms and cellular pathways resulting in polyQ neurotoxicity and pathogenesis are a prerequisite for the development of effective treatments for the corresponding disorders. In an attempt to contribute to this process we intended to conduct a genome-wide high-throughput modifier screen in order to identify genetic modifiers of polyQ neurotoxicity in *Drosophila melanogaster*. This should be accomplished first of all by characterisation of a feasible disease model exhibiting a readily accessible readout for the large scale experiments. Expression of a human variant of truncated Ataxin-3, harbouring a stretch of 78 glutamines, in the compound eye results in an REP. This REP combines pathological involvement of neuronal photoreceptor cells with an easy exterior observability of neurodegeneration. By means of RNA interference we planned to knockdown a genome-wide set of potential modifier genes, thereby evaluating the impact of the gene silencing on the REP. For this purpose, we obtained a set of fly RNAi strains from the VDRC representing all *Drosophila* genes known to have an orthologue in humans. A genetic modifier screen with these ~7,500 genes would represent the most comprehensive endeavour in this field and setting so far. The gene knockdown approach, the *in vivo* situation and the easy assessment of neurotoxicity modification mark the advantages of this work in comparison to previously conducted modifier screens. By subsequent thorough analysis and processing of our results and the obtained modifiers we hope to aid in conceiving polyQ diseases better and opening avenues for therapeutic approaches.

4 Material and Methods

4.1 Chemicals, reagents and equipment

Composition of reagents and buffers is specified in **Table 2** and referred to as such with the respective name in the text.

Table 2. Chemicals and reagents.

Name	Specification/Composition	Source/Manufacturer
Acridine Orange	3,6-bis[Dimethylamino]acridin (A-6014)	Sigma, USA
Acrylamide	Acrylamide 2K (30 %)	AppliChem, Germany
APS	Ammonium persulphate ≥ 98 % (9592.2)	Roth, Germany
Bromophenol blue	(A512.1)	Roth, Germany
CaCl ₂ x 2H ₂ O	Calciumchloride dihydrate ≥ 99 % p.a. (5239.2)	Fluka, Germany
Chloroform	Trichlormethane ≥ 99 % (3313.1)	Roth, Germany
Citrate buffer	1.8 mM citric acid 8.2 mM sodium citrate, pH 6.0	
Citric acid	(1.00244.1000)	Merck, Germany
DEPC	Diethylpyrocarbonate (K028.1)	Roth, Germany
<i>Drosophila's</i> Ringer	182 mM KCl 46 mM NaCl 3 mM CaCl ₂ x 2H ₂ O 10 mM Tris, pH 7.2	
DTT	1,4-Dithiothreitol (6908.1)	Roth, Germany
Entellan	(1.07961.0500)	Merck, Germany
Ethanol	≥ 99.8 % p.a. (9065.4)	Roth, Germany
Fluoromount	Fluoromount-G (0100-01)	Southern Biotech, USA
Glycerol	99 % (G5516-1L)	Sigma, USA
Glycine	≥ 99 % p.a. (3908.2)	Roth, Germany
HEPES	≥ 99.5 % p.a. (9105.4)	Roth, Germany
ECL solution	Immun-Star™ WesternC™ Kit (170-5070)	Bio-Rad, USA
Isopropanol	2-Propanol (T910.1)	Roth, Germany
KCl	Potassium chloride, ≥ 95.5 % p.a. (6781.1)	Roth, Germany
KH ₂ PO ₄	Potassium dihydrogen phosphate, ≥ 99 % p.a.	Roth, Germany

Laemmli buffer (5x)	250 mM Tris, pH 6.8 10 % (v/v) SDS 1.25 % (w/v) bromophenol blue 10mM EDTA 0.03 % (v/v) β -mercaptoethanol 50 % (v/v) glycerol	
Methanol	(717.1)	Roth, Germany
Methyl benzoate	(822330.1000)	Merck, Germany
MgCl ₂	Magnesium chloride \geq 98,5 % p.a. (KK36.1)	Roth, Germany
NaH ₂ PO ₄ x H ₂ O	Monosodium phosphate monohydrate, \geq 99 % p.a. (1.06342.1000)	Merck, Germany
NaCl	Sodium chloride, \geq 95.5 % p.a.	Roth, Germany
Na ₂ HPO ₄ x H ₂ O	Disodium phosphate monohydrate, \geq 99.5 % p.a. (1.06580.1000)	Merck, Germany
NaHCO ₃	Sodium hydrogen carbonate, \geq 99 % pure (8551.1)	Roth, Germany
NGS	Normal goat serum (S-2007)	Sigma, USA
Nitrocellulose membrane	Protran® BA 83 (10 402 396)	Whatman, Germany
Paraffin	32.3 % Paraffin 42-44 (107150) 32.3 % Paraffin 51-53 (107157) 32.3 % Paraffin 57-60 (107158) 3.2 % bees wax	Merck, Germany (Paraffin) Roth, Germany (beeswax)
PBS (0.01 M)	Phosphate-buffered saline 8 mM Na ₂ HPO ₄ x H ₂ O 1.8 mM NaH ₂ PO ₄ x H ₂ O 0.1 M NaCl	
PBS-T	0.14 M NaCl 6 mM Na ₂ HPO ₄ 2.7 mM KCl 1.5 mM KH ₂ PO ₄ 0.4 % Triton-X100	
PFA	4 % paraformaldehyde (0335.2) in PBS/PBS-T	Roth, Germany
Phalloidin	Alexa Fluor® 568 Phalloidin	Invitrogen, Germany
Resolving gel buffer (SDS-PAGE)	0.4 % SDS 1.5 M Tris, pH 8.8	
RIPA lysis buffer	50 mM Tris, pH 8.0 0.15 M NaCl 0.1 % (v/v) SDS 1 % NP-40 0.5 % Sodium deoxycholate Protease inhibitor (Roche)	
Running buffer (SDS-PAGE)	0.1 M Tris 1 M glycine 0.5 % SDS	
SDS	Sodium dodecyl sulphate, AccuGene 10 % (51213)	Cambrex, USA

Skim milk	Milk powder (T145.2)	Roth, Germany
Sodium citrate	(1.06448.0500)	Merck, Germany
Stacking gel buffer (SDS-PAGE)	4 % SDS 0.25 M Tris, pH 6.8	
Stripping buffer (WB)	0.2 M glycine 0.5 M NaCl pH 2.8	
Sucrose	D(+)-saccharose \geq 99.5 % p.a. (4621.1)	Roth, Germany
TBS	25 mM Tris 140 mM NaCl pH 7.5	
TBS-T	25 mM Tris 140 mM NaCl pH 7.5 0.05 % Tween-20	
TEMED	N,N,N',N'-Tetramethylethylendiamide	AppliChem, Germany
Transfer buffer (WB)	25 mM Tris 192 mM glycine 20 % (v/v) methanol	
Tris	\geq 99.3 % (AE15.2)	Roth, Germany
Triton-X100		Sigma, USA
Tween®20	(9127.1)	Roth, Germany
Vectashield	Vectashield mounting medium w/ and w/o DAPI	Vector, USA
Xylene		Otto Fischar, Germany

Table 3. Equipment.

Name/Specification	Manufacturer
Microtome HM 360	Thermo Scientific, Germany
Cryotome CM3050 S	Leica, Germany
Zoom stereo microscope SZ51 with KL200 LED light source	Olympus, Germany
Biological microscope CX31	Olympus, Germany
Zoom stereo microscope SZX10 with S80-55 RL ring light and SC30 digital camera	Olympus, Germany
Routine microscope CKX41 (inverted) with U-RFLT50 light source and SC30 camera	Olympus, Germany

Research microscope BX51 with X-Cite® 120Q light source and DP72 digital camera	Olympus, Germany
Tissue homogenizer SpeedMill P12	Analytik Jena, Germany
Chemiluminescence documentation system Alliance LD4.77.WL.Auto	Biometra, Germany
Scanning electron microscope ESEM XL 30 FEG	FEI, Eindhoven, Netherlands
Multimode microplate reader Infinite® M200	Tecan, Germany

Table 4. Software and online resources.

Name	Application
Adobe® Illustrator® CS4	Creation of illustrations
Adobe® Photoshop® CS4	Image processing
ImageJ 1.42	Counting of photoreceptor neurons
GNU Image Manipulation Program (GIMP) 2.6	Image processing, compilation of figures
GraphPad® Prism™ 5	Statistical analysis
Olympus Cell A	Documentation of eye phenotypes
Olympus Cell F	Documentation of histological, immunohistochemical and cytochemical micrographs
Alliance UVItec 15.11	Documentation of Western blots and filter retardation assays
BioDoc Analyse 2.1	Quantification of Western blots and filter retardation assays
http://blast.ncbi.nlm.nih.gov/	Alignments for determination of gene orthologues between <i>Drosophila melanogaster</i> and <i>Homo sapiens</i>
http://www.ncbi.nlm.nih.gov/homologene	Identification of gene orthologues between <i>Drosophila melanogaster</i> and <i>Homo sapiens</i>
http://www.ihop-net.org/UniPub/iHOP/	Identification of gene orthologues between <i>Drosophila melanogaster</i> and <i>Homo sapiens</i>

4.2 Fly experiments

In this work, genes are generally set in italics, *Drosophila* genes are written in small letters in contrast to human orthologue genes which are written in capital letters. Gene names are phrased as the official short form or designation according to NCBI Gene database [269]. If not stated otherwise, candidate genes are referred to as the fly variant. Transgenes, fly genotypes and fly stocks are written in italics and as proposed by FlyBase nomenclature [270].

4.2.1 Transgenic flies and housing conditions

Fly stocks were maintained on standard cornmeal-agar-yeast-molasses-based food at 18 °C. Standard crossbreeding and other experiments with larvae and adult *Drosophila* were conducted on 25 °C. For adult-onset expression, GAL80-expressing flies were shifted from permissive temperature at 18 °C to restrictive temperature of 29 °C.

Table 5. Utilised *Drosophila melanogaster* strains.

Transgenic line	Genotype ¹	Source
Actin5C-GAL4	<i>y[1]w[*];P{w[+mC]=Act5C-GAL4}25F01/CyO,y[+]</i>	Bloomington #4414
CxD/TM3	<i>y[1],w[*];;CxD/TM3,Sb[1],Ser[1]</i>	Bloomington #6309
elav ^{C155} -GAL4	<i>P{w[+mW.hs]=GawB}elav[C155]</i>	Bloomington #458
elav-tub-GAL80	<i>P{w[+mW.hs]=GawB}elav[C155];P{w[+mC]=tubP-GAL80[ts]}20</i>	created by Malte Butzlaff (original GAL80 stock: Bloomington #7019)
FM7	<i>FM7a</i>	Bloomington #785
GMR-GAL4	<i>w[*];P{w[+mC]=GAL4-ninaE.GMR}12</i>	Bloomington #1104
Oregon-R-C	<i>wild type</i>	Bloomington #5
Rhodopsin-GAL4	<i>P{ry[+t7.2]=rh1-GAL4}3, ry[506]</i>	Bloomington #8691
sal/CyO	<i>salm[1],cn[1],bw[1]sp[1]/CyO</i>	Bloomington #3274
UAS-ATXN1 Q82	<i>y[1]w[118] P{[+]=UAS-SCA1.82Q}[F7]</i>	gift of Juan Botas [136]

UAS-eGFP	$w[*];P\{w[+]=UAS-eGFP\}\#4.2/CyO$	created by Aaron Voigt
UAS-Htt Exon1 Q93	$w[*];P\{w[+]=UAS-Q93ex1\}K6,9,15R$	gift of Lawrence Marsh [75]
UAS-lacZ	$P\{w[+mC]=UAS-lacZ.Exel\}2$	Bloomington #8529
UAS-SCA3-Q84	$w[*];;P\{w[+]=UAS-MJD-Q84\}7.2/TM3,Sb$	gift of Nancy Bonini [209]
UAS-SCA3tr-Q27	$w[*];;P\{w[+mC]=UAS-Hsap\MJD.tr-Q27\}N18.3d$	Bloomington #8149
UAS-SCA3tr-Q78	$w[*];P\{w[+mC]=UAS-Hsap\MJD.tr-Q78\}c.211.2$	Bloomington #8150
UAS-Tau[R406W]	$w[*];;P\{w[+mC]=UAS-hTau[R406W]\}$	gift of Mel Feany [271]

¹ genotype as suggested by Flybase [270].

RNAi fly strains comprising the human orthologue sublibrary were purchased from the Vienna *Drosophila* RNAi Centre (VDRC) [250] where they have been generated by random integration of shRNA-transcribing inverted repeats under *UAS-GAL4* control into the *Drosophila* genome (*UAS-shRNA*).

The 7,488 RNAi lines for the human orthologue sublibrary used in this study were selected by the VDRC considering known or predicted human orthologues to the fly genes (see **Appendix Table 3** for complete list).

4.2.2 Mating procedures

Mating procedures for the subsequent screens were essentially the same. Screening for eye changes by shRNA expression itself was conducted using the *GMR-GAL4* line as a control. *GMR-GAL4* and *UAS-SCA3tr-Q78* strains were recombined in order to generate the screening stock for the polyQ modifier screen (*GMR_SCA3tr-Q78*). For the screening of polyQ specificity of RNAi candidates, flies overexpressing the mutant *tau* transgene *UAS-Tau[R406W]* in the eye were utilised (*GMR_Tau[R406W]*). For screening purposes, stocks were crossbred with *UAS-shRNA* lines from the VDRC.

The random integrations of shRNA were located on chromosomes one, two and three. RNAi lines with integration on the first chromosome (X) have been generated utilising an artificial double X (dX) gonosome (male: XY; female: dXY) with combination of three X chromosomes (dXX) being lethal. Integrations are found on the single X

chromosome, leading to the restriction of the shRNA transgene to male carriers. Thus, male flies of the RNAi strains were generally crossbred to virgin female flies of the screening stocks and effects of the gene knockdown were assessed in female progeny.

Table 6. Stocks utilised for screening approaches.

Screening stock	Genotype
<i>GMR_GAL4</i>	$w[*]; P\{w[+mC]=GAL4-ninaE.GMR\}12$
<i>GMR_SCA3tr-Q78</i>	$y[*]w[*]; P\{w[+mC]=GAL4-ninaE.GMR\}12, P\{w[+]=UAS-MJD-trQ78\}Strong/CyO$
<i>GMR_Tau[R406W]</i>	$w[*]; P\{w[+mC]=GAL4-ninaE.GMR\}12/CyO; P\{w[+]=UAS-Tau[R406W]\}/TM3,Sb$

4.2.3 Evaluation of rough eye phenotype modification

For assessment of REP modulation, at least five female flies were analysed for changes in the severity of eye degeneration. Modifications by the induction of RNAi in polyQ and tau models were categorized as follows: “wild type-like phenotype (1)”, obvious REP suppression (2)”, “subtle REP suppression (3)”, “no change of REP (4)”, “subtle enhancement of REP (5)”, “obvious enhancement of REP (6)” and “lethal (7)”. For the *GMR-GAL4* screening only the “no change” and enhancement terms apply. RNAi lines exhibiting such effects in the *GMR-GAL4* control flies were excluded from subsequent experiments due to impact unconnected to expression of elongated polyQ. Designation of an RNAi line as polyQ modifier candidate required no change in control flies and an at least obvious enhancement/suppression of the REP in three independent experiments. Candidate lines were tested for polyQ specificity by rescreening with *Tau[R406W]* screening stock. RNAi lines exhibiting similar effects in both models were excluded from the polyQ candidate set and remainder strains were subjected to more detailed analysis.

Data on screen results were managed and stored making use of a databank generated with *MySQL* by Dr. Malte Butzlaff (Dept. of Neurology, Aachen).

4.2.4 Documentation of eye phenotypes

Drosophila compound eyes were pictured using an Olympus zoom stereo microscope (**Table 3**) at 6.3x magnification and Cell A software (Table 4). Eye documentation with scanning electron microscopy (SEM) was conducted on unfixated and uncoated flies utilising the ESEM scanning electron microscope (**Table 3**) in low vacuum mode (0.8-1.5 Torr) and an accelerating voltage of 10 kV. GIMP 2.6 and Adobe® Photoshop® CS4 software was used for rotating and cropping of images. All whole compound eye images compiled in this work feature dorsal-up and anterior-left orientation.

4.2.5 Dissection and staining of eye imaginal discs

Dissection of L3 *Drosophila* larvae was performed as described previously [272]. For staining with vital dye, preparation was conducted in *Drosophila's* Ringer solution (**Table 2**), otherwise PBS-T was used. For subsequent immunohistochemistry, isolated eye discs were subjected to fixation in 4 % paraformaldehyde (PFA) in PBS-T for 30 min, followed by several washing steps in PBS-T. Subsequent to blocking with 4 % normal goat serum (NGS), tissue was incubated with an antibody directed against the HA-tag of the truncated Ataxin-3 protein (mouse anti-HA, Covance) over night at 4 °C. Primary antibody was detected with an Alexa Fluor® 488-coupled secondary anti-mouse antibody. Tissue was mounted in DAPI-containing Vectashield mounting medium on glass slides and imaged afterwards using an Olympus BX51 fluorescence microscope equipped with 20x and 40x objectives.

For acridine orange staining, vital dye was dissolved in *Drosophila's* ringer solution to achieve a concentration of 1.6×10^{-6} M for dissection. Isolated eye discs were placed on a glass slide, fastened with a cover slide and immediately visualised using the same microscope properties as described for immunohistochemistry.

4.2.6 Longevity analysis

For evaluation of life span, male flies with the respective genotype were raised and selected at 18 °C (for adult-onset system with temperature-sensitive GAL80) or 25 °C and grouped into vials containing 20 flies maximum. Longevity experiments were conducted at

25 °C for normal UAS/GAL4 strains; lines containing GAL80 were shifted to the restrictive temperature of 29 °C for onset of transgene expression. Flies were transferred to fresh food twice a week and death events were counted at least every second day. A minimum of 20 flies per genotype were scored for every longevity assay. GraphPad Prism 5 was used for Kaplan-Meyer plotting and statistical analysis, featuring Log-Rank test for comparison of two longevity curves.

4.2.7 Protein collection from fly heads

The procedure was utilised for eye-specific and pan-neural transgene expressing strains alike. Flies were placed in reaction tubes and flash frozen in liquid nitrogen. Frozen flies were vortexed for separation of heads from bodies. Heads were transferred to vials containing radioimmunoprecipitation assay (RIPA) buffer (10 µL per head) and a small quantity of ceramic beads. The samples were homogenised with the SpeedMill P12 homogeniser (2x2 min, predefined programme for insect tissues). Subsequent to homogenisation, samples were centrifuged in order to pellet the beads and crude debris (13,300 rpm, 5 min, 4 °C), followed by collection of the supernatant and an additional centrifugation step (13,300 rpm, 5 min, 4 °C) for clearing. Protein concentration was measured using the Bio-Rad Dc Protein Assay Kit and the Tecan® multimodal microplate reader.

4.2.8 Immunoblotting

For Western blot analysis, protein samples were diluted in loading buffer (5x *Laemmli*) and boiled (95 °C, 5 min) before loading onto a polyacrylamide gel (10 %, 12 % or 4-12 % gradient gels) and subsequent SDS-PAGE (run at 100 V for 90 min with running buffer). Resolved proteins were transferred onto nitrocellulose membrane (225 mA per gel for 90 min with transfer buffer). The membranes were then blocked with skim milk (5 % in TBS-T for 60 min) followed by incubation with the primary antibody at 4 °C overnight (in 0.5 % skim milk in TBS-T, for antibody concentrations see **Table 7**).

Table 7. Antibodies utilised for *Drosophila* head and cell lysate immunoblotting and for immunohistochemical stainings.

Antibody	Species	Dilution	Manufacturer
primary antibodies			
anti-haemagglutinin	mouse monoclonal	1:500	Covance, USA
anti-polyglutamine	mouse monoclonal	1:1,000	Millipore, USA
anti-myc tag	mouse monoclonal	1:1,000	Millipore, USA
anti-GFP	mouse monoclonal	1:1,000	Roche, Germany
anti-TRMT2A	rabbit polyclonal	1:750	Sigma-Aldrich, USA
anti- β -tubulin	mouse monoclonal	1:500	DSHB, USA
anti-VDAC/porin	rabbit polyclonal	1:1,000	Abcam, UK
anti-syntaxin	mouse monoclonal	1:2,500	DSHB, USA
secondary antibodies			
ECL anti-mouse IgG, HRP-coupled	sheep	1:10,000	GE Healthcare, Germany
ECL anti-rabbit IgG, HRP-coupled	donkey	1:10,000	GE Healthcare, Germany
Alexa Fluor® 488 anti-mouse IgG (H+L)	goat	1:500	Invitrogen, Germany

After three washing steps of 5 min in TBS-T, membranes were probed with appropriate secondary antibodies for 60 min at room temperature. Following three additional washings in TBS-T, chemiluminescence signal was induced using Immun-Star™ ECL solution (Bio-Rad, Germany) as a HRP substrate and captured with Alliance LD4 documentation system (Biometra, Germany) and Alliance UVItc software. Band intensity was quantified utilising BioDoc Analyse software (Biometra, Germany).

4.2.9 Filter Retardation Assay

Filter retardation assays were mainly conducted as described previously [273-275]. Equal protein amounts (15 μ g) of RIPA fly head lysates were adjusted to 2 % SDS and 50 mM dithiothreitol followed by heating to 100 °C for 5 min. Using a dot blot filtration unit, the resulting solutions were filtered through a 0.2 μ m nitrocellulose membrane

(Whatman, UK)) previously equilibrated with 0.1 % SDS in TBS and afterwards washed in TBS-T. Membranes were further processed for immunodetection as described in section 4.2.8 by blocking and probing with primary (anti-HA, anti-GFP, anti-myc) and secondary antibodies followed by documentation.

For assessment of the aggregate load of the individual polyQ-shRNA-coexpressing fly lines, results of band intensity measurements were normalised to that of the polyQ control set as a hypothetical mean of 1.0 and calculated with One-sample t-test. If applicable, lysates from three independent crossbreeds were utilised.

4.2.10 Histological and immunohistochemical staining of paraffin sections

For paraffin sections, heads of female flies were fixated in 4 % paraformaldehyde/PBS-T for 60 min and subsequently subjected to dehydration in an ascending alcohol series (30 min in each: 70 %, 80 %, 90 %, 2x100 % ethanol). Fly heads were incubated in methyl benzoate for 60 min and three times in paraffin at 62 °C for 30 min each before embedding and hardening at room temperature overnight. Embedded fly heads were cut into 6 µm thick frontal sections with Feather C35 single-use blades using a Thermo Scientific microtome. For staining, sections were incubated in xylene for 20 min twice and rehydrated in an descending alcohol series (5 min in each: 2x100 %, 90 %, 80 %, 70 % ethanol) followed by rinsing in PBS.

For toluidine blue histological staining, sections were incubated for 5 min in 0.1 % toluidine blue solution with 2.5 % NaHCO₃, rinsed with deionised water and dehydrated in an ascending alcohol series (as described above), followed by dual incubation in xylene for 10 min each. Finally, sections were mounted with entellan and documented using an Olympus BX51 microscope and Cell F software.

For immunohistochemical staining, sections were subjected to heating in citrate buffer (**Table 2**) at 1000 W for 10 min in a microwave oven in order to demask protein epitopes. Afterwards, sections were washed in PBS for 5 min, blocked for 30 min with 4 % normal goat serum and probed with primary antibody in 4 % NGS/PBS for 3 h at 37 °C. Following washing in PBS for 5 min, sections were incubated with Alexa Fluor® 488-coupled anti-mouse secondary antibody (Invitrogen, see **Table 7**) for 60 min at room temperature. Rinsing in PBS was conducted prior to mounting of the sections in Vectashield® (Vector Laboratories, UK) mounting medium (with or without DAPI). For

documentation of the slides Cell F software and an Olympus BX51 microscope equipped with a fluorescence light source were utilised.

4.2.11 Immunohistochemical staining of cryo sections

For preparation of cryo sections, heads of female flies were fixated in 4 % paraformaldehyde/PBS-T overnight, followed by cryoprotection with 10 % sucrose for 12 h and 30 % sucrose overnight. Specimens were cut into 16 µm thick frontal sections using a Leica cryostat and stored at -20 °C.

For immunostaining, sections were rinsed for 5 min in PBS and immediately blocked with 4 % NGS/PBS, followed by primary antibody incubation (**Table 7**) in 4 % NGS/PBS for 3 h at 37 °C. Afterwards, sections were washed briefly in PBS and probed with Alexa Fluor® 488-coupled anti-mouse secondary antibody for 60 min at room temperature. Eventually, sections were washed in PBS and mounted in Vectashield® mounting medium. Visualisation was done with an Olympus BX51 microscope equipped with a fluorescent light source and Cell F software.

4.2.12 Semi-thin tangential sectioning of fly heads and photoreceptor quantification

For preparation of semi-thin sections for quantification of photoreceptor cells, fly heads of respective genotypes were fixated in 4 % PFA/PBS-T overnight. Subsequently, heads were dehydrated in an ascending alcohol series (30 min in each: 70 %, 80 %, 90 %, 2x100 %) and equilibrated in LR White embedding medium with LR White catalyst (Fluka, USA) for 3x1 h. Following this, LR White accelerator was added and resin left for hardening at room temperature for 24 h. After setting, specimens were roughly cut to size with razorblades and fine trimmed utilising glass blades. For 1 µm tangential sectioning of fly heads diamond blades and a Thermo Scientific microtome were employed. Tissue was stained with toluidine blue for 5 min and allowed to dry prior to mounting with Entellan®. Visualisation was done using an Olympus BX51 microscope and Cell F software.

For quantification, rhabdomeres as an indicator of photoreceptor (PR) neurons were counted in 50 ommatidia of n=3 individuals per genotype and presented as mean PR count ± standard error of the mean (SEM) per ommatidium. Two-tailed Mann-Whitney test was used to calculate the p-value when comparing the photoreceptor counts between two

groups. In experiments with three groups, Kruskal-Wallis test was performed followed by Dunn post-tests.

4.3 Cell culture experiments

4.3.1 Cell culture conditions and media

Human HEK293 cells were maintained in Dulbecco's modified Eagle's medium (DMEM, PAN Biotech, Germany) supplemented with 10 % fetal calf serum (FCS, Biochrom AG, Germany), 100 units/mL penicillin and 100 mg/mL streptomycin (both Biochrom AG, Germany), in a humidified atmosphere of 5 % CO₂/95 % air at 37 °C (Thermo Scientific HERACell 150i incubator). For selection of stably transduced cells with shRNA, 0.5 µg/mL puromycin (Invitrogen, Germany) was added.

4.3.2 Generation of stable shRNA-expressing cells

Silencing of *TRMT2A* expression in HEK293 cells was accomplished by infection of cells with lentiviral transduction particles carrying an inverted repeat sequence in a lentiviral plasmid vector (*pLKO.1-puro*). The sequence is integrated into the host cell DNA and shRNA directed against the *TRMT2A* mRNA is expressed under the control of a human phosphoglycerate kinase eukaryotic promoter. Commercially available transduction particles were all purchased from Sigma-Aldrich (as listed in **Table 8**). shRNA transduction particles having no known human target sequence were used as a negative control of expression knockdown, activating the RNAi machinery of the cell without affecting the expression of any gene.

Table 8. Lentiviral clones and non-target strain utilised for *TRMT2A* silencing experiments in HEK293 cells.

Lentiviral clone ID	Sequence
MISSION® shRNA Lentiviral Transduction Particles	
NM_182984.2-856s1c1	CCGGGCAGACTGAGTATCGTAATAACTC- GAGTTATTACGATACTCAGTCTGCTTTTTTG
NM_182984.2-1574s1c1	CCGGCAGGACAATGAGTTGAGTAATCTC- GAGATTACTCAACTCATTGTCCTGTTTTTG

NM_182984.2-736s1c1	CCGGGCAGAACTTGCCAAGGAAATCTC- GAGATTTTCCTTGGCAAGTTTCTGCTTTTTTG
NM_182984.2-1985s1c1	CCGGCCAGATAACACCCTACAAGAACTC- GAGTTCTTGTAGGGTGTATCTGGTTTTTTG
NM_182984.2-1505s1c1	CCGGCGGAAGGTAAGAGGGTCATTCTC- GAGAATGACCCTCTTTACCTTCCGTTTTTTG

MISSION® Non-Target shRNA Control Transduction Particles

SHC002V (Product No.)	CCGGCAACAAGATGAAGAGCACCAACTC- GAGTTGGTGTCTTCATCTTGTTGTTTTT
-----------------------	---

Transfection of HEK293 cells with lentiviral transduction particles was completed following manufacturer's instructions by Daniela Otten (Department of Biochemistry, University Medical Centre Aachen). Multiplicities of infection (MOI) of 2, 5, 10 and 15 were utilised. Puromycin-resistant colonies were selected and cultured further, decrease of TRMT2A protein levels due to gene silencing was assessed by Western blot analysis.

4.3.3 Plasmid transfection

Transfection of plasmids into HEK293 cells was accomplished using Metafectene® (Biontex, Germany) following manufacturer's instructions. Cells were seeded on poly-L-lysine (PLL)-coated plates (35,000 cells/cm²) and then transfected 48 h before experimentation. Cells and expression of GFP-tagged constructs were visualised with an Olympus inverse cell culture microscope equipped with a fluorescence light source.

4.3.4 Protein collection from cell culture and immunoblotting

Plated cells were washed in ice cold PBS and then lysed in RIPA buffer under agitation for 30 min at 4 °C. Samples were centrifuged for 15 min at 13,300 rpm at 4 °C and supernatants were collected. Protein concentrations were measured using the Bio-Rad Dc Protein Assay and Tecan® multimode microplate reader. Western blotting was then performed as outlined in chapter 4.2.8.

4.3.5 Cytochemistry

Cells were plated on laminin (mouse, Sigma, Germany)-coated glass slips. 48 hours after transfection with GFP-coupled *huntingtin* transgene plasmids, cells were washed once in PBS and fixed in 4 % PFA for 30 min at RT. After three washes in PBS, cells were incubated with Alexa Fluor® 568-coupled phalloidin (Invitrogen, Germany; 1:500 in PBS-T) for 20 min at room temperature. Subsequently, cells were washed three times in PBS and nuclei were counterstained by briefly rinsing the cells in DAPI solution (2 µg/mL). Cells were again washed thrice in PBS before being mounted on glass slides using Fluoromount-G™ (Southern Biotech, USA). GFP-positive cells and thereof inclusion-positive cells were counted and statistics were calculated with unpaired t-test using GraphPad Prism 5.

5 Results

5.1 Characterisation of a SCA3 fly model for the modifier screen

We intended to conduct an RNAi screen to identify genetic modifiers of polyQ-induced neurotoxicity in *Drosophila*. In order to achieve this goal, a screening stock was generated by recombination of a truncated version of the human SCA3 causative gene *ATXN3* ($P\{w[+mC]=UAS-Hsap\MJD.tr-Q78\}$) [219] (from now on termed *SCA3tr-Q78*) with the GMR-GAL4 ($w[*];P\{w[+mC]=GAL4-ninaE.GMR\}12$) driver. The resulting fly line with $w[*];P\{w[+mC]=GAL4-ninaE.GMR\}12, P\{w[+mC]=UAS-Hsap\MJD.tr-Q78\}/CyO$ (referred to as *GMR_SCA3tr-Q78* in the text) was used for screening. This disease transgene codes for a carboxy-terminal fragment of the Ataxin-3 protein comprised of 12 Ataxin-3 amino acids together with a haemagglutinin (HA) tag upstream of the polyQ tract with 78 repeats. The polyQ tract is flanked downstream by the residual 43 amino acids of the protein isoform 1a. For comparison with different polyQ settings, a similar transgenic fly line expressing truncated Ataxin-3 with a normal polyQ tract of 27 repeats ($P\{w[+mC]=UAS-Hsap\MJD.tr-Q27\}$) and a full length *ATXN3* fly line with 84 glutamines ($P\{w[+mC]=UAS-SCA3.fl-Q84.myc\}$) [209] were utilised.

Additionally, a fly line expressing a mutated form of human microtubule-associated protein tau gene, *Tau[R406W]* ($P\{w[+mC]=UAS-hTau[R406W]\}$) [271] was employed. By means of this unrelated disease model for frontotemporal dementia (FTD) the specificity of the obtained modifiers for polyQ-induced neurotoxicity was tested.

5.1.1 Phenotypes of the disease model flies

In order to assess polyQ-induced neurotoxicity and the modulation thereof, the rough eye phenotype of *GMR_SCA3tr-Q78* was used as readout. The REP reflects the demise of photoreceptor neurons [219] induced by expression of the toxic gene product in postmitotic cells of the *Drosophila* compound eye [252]. The driver line itself served as a reference phenotype throughout the screen (**Figure 6B**) instead of a wild type fly (**Figure 6A**) with which RNAi effects alone could not be analysed. Overexpression of a non-toxic *lacZ* transgene (coding for β galactosidase, $P\{w[+mC]=UAS-lacZ.Exel\}2$) did not show vast

changes compared to the control phenotype (**Figure 6C**). Both featured a subtly roughened eye phenotype at 25 °C, temperature increase to 29 °C intensified the severity of the *GMR-GAL4* phenotype (not shown). Neither expression of the normal length truncated Ataxin-3, *SCA3tr-Q27* (Figure 6D) nor of the full-length *SCA-Q84* (**Figure 6F**) resulted in an overt REP although *SCA3-Q84* eyes were slightly roughened, comparable to *lacZ* phenotype. GMR-mediated targeting of *SCA3tr-Q78* expression to the eye however led to a severe degenerative eye phenotype as described previously [219] (**Figure 6H**). Pigmentation of the compound eye is greatly reduced with only minor retention of colour at the rims. Additionally, the surface texture is disturbed with disarranged sensory bristles and occasionally appearing necrotic spots and dints, hinting to degeneration of underlying eye structures. Nevertheless, eye size itself appears unaffected by the otherwise detrimental consequences of polyQ expression. Finally, overexpression of the *Tau[R406W]* transgene resulted in a heavy REP presenting with deranged surface and overall shrinkage of the eye, yet eye colour is retained (**see Appendix Figure 1**). The eye morphology of SCA3 flies visible with light microscopy is also reflected in scanning electron micrographs. Whereas the surfaces of *SCAtr-Q27* and full length *SCA3-Q84* fly eyes appear regular and exhibit no predominant deterioration, the eyes of *SCA3tr-Q78* flies are severely compromised in structure and shape. The eye is collapsed and features disordered sensory bristles in conjunction with a disorganised ommatidial pattern. Overall collapse of the compound eye may be caused by loss of underlying retinal tissue due to SCA3-induced degeneration, a process obviously not taking place in the other two SCA3 models, at least not to the same extent.

For investigations of neurodegenerative diseases like SCA3 in flies, it would be reasonable to evaluate the effect of *SCA3tr-Q78* overexpression in photoreceptor neurons, but also in other neuron populations or the entire nervous system. However, pan-neural expression of the *SCA3tr-Q78* transgene results in pupal lethality and yielded no viable progeny, neither did ubiquitous Ataxin-3 production, confirming previous reports [219].

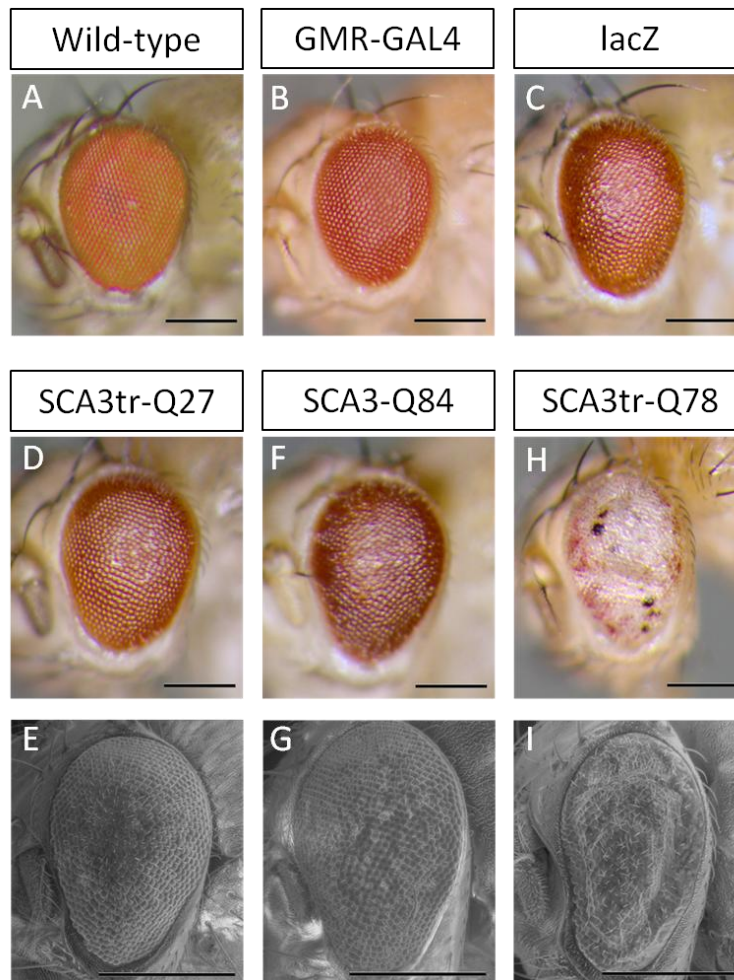


Figure 6. Phenotypes induced by GMR-mediated expression of different transgenes.

Compound eye phenotypes of wild type (A) and control flies (B, C) in comparison to flies bearing neurodegenerative disease-associated transgenes (D-I). In contrast to wild type eyes (A), control *GMR-GAL4* flies exhibit a subtly roughened eye surface (B) slightly worsened by expression of a *lacZ* control transgene (C). Expression of normal length truncated SCA3 (D) and full-length elongated SCA3 (F) transgenes induces mildly roughened eye phenotypes whereas induction of a truncated disease gene results in a heavy REP with deteriorated surface and texture of the compound eye featuring dints and necrotic spots (H). Scanning electron micrographs underpin the light microscopy findings, displaying subtle surface changes for *SCA3tr-Q27* (E) and *SCA3-Q84* (G) and showing seriously compromised eye morphology in *SCA3tr-Q78* flies (I).

Orientation of images is dorsal-up and anterior-left, all scale bars apply to 200 μ m respectively.

5.1.2 Assessment of *SCA3tr-Q78* protein expression and effects in the eye

Expression of neurotoxic truncated Ataxin-3 protein is reflected in the demise of postmitotic cells of the eye and the resulting rough eye phenotype. Detection of monomeric polyQ protein in adult flies with biochemical methods like Western blot proved to be rather complicated (compare [276], **Figure 7A**) since detectable protein amounts were very low (molecular mass \sim 32 kDa). SDS-insoluble aggregates resided in the stacking gel of polyacrylamide gels. Higher molecular strong bands were visible between 50 and 75 kDa,

presumptively representing dimers of truncated Ataxin-3 (**Figure 7A**). Protein levels reached a peak shortly after hatching, decreasing drastically at seven days post eclosion (dpe) and being hardly detectable at 12 dpe. Since there is no *ATXN3* fly orthologue, levels of transgene expression levels could not be compared to endogenous protein levels. The presence of SDS-insoluble truncated Ataxin-3 aggregates could also be detected in freshly hatched flies by filter retardation assay. The aggregate load in head lysates of SCA3 flies was constant on a high level throughout a period of 12 days post eclosion (**Figure 7B**).

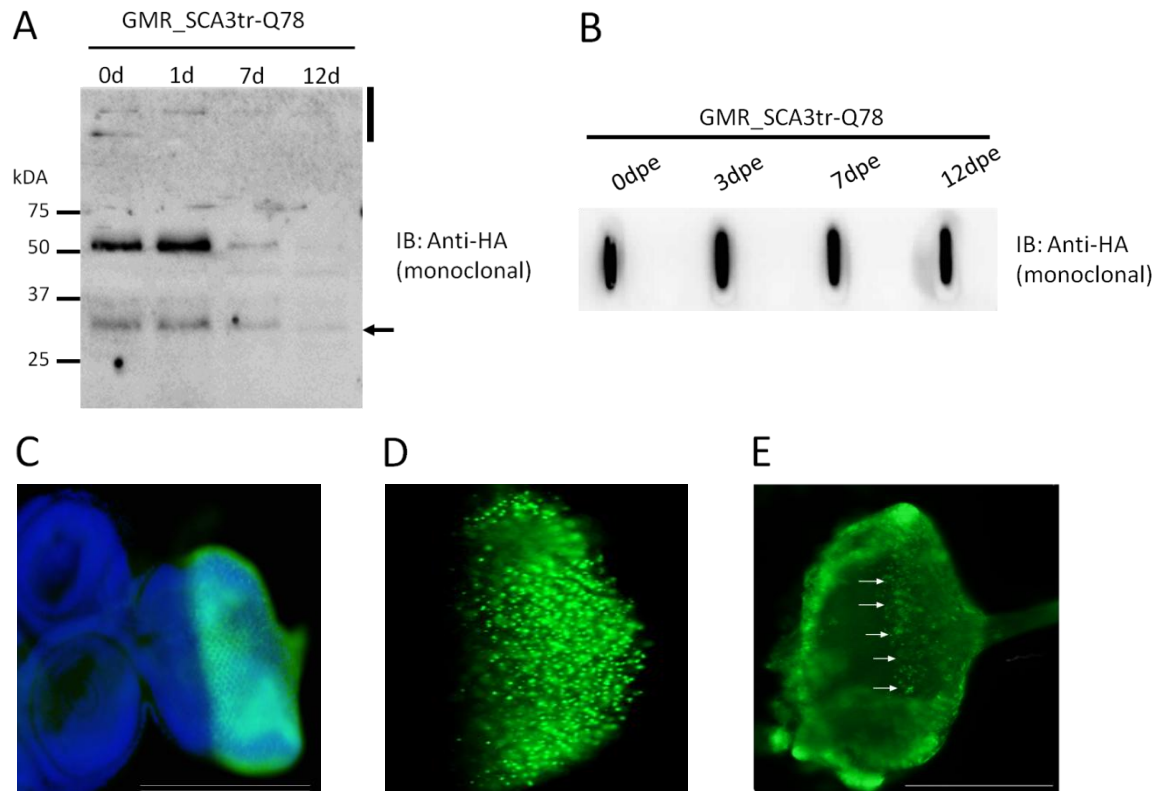


Figure 7. Biochemical detection of SCA3tr-Q78 protein levels and aggregation together with verification of SCA3tr-Q78 expression, aggregation and induced cell death in larval imaginal discs.

(A) Immunoblot for SCA3tr-Q78 protein levels in flies of different age, showing weak protein signal at ~32 kDa (arrow) and higher molecular strong signals above 50 kDa just after and one day post eclosion. Aggregated protein traces are retained in the stacking gel (bar). Protein levels at 7 dpe and 12 dpe are hardly detectable. **(B)** Filter retardation assay of SCA3 fly head lysates exhibits strong constant signal for SDS-insoluble Ataxin-3 aggregates already present at eclosion time. **(C)** Detection of HA-tagged truncated Ataxin-3 in the L3 larval imaginal disc posterior (right) of the morphogenetic furrow. **(D)** Truncated Ataxin-3 forms aggregates in the eye discs of *SCA3tr-Q78* L3 larvae. **(E)** Cell death in *SCA3tr-Q78* larval eye discs detected by acridine orange staining is correlated to the expression of truncated Ataxin-3 (arrows mark morphogenetic furrow and border of cell death).

Genotype of *SCA3tr-Q78* flies used: *w; GMR-GAL4/UAS-SCA3tr-Q78*

Orientation is anterior-left. Blue in **(C)**, nuclei stained with DAPI; green in **(C)** and **(D)**, SCA3tr-Q78 stained with mouse anti-HA antibody; green in **(E)**, acridine orange. Scale bars in **(C)** and **(E)** apply to 100 μ m respectively.

Expression of the *glass* multiple reporter (GMR) is initiated with the progression of the morphogenetic furrow (MF) in a presumptive eye structure, the larval imaginal eye disc, after 12 h of larval third instar (L3) [252]. The MF demarcates the border between yet uncommitted cells anterior and postmitotic neuronal progenitor cells posterior to the MF [277, 278]. Concomitantly with onset of GMR expression and thereby GAL4 activation, induction of *SCA3tr-Q78* via its UAS sequence takes place. This leads to first nuclear inclusions detectable at mid-third instar and morphological defects three days later in early pupal stages [219]. Consequently, expression of expanded polyQ protein can be discerned with antibodies directed against the HA tag in eye discs of *SCA3tr-Q78* L3 larvae (**Figure 7C**). *SCA3* fly eye discs also exhibit protein aggregation and inclusions in targeted cells as already shown previously [219] (**Figure 7D**).

Ataxin-3 with an expanded polyQ stretch has been described to induce apoptotic cell death [213, 279, 280]. In order to detect dying cells during eye morphogenesis, the fluorescent vital dye acridine orange (AO) was utilised. The compound crosses the cellular plasma membrane and intercalates into the DNA, emitting a bright green to orange signal of the nucleus with condensed chromatin in apoptotic cells. By these means cell death in larval eye discs of polyQ flies could be detected (**Figure 7E**) [281] and is co-localised with the expression of truncated Ataxin-3. Thus, the basis of the observed rough eye phenotype of the adult polyQ flies already at hatching can be traced back to the expression of toxic truncated Ataxin-3 and its aggregation in nuclear inclusions already at larval stages.

Production of the truncated *ATXN3* gene product continues at pupal stages and in adult flies, resulting in a REP. Frontal fly head sections reveal greatly disturbed eye morphology with degenerated retinal structures and heavy cell loss (**Figure 8E**) compared to highly ordered, intact retinal structure in GMR control (**Figure 8A**). LacZ-expressing flies (**Figure 8C**) reveal slightly thinner retinae, but predominantly retained morphology.

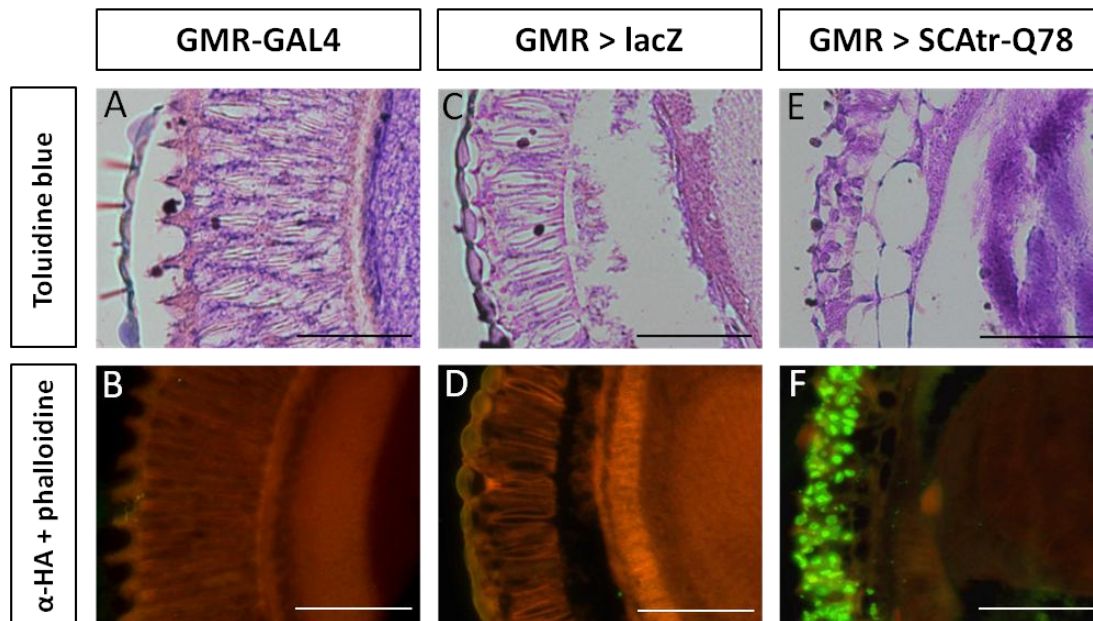


Figure 8. Histological and immunohistochemical analysis of utilised fly models.

(A) Frontal sections of GMR control fly heads stained with toluidine blue exhibit ordered dense retinal structure and (B) prove negative for expression of HA-tagged truncated Ataxin-3. (C) Retina of lacZ-expressing flies is reduced in thickness and less dense than that of control flies, however, it shows regular patterning of profound eye structures (detachment of the retina from underlying tissue is a sectioning artefact). (D) LacZ fly head sections are negative for Ataxin-3 staining. (E) Frontal sections of *GMR_SCA3tr-Q78* fly heads reveal severely degenerated retina and deeper eye structures with merely no retained structured tissue. (F) Remaining cells feature heavy HA-positive Ataxin-3 inclusions.

All pictures represent central parts of the fly retina. Red in (B, D, F), F-actin stained with Alexa Fluor 568-coupled phalloidin; green in (F), SCA3tr-Q78 stained with mouse anti-HA antibody. All scale bars apply to 50 μm respectively.

Immunohistochemistry approaches exhibit strong staining for HA-tagged polyQ protein and marked aggregates in remainder of GMR-polyQ fly retinae (Figure 8F) which are neither found in *GMR-GAL4* controls (Figure 8B) nor in flies expressing non-toxic lacZ (Figure 8D).

5.1.3 Evaluation of photoreceptor integrity

In an attempt to quantify polyQ-induced neurodegeneration of the rough eye we intended to count photoreceptor (PR) neurons, a direct target of toxic protein expression by *GMR-GAL4*, and assess the changes in their stereotypic distribution pattern. In control eyes, there is a trapezoid pattern of seven out of eight photoreceptors visible for each ommatidium. The seventh and eighth PRs are located on top of each other and thus cannot be visualised separately. Neurodegeneration as a consequence of polyQ toxicity is destined to diminish photoreceptor count. Semi-thin sagittal sectioning of the eye was used for evaluation of photoreceptor integrity after histological staining.

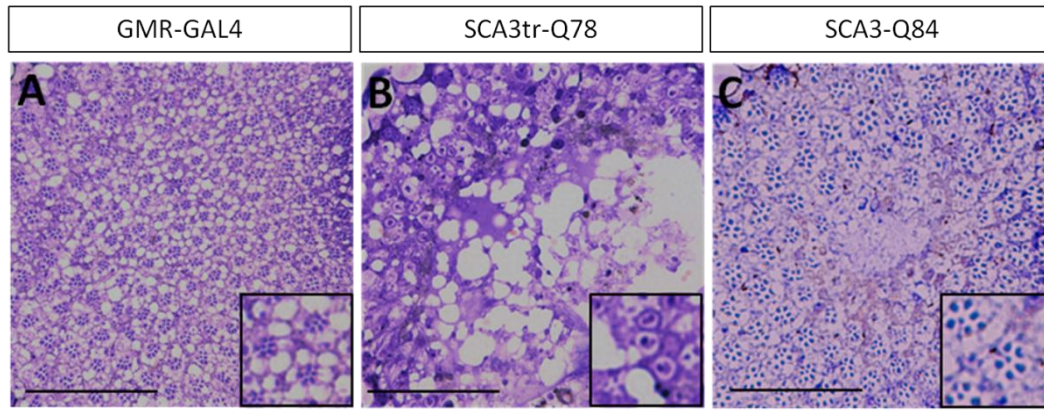


Figure 9. Photoreceptors in semi-thin sections of SCA3 disease models.

(A) Photoreceptors of control flies appear in an ordered fashion with a regular rhabdomere count of seven. **(B)** Truncated SCA3 gene expression results in severely degenerated eye tissue with hardly any PR neurons left and vast cell-free areas. **(C)** In flies with full-length expanded SCA3 expression, ommatidial structure and PR count is predominantly retained as in the control with slight loosening up of overall tissue structure. *GMR-GAL4* driver **(A)** was used to activate expression **(B, C)** and driver-only served as control. Insets show detailed a view of semi-thin sections of compound eyes. All scale bars apply to 50 μm .

Counting of photoreceptors in the *GMR-GAL4* control flies resulted in an if at all slightly reduced number of visible neurons, mainly probably due to mild GAL4 toxicity. However, photoreceptors with toxic elongated polyQ expression exhibit severe neuronal loss and eyes present with overt lack of ommatidia themselves. In contrast to the truncated protein, full-length Ataxin-3 with 84 glutamines exhibited no decrease in rhabdomere number compared to the GMR control. Only the strict trapezoid pattern of the photoreceptor neurons was distorted to some degree. Concluding from this one can say that the exterior rough eye phenotype of disease flies indeed has its origin in the degeneration of photoreceptor neurons in the single ommatidia of the compound eye.

5.2 Modifier screen for polyQ-induced neurotoxicity

In order to conduct an RNAi-based screen for modifiers of polyQ-induced neurotoxicity, a subset of RNAi fly lines from the Vienna *Drosophila* RNAi Centre (VDRC) was obtained, comprised of 7,488 lines corresponding to 6,930 different genes. To our knowledge this represents the largest number of genes investigated in a modifier screen in *Drosophila* so far. The RNAi lines were chosen by the VDRC as silencing fly orthologues to human genes (termed human orthologue RNAi sublibrary). These RNAi library strains were subjected to consecutive steps of screening to reveal genetic interactors of truncated

Ataxin-3 protein in the course of SCA3 pathogenesis modelled in *Drosophila* eyes (summarised in Figure 10).

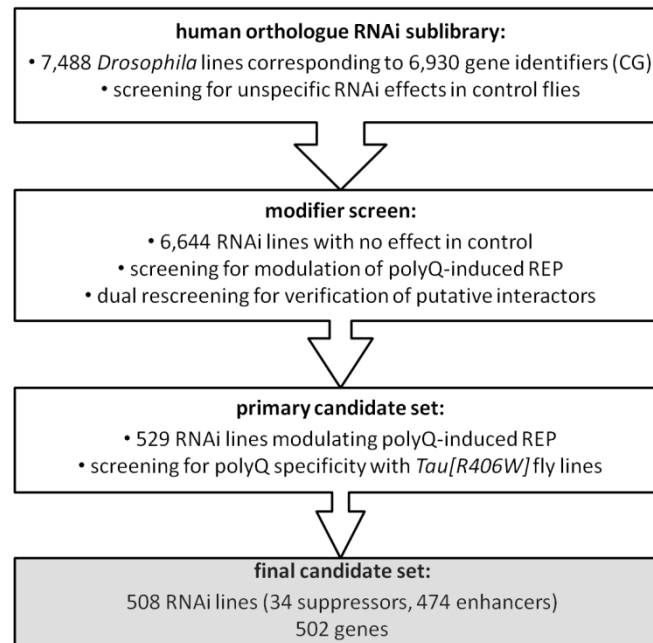


Figure 10. Flow chart of the implemented screen to identify modifiers of SCA3-induced toxicity including subsequent analysis of primary screen candidates.

The screening process is depicted, including the results of each consecutive screening step explained in chapter 5.2.

5.2.1 Screen for unspecific RNAi effects in control flies

To exclude RNAi lines from subsequent screening that *per se* induce a change of external eye structures, the complete RNAi sublibrary was crossbred with the *GMR-GAL4* driver line. RNAi lines subtly or obviously worsening the eye appearance of the *GMR-GAL4* line in the F1 generation were not considered for screening as gene silencing in this case apparently has deleterious effects apart from expression of a toxic protein. According to this paradigm, 844 RNAi lines were excluded from further investigation due to their modification in control (**Figures 9, 11**).

5.2.2 Primary screen for polyglutamine modifiers

Subsequent to exclusion of effectors in control flies, the primary screen was conducted by crossbreeding the remaining 6,644 RNAi lines with the *GMR_SCA3tr-Q78* flies. As a result, F1 flies co-expressed truncated Ataxin-3 with 78 polyglutamine repeats and the respective shRNA. Modification of REP was assessed in the F1 generation with respect to

change of severity of degeneration, pigmentation and overall eye morphology. Potential candidates exhibiting a modulation of REP after the primary screening were subjected to dual rescreening for verification. Out of all lines investigated, 6,115 did not show any change in polyQ-induced rough eye phenotype and were therefore not considered as candidates. 529 RNAi lines exhibited an overt change of the polyQ-induced REP, as obvious suppression or enhancement was observed. In case *SCA3tr-Q78* expression in combination with gene silencing yielded no viable offspring, this was considered as a lethal enhancement (**Figure 11**). It is reasonable to assume that alterations of the REP in either direction reflect amelioration or increment of Ataxin-3-induced toxicity.

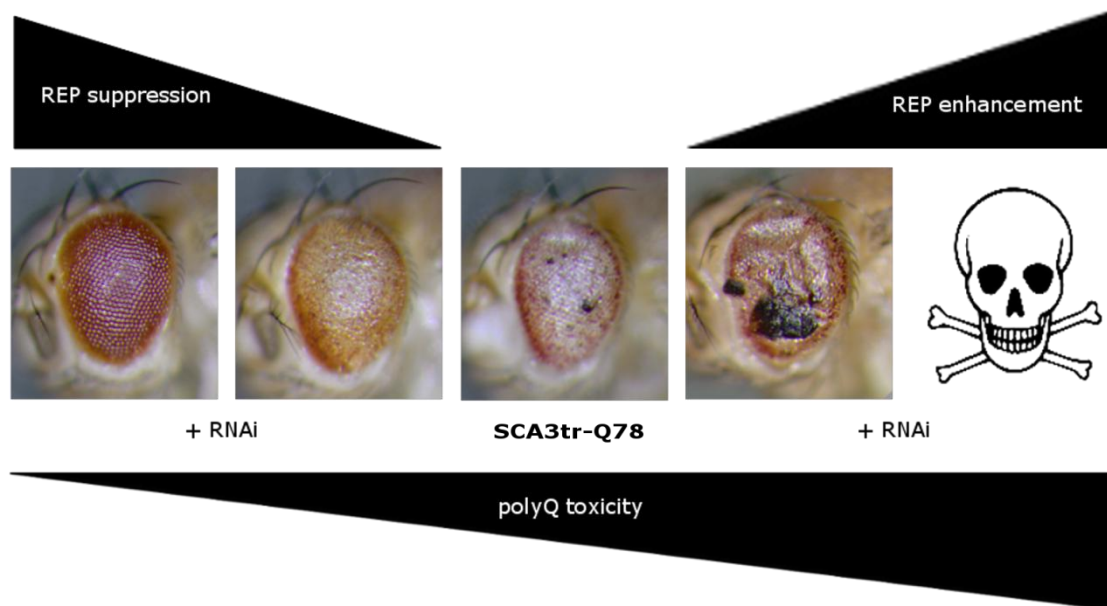


Figure 11. Modification of the *SCA3tr-Q78*-induced phenotype by enhancing and suppressing candidate RNAi lines.

Only obvious alteration of the *SCA3* REP in either direction was considered. It was assumed that modification of the screen REP by knockdown of a candidate gene reflects amelioration or increase in polyQ toxicity in affected cells respectively.

Expression of 36 shRNAs in *SCA3* flies led to a suppression of the phenotype in F1 generation (obvious amelioration of REP or WT-like eye), but the overwhelming majority of modifiers were enhancers with 493 RNAi lines leading to an obviously worsened phenotype or no offspring at all. Knockdown of 457 genes out of these 483 enhancing candidates lead to a lethal outcome after crossbreeding with *SCA3tr-Q78* flies (complete list of modifier RNAi lines in **Appendix Table 1**). Naturally it was not possible to analyse these candidates morphologically in further detail and focus was put on the other candidates, especially on the suppressors (modifier RNAi lines with viable progeny listed in **Table 9**).

In one suppressor case, silencing of the same gene (*Hsc70-4*) by two different RNAi lines (transformant IDs 26465 and 50222) yielded suppression of REP for both strains.

RNAi lines modifying SCA3tr-Q78-induced REP and having viable progeny (**Table 9**) were categorised according to their GO term (process) as proposed by the Gene Ontology Annotation Database [282]. Categories and respective number of modifier lines are as follows: protein folding and stress response (7), transcription/chromatin modification (7), nucleic acid metabolism (9), transport and secretion (4), signalling (6), lipid metabolism (4), ubiquitin- and proteasome-related pathways (4), development, differentiation and cell death (9), miscellaneous (15) and unknown function (7) (**Table 9, Figure 12**). Lethal candidate lines were not categorised, yet selected candidates were utilised for computational analysis (data not shown) and are discussed in chapter 6.

Apart from the primary candidates utilised for further analysis, a total of 1,002 RNAi lines resulted in subtle modification of the REP, 217 of them subtle suppressors and 785 subtle enhancers. This group was not investigated beyond this point due to unclear origin of the modification and possible interindividual differences in the eye phenotypes. However, subtle candidates might prove helpful for computational analysis.

Table 9. List of candidates with viable progeny modifying Ataxin-3-induced REP in *Drosophila*.

Transformant ID ¹	<i>Drosophila</i> gene ²	Human orthologue ³	Process ⁴	Δ SCA3 REP ⁵
Protein folding and stress response				
26465	<i>Hsc70-4</i>	<i>HSPA1L</i>	Stress and unfolded protein response	S
50222	<i>Hsc70-4</i>	<i>HSPA1L</i>	Stress and unfolded protein response	S
23637	<i>Droj-2</i>	<i>DNAJA4</i>	Protein folding	S
45596	<i>Hsc70-1</i>	<i>HSPA8</i>	Stress response	S
41696	<i>Hop</i>	<i>STIP1</i>	Stress response	S
33581	<i>CG2887</i>	<i>DNAJB1P1</i>	Protein folding (D)	E
48692	<i>Hsf</i>	<i>LOC644383</i>	Response to heat (D),	E
Transcription/Chromatin modification				
11219	<i>RpII15</i>	<i>POLR2I</i>	Transcription	S
3780	<i>dve-s</i>	<i>GBX1</i>	Transcription regulaton	S
41530	<i>Brd8</i>	<i>BRD8</i>	Transcription regulation	S

6282	<i>EloA</i>	<i>TCEB3</i>	Transcription regulation	S
43802	<i>MRG15</i>	<i>MORF4L1</i>	Transcription regulation	S
28386	<i>salr</i>	<i>SALL1</i>	Transcription regulation	E
5684	<i>chm</i>	<i>KAT7</i>	Chromatin modification	E
Nucleic acid metabolism				
34713	<i>CG3808</i>	<i>TRMT2A</i>	RNA processing	S
26475	<i>CG4266</i>	<i>SCAF8</i>	RNA splicing	S
43870	<i>DNApol-α50</i>	<i>PRIM1</i>	DNA replication	S
36025	<i>tsu</i>	<i>RBM8A</i>	RNA metabolism	E
31777	<i>CG13298</i>	<i>SF3B14</i>	RNA splicing	E
23659	<i>Smg5</i>	<i>SMG5</i>	RNA metabolism	E
24725	<i>CG3225</i>	<i>DHX35</i>	RNA splicing	E
24070	<i>CG9601</i>	<i>PNKP</i>	DNA damage response	E
10942	<i>Gnf1</i>	<i>RFC1</i>	DNA replication and repair	E
Transport and secretion				
33262	<i>CG5687</i>	<i>SLC5A8</i>	Ion transport	S
20536	<i>CCS</i>	<i>CCS</i>	Metal ion transport	E
20183	<i>Cha</i>	<i>CHAT</i>	Neurotransmitter secretion	E
8620	<i>CG4288</i>	<i>SLC17A5</i>	Transmembrane transport	E
Signalling				
8780	<i>CG17048</i>	<i>RASGRP1</i>	Ras protein signal transduction	S
25030	<i>5PtaseI</i>	<i>INPP5A</i>	Cell communication	S
31257	<i>Gbeta13F</i>	<i>GNB1</i>	G protein coupled ACh receptor signalling pathway	S
1326	<i>AR-2</i>	<i>KISS1R</i>	G protein-coupled receptor signalling pathway	E
36153	<i>CG34372</i>	<i>DEF6</i>	G-protein coupled receptor signalling pathway (D)	E
32370	<i>stai</i>	<i>ODZ3</i>	Signal transduction	E
Lipid metabolism				
8070	<i>bwa</i>	<i>ACER2</i>	Lipid metabolism	S
30186	<i>CG15534</i>	<i>SMPD1</i>	Sphingomyelin catabolic process	E
42798	<i>Dnz1</i>	<i>ZDHHC3</i>	Protein palmitoylation	E
10020	<i>Spt-I</i>	<i>SPTLC1</i>	Sphingolipid biosynthesis	E

Ubiquitin- and proteasome-related pathways

37221	<i>CG9153</i>	<i>HERC4</i>	Protein ubiquitination	S
24030	<i>Trbd</i>	<i>ZRANB1</i>	Protein deubiquitination	S
43606	<i>CG6758</i>	<i>FBXO42</i>	Protein ubiquitination	S
37930	<i>CG14619</i>	-	Protein deubiquitination (D)	S

Development, differentiation and cell death

23121	<i>LanB1</i>	<i>LAMB2</i>	Cell morphogenesis	S
16040	<i>Hrb27C</i>	<i>DAZAP1</i>	Differentiation	S
35147	<i>l(3)neo38</i>	<i>ZNF541</i>	Cell differentiation	E
47569	<i>CG12935</i>	<i>TMEM223</i>	Nervous system development (D)	E
21293	<i>CG31048</i>	<i>DOCK3</i>	Axonal outgrowth	E
19450	<i>CG15399</i>	<i>CHODL</i>	Muscle organ development	E
41960	<i>Exn</i>	<i>NGEF</i>	Apoptosis	E
33837	<i>Pkcdelta</i>	<i>PRKCD</i>	Apoptosis	E
13005	<i>Dab</i>	-	Differentiation/Neurogenesis (D)	S

Miscellaneous

7903	<i>ppk14</i>	<i>TREM2</i>	Axonal guidance	S
17196	<i>DCX-EMAP</i>	<i>CYP2E1</i>	Steroid metabolic process	S
16182	<i>aux</i>	<i>GAK</i>	Cell cycle	S
8408	<i>Cad88C</i>	<i>CDH7</i>	Cell-cell adhesion	S
44362	<i>slmo</i>	<i>SLMO2</i>	Spermatogenesis (D)	S
19066	<i>Doa</i>	<i>CLK2</i>	Protein phosphorylation	S
22590	<i>timeout</i>	<i>TIMELESS</i>	Mitosis	E
24885	<i>DAAM</i>	<i>DAAM2</i>	Actin cytoskeleton organization	E
40478	<i>Marf</i>	<i>MFN2</i>	Mitochondrial fusion	E
44114	<i>CG11722</i>	<i>NDUFAF4</i>	Mitochondrial respiratory chain complex I assembly	E
48062	<i>CG1695</i>	<i>SGSM1</i>	Regulation of Rab GTPase activity	E
22454	<i>CG6873</i>	<i>ADAM12</i>	Cell adhesion	E
30717	<i>CG33128</i>	<i>REN</i>	Proteolysis	E
36572	<i>Sbp2</i>	<i>SECISBP2</i>	Translation	E
15789	<i>Mal-A1</i>	-	Carbohydrate metabolic process (D)	S

Unknown function

46473	<i>CG17919</i>	<i>LOC647307</i>	-	S
23843	<i>roq</i>	<i>RC3H2</i>	-	S
40006	<i>CG15618</i>	<i>THADA</i>	-	S
40044	<i>CG16890</i>	<i>FRA10AC1</i>	-	S
43612	<i>CG14966</i>	<i>C15orf40</i>	-	E
29711	<i>CG6115</i>	<i>LOC493754</i>	-	E
49792	<i>CG3678</i>	<i>TTC35</i>	-	E

¹ As indicated by VDRC.

² *Drosophila* gene as listed in Gene Database of NCBI [3].

³ Human orthologue according to HomoloGene Database [283] or obtained from BLAST analysis [284]. Symbol as listed in Gene Database of NCBI [3].

⁴ Referred to as biological process of the human orthologue gene according to GO term listed in Gene Ontology Annotation Database [282], otherwise marked with D for predicted process of *Drosophila* gene.

⁵ Modification of SCA3tr-Q78-induced REP after GMR-GAL4-mediated expression of shRNA.

S, Suppression; E, Enhancement (both in case of RNAi of respective gene)

5.2.3 Specificity of RNAi effects for SCA3tr-Q78-induced neurotoxicity

In order to narrow down the candidates found in the primary screen to those modulating specifically SCA3tr-Q78 neurotoxicity without affecting other disease proteins, RNAi silencing of modifier genes was induced in flies expressing *Tau[R406W]*. By comparing the polyQ screen data with results from this verification experiment with an unrelated pathogenesis model, target genes that exclusively act on polyglutamine-induced effects should be identified. Only 4 % (21 lines) of the RNAi candidates displayed a similar modification of the *Tau[R406W]*-induced REP (two suppressors, 19 enhancers). These candidates were not considered specific for polyglutamine, nevertheless they are included in the set of Ataxin-3 action modifiers. Two RNAi lines (with shRNA against *Drosophila* genes *aux* and *CG3808*) were found to modulate *Tau[R406W]*- and SCA3tr-Q78-induced REPs in opposite directions, suppressing polyQ- and enhancing *Tau*-induced phenotypes. Due to different modulation in the two disease models, *aux* and *CG3808* were still termed modifier candidates specific for SCA3tr-Q78 neurotoxicity.

In conclusion, we obtained a total of 508 RNAi lines (34 suppressors, 474 enhancers) corresponding to 502 *Drosophila* genes. Silencing of these genes is assumed to modify Ataxin-3-induced neurodegeneration in the fly compound eye (see **Figures 10, 12**).

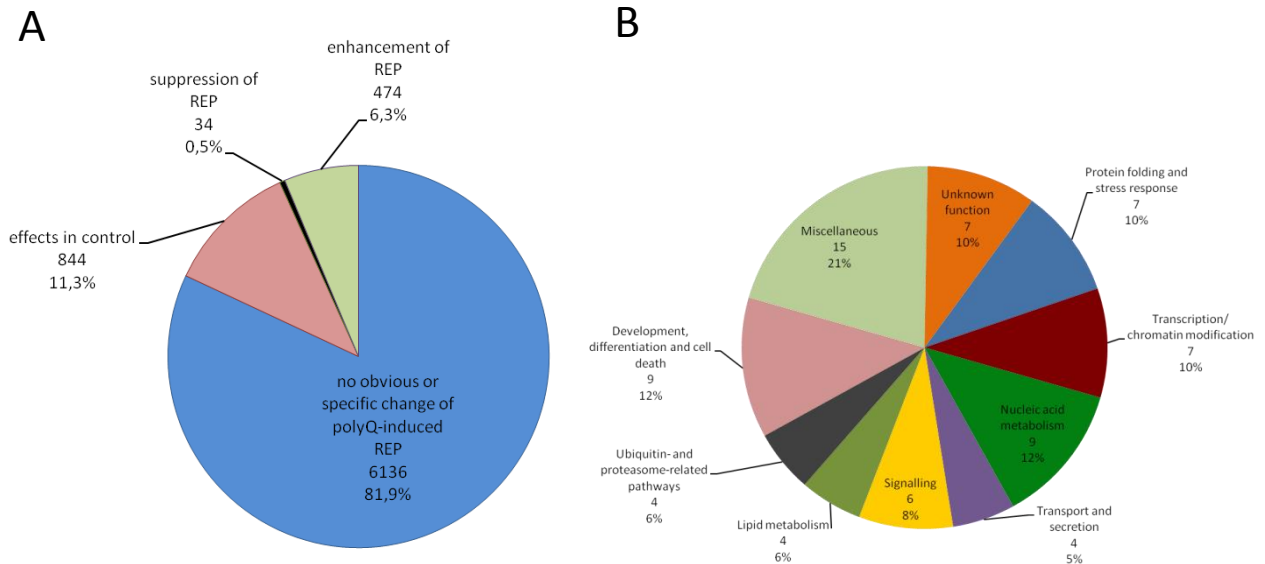


Figure 12. Summary of the *SCA3tr-Q78* modifier screen and overview of modifier categories.

(A) Of the 7,488 utilised RNAi lines, 844 showed disturbed external eye structures after being crossed to *GMR-GAL4* and were excluded from further screening. Screening identified 34 suppressors and 474 enhancers. The remaining 6,136 lines had no impact on REP or showed similar effects in the Tau screen, hence were not considered specific for polyQ. **(B)** Depiction of biological processes of silenced candidate genes.

5.2.4 Evaluation of gene silencing by RNAi lines

Given the large number of candidate genes, it was not possible to quantify silencing of RNAi target genes on mRNA levels. Nevertheless, in an attempt to evaluate the RNAi effect of the screened fly lines in a sampled fashion, the results of ubiquitous expression of the UAS-shRNA were assessed. For this experiment the human orthologue sublibrary was searched for genes that have been reported in the literature to be crucial for survival. These amounted to 59 lines representing 54 genes subsequently crossbred with the *actin5C-GAL4* driver line ($P\{w[+mC]=Act5C-GAL4\}25F01$). It was assumed that effective silencing of target genes would lead to a reduced number or complete lack in offspring due to vital importance of the downregulated genes.

Ubiquitous silencing of this set of essential genes indeed eventuated in a lethal outcome in F1 generation for 45 of the 59 tested RNAi lines (76.2 %), the remainder showing a reduced number of offspring (summarised in **Appendix Table 2**). Additionally, select suppressor candidates from the RNAi screen were able to rescue lethality in offspring pan-neurally expressing *SCA3tr-Q78* (data not shown). Concluding from these results it was assumed that the majority of the RNAi lines yield effective silencing of their target genes.

5.3 Impact of modifiers on polyQ toxicity and aggregation

The modulation of the exterior polyQ-induced rough eye phenotype served as a readout of neurotoxicity and its modulation by modifier candidates. Additionally, integrity of eye structure and the connection between aggregation and neurodegeneration can be analysed in greater detail by histological and immunohistochemical approaches on the one hand and biochemical filtration methods on the other hand. We utilised both for certain candidate genes in order to gain insight into the modes of action of the discovered modifiers.

5.3.1 Evaluation of tissue integrity of *SCA3^{tr-Q78}-shRNA-coexpressing* flies

A suitable approach to study morphology and thereby integrity of the compound eye is frontal sectioning of fly heads and the subsequent histological staining of the tissue. The morphological changes of the eye surface of polyQ flies originate from the degeneration of the underlying tissue of the compound eye. Namely, photoreceptor and adjacent cell architecture are severely deteriorated, leading to the overt rough eye phenotype and eventually collapse of the eye.

Selected suppressor candidates were used in order to assess preservation of deeper eye tissue in contrast to retinal damage in polyQ flies. Flies co-expressing polyQ protein and enhancer RNAi could not be analysed due to severe degeneration of eye structure. As expected, silencing of genes leading to improvement of REP was also able to alleviate the detrimental effects of polyQ expression in the retina, albeit to different degrees (**Figure 13**). For example, the two RNAi lines for knockdown of Hsc70-4 (Transformant IDs 50222/26465) both ameliorated cell demise in the retina of SCA3 flies in line with their suppression effect on REP in the RNAi screen. Nevertheless, the effect of tissue preservation was significantly different for these shRNAs, with line 50222 showing almost wild-type retinal extend and structure whereas line 26465 exhibited good external phenotype mitigation yet retinal organisation presented diffuse and width was decreased.

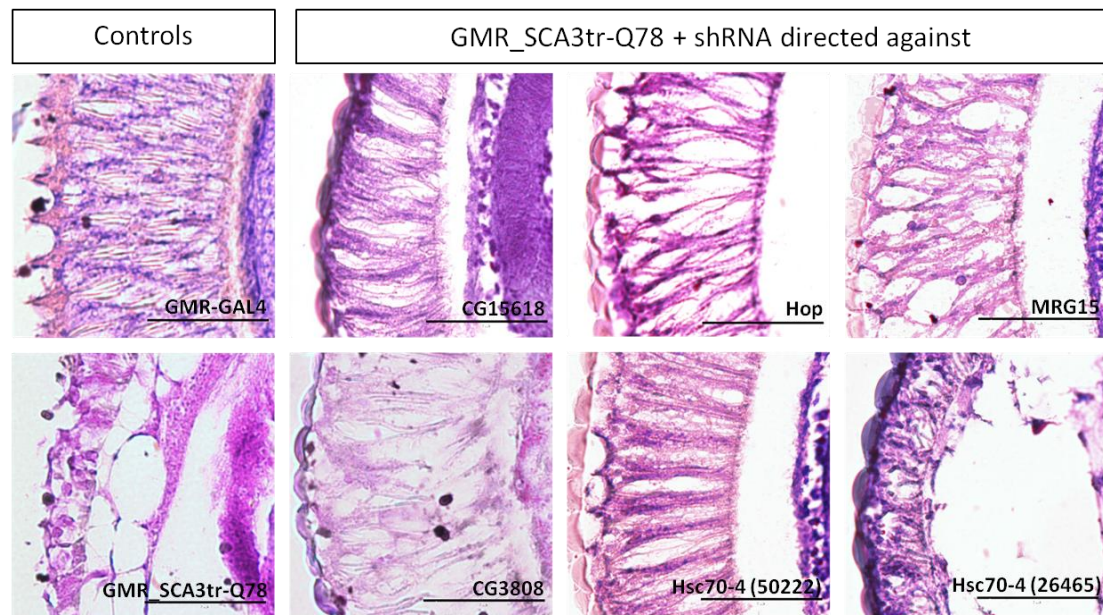


Figure 13. Influence of selected shRNAs on tissue integrity of *SCA3tr-Q78* fly head sections.

Control sections feature intact retinal tissue in *GMR-GAL4* and serious degeneration of eye tissue in *SCA3tr-Q78* fly sections. Following introduction of shRNA lines suppressing Ataxin-3-induced REP, retinal thickness is improved to different degrees and retinal tissue architecture is restored towards *GMR* control situation. All scale bars apply to 50 μm respectively.

5.3.2 Filter retardation analysis of RNAi influence on polyQ aggregates

Due to the proposed toxicity of certain polyQ aggregate species and the possible influence of modifier gene knockdown thereon, it was intended to biochemically study whether there is an impact of silencing of screened modifier genes on the levels of SDS-insoluble polyQ aggregates as previously described [276].

In order to address this question, expanded polyQ protein was co-expressed together with the candidate shRNA in the eye. Where possible, offspring were collected and SDS-treated head lysates were subjected to filter retardation assay (FRA) analysis. Filtration of the protein lysates through a nitrocellulose membrane would lead to trapping of aggregates exceeding a certain size (0.2 μm), allowing for assessment of polyQ aggregate load. Of course, lethal enhancers could not be analysed due to the absence of viable progeny. The hypothesis was that REP-suppressing candidates would decrease toxic aggregate levels, whereas enhancer shRNA expression would result in higher aggregate load. Nevertheless only a minor number of suppressor candidates was observed to effectively ameliorating aggregate number (6/34, 17.6 %) with shRNA against *CG3808* being the most potent aggregation suppressor. On the contrary, a considerable large group did not change

aggregate levels significantly or even enhanced (2/34, 5.8 %) the cellular polyQ aggregate burden after normalisation to polyQ control. Additionally, the majority of enhancer RNAi candidates exhibited a trend towards decreasing aggregate levels with only a few gene knockdowns resulting in higher aggregate load. However, absolute number of significant changes is smaller in enhancers compared to suppressors. Concluding from these results, aggregate levels in this experimental setting do not appear to correlate to exterior REP and *vice versa* (Figure 14).

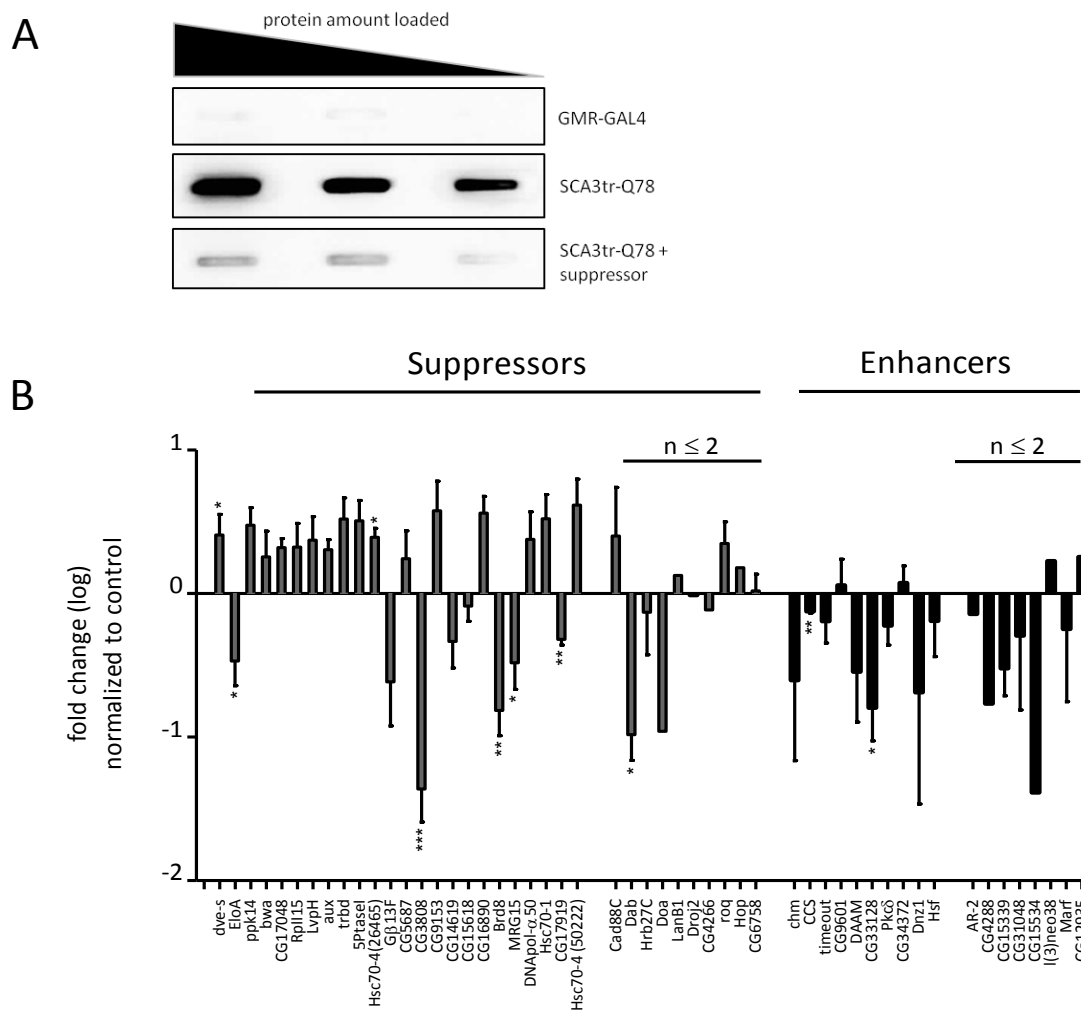


Figure 14. Analysis of SDS-insoluble SCA3tr-Q78 aggregate load with shRNA modifiers.

(A) Exemplary filter retardation analysis for visualisation of aggregate load. GMR-GAL4 control is negative, *SCA3tr-Q78* lysates exhibit heavy aggregation which is mitigated by suppressor shRNA. (B) Densitometric measurement of filter retardation analysis compared to *SCA3tr-Q78* for suppressors and enhancers of polyQ-induced toxicity. $n \geq 3$ if not indicated otherwise. Significant changes are: * $p < 0.05$; ** $p < 0.01$; *** $p < 0.001$.

5.3.3 RNAi effects on polyQ inclusions *in situ*

Expression of expanded polyQ protein leads to formation of protein aggregates in the compound eye as shown before and verified biochemically by the filter retardation experiments. Aggregation of toxic gene products is a hallmark of polyQ disease and considered to be at least in part causative for neurotoxicity and degeneration. On a microscopic level, inclusion bodies in retinal cells are detectable, presumably consisting of diverse polyQ aggregate species and various other proteins recruited to the agglomerate. In the eyes of the offspring of polyQ flies and flies concomitantly expressing modifier shRNA we intended to address the question whether improvement or worsening of the REP corresponds to the aggregate load *in situ*.

In the frontal head sections representative for select candidates we were however not able to show a robust connection between decrease of inclusions in the eye tissue and change of the REP. Three of the analysed RNAi lines featured a reduction of SDS-insoluble aggregates in filter retardation assays (Brd8, CG17919, CG33128, **Figure 15A-C**) with the latter being an enhancer of the REP. The two suppressor lines still featured inclusions, however to a seemingly decreased amount. The CG33128 shRNA (**Figure 15C**) led to an enhanced number of inclusions and concomitantly had the worst tissue integrity. The suppressor lines at least presented with improved retinal morphology compared to polyQ alone. Two lines with increased SDS-insoluble aggregate load in filter retardation analysis, CG17048 and Hsc70-4 (26465) (**Figure 15D, E**), had clearly delimited small inclusions in moderate numbers in parallel with an overall well-preserved tissue integrity. Thus, there was no clear trend such that modified eye structure and therefore altered neurotoxicity have their origin in a differential number of immunohistochemically detectable aggregates.

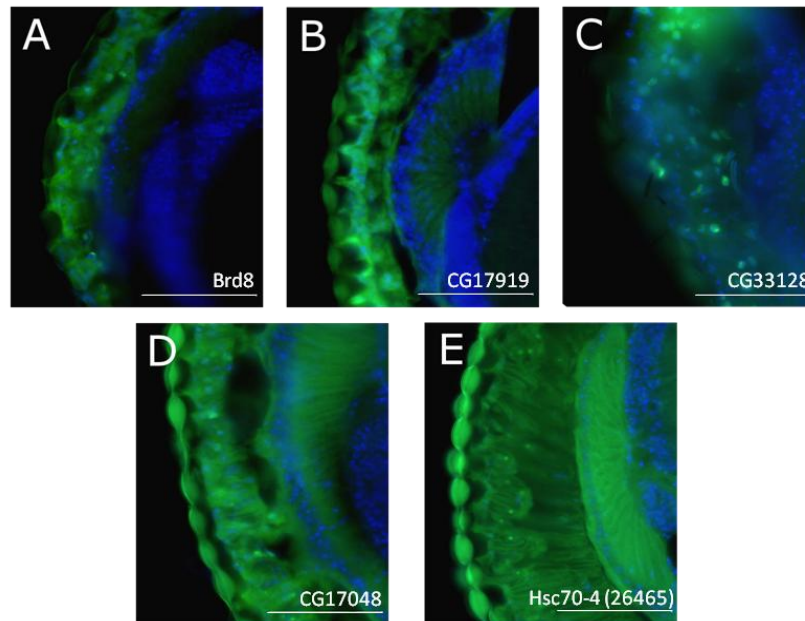


Figure 15. Influence of RNAi on microscopically detectable Ataxin-3 inclusions *in situ*.

RNAi effects differently affect inclusions of SCA3tr-Q78 protein in fly eyes. Whereas two out of the group of suppressors of SDS-insoluble aggregates had diffusely demarcated and seemingly less inclusions (**A, B**), the third one appeared to have high inclusion numbers and disturbed retinal morphology (**C**). Aggregate enhancers in FRA exhibited distinct small inclusions in moderate numbers, tissue integrity is well preserved (**D, E**).

Blue, cell nuclei stained with DAPI; green, SCA3tr-Q78 stained with mouse anti-HA antibody. All scale bars apply to 50 μm respectively.

5.4 Summary of RNAi screen results

We conducted a large-scale RNAi screen in *Drosophila* in order to identify genes that if silenced are capable of modifying polyQ toxicity. After excluding vitally crucial genes from the analysis, our efforts resulted in a set of 502 candidate genes. Knockdown of the vast majority of interactors together with elongated polyQ expression led to lethality in the progeny and pre-empted further investigations. Nevertheless, we were able to analyse several of 68 non-lethal candidates in more detail.

Histological and immunohistological evaluation revealed that suppressor candidates are to a certain degree capable of ameliorating the degeneration of eye tissue and photoreceptors responsible for the REP. However, the amount of exterior improvement of the REP is not consistently reflected in the preservation of the underlying eye structures. Tissue of enhancing candidates is rendered impossible to investigate since degeneration of the eye tissue is already too severe upon polyQ expression alone. Additionally, examination of aggregate formation in the eye of elongated polyQ-expressing flies showed heavy inclusion load in *SCA3tr-Q78* flies. Improvement of REP by suppressors did not correlate to

their capability to prevent inclusion body formation. Contrary to our assumption, the improvement or aggravation of the REP by the modifiers could not be conclusively explained by their impact on SDS-insoluble aggregates in filter retardation analysis.

As a result of the consistently beneficial outcome of its silencing for polyQ toxicity in histological as well as biochemical testing, we chose the *Drosophila* gene *CG3808*, orthologous to the human *tRNA methyltransferase homologue 2A (TRMT2A)*, for subsequent analysis.

5.5 Analysis of the effect of *TRMT2A* silencing on polyQ toxicity in *Drosophila*

Silencing of *CG3808*, the *Drosophila* orthologue of *TRMT2A*, showed promising results in ameliorating the detrimental effects of elongated SCA3 protein. Thus, we addressed the question whether *CG3808* knockdown would also prove beneficial during more detailed analysis and in other polyQ models apart from *SCA3tr-Q78*. Firstly, we assessed the capability of the RNAi to overcome lethality induced by pan-neural expression of *SCA3tr-Q78*. Indeed, co-expression of shRNA and *SCA3tr-Q78* in all neural cells resulted in viable progeny with no overt abnormalities. Additionally, ubiquitous silencing of *CG3808* by the means of RNAi did not render the offspring fatal and had no negative influence on overall life time of the respective flies, demonstrating that the protein is not of vital importance in *Drosophila* (data not shown).

For evaluation of *CG3808* RNAi effects we again utilised histological and biochemical methods together with assessment of longevity. Finally, we transferred experiments to a cellular model in an attempt to verify the progress accomplished in *Drosophila* in a mammalian model.

5.5.1 Impact of *TRMT2A* silencing on polyglutamine-induced REPs

Expression of *SCA3tr-Q78* in the compound eye led to a rough eye phenotype visible with light (**Figure 16A**) as well as scanning electron microscopy (SEM, **Figure 16B**). The SEM findings are in line with results obtained from REP pictures, namely the eyes presenting with heavily disarranged surface and even collapsed eye morphology probably due to underlying tissue degeneration. Silencing of *CG3808* by RNAi led to amelioration of *SCA3tr-Q78*-induced REP with restored patterning and morphology of the exterior eye

surface. For another polyQ fly model, inducing a REP with exon 1 of the *huntingtin* gene under GMR control, similar observations were made. This *htt* transgene contains 97 glutamine repeats ($w[*];P\{w[+]=UAS-Q97ex1\}K6,9,15R$) and downregulation of *CG3808* expression was sufficient to rescue the Htt-induced REP (**Figure 16C, D**), reversing the phenotype to almost wild type (**Figure 16H**). This was underpinned by SEM analysis, exhibiting a predominantly ordered surface without signs of degeneration (**Figure 16I**). Introduction of shRNA against *CG3808* into a model for SCA1 with full-length ATXN1 Q82 expression ($y[1]w[118]P\{[+]=UAS-SCA1.82Q\}[F7]$, **Figure 16E**) yielded improvement of the degenerative eye phenotype to great extent as well (**Figure 16J**).

Concluding, knockdown of *CG3808* expression is obviously capable of exerting neuroprotective effects in the course of eye degeneration caused by several different polyQ proteins.

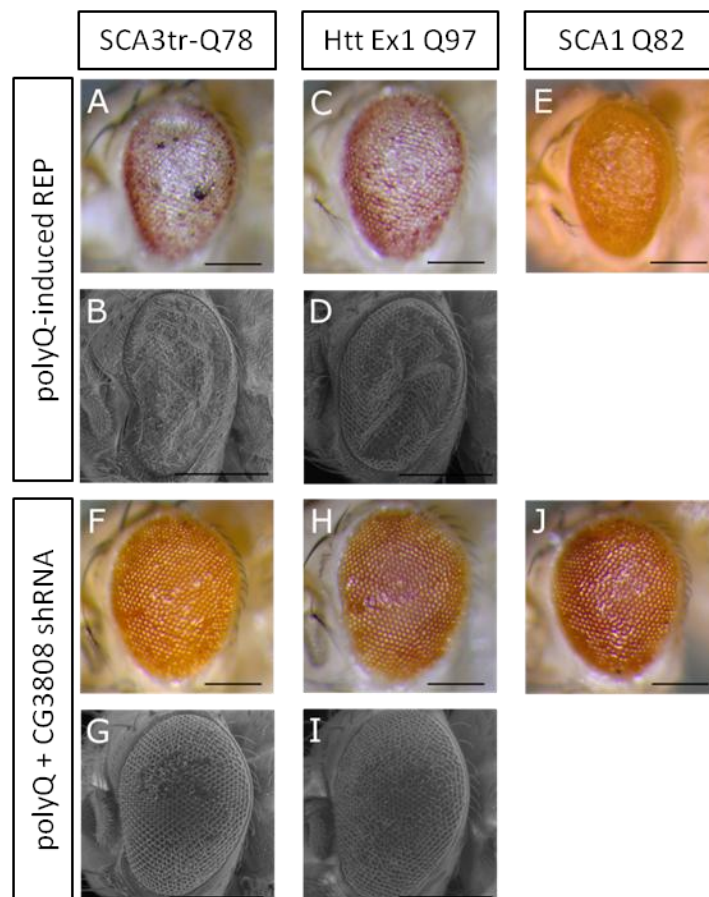


Figure 16. Rescue of polyQ-induced REP by shRNA against *CG3808*.

Elongated polyQ proteins responsible for SCA3 (**A, B**), HD (**C, D**) and SCA1 (**E**) induced an REP in flies visible by light and scanning electron microscopy. Induction of shRNA directed against *CG3808* transcripts mitigates this REP to almost wild type situation (**F-J**).

All scale bars apply to 200 μm .

5.5.2 Evaluation of photoreceptor integrity of polyQ flies with *TRMT2A* knockdown

Semi-thin sagittal sections of fly eyes expressing variants of Ataxin-1 and Ataxin-3 under control of GMR-GAL4 (*GMR_SCA1 Q82* and *GMR_SCA3tr-Q78* respectively) display severe degeneration of photoreceptor neurons as a consequence of polyQ neurotoxicity. Co-expression of shRNA against *CG3808* on the contrary was capable of ameliorating the detrimental effects in the eye (**Figure 17A**). Quantification of photoreceptor neurons per ommatidium showed a severely decreased PR count in *GMR_SCA3tr-Q78* (1.16 ± 0.06) flies and a moderately decreased one (4.24 ± 0.27) in the *GMR_SCA1Q82* model. Silencing of *CG3808* rescued PR degeneration almost to the level of GMR control conditions (6.85 ± 0.03) in *GMR_SCA3tr-Q78* (6.31 ± 0.09) and *GMR_SCA1 Q82* (6.64 ± 0.05) models (**Figure 17B**). Additionally, stereotypic patterning in the ommatidia was visible again in *GMR_SCA3tr-Q78* flies in combination with *CG3808* silencing. These results could be recapitulated also in the flies expressing the elongated full-length form of Ataxin-1 (*GMR>SCA1 Q82*, **Figure 17A**) and at least qualitatively with a transgene of exon 1 of *HTT* with 97 glutamine repeats (*GMR_HTT Exon1 Q97*, not shown). Therefore, silencing of *CG3808* seems to have a strong neuroprotective effect opposing polyQ toxicity in the *Drosophila* eye.

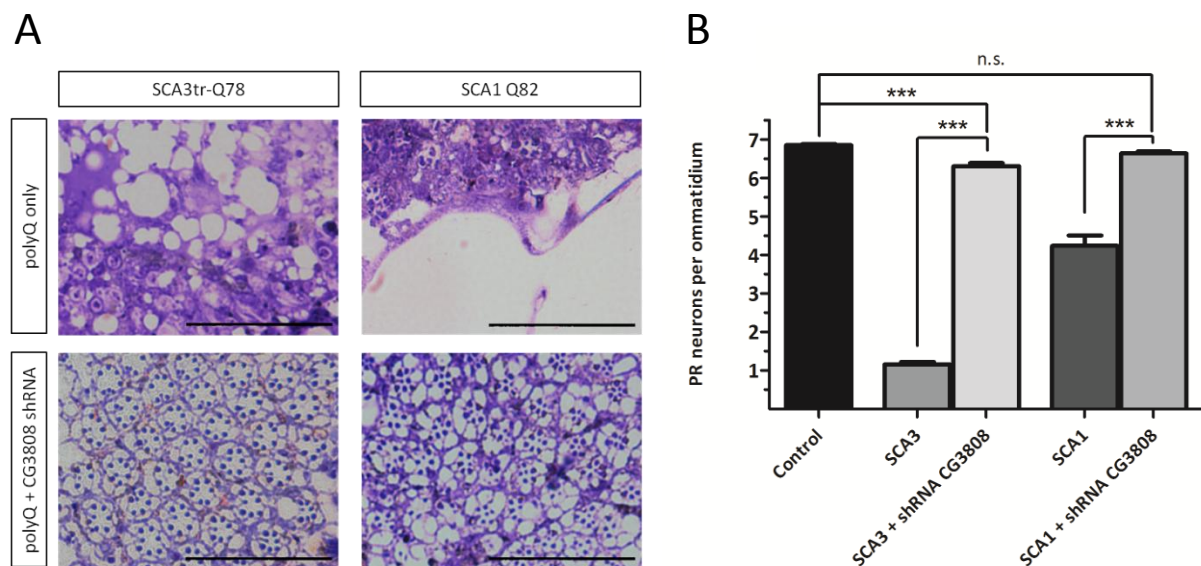


Figure 17. Evaluation of photoreceptor integrity in polyQ flies with *CG3808* RNAi.

(A) Depiction of PR neuron degeneration in polyQ models for SCA3 and SCA1 (upper panel) and rescue of number and patterning of PRs by silencing of *CG3808* via RNAi (lower panel). (B) Quantification of PR number in SCA3 and SCA1 fly models compared to GMR control. Significant PR loss was rescued to a great extent by expression of shRNA against *CG3808*.

All scale bars in (A) apply to 50 μ m respectively. Kruskal-Wallis test with Dunn's Multiple Comparison test was used for statistics in (B), significant changes are: *** $p < 0.001$; n.s., not significant.

5.5.3 Assessment of adult-onset polyQ fly longevity

In order to more closely mimic the disease situation in humans with late onset and progressive degeneration, further experiments in a pan-neural adult-onset model for polyQ diseases were performed. Therefore an *elav-GAL4* fly strain with additional ubiquitous expression of the temperature-sensitive yeast transcriptional repressor GAL80^{ts} ($P\{w[+mW.hs]=GawB\}elav[C155]; P\{w[+mC]=tubP-GAL80[ts]\}20$) [285] (referred to as *elav-GAL80* in the text) was used. GAL80 is a competitor of GAL4 in binding to the UAS without activating properties, thereby preventing subsequent induction of gene expression at permissive temperature (≤ 20 °C). Upon shifting to restrictive temperature (≥ 25 °C), GAL80 is unfolded, which prevents blockage of GAL4, consequently allowing GAL4-UAS binding and gene expression. Protein aggregation analysis and longevity experiments were performed making use of this system, facilitating pan-neural expression of *SCA3tr-Q78* only following temperature shift from 18 °C to 29 °C.

Induction of polyQ expression could be shown in Western blot experiments climaxing four days post temperature shift and declining afterwards probably due to cell demise (**Figure 18A**). Aggregation of truncated Ataxin-3 was shown to be absent before induction of *SCA3tr-Q78* expression on permissive temperature and to increase rapidly within a timeframe of 7 days after temperature shift (**Figure 18B, C**).

Overall lifetime of polyQ-expressing flies is a feasible tool for evaluation of toxicity and neurodegeneration. *SCA3tr-Q78* flies showed no abnormalities at restrictive temperature due to absent toxic protein expression. However, locomotive abilities of the flies deteriorated fast after induction of expression concomitantly with a rapid decline in survival time resulting in a median survival time (timepoint when 50 % of flies of overall flies are still alive) of only 10 days. Flies with adult-onset expression of a non-toxic control transgene ($P\{w[+mC]=UAS-eGFP\}$) had an almost three times longer mean survival (27 days). Eventually, co-expression of *SCA3tr-Q78* and shRNA against *CG3808* increased median survival significantly to about 18 days. Therefore, silencing of this methyl transferase proved to be beneficial in alleviating detrimental polyQ effects on longevity, despite limitations compared to non-polyQ transgene expression.

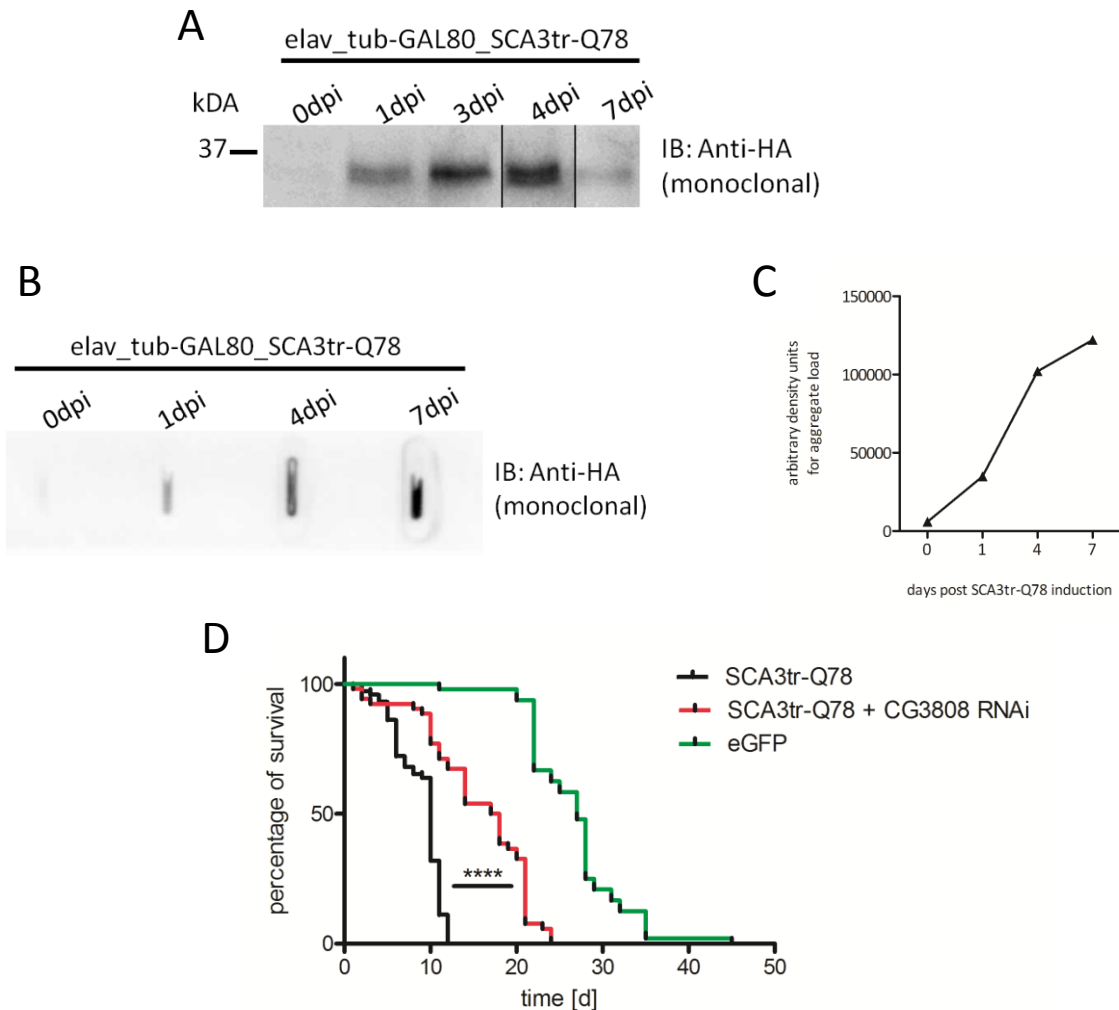


Figure 18. Adult-onset model of *SCA3tr-Q78* in *Drosophila* and extension of polyQ fly life time by *CG3808* RNAi.

(A) Protein levels of truncated Ataxin-3 in adult-onset fly model are detectable one day post induction (dpi) by temperature shift and increase until 4 dpi. At 7 dpi, levels have already declined. (B, C) Aggregate load of SCA3tr-Q78 in adult-onset fly heads increases steadily after induction over a course of 7 days. (D) Expression of shRNA against *CG3808* is sufficient to significantly prolong median survival and overall lifetime of pan-neural adult-onset SCA3tr-Q78 flies, although not to control levels (eGFP).

Log-rank test was used for statistics in (D), significant changes are: **** $p < 0.0001$.

5.5.4 Influence of *CG3808* downregulation on aggregate formation in *Drosophila*

As already demonstrated, targeting of *SCA3tr-Q78* expression to the eye leads to aggregate formation and gives rise to inclusion bodies of elongated polyQ protein and eye degeneration. By co-expression of shRNA against *CG3808* the anti-aggregation properties of this gene knockdown could be shown *in situ* and in filter retardation analysis.

Paraffin frontal fly head sections were probed with an antibody directed against the HA-tag of the polyQ protein. It could be observed that induction of *CG3808* RNAi is capable

of preventing assembly of inclusion bodies in the compound eye retina, concomitantly preserving the structure and architecture of the tissue to great extent. Additionally, aggregation of elongated full-length Ataxin-1 in the retina and impact of *CG3808* induction thereon was estimated. Ataxin-1 did not show pronounced formation of inclusion, yet rather was localised to the nucleus. *CG3808* RNAi did not feature an obvious change of Ataxin-1 distribution or amount, however, retinal structure appeared improved (**Figure 19A**).

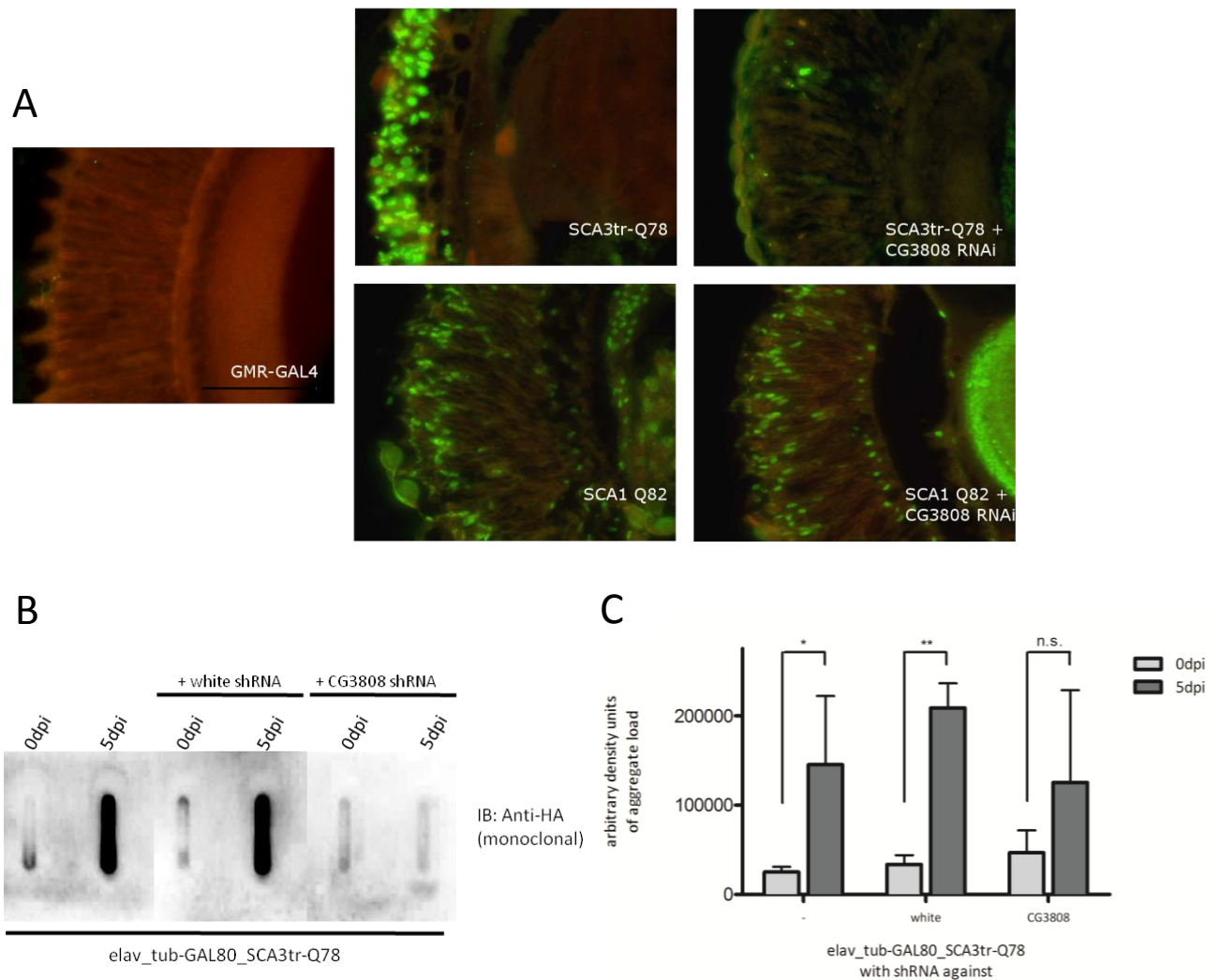


Figure 19. Overview of anti-aggregation effects of *CG3808* RNAi in different polyQ models and settings.

(A) Induction of *CG3808* RNAi leads to a prominent decrease of inclusion number in the retina of SCA3 model flies (upper row). Ataxin-1 protein does not seem to form inclusion in SCA1 flies and *CG3808* RNAi does not influence distribution or protein amount in the retina. **(B)** Adult-onset co-expression of *CG3808* shRNA with *SCA3tr-Q78* ameliorates aggregate load in fly head lysates also compared to an RNAi control (*white* shRNA). **(C)** Quantification of aggregate load in adult-onset SCA3 flies after introduction of control and *CG3808* shRNA.

Scale bar in **(A)** applies to 50 μm . Red in **(A)**, F-actin stained with Alexa Fluor[®] 568-linked phalloidin; green in **(A)** upper row, SCA3tr-Q78 stained with mouse anti-HA antibody; lower row, SCA1 Q82 stained with mouse anti-polyQ antibody. t-test was used for statistics in **(C)**, significant changes are: * $p < 0.05$; ** $p < 0.01$; n.s., not significant.

The potent aggregate-reducing capacity of *CG3808* downregulation has already been shown for eye-expressed polyQ protein (see chapter 5.3.2, **Figure 14 B**). Nevertheless, expression of *SCA3tr-Q78* and of *CG3808* shRNA under GMR control does not reflect the pathogenic situation in humans with respect to late disease onset. Therefore, *elav-GAL80* fly strains for pan-neural adult-onset expression were utilised. Induction of polyQ expression alone by temperature shift produced a significant increase in SDS-insoluble aggregates five days post induction as detected by filter retardation assay (**Figure 19B, C**). Introduction of a control shRNA against *white* gene expression also showed a significant rise in aggregate load, whereas the moderate increase in flies expressing both polyQ and *CG3808* RNAi was not statistically significant (**Figure 19C**). From these findings one can conclude that silencing of *CG3808* expression is capable of decelerating the formation and/or accumulation of potentially toxic polyQ aggregates.

5.6 Impact of *TRMT2A* knockdown on polyQ toxicity in a mammalian system

All experiments so far have been conducted in fly polyQ models with shRNA targeting the expression of the fly orthologue *CG3808* of the human *TRMT2A* gene. Unfortunately, there are no classical loss-of-function alleles of *CG3808* available. In addition, the lack of independent RNAi lines to silence *CG3808* prevented us from confirming our findings. Although *Drosophila* proved to be a feasible and beneficial tool for analysis of polyQ modifier genes, it is of crucial importance to confer the insights gained regarding amelioration of aggregation and toxicity to a mammalian system. Moreover, reconfirmation of the beneficial effects of *TRMT2A* silencing in the context of polyQ-induced toxicity in a vertebrate system would be desirable. Demonstrating the favourable activity of *TRMT2A* silencing in polyQ diseases would eventually deduce a universal mechanism conserved between flies and vertebrates, highlighting the experimental rationale of our screen.

5.6.1 Generation of stable *TRMT2A* knockdown HEK cells

For the cell culture experiments human embryonic kidney cells (HEK293) were utilised. The high transfection efficiency and general robustness regarding both growth and protein production rendered HEK cells a feasible model system for the polyQ investigations.

For stable silencing of *TRMT2A* expression, five different shRNA lentiviral transduction particles, targeting individual human *TRMT2A* mRNA sequences, were purchased for treatment of HEK293 cells. Additionally, one non-target shRNA control viral strain was used, coding for an shRNA without any known cellular targets. Subsequent to viral transduction (at Department of Biochemistry, University Medical Centre Aachen) with different multiplicities of infection (MOI), cell colonies having the shRNA stably integrated in their genome were selected. Western blot analysis was utilised for evaluation of successful *TRMT2A* downregulation. Viral strains #856 and #1574 exhibited almost complete silencing of *TRMT2A* expression, regardless of deployed MOI. Strains #736 and #1502 induced slight downregulation of expression, whereas transduction with strain #1485 did not result in overt changes of expression levels. Scrambled shRNA viral transduction had no impact on *TRMT2A* protein levels and proved to be adequate as control. All expressional levels were compared to the amount of β -tubulin as control (**Figure 20A**).

Consequently, cells transduced with strains #856 and #1574 featured feasible prerequisites for further experiments regarding polyQ toxicity in a mammalian model system. Eventually cells with stable *TRMT2A* knockdown (derived from infection with strain #1574) were used (**Figure 20B, C**). Additionally, *TRMT2A* silencing was confirmed by mass-spectrometric analysis (see chapter 5.7).

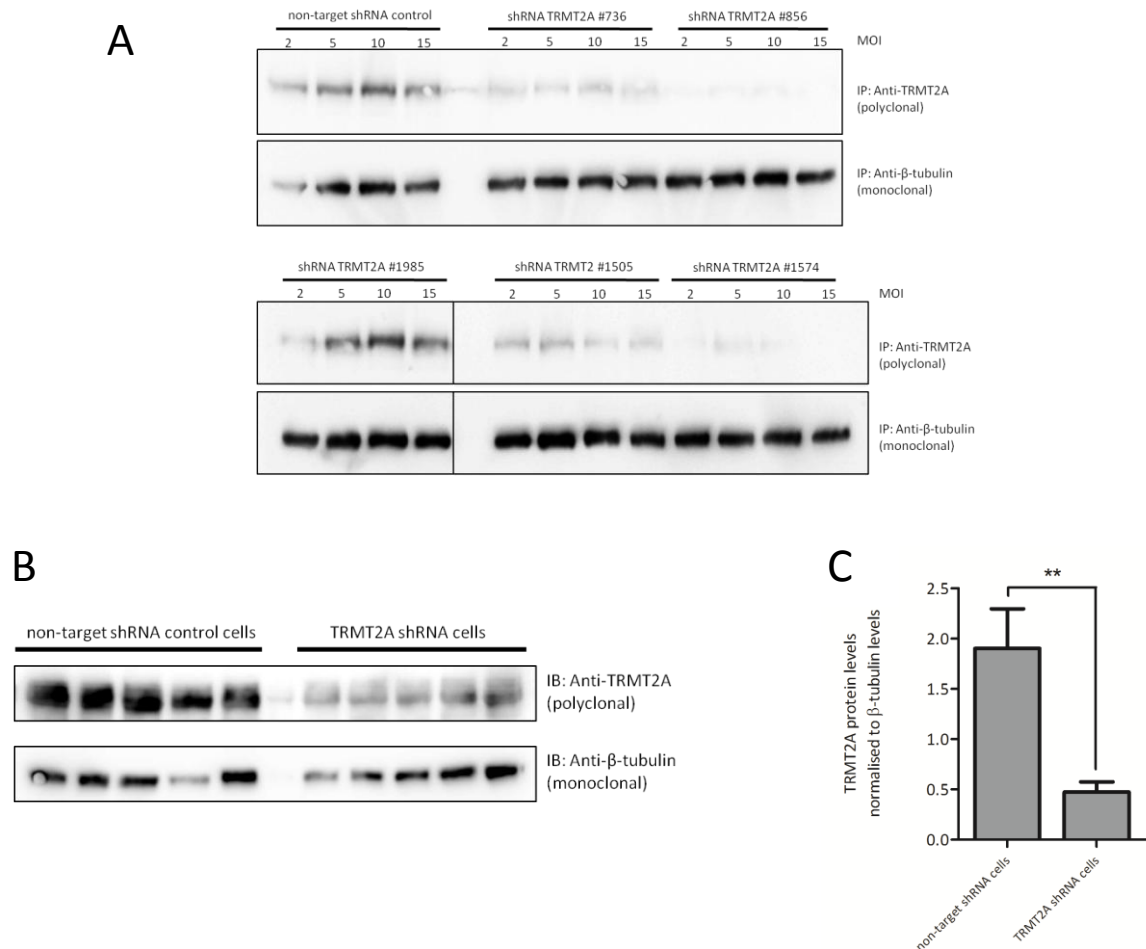


Figure 20. Stable shRNA-mediated silencing of *TRMT2A* expression after viral transduction of HEK293 cells.

(A) Subsequent to transduction of shRNA against *TRMT2A* by lentiviral particles, protein levels of viral strains #856 and #1574 were reduced most efficiently of all tested lines. Non-target shRNA control showed no marked change in *TRMT2A* protein levels. (B) Exemplary Western blot of decreased *TRMT2A* protein levels in ultimately utilised line #1574 HEK cells compared to scrambled shRNA control. (C) Quantification of *TRMT2A* protein levels in line #1574 HEK cells compared to control.

t-test was used for statistics in (C), significant changes are ** $p < 0.01$.

5.6.2 Transfection of stable *TRMT2A* knockdown cells with polyQ constructs

For replication of *Drosophila* results in mammalian cells, the impact of *TRMT2A* knockdown on polyQ aggregation was investigated. Therefore, stably transduced HEK293 cells were transfected with different *huntingtin* constructs harbouring either a 25 repeats polyQ tract (*GFP-HttQ25*) or a pathological tract of 103 glutamines (*GFP-HttQ103*, both kind gift by Jan Senderek, ETH Zürich). PolyQ protein expression and aggregation could be visualised and monitored via a carboxy-terminal GFP-tag and fluorescence microscopy. Whereas normal Huntingtin was equally distributed throughout the cytoplasm (Figure 21A, upper row), the expanded polyQ tracts rendered the protein prone to

aggregation, resulting in peri- or intranuclear inclusions (**Figure 21A, lower row**). For expression of mutant polyQ constructs, protein aggregation or cell toxicity no obvious discrepancies could be discerned between control and knockdown cells. Nevertheless, quantification of GFP-positive cells with inclusions showed a slight, however significant increment for inclusion bodies (**Figure 21B**) from control cells (**Figure 21A, left column**) to the most potent knockdown cell line, #1574 (**Figure 21A, right column**).

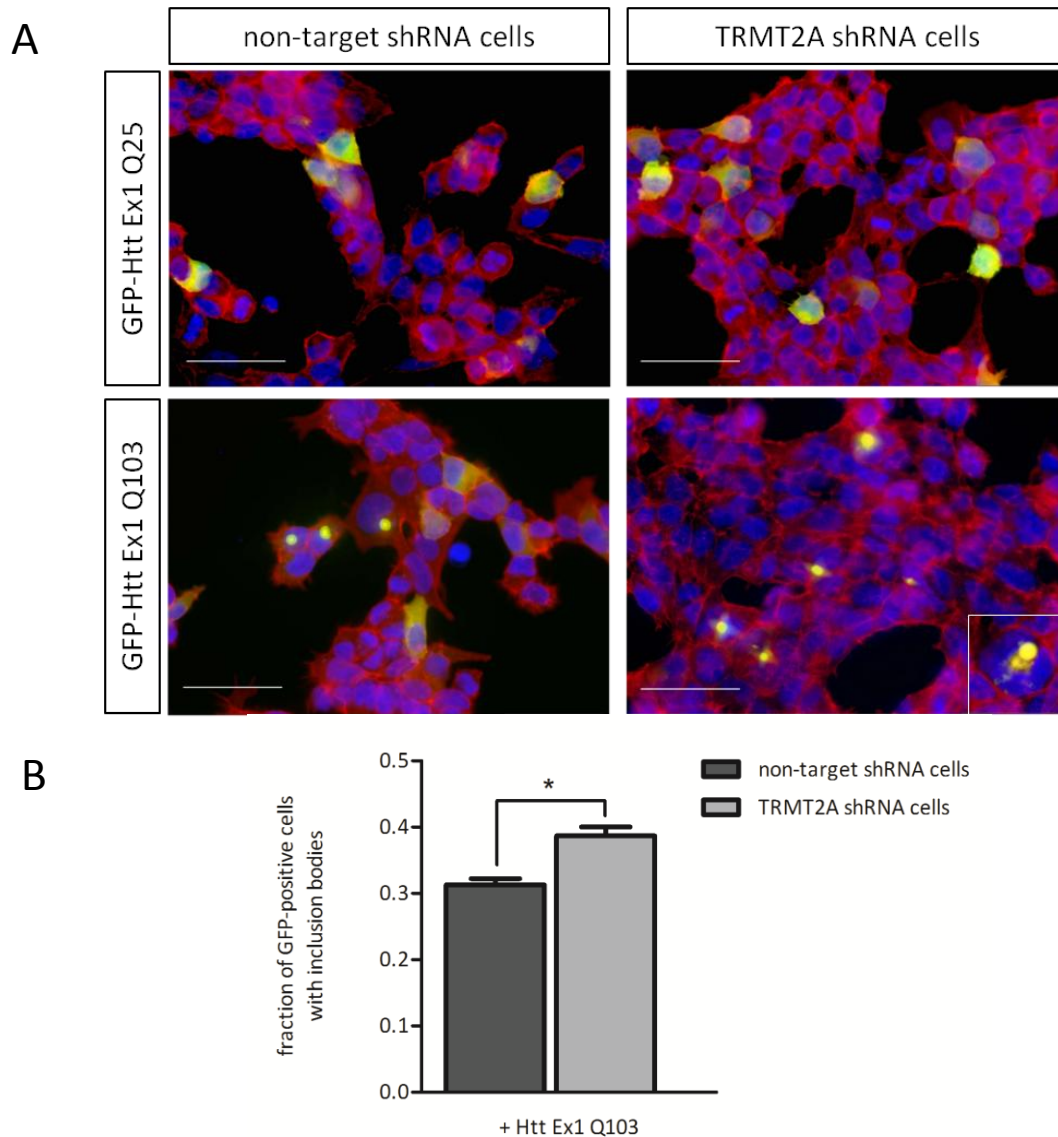


Figure 21. Aggregation properties of normal and expanded Huntingtin in control and *TRMT2A* knockdown HEK cells.

(A) Transfection of HEK cells with normal GFP-tagged Huntingtin (Q25, upper row) led to cytoplasmic distribution of polyQ protein in control and knockdown cells. Expanded Huntingtin (Q103, lower row) forms prominent inclusion bodies in control and knockdown cells alike (detailed view in inset right lower row). **(B)** Significant increase in the fraction of transfected *TRMT2A* knockdown cells bearing inclusion bodies compared to control.

All scale bars in **(A)** apply to 50 μm . t-test was used for statistics in **(B)**, significant changes are * $p < 0.05$.

5.6.3 Investigation of aggregation in polyQ-transfected knockdown cells

Apart from microscopic evaluation, polyQ aggregation under the influence of *TRMT2A* knockdown was also investigated biochemically. Utilising the filter retardation assay, the formation of SDS-insoluble aggregates of two different *huntingtin* constructs was assessed in control and knockdown cells. One construct was the afore utilised exon 1 Huntingtin with a GFP-tag (*GFP-HttQ103*), the second one expresses Huntingtin with the 590 N-terminal amino acids and a myc-tag (*myc-Htt590*). As expected, non-expanded polyQ protein (in both constructs Q25) did not show increased susceptibility to aggregation and was not retained on the filter membrane neither in control nor in knockdown cells (**Figure 22A**). Upon *GFP-HttQ103* and *myc-Htt590* Q97 expression, control cells faced heavy polyQ protein aggregation. In line with the *Drosophila* findings, *TRMT2A* knockdown resulted in a significant amelioration of SDS-insoluble aggregate load in HEK293 cells trapped on the membrane (**Figure 22A**). Therefore, *TRMT2A* knockdown seems to be sufficient to significantly alleviate SDS-insoluble polyQ aggregate load in mammalian cells.

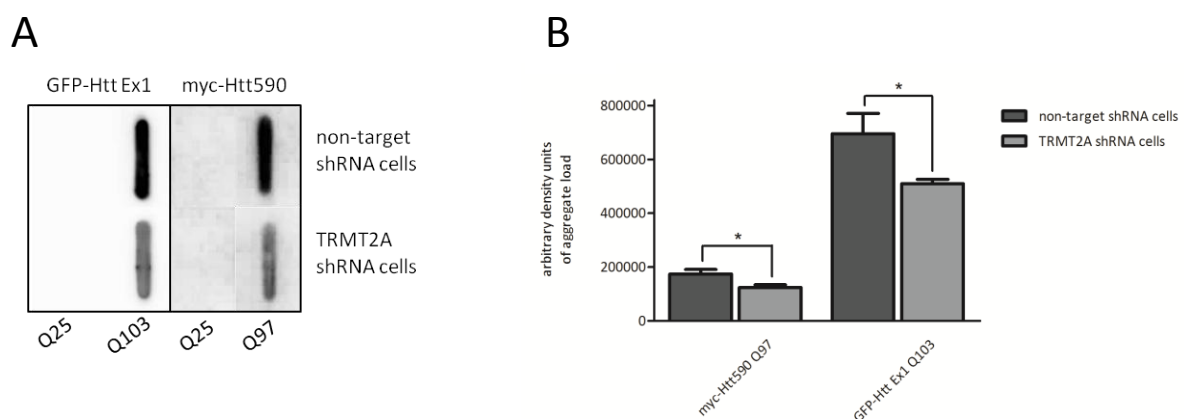


Figure 22. Impact of *TRMT2A* knockdown on different SDS-insoluble Huntingtin aggregates.

(A) Q25-Huntingtin shows no SDS-insoluble protein aggregates, Q103 and Q97 proteins result in heavy aggregate load in control cells which is mitigated in *TRMT2A* knockdown cells. **(B)** Quantification of decrease in Huntingtin aggregate load in *TRMT2A* knockdown cells compared to control.

For protein detection in **(A)**, mouse anti-GFP and mouse anti-myc antibodies were used. t-test was used for statistics in **(B)**, significant changes are * $p < 0.05$

In conclusion, silencing of *TRMT2A* expression in mammalian cells partially was capable of recapitulating alleviating effects on SDS-insoluble polyQ aggregates. A dissolving effect like for RNAi of *CG3808* affecting *in situ* polyQ inclusion could not be verified. Yet it remains to be solved how the consequences of *TRMT2A* silencing are brought about mechanistically on a molecular level.

5.7 Attempts on revelation of the molecular mechanism of *TRMT2A* knockdown on polyQ proteins

The methylation of tRNA bases by their respective methyltransferases such as *TRMT2A* is an important factor during translation for processes like binding of aminoacyl-tRNA synthetases, aminoacylation itself and binding of the tRNA to the ribosome. Concluding from that it might be possible that silencing of *TRMT2A* hampers one of these processes and leads to differential translation of polyQ proteins. Exchange of a single glutamine within the polyQ stretch for a different amino acid alters the conformational properties, therefore possibly mitigating toxicity. In order to account for this possible mechanism, it was intended to analyse the peptide sequence of polyQ proteins by matrix-assisted laser desorption/ionisation-time of flight mass spectrometry (MALDI-TOF MS) after silencing of *TRMT2A* expression. Isolation of SCA3tr-Q78 protein from *CG3808*-silenced flies with immunoprecipitation approaches proved to be difficult due to the previously mentioned low levels of available monomeric protein. Therefore, lysates of *TRMT2A* knockdown HEK cells overexpressing myc-tagged Huntingtin Q25 were prepared for analysis by Fabian Hosp (Department Cellular Signalling and Mass Spectrometry, Max Delbrück Center for Molecular Medicine, Berlin, Head: Prof. Matthias Selbach). Owing to the required tryptic digestion of the proteins prior to MS analysis and the absence of appropriate motifs in the polyQ stretch, a non-elongated form of Huntingtin was chosen to allow for ionisation of the peptide. Nevertheless, it was not possible to ionise the polyQ peptide in order to analyse the mass of the polyQ stretch in MALDI-TOF experiments, which prevented indication of a putative amino acid change in the polyQ sequence. Other peptides of the *huntingtin* transgene product could be identified, proving occurrence of the protein in general. Assuming a generally reduced specificity in translation upon *TRMT2A* silencing, a replacement of glutamine in other proteins and apart from the polyQ stretch might have been an indirect endorsement of the amino acid exchange hypothesis. An investigation of glutamine modifications in the global protein content of the cell lysates yielded no particularly increased accumulation of alterations in the amino acid sequence in the *TRMT2A* knockdown cells.

Another possible path of verification of the assumption regarding the *TRMT2A* mode of action on polyQ proteins is the introduction of novel sites for proteolytical digestion as a side effect of the introduction of an erratic amino acid into the polyQ stretch.

Due to the close relationship of glutamine and glutamate and the fact that the evolution of different tRNAs for glutamine and glutamate is relatively new in evolution, it stands to reason that the exchanged amino acid for glutamine is likely glutamate. Introduction of glutamate into the polyQ stretch would generate a target site for a glutamyl endopeptidase. In this case, treatment of polyQ stretches derived from *TRMT2A* knockdown cells would most probably result in fragmentation of the polyQ tract. This in turn could be visualised in Western blot analysis due to mass shift of the specific protein bands. Initial experiments with a plasmid expressing a HA-tagged expanded polyQ tract (gift from Junying Yuan, Department of Cell Biology, Harvard Medical School, Boston) in *TRMT2A*-silenced HEK cells have already started, but have not yielded conclusive results yet.

6 Discussion

6.1 Characterisation of the utilised polyQ *Drosophila* model

In an attempt to identify novel genetic modifiers of Ataxin-3-induced neurotoxicity we utilised an established *Drosophila* model [256]. Expression of the *SCA3tr-Q78* transgene results in a truncated Ataxin-3 protein containing a polyQ stretch of 78 repeats and residual amino acids N- and C-terminally of the tract together with an N-terminal hemagglutinin tag. However, the Josephin domain and the ubiquitin-interacting motifs of the protein are lacking, thereby compromising the enzymatic activity of the truncated protein as a deubiquitinating enzyme and transcriptional repressor. Expression of the transgene in all postmitotic cells of the *Drosophila* compound eye exerted severe neurodegeneration resulting in alteration of the exterior eye structure, a so-called rough eye phenotype (REP). The REP is characterised by depigmentation, disturbance of texture and ommatidial pattern, dints and necrotic spot formation. These effects obviously have their origin in polyQ toxicity. The deleterious visible changes are a continuation of the heavily destructed internal eye structures featuring decreased retinal thickness and compromised tissue integrity due to a loss of cell mass. As a result of polyQ protein toxicity, the stereotypic number and pattern of photoreceptor neurons is decreased and disrupted respectively, demonstrating the feasibility and transferability of this modelling approach for neurological disorders. At the same time, the easy accessibility for evaluation is an important advantage of the eye-specific polyQ protein expression. Induction of the *SCA3* transgene in all neural cells already at embryonic stages results in pupal lethality as shown before [219] and therefore cannot be utilised in assessment of polyQ effects and modifier screening.

Changes in polyQ-induced REPs have been previously used to identify modifiers of toxicity [28, 136, 256]. For example, co-expression of the viral antiapoptotic caspase inhibitor p35 is capable of at least partially mitigating the rough eye phenotype of the *SCA3tr-Q78* fly model, hinting to the presence of apoptotic processes in the course of polyQ-induced cell degeneration [219]. This is supported by the discovery of cell death in polyQ-expressing cells in the larval eye imaginal discs of *SCA3tr-Q78* flies eventually manifesting in an impaired adult structure. However, the introduction of *p35* was not consistently as beneficial as previously described [219] and could not fully cope with the massive

neurotoxic effects of the SCA3tr-Q78 protein. Additionally, the protective p35 action obviously cannot be generalised for polyQ diseases since no mitigating effect has been observed for overexpression of toxic *huntingtin* transgenes [259].

The presence of SCA3tr-Q78 protein in flies can be verified on the one hand indirectly by the obvious pernicious effects triggered in the compound eye and on the other hand directly by immunostaining of eye imaginal discs as well as adult eye sections. Both show robust *SCA3tr-Q78* expression coinciding with the onset of aggregation already in larval tissue. This explains why model flies already feature an REP at the time of hatching since the first morphological defects set in as early as in pupal stages. Despite the advantages of this robust degeneration phenotype and the mimicking of vertebrate disease processes, this early manifestation of polyQ toxicity consequences does not entirely reflect the late-onset situation of polyQ disease in humans and the overall pathogenesis is restricted to the photoreceptor subset of neurons. The high toxicity of SCA3tr-Q78 in this model may be explained with the truncation of the protein which is thought to be the process finally initiating aggregation. Eye-specific and pan-neural expression of the full length Ataxin-3 with an elongated stretch of 84 glutamines does not result in an overt eye phenotype at hatching yet exhibits late-stage and progressive neurodegeneration [209]. Possibly, these findings have their origin in the fact that the more toxic truncated variant of Ataxin-3 is produced in the first place whereas the full-length version initially has to be proteolytically processed before being rendered toxic. In addition, differences in the expression levels of the two transgenes might account for changes in toxicity. It is only when the cell's capacity to cope with the overload of toxic protein is exhausted that the toxic influences of the truncated proteins set in, which naturally happens faster with the originally shortened form. Expression of the admittedly truncated yet normal form of Ataxin-3 with 27 glutamine repeats does not exert any of the detrimental effects mentioned before, proving the crucial role of polyQ repeat elongation above a certain threshold.

Investigation of actual levels of truncated Ataxin-3 in *Drosophila* is rendered difficult by the highly aggregative nature of the protein, draining the pool of detectable monomeric protein and increasing the amount of aggregated protein not accessible to Western blot analysis. Given the large extend of photoreceptor loss in *GMR_SCA3tr-Q78* flies, it is also reasonable to assume that substantial amounts of cells have already demised shortly after hatching. Thus the lack of protein production of these cells may account for low detection of the protein. Despite the lack of quantifiable biochemical detection of truncated Ataxin-3

in our disease model, there is sufficient evidence for *SCA3tr-Q78* transgene expression combined with several options for analysis of genetic interactions. Despite frequent gene homologies between vertebrates and invertebrates, to date no *ATXN3* orthologue has been described in *Drosophila*. Therefore no endogenous Ataxin-3 can interfere with transgene expression, protein levels or aggregation in a way that has been previously described [209], meaning there is full penetrance of toxic polyQ effects in *SCA3tr-Q78*-expressing flies.

A *Drosophila* model for frontotemporal dementia (FTD) and Parkinsonism linked to chromosome 17 comprising a mutant form of the *mapt* gene (coding for Tau[R406W]) [271] was used to determine the specificity of the obtained experimental results for polyQ-induced toxicity. Targeting production of Tau[R406W] to postmitotic cells of the eye results in a severe REP presenting with disturbed external eye morphology and decreased eye size. Since function of normal Tau as well as mutant *tau*-induced pathogenesis are believed to be different from that of polyQ toxicity, modifiers exhibiting similar results in both disease models are unlikely to be specific for one of the proteins and are not analysed further as such.

6.2 Modifiers of Ataxin-3-induced REP in *Drosophila*

In the primary screen for modifiers of Ataxin-3-induced neurotoxicity, 529 RNAi lines were identified to change the polyQ-induced REP. Of this group, 21 RNAi strains also exhibited similar modulation of Tau[R406W]-induced degeneration and were therefore not considered specific for Ataxin-3, yet not excluded from further analysis. Finally, 508 RNAi lines representing 502 genes were identified as modulators of Ataxin-3-induced neurotoxicity in the *Drosophila* eye. Silencing of gene expression by 34 of these lines resulted in suppression of the REP, whereas 474 shRNAs rendered the REP more severe with the vast majority of lines being lethal in disease model progeny. These numbers are completed with 2 suppressing and 19 enhancing candidates featuring the same result in the Tau verification screen. By previous screening of the entire RNAi sublibrary devoted for the polyQ screen it was assured that the candidate genes are specific for the disease condition and are not of vital importance.

The high number of genes leading to lethal interactions appears surprising since expression of the toxic polyQ protein species during the screen is confined to differentiated

cells of the eye which should not interfere with the viability of the flies. This seeming contradiction may be explained by the fact that silencing of gene expression drains the cell of important regulatory mechanisms normally keeping the toxic effects of polyQ proteins at bay. Furthermore, the truncated Ataxin-3 used in the screen proved to be a highly toxic protein, not allowing for pan-neural expression and leading to a severe neurodegenerative phenotype. It stands to reason that massive cell demise in the course of the expression of elongated polyQ protein is even enhanced in combination with the lack of ameliorating gene action silenced by RNAi. Therefore, the extent of cell death might just overwhelm the capacity of the phagocytic clearance responsible for the uptake of apoptotic cell remainders [286, 287]. As a consequence, cellular debris and released polyQ aggregates would compromise the physiological functioning of adjacent tissues during development or even penetrate and infect other cells [275]. On top of that, GMR-positive cells and therefore polyQ protein expression have also been described to be present in non-retinal areas of the brain [252] whose demise may add to the detrimental effects of developing compound eye degeneration. Eventually, neighbouring neural tissue originally without polyQ protein expression is indirectly affected by polyQ toxicity and normal fly morphogenesis and hatching is prevented.

As a consequence of the large number of lethal candidates, only the RNAi lines producing vital offspring and having analyzable phenotypes were investigated further and grouped into categories reflecting the biological processes they are involved in. Nevertheless, the entire list of candidate lines was utilised for comparison of the results with the outcome of previously conducted modifier screens.

6.2.1 Comparison to related polyQ modifier screens

There are plenty screening approaches that have been implemented in order to discover and investigate modifiers of Ataxin-3 and other polyQ proteins in the physiological and disease state. The results obtained in the present work were compared to the outcome of three studies: an RNAi-based screen for modifiers of polyQ aggregation in *C. elegans* by Nollen *et al.* [267]; a genome-wide screen for modulators of Htt aggregation in *Drosophila* cells by Zhang *et al.* [268] and a genome-wide modifier screen for Ataxin-3-induced neurotoxicity based on misexpression of endogenous *Drosophila* genes by Bilen and Bonini [256].

The categories of candidates obtained in the published screens resemble those specified in **Table 9** representative for the complete modifier list. Zhang *et al.* identified for example chaperones, phosphatases/kinases, proteins involved in transcription and ubiquitin/proteasome pathways. Nollen *et al.* presented candidates grouping into the biological processes of protein synthesis, folding, transport, degradation and additionally RNA synthesis and processing. Bilen and Bonini for their part revealed genetic interactors acting as chaperones, in the ubiquitin pathway or having miscellaneous functions.

Comparing the three screens, the relatively high disparity in the number of obtained candidate genes is striking. Whereas the Bilen screen produced only 18 candidate genes, all other screens exhibit candidate numbers ten times and more as much, with the present work even yielding over five hundred modifiers of polyQ toxic action. This may speak in favour of a greater coverage of the genome by RNAi-based approaches compared to random misexpression of endogenous genes. Additionally, it is reasonable to assume that a loss-of-function of a gene product in a polyQ-burdened cell is more likely to occur and actually have an influence on toxicity than the artificial overexpression of a given gene. On the other hand, an unreasonable high number of candidate genes could also be an indicator for a high percentage of false-positive candidates produced by bystander effects not correlated to polyQ activity. Taking this into account, the chances of such false-positive modifier genes were minimised as far as possible by prior screening for RNAi effects in control flies and replication of crossbreeding for primary candidate hits. The at least in part comparable high numbers of the Nollen and Zhang screens and the present work should nevertheless not hide the fact that the first two were conducted in different models (*C. elegans* and *Drosophila* cells, respectively) and were designed to investigate aggregation of polyQ proteins, not neurotoxicity as in the Bilen and the genome-wide RNAi screen. Consequently, results and possible similarities between all the screens should be taken cautiously. Although the Bilen and Bonini screen uses the same fly model and shares 22 % of its candidate genes with the ones from this work, the higher number of overlapping modifiers in the other screens probably has its origin in the methodically similar RNAi approach (**Figure 23**).

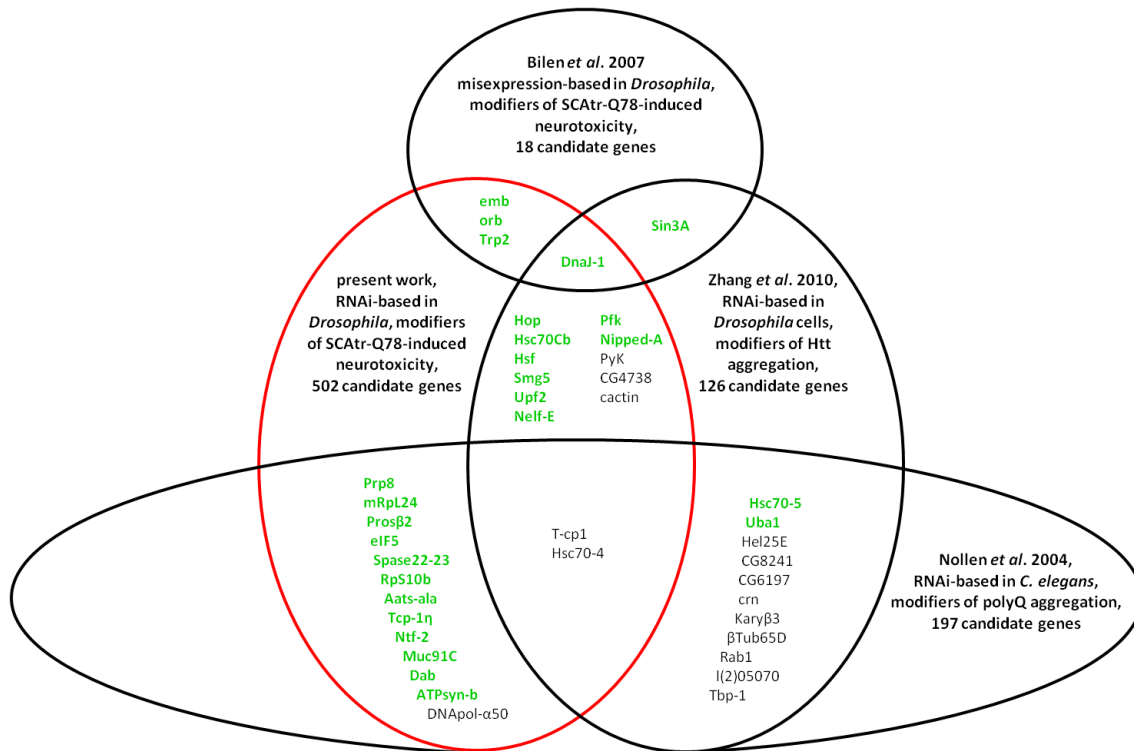


Figure 23. Overlap between screens for genetic modifiers of polyQ-induced neurotoxicity or aggregation.

Venn-like diagram showing genes mutually obtained as genetic modifiers in diverse polyQ protein disease models and screens. Depicted are only candidate genes shared by the different screens, not modifiers unique for one of the single screens. The present work is marked with red encircling. Modifier candidates genetically acting in the same direction (increasing or ameliorating toxicity/aggregation) are marked in green, candidates with opposing direction of action are grey.

Gene symbols are those for *Drosophila* as listed in Gene Database of NCBI [3].

6.2.2 Chaperones as polyQ misfolding and aggregation modifiers

What is evident yet not surprising in all the screens is the high portion of chaperone-related candidate genes. Chaperones and heat shock proteins have been implicated earlier in the amelioration of polyQ toxicity and aggregation [26, 30, 222, 288, 289]. Therefore, depletion of chaperones and their regulatory proteins mostly results in enhanced neurotoxicity and aggregation, whereas the opposite is the case upon increase of chaperone levels. Indeed, co-expression of human chaperone HSP70 substantially suppressed the REP of *GMR_SCA3tr-Q78* flies (not shown). In whole, eight modifier genes of the chaperone class of proteins are shared in different combinations by the four previously described modifier screens. *DnaJ-1* for example is a genetic suppressor of polyQ-induced neurotoxicity in the present work (enhancer if gene is silenced). An ameliorating influence on polyQ aggregation and neurotoxicity was shown by the Zhang and Bilen screens, also

confirmed by a fourth screen on polyQ by Kazemi-Esfarjani and Benzer [28]. A different chaperone-coding gene, *Hsc70-4*, has been published to mitigate SCA3tr-Q78 aggregation, and knockdown in the *C. elegans* screen facilitated aggregate formation. However, Zhang *et al.* reported the *Hsc70-4* gene product to be an enhancer of Htt aggregation and also in the work at hand, silencing of *Hsc70-4* produced an obvious suppression of the REP. The fact that in the present work two RNAi lines for *Hsc70-4* produced comparable effects not only proves the principle of the screen, but additionally renders the obtained result credible. Modulating the activity of this gene might influence aggregation indirectly by interfering with protein functions apart from stress response, in the case of *Hsc70-4* for example clathrin-dependent endocytosis [290, 291]. Despite that, overall chaperone functioning occupies a pivotal role in polyQ protein misfolding and aggregation by retaining or restoring native protein conformation. Thereby, chaperones interfere with the earliest steps of pathogenesis and putatively prevent accumulation and aggregation of toxic proteins in the first place.

6.2.3 Components of the UPS in polyQ pathogenesis

The next noteworthy functional group of modifiers is that of genes involved in ubiquitin- and proteasomal pathways. Ubiquitination of misfolded or dysfunctional proteins and their subsequent degradation by the proteasome is one of the key cellular processes to fight accumulation and aggregation of potentially toxic proteins. Naturally, genes involved in this pathway emerge as modifiers of neurotoxicity as well as aggregation. The RNAi-based screens on *C. elegans* and the present work have the UPS-related candidate *Prosβ2* in common, which genetically acts as a suppressor of aggregation/neurotoxicity in both screens. Another UPS example, *l(2)05070*, was identified as aggregation enhancer in the Zhang screen unlike being a suppressor in the Nollen work. To add to these findings, in the present screen four members of the UPS pathway have been identified as genetically enhancing candidates (**Table 9**) being responsible for either protein ubiquitination or deubiquitination. Additional to the UPS-related genes in **Table 9**, other UPS pathway genes exhibiting lethal effects when knocked down are also listed in **Appendix Table 1**, for example *Uch-L3*, encoding a deubiquitinating hydrolase described as a part of the regulatory complex of the 26S proteasome [292]. One can conclude from these results that with regard to the UPS-related modifiers, a general statement about the impact of the

single components of the pathway on polyQ proteins is not possible. Instead it is necessary to take into account the specificity of the modifier protein (ubiquitinating or deubiquitinating) and its respective substrate protein and affected cellular process. Despite that, a lack of structural constituents of the proteasome, like *Prosβ2*, is in almost every case detrimental for the cell when facing an increased burden of misfolded protein or protein aggregation. An impact of ubiquitination on the physiological function of truncated Ataxin-3 used in the present screen can be excluded since the protein lacks its enzymatically active domains.

In conclusion, by modulating the clearance of misfolded proteins, the members of the UPS pathway are of vital importance for cellular coping with elongated polyQ proteins and are potent modifiers of polyQ toxicity.

6.2.4 PolyQ-induced neurotoxicity modifiers involved in transcriptional regulation

As already mentioned in chapter 2.2.2, transcriptional dysregulation plays an important role in the course of polyQ pathogenesis either by loss-of-function of a mutated regulatory polyQ protein or interference of aggregates or the like with transcription itself. Like in the case of the UPS pathway, no generalised assumption can be made about an overall beneficial or harmful effect of transcriptional regulators on polyQ toxicity. Enhancement of the REP by silencing of *chm* (a histone acetyl transferase, HAT) is in line with the proposed beneficial effect of increasing HAT expression in polyQ disease [72]. Although also representing a HAT and being involved in cell cycle control via *cdc2* [293], silencing of *MRG15* led to suppression of the REP, demonstrating the possible opposing effects of genes with similar function. The same effect was observed for *MRG15* knockdown in the *Tau[R406W]* model, hinting to a rather unspecific disadvantageous influence of *MRG15* in cells affected by toxic proteins. One could speculate about a scenario in which acetylation of the *cdc2* promoter and thereby facilitation of transcription initiates a new mitotic cycle in S phase. Activation of the cell cycle in neurons will drive the anyhow polyQ-stricken cells into apoptosis. This hypothesis demonstrates the detailed consideration of the specific processes the candidate genes are influencing with respect to polyQ toxicity.

6.2.5 Nuclear transport proteins are modifiers of polyQ toxicity

Export from the nuclear compartment via a nuclear export signal (NES) has been shown to be implicated in polyQ pathogenesis. The *Drosophila* orthologue for human *exportin-1* (*Xpo1*), *embargoed* (*emb*), exhibited specificity for export of elongated polyQ proteins and disruption of this process increased polyQ toxicity by polyQ interference with transcription [294]. The deleterious effect of *emb* silencing was confirmed in the present work as well as in the screen of Bilen and Bonini [256]. Additionally, the genome-wide RNAi screen revealed another nuclear transporter, *Exportin-6* (*Exp6*), as being involved in polyQ protein translocation since silencing of this gene resulted in lethality of polyQ flies. Studies have shown that the nuclear environment putatively fosters seeding of polyQ aggregates [295] and aggregation-prone polyQ fragments accumulate in the nucleus after escaping the cytoplasmic protein quality control [296]. Surprisingly, the RNAi screen in *SCA3tr-Q78*-expressing flies additionally revealed several importins, facilitating nuclear import, as being detrimental when knocked down. Among them are *Trn*, homologous to *transportin-1* (*TNPO1*) and *moleskin* (*msk*), orthologue of *importin-7* (*IP07*), furthermore some import-related nuclear pores. It is not clear why a process opposed to nuclear export features the same findings after disruption. Computational analysis identified *msk* as a member of a gene cluster mainly involved in ribosomal and RNA biogenesis with the central gene *Nop56* having recently been linked to SCA36 [297] (not shown). Possibly, the impact of nuclear import on polyQ toxicity is rather indirectly mediated by transcriptional and translational processes.

6.2.6 Further remarks on polyQ toxicity modifiers and the RNAi screen

Several other genes previously implicated in polyQ neurotoxicity and pathogenesis were identified in the present RNAi screen. Silencing of the *Drosophila huntingtin* orthologue had a lethal outcome in polyQ flies connecting SCA3 with the disease gene for Huntington's disease. In the case of another polyQ disorder, SCA2, and its disease gene *ATXN2*, no interaction could be proven despite findings reported previously [298]. Another noteworthy fact is the underrepresentation of autophagy-related genes in the screen results, a finding opposed to the described pivotal role of autophagy in mitigation of polyQ-related neurodegeneration (reviewed in [299]). Only one autophagy gene, *Atg6*, was shown

to potentially suppress SCA3tr-Q78 toxicity in its native state. A reason for this may be the prior screening for RNAi effects in GMR control flies. Members of the autophagy system and also several other genes (chaperones, structural cell constituents, transcription factors, proteasomal components etc.) are with high probability of vital importance for cellular survival themselves. In case that RNAi of these genes already exhibits changes in control flies, they were prevented from evolving as candidates for polyQ toxicity modulation due to the experimental design. However, this does not mean that they do not somehow interfere with elongated polyQ activity.

Representing a novel revelation, the biological process of lipid metabolism and, more precisely, of sphingolipid metabolism showed interesting influence on polyQ toxicity. Four members of this biological process are listed in **Table 9** as obvious modifiers of polyQ-induced REP and several others exhibited lethal outcome following knockdown in *SCA3tr-Q78* flies. Since sphingolipid pathways have been implicated in neurodegeneration [300] and impinge on diverse crucial cellular processes (apoptosis, differentiation, proliferation [301]), it would be worthwhile to further investigate the intertwining of these lipid-related mechanisms with respect to their impact on polyQ toxicity.

The relatively small overlap between the polyQ RNAi screen and the findings made in *Tau[R406W]*-expressing flies underlines the specificity of the discovered modifiers for SCA3-linked pathogenesis. Nevertheless, the majority of genes being modifiers in both screens exhibit the same mode of change in their respective REP. For some candidates, this might be explained by the general importance of these genes in cellular coping strategies against proteotoxic stress. *Prosβ2* and *Rpn9*, both structural constituents of the proteasome, are examples for fundamental genes in order to fight misfolded/aggregated proteins. Due to the fact that silencing *Prosβ2* and *Rpn9* had no effect in control flies, a general necessity for survival cannot be deduced from the lethal outcome of silencing of these two genes in the disease models.

6.3 Aggregation in *SCA3tr-Q78*-shRNA-coexpressing flies

It has been shown previously biochemically [276] and immunohistochemically [256] that several genes, especially chaperones, feature aggregate-mitigating properties on polyQ proteins. Despite these findings, the conduction of a large-scale analysis of aggregation with filter retardation approaches yielded contradictory results. Whereas

some, yet by far not the majority of REP suppressor candidates decreased the load of SDS-insoluble polyQ aggregates, this was also the case for a number of REP enhancers. Given the proposed connection between aggregate formation and polyQ neurotoxicity, these results are at least surprising and cannot be explained by slight changes in deployed protein amount during the experiment. It might well be that the mode of sample preparation depletes a certain amount of higher molecular aggregates; however, these are not considered to be the actual toxic species. One reasonable explanation for the differential outcome of REP suppressors may be the high number of investigated genes compared to previous studies, producing a more comprehensive image of aggregation modulation. Furthermore, the influences of the various modifiers on polyQ aggregation might be more complex and cannot be reduced to simple molecular mechanisms somehow being related to aggregation. The reason for the missing correlation between SDS-insoluble aggregates, microscopically visible inclusions and polyQ neurotoxicity lies presumably in the differential nature of the aggregate species. Inclusions are considered to be rather beneficial for the cell, protecting it from the detrimental effects of the unbound, yet SDS-insoluble polyQ oligomers. Here again, further investigations are necessary prior to giving a reliable statement about advantageous or disadvantageous effects of modifiers on the various aggregation states.

6.4 The role of TRMT2A in polyQ pathogenesis

Knockdown of the *Drosophila* orthologue of *tRNA methyltransferase 2 homologue A* (*TRMT2A*), *CG3808*, in the *SCA3tr-Q78* modifier screen exhibited some of the most potent effects with regard to the suppression of the REP and amelioration of polyQ aggregate load. Furthermore, *CG3808* silencing in *Drosophila* rescued lethality of flies with pan-neural expression of *SCA3tr-Q78*, restored photoreceptor neuron loss and prolonged polyQ-compromised longevity in an adult-onset disease model. Moreover, select findings could also be extended to fly models for other polyQ disorders like HD and SCA1. Given the fact that these are complete novel observations and tRNA methyltransferases have never before been implicated in polyQ pathogenesis, nor is there an obvious mechanistic connection, these results are rather surprising. Eventually, effects like mitigation of aggregate load could be even recapitulated in mammalian HEK cells stably transfected with shRNA against *TRMT2A*.

Studies on patient tissue presented an association between the expression of *TRMT2A* in humans and the recurrence in breast cancer in a subset of patients [302]. Apart from that, the only link to neurological disorders is a putative connection of a single nucleotide polymorphisms in the *TRMT2A* gene with schizophrenia [303]

The process of tRNA methylation is a crucial event in the high-fidelity translation of mRNA into polypeptides. tRNA methyltransferase enzymes are according to their specificity capable of linking a methyl group to a tRNA base, hereby changing the chemical properties of this residue. Dependent on the location of the mentioned nucleotide, tRNA methylation interferes with different mechanisms prior to and during translation of mRNA into proteins and exhibits a pivotal influence upon tRNA stability and maturation [304-306]. It is reasonable to assume that silencing of methyltransferase expression and thus lacking tRNA modification might hamper one of these processes. As a consequence, aminoacylation of tRNA may decline in fidelity, leaving the tRNA associated with an incorrect amino acid. Upon introduction of this false component into the polypeptide chain, the chemical properties of the resulting protein are likely to be altered in conformation due to changed molecular interactions and also with respect to enzymatic activity caused by modified active sites.

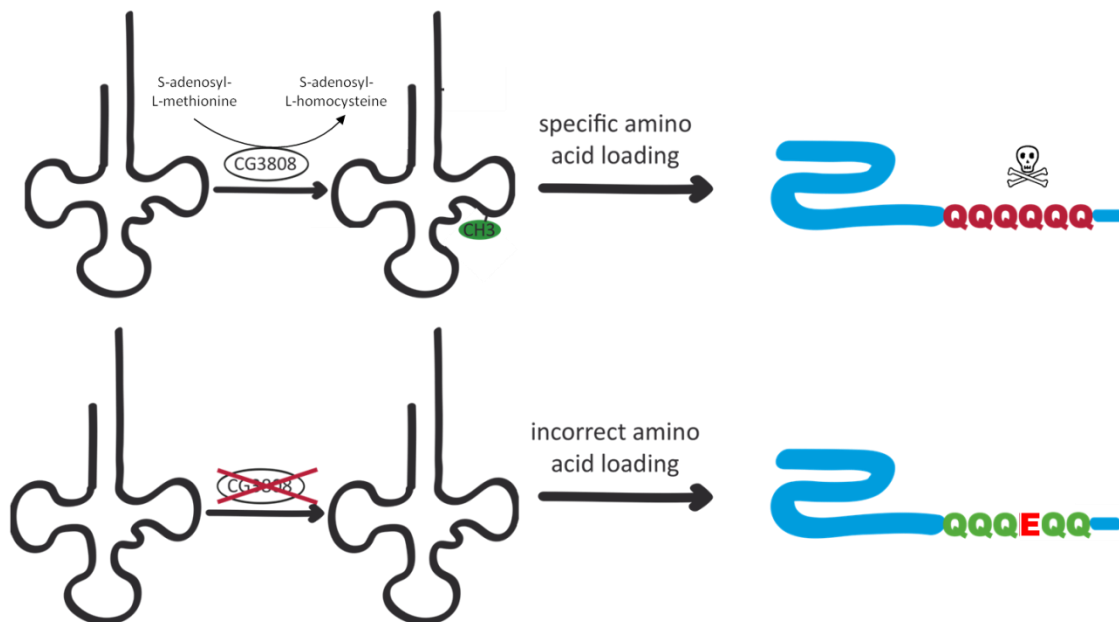


Figure 24. Putative mechanistic explanation of polyQ toxicity amelioration by *TRMT2A* knockdown.

(A) Under normal conditions, the *Drosophila TRMT2A* orthologue, *CG3808*, transfers a methyl group onto uridine 54 of the tRNA. Thereby, high-fidelity amino acid loading is ensured. In the case of mutated polyQ disease genes, this results in an elongated glutamine repeat domain which is detrimental for the cell. (B) Silencing of *CG3808* and consecutive lack of tRNA methylation may render tRNA-amino acid linkage inaccurate, resulting in introduction of a different amino acid into the polyQ stretch (here E, glutamate). This would decrease toxicity of the polyQ domain to a great extent.

Taking into account the generalised effect of *TRMT2A* knockdown in diverse polyQ models, the variances are more probable to be confined to the polyQ tract, the only common feature of the disease proteins. Unfortunately, until now we were not able to prove this hypothesis due to experimental restrictions, like impossible analysis of the polyQ stretch by mass spectrometry, or show experimental evidence for specificity of the putative mechanism for polyQ proteins. However, *CG3808* silencing failed to show an effect on the REP of other neurodegenerative disease models (TDP-43, not shown) or exhibited a different REP modification in the *Tau[R406W]* flies (lethal, not shown). Therefore, a certain specificity for polyQ proteins was substantiated. Hopefully, future experiments profiting from the putative erratic introduction of amino acids in the polyQ domain following *TRMT2A* silencing will shed more light on the mechanistic basis of methyltransferase silencing and polyQ pathogenesis. The significant increase of polyQ inclusion bodies in *TRMT2A* knockdown cells leaves additional room for speculations as to how this presumably beneficial detoxification process is brought about following *TRMT2A* silencing. A slightly different explanatory approach is conceivable with respect to target specificity of *TRMT2A*. It transfers a methyl group onto uridine at position 54 of the tRNA, producing 5-methyluridine (ribothymidine) in the T-loop structure (**Figure 25A**) [307]. Disruption of this process may lead to subsequent hampering of T-loop-related processes in the course of translation, for example binding to the ribosome or distinct aminoacylation. Since no general disturbance of protein production was observed, interference with translational processes according to this theory would be confined to specific amino acids and proteins like polyQ by unknown mechanisms.

Although investigations on the molecular basis of the *TRMT2A* influence on polyQ toxicity have not yielded enlightening results so far, the remarkable findings described in this work make this protein and its related processes a worthwhile target of further experimentation.

7 Summary and Concluding Remarks

Almost two decades have passed since the discovery of the elongated polyQ stretch as the molecular pathological basis of polyQ diseases. Despite this time of extensive scientific effort, it is still not clear which cellular pathways and mechanisms ultimately lead to polyQ toxicity or what the definite toxic species during pathogenesis is. Numerous approaches have focused on single molecular processes and yielded insight into their impact on polyQ proteins, nevertheless we are still lacking a comprehensive overview or network of polyQ pathogenesis and the cellular proteins involved therein. The respective knowledge is an imperative prerequisite in order to develop feasible treatment approaches to eventually cure these devastating disorders.

In an attempt to contribute to revelation of disease mechanisms and modulations thereof, we conducted a large-scale RNAi screen for modifiers of truncated SCA3 protein-induced neurotoxicity in *Drosophila*. As a result we were able to obtain a set of potential genetic interactors of polyQ proteins in the course of the disease. Together with already known modifier genes like chaperones, UPS pathway members and nuclear exportins, the experiments yielded novel genes involved in processes previously not described for polyQ disease. Genes responsible for sphingolipid metabolism seem to play a role in the emergence of neurodegeneration as well as nuclear importins and genes responsible for ribosome biogenesis. The results furthermore revealed the strong potency of the tRNA methyltransferase TRMT2A and its *Drosophila* equivalent CG3808 to modify polyQ toxicity by so far unknown mechanisms.

Concluding, the genes obtained as polyQ neurotoxicity modulators during the RNAi screen and in subsequent experiments provide a promising entity of genetic interactors of polyQ protein and a valuable pool for future research in order to shed light on polyQ pathogenesis.

8 Bibliography

1. Bates, G., *Huntingtin aggregation and toxicity in Huntington's disease*. *Lancet*, 2003. **361**(9369): p. 1642-4.
2. Takahashi, T., S. Katada, and O. Onodera, *Polyglutamine Diseases: Where Does Toxicity Come From? What Is Toxicity? Where Are We Going?* *J Mol Cell Biol*, 2010.
3. *NCBI Gene*. November/December 2011; Available from: <http://www.ncbi.nlm.nih.gov/gene/>.
4. Schols, L., et al., *Autosomal dominant cerebellar ataxias: clinical features, genetics, and pathogenesis*. *Lancet Neurol*, 2004. **3**(5): p. 291-304.
5. Walker, L.C. and H. LeVine, *The cerebral proteopathies: neurodegenerative disorders of protein conformation and assembly*. *Mol Neurobiol*, 2000. **21**(1-2): p. 83-95.
6. Luheshi, L.M., D.C. Crowther, and C.M. Dobson, *Protein misfolding and disease: from the test tube to the organism*. *Curr Opin Chem Biol*, 2008. **12**(1): p. 25-31.
7. La Spada, A.R. and J.P. Taylor, *Repeat expansion disease: progress and puzzles in disease pathogenesis*. *Nat Rev Genet*, 2010.
8. Orr, H.T. and H.Y. Zoghbi, *Trinucleotide repeat disorders*. *Annu Rev Neurosci*, 2007. **30**: p. 575-621.
9. La Spada, A.R., H.L. Paulson, and K.H. Fischbeck, *Trinucleotide repeat expansion in neurological disease*. *Ann Neurol*, 1994. **36**(6): p. 814-22.
10. Zoghbi, H.Y. and H.T. Orr, *Glutamine repeats and neurodegeneration*. *Annu Rev Neurosci*, 2000. **23**: p. 217-47.
11. Igarashi, S., et al., *Strong correlation between the number of CAG repeats in androgen receptor genes and the clinical onset of features of spinal and bulbar muscular atrophy*. *Neurology*, 1992. **42**(12): p. 2300-2.
12. Orr, H.T., *Beyond the Qs in the polyglutamine diseases*. *Genes Dev*, 2001. **15**(8): p. 925-32.
13. Gatchel, J.R. and H.Y. Zoghbi, *Diseases of unstable repeat expansion: mechanisms and common principles*. *Nat Rev Genet*, 2005. **6**(10): p. 743-55.
14. Bird, T.D., *Hereditary Ataxia Overview*. 1993.
15. Klement, I.A., et al., *Ataxin-1 nuclear localization and aggregation: role in polyglutamine-induced disease in SCA1 transgenic mice*. *Cell*, 1998. **95**(1): p. 41-53.
16. Saudou, F., et al., *Huntingtin acts in the nucleus to induce apoptosis but death does not correlate with the formation of intranuclear inclusions*. *Cell*, 1998. **95**(1): p. 55-66.
17. Stott, K., et al., *Incorporation of glutamine repeats makes protein oligomerize: implications for neurodegenerative diseases*. *Proc Natl Acad Sci U S A*, 1995. **92**(14): p. 6509-13.
18. Lathrop, R.H., et al., *Modeling protein homopolymeric repeats: possible polyglutamine structural motifs for Huntington's disease*. *Proc Int Conf Intell Syst Mol Biol*, 1998. **6**: p. 105-14.
19. Tanaka, M., et al., *Intra- and intermolecular beta-pleated sheet formation in glutamine-repeat inserted myoglobin as a model for polyglutamine diseases*. *J Biol Chem*, 2001. **276**(48): p. 45470-5.
20. Perutz, M.F., et al., *Amyloid fibers are water-filled nanotubes*. *Proc Natl Acad Sci U S A*, 2002. **99**(8): p. 5591-5.
21. Thakur, A.K. and R. Wetzel, *Mutational analysis of the structural organization of polyglutamine aggregates*. *Proc Natl Acad Sci U S A*, 2002. **99**(26): p. 17014-9.

22. Nagai, Y., et al., *A toxic monomeric conformer of the polyglutamine protein*. Nat Struct Mol Biol, 2007. **14**(4): p. 332-40.
23. Takahashi, T., et al., *Soluble polyglutamine oligomers formed prior to inclusion body formation are cytotoxic*. Hum Mol Genet, 2008. **17**(3): p. 345-56.
24. Walsh, D.M., et al., *Naturally secreted oligomers of amyloid beta protein potently inhibit hippocampal long-term potentiation in vivo*. Nature, 2002. **416**(6880): p. 535-9.
25. Perutz, M.F., et al., *Glutamine repeats as polar zippers: their possible role in inherited neurodegenerative diseases*. Proc Natl Acad Sci U S A, 1994. **91**(12): p. 5355-8.
26. Behrends, C., et al., *Chaperonin TRiC promotes the assembly of polyQ expansion proteins into nontoxic oligomers*. Mol Cell, 2006. **23**(6): p. 887-97.
27. Scherzinger, E., et al., *Self-assembly of polyglutamine-containing huntingtin fragments into amyloid-like fibrils: implications for Huntington's disease pathology*. Proc Natl Acad Sci U S A, 1999. **96**(8): p. 4604-9.
28. Kazemi-Esfarjani, P. and S. Benzer, *Genetic suppression of polyglutamine toxicity in Drosophila*. Science, 2000. **287**(5459): p. 1837-40.
29. Muchowski, P.J. and J.L. Wacker, *Modulation of neurodegeneration by molecular chaperones*. Nat Rev Neurosci, 2005. **6**(1): p. 11-22.
30. Warrick, J.M., et al., *Suppression of polyglutamine-mediated neurodegeneration in Drosophila by the molecular chaperone HSP70*. Nat Genet, 1999. **23**(4): p. 425-8.
31. Li, M., et al., *Soluble androgen receptor oligomers underlie pathology in a mouse model of spinobulbar muscular atrophy*. J Biol Chem, 2007. **282**(5): p. 3157-64.
32. Poirier, M.A., et al., *Huntingtin spheroids and protofibrils as precursors in polyglutamine fibrilization*. J Biol Chem, 2002. **277**(43): p. 41032-7.
33. Kaye, R., et al., *Common structure of soluble amyloid oligomers implies common mechanism of pathogenesis*. Science, 2003. **300**(5618): p. 486-9.
34. Sanchez, I., C. Mahlke, and J. Yuan, *Pivotal role of oligomerization in expanded polyglutamine neurodegenerative disorders*. Nature, 2003. **421**(6921): p. 373-9.
35. Mangiarini, L., et al., *Exon 1 of the HD gene with an expanded CAG repeat is sufficient to cause a progressive neurological phenotype in transgenic mice*. Cell, 1996. **87**(3): p. 493-506.
36. Kaye, R., et al., *Fibril specific, conformation dependent antibodies recognize a generic epitope common to amyloid fibrils and fibrillar oligomers that is absent in prefibrillar oligomers*. Mol Neurodegener, 2007. **2**: p. 18.
37. Davies, S.W., et al., *Formation of neuronal intranuclear inclusions underlies the neurological dysfunction in mice transgenic for the HD mutation*. Cell, 1997. **90**(3): p. 537-48.
38. Ross, C.A., *Intranuclear neuronal inclusions: a common pathogenic mechanism for glutamine-repeat neurodegenerative diseases?* Neuron, 1997. **19**(6): p. 1147-50.
39. Martindale, D., et al., *Length of huntingtin and its polyglutamine tract influences localization and frequency of intracellular aggregates*. Nat Genet, 1998. **18**(2): p. 150-4.
40. Yamada, M., S. Tsuji, and H. Takahashi, *Pathology of CAG repeat diseases*. Neuropathology, 2000. **20**(4): p. 319-25.
41. Trotter, Y., et al., *Polyglutamine expansion as a pathological epitope in Huntington's disease and four dominant cerebellar ataxias*. Nature, 1995. **378**(6555): p. 403-6.
42. Nucifora, F.C., Jr., et al., *Interference by huntingtin and atrophin-1 with cbp-mediated transcription leading to cellular toxicity*. Science, 2001. **291**(5512): p. 2423-8.
43. Morfini, G., G. Pigino, and S.T. Brady, *Polyglutamine expansion diseases: failing to deliver*. Trends Mol Med, 2005. **11**(2): p. 64-70.

44. Kim, M., et al., *Mutant huntingtin expression in clonal striatal cells: dissociation of inclusion formation and neuronal survival by caspase inhibition*. J Neurosci, 1999. **19**(3): p. 964-73.
45. Yu, Z.X., et al., *Huntingtin inclusions do not deplete polyglutamine-containing transcription factors in HD mice*. Hum Mol Genet, 2002. **11**(8): p. 905-14.
46. Arrasate, M., et al., *Inclusion body formation reduces levels of mutant huntingtin and the risk of neuronal death*. Nature, 2004. **431**(7010): p. 805-10.
47. Walker, F.O., *Huntington's disease*. Lancet, 2007. **369**(9557): p. 218-28.
48. Robitaille, Y., et al., *The neuropathology of CAG repeat diseases: review and update of genetic and molecular features*. Brain Pathol, 1997. **7**(3): p. 901-26.
49. Rub, U., et al., *Degeneration of the central vestibular system in spinocerebellar ataxia type 3 (SCA3) patients and its possible clinical significance*. Neuropathol Appl Neurobiol, 2004. **30**(4): p. 402-14.
50. Rub, U., E.R. Brunt, and T. Deller, *New insights into the pathoanatomy of spinocerebellar ataxia type 3 (Machado-Joseph disease)*. Curr Opin Neurol, 2008. **21**(2): p. 111-6.
51. Li, S. and X.J. Li, *Multiple pathways contribute to the pathogenesis of Huntington disease*. Mol Neurodegener, 2006. **1**: p. 19.
52. Lam, Y.C., et al., *ATAXIN-1 interacts with the repressor Capicua in its native complex to cause SCA1 neuropathology*. Cell, 2006. **127**(7): p. 1335-47.
53. Lim, J., et al., *Opposing effects of polyglutamine expansion on native protein complexes contribute to SCA1*. Nature, 2008. **452**(7188): p. 713-8.
54. Zoghbi, H.Y. and H.T. Orr, *Pathogenic mechanisms of a polyglutamine-mediated neurodegenerative disease, spinocerebellar ataxia type 1*. J Biol Chem, 2009. **284**(12): p. 7425-9.
55. Palazzolo, I., et al., *Akt blocks ligand binding and protects against expanded polyglutamine androgen receptor toxicity*. Hum Mol Genet, 2007. **16**(13): p. 1593-603.
56. Humbert, S., et al., *The IGF-1/Akt pathway is neuroprotective in Huntington's disease and involves Huntingtin phosphorylation by Akt*. Dev Cell, 2002. **2**(6): p. 831-7.
57. Warby, S.C., et al., *Huntingtin phosphorylation on serine 421 is significantly reduced in the striatum and by polyglutamine expansion in vivo*. Hum Mol Genet, 2005. **14**(11): p. 1569-77.
58. Chen, H.K., et al., *Interaction of Akt-phosphorylated ataxin-1 with 14-3-3 mediates neurodegeneration in spinocerebellar ataxia type 1*. Cell, 2003. **113**(4): p. 457-68.
59. Terashima, T., et al., *SUMO-1 co-localized with mutant atrophin-1 with expanded polyglutamines accelerates intranuclear aggregation and cell death*. Neuroreport, 2002. **13**(17): p. 2359-64.
60. Steffan, J.S., et al., *SUMO modification of Huntingtin and Huntington's disease pathology*. Science, 2004. **304**(5667): p. 100-4.
61. Subramaniam, S., et al., *Rhes, a striatal specific protein, mediates mutant-huntingtin cytotoxicity*. Science, 2009. **324**(5932): p. 1327-30.
62. Goti, D., et al., *A mutant ataxin-3 putative-cleavage fragment in brains of Machado-Joseph disease patients and transgenic mice is cytotoxic above a critical concentration*. J Neurosci, 2004. **24**(45): p. 10266-79.
63. Hoffner, G., M.L. Island, and P. Djian, *Purification of neuronal inclusions of patients with Huntington's disease reveals a broad range of N-terminal fragments of expanded huntingtin and insoluble polymers*. J Neurochem, 2005. **95**(1): p. 125-36.

64. Colomer Gould, V.F., et al., *A mutant ataxin-3 fragment results from processing at a site N-terminal to amino acid 190 in brain of Machado-Joseph disease-like transgenic mice*. *Neurobiol Dis*, 2007. **27**(3): p. 362-9.
65. Berke, S.J., et al., *Caspase-mediated proteolysis of the polyglutamine disease protein ataxin-3*. *J Neurochem*, 2004. **89**(4): p. 908-18.
66. Luo, S., et al., *Cdk5 phosphorylation of huntingtin reduces its cleavage by caspases: implications for mutant huntingtin toxicity*. *J Cell Biol*, 2005. **169**(4): p. 647-56.
67. Schilling, B., et al., *Huntingtin phosphorylation sites mapped by mass spectrometry. Modulation of cleavage and toxicity*. *J Biol Chem*, 2006. **281**(33): p. 23686-97.
68. Shimohata, T., et al., *Expanded polyglutamine stretches interact with TAFII130, interfering with CREB-dependent transcription*. *Nat Genet*, 2000. **26**(1): p. 29-36.
69. Dunah, A.W., et al., *Sp1 and TAFII130 transcriptional activity disrupted in early Huntington's disease*. *Science*, 2002. **296**(5576): p. 2238-43.
70. Luthi-Carter, R., et al., *Polyglutamine and transcription: gene expression changes shared by DRPLA and Huntington's disease mouse models reveal context-independent effects*. *Hum Mol Genet*, 2002. **11**(17): p. 1927-37.
71. Sadri-Vakili, G., et al., *Histones associated with downregulated genes are hypoacetylated in Huntington's disease models*. *Hum Mol Genet*, 2007. **16**(11): p. 1293-306.
72. Selvi, B.R., et al., *Tuning acetylation levels with HAT activators: therapeutic strategy in neurodegenerative diseases*. *Biochim Biophys Acta*, 2010.
73. Butler, R. and G.P. Bates, *Histone deacetylase inhibitors as therapeutics for polyglutamine disorders*. *Nat Rev Neurosci*, 2006. **7**(10): p. 784-96.
74. Sadri-Vakili, G. and J.H. Cha, *Histone deacetylase inhibitors: a novel therapeutic approach to Huntington's disease (complex mechanism of neuronal death)*. *Curr Alzheimer Res*, 2006. **3**(4): p. 403-8.
75. Steffan, J.S., et al., *Histone deacetylase inhibitors arrest polyglutamine-dependent neurodegeneration in Drosophila*. *Nature*, 2001. **413**(6857): p. 739-43.
76. Hockly, E., et al., *Suberoylanilide hydroxamic acid, a histone deacetylase inhibitor, ameliorates motor deficits in a mouse model of Huntington's disease*. *Proc Natl Acad Sci U S A*, 2003. **100**(4): p. 2041-6.
77. Evert, B.O., et al., *Ataxin-3 represses transcription via chromatin binding, interaction with histone deacetylase 3, and histone deacetylation*. *J Neurosci*, 2006. **26**(44): p. 11474-86.
78. Paulson, H.L., et al., *Intranuclear inclusions of expanded polyglutamine protein in spinocerebellar ataxia type 3*. *Neuron*, 1997. **19**(2): p. 333-44.
79. Chai, Y., et al., *Evidence for proteasome involvement in polyglutamine disease: localization to nuclear inclusions in SCA3/MJD and suppression of polyglutamine aggregation in vitro*. *Hum Mol Genet*, 1999. **8**(4): p. 673-82.
80. Bence, N.F., R.M. Sampat, and R.R. Kopito, *Impairment of the ubiquitin-proteasome system by protein aggregation*. *Science*, 2001. **292**(5521): p. 1552-5.
81. Bennett, E.J., et al., *Global changes to the ubiquitin system in Huntington's disease*. *Nature*, 2007. **448**(7154): p. 704-8.
82. Venkatraman, P., et al., *Eukaryotic proteasomes cannot digest polyglutamine sequences and release them during degradation of polyglutamine-containing proteins*. *Mol Cell*, 2004. **14**(1): p. 95-104.
83. de Pril, R., et al., *Accumulation of aberrant ubiquitin induces aggregate formation and cell death in polyglutamine diseases*. *Hum Mol Genet*, 2004. **13**(16): p. 1803-13.

84. Bowman, A.B., et al., *Neuronal dysfunction in a polyglutamine disease model occurs in the absence of ubiquitin-proteasome system impairment and inversely correlates with the degree of nuclear inclusion formation*. Hum Mol Genet, 2005. **14**(5): p. 679-91.
85. Bett, J.S., et al., *Proteasome impairment does not contribute to pathogenesis in R6/2 Huntington's disease mice: exclusion of proteasome activator REGgamma as a therapeutic target*. Hum Mol Genet, 2006. **15**(1): p. 33-44.
86. Bett, J.S., et al., *The ubiquitin-proteasome reporter GFPu does not accumulate in neurons of the R6/2 transgenic mouse model of Huntington's disease*. PLoS One, 2009. **4**(4): p. e5128.
87. Todi, S.V., et al., *Ubiquitination directly enhances activity of the deubiquitinating enzyme ataxin-3*. EMBO J, 2009. **28**(4): p. 372-82.
88. Lin, M.T. and M.F. Beal, *Mitochondrial dysfunction and oxidative stress in neurodegenerative diseases*. Nature, 2006. **443**(7113): p. 787-95.
89. Bossy-Wetzell, E., A. Petrilli, and A.B. Knott, *Mutant huntingtin and mitochondrial dysfunction*. Trends Neurosci, 2008. **31**(12): p. 609-16.
90. Browne, S.E., et al., *Oxidative damage and metabolic dysfunction in Huntington's disease: selective vulnerability of the basal ganglia*. Ann Neurol, 1997. **41**(5): p. 646-53.
91. Panov, A.V., et al., *Early mitochondrial calcium defects in Huntington's disease are a direct effect of polyglutamines*. Nat Neurosci, 2002. **5**(8): p. 731-6.
92. Cui, L., et al., *Transcriptional repression of PGC-1alpha by mutant huntingtin leads to mitochondrial dysfunction and neurodegeneration*. Cell, 2006. **127**(1): p. 59-69.
93. Song, W., et al., *Mutant huntingtin binds the mitochondrial fission GTPase dynamin-related protein-1 and increases its enzymatic activity*. Nat Med, 2011.
94. Andreassen, O.A., et al., *Creatine increase survival and delays motor symptoms in a transgenic animal model of Huntington's disease*. Neurobiol Dis, 2001. **8**(3): p. 479-91.
95. Schilling, G., et al., *Coenzyme Q10 and remacemide hydrochloride ameliorate motor deficits in a Huntington's disease transgenic mouse model*. Neurosci Lett, 2001. **315**(3): p. 149-53.
96. Schilling, G., et al., *Environmental, pharmacological, and genetic modulation of the HD phenotype in transgenic mice*. Exp Neurol, 2004. **187**(1): p. 137-49.
97. Gunawardena, S., et al., *Disruption of axonal transport by loss of huntingtin or expression of pathogenic polyQ proteins in Drosophila*. Neuron, 2003. **40**(1): p. 25-40.
98. Caviston, J.P., et al., *Huntingtin facilitates dynein/dynactin-mediated vesicle transport*. Proc Natl Acad Sci U S A, 2007. **104**(24): p. 10045-50.
99. Szebenyi, G., et al., *Neuropathogenic forms of huntingtin and androgen receptor inhibit fast axonal transport*. Neuron, 2003. **40**(1): p. 41-52.
100. Feany, M.B. and A.R. La Spada, *Polyglutamines stop traffic: axonal transport as a common target in neurodegenerative diseases*. Neuron, 2003. **40**(1): p. 1-2.
101. Lee, W.C., M. Yoshihara, and J.T. Littleton, *Cytoplasmic aggregates trap polyglutamine-containing proteins and block axonal transport in a Drosophila model of Huntington's disease*. Proc Natl Acad Sci U S A, 2004. **101**(9): p. 3224-9.
102. Sinadinos, C., et al., *Live axonal transport disruption by mutant huntingtin fragments in Drosophila motor neuron axons*. Neurobiol Dis, 2009. **34**(2): p. 389-95.
103. Vonsattel, J.P., et al., *Neuropathological classification of Huntington's disease*. J Neuropathol Exp Neurol, 1985. **44**(6): p. 559-77.
104. Reis, S.A., et al., *Striatal neurons expressing full-length mutant huntingtin exhibit decreased N-cadherin and altered neuritogenesis*. Hum Mol Genet, 2011. **20**(12): p. 2344-55.

105. Fossale, E., et al., *Differential effects of the Huntington's disease CAG mutation in striatum and cerebellum are quantitative not qualitative*. Hum Mol Genet, 2011.
106. Warby, S.C., R.K. Graham, and M.R. Hayden, *Huntington Disease*. 1993.
107. *A novel gene containing a trinucleotide repeat that is expanded and unstable on Huntington's disease chromosomes. The Huntington's Disease Collaborative Research Group*. Cell, 1993. **72**(6): p. 971-83.
108. Chong, S.S., et al., *Contribution of DNA sequence and CAG size to mutation frequencies of intermediate alleles for Huntington disease: evidence from single sperm analyses*. Hum Mol Genet, 1997. **6**(2): p. 301-9.
109. Nance, M.A., et al., *Analysis of a very large trinucleotide repeat in a patient with juvenile Huntington's disease*. Neurology, 1999. **52**(2): p. 392-4.
110. Strong, T.V., et al., *Widespread expression of the human and rat Huntington's disease gene in brain and nonneural tissues*. Nat Genet, 1993. **5**(3): p. 259-65.
111. Bhide, P.G., et al., *Expression of normal and mutant huntingtin in the developing brain*. J Neurosci, 1996. **16**(17): p. 5523-35.
112. Cattaneo, E., C. Zuccato, and M. Tartari, *Normal huntingtin function: an alternative approach to Huntington's disease*. Nat Rev Neurosci, 2005. **6**(12): p. 919-30.
113. Andrade, M.A. and P. Bork, *HEAT repeats in the Huntington's disease protein*. Nat Genet, 1995. **11**(2): p. 115-6.
114. Goehler, H., et al., *A protein interaction network links GIT1, an enhancer of huntingtin aggregation, to Huntington's disease*. Mol Cell, 2004. **15**(6): p. 853-65.
115. Nasir, J., et al., *Targeted disruption of the Huntington's disease gene results in embryonic lethality and behavioral and morphological changes in heterozygotes*. Cell, 1995. **81**(5): p. 811-23.
116. Zuccato, C., et al., *Loss of huntingtin-mediated BDNF gene transcription in Huntington's disease*. Science, 2001. **293**(5529): p. 493-8.
117. Hoffner, G., P. Kahlem, and P. Djian, *Perinuclear localization of huntingtin as a consequence of its binding to microtubules through an interaction with beta-tubulin: relevance to Huntington's disease*. J Cell Sci, 2002. **115**(Pt 5): p. 941-8.
118. DiFiglia, M., et al., *Huntingtin is a cytoplasmic protein associated with vesicles in human and rat brain neurons*. Neuron, 1995. **14**(5): p. 1075-81.
119. Durr, A., *Autosomal dominant cerebellar ataxias: polyglutamine expansions and beyond*. Lancet Neurol, 2010. **9**(9): p. 885-94.
120. McMurray, C.T., *Mechanisms of trinucleotide repeat instability during human development*. Nat Rev Genet. **11**(11): p. 786-99.
121. Mirkin, S.M., *Expandable DNA repeats and human disease*. Nature, 2007. **447**(7147): p. 932-40.
122. Kovtun, I.V. and C.T. McMurray, *Features of trinucleotide repeat instability in vivo*. Cell Res, 2008. **18**(1): p. 198-213.
123. Orr, H.T., et al., *Expansion of an unstable trinucleotide CAG repeat in spinocerebellar ataxia type 1*. Nat Genet, 1993. **4**(3): p. 221-6.
124. Bryer, A., et al., *The hereditary adult-onset ataxias in South Africa*. J Neurol Sci, 2003. **216**(1): p. 47-54.
125. Brusco, A., et al., *Molecular genetics of hereditary spinocerebellar ataxia: mutation analysis of spinocerebellar ataxia genes and CAG/CTG repeat expansion detection in 225 Italian families*. Arch Neurol, 2004. **61**(5): p. 727-33.
126. Sh, S. and T. Ashizawa, *Spinocerebellar Ataxia Type 1*. 1993.
127. Sasaki, H., et al., *Clinical features and natural history of spinocerebellar ataxia type 1*. Acta Neurol Scand, 1996. **93**(1): p. 64-71.

128. Schols, L., et al., *Autosomal dominant cerebellar ataxia: phenotypic differences in genetically defined subtypes?* Ann Neurol, 1997. **42**(6): p. 924-32.
129. Servadio, A., et al., *Expression analysis of the ataxin-1 protein in tissues from normal and spinocerebellar ataxia type 1 individuals.* Nat Genet, 1995. **10**(1): p. 94-8.
130. Matilla, A., et al., *Mice lacking ataxin-1 display learning deficits and decreased hippocampal paired-pulse facilitation.* J Neurosci, 1998. **18**(14): p. 5508-16.
131. Goldfarb, L.G., et al., *Unstable triplet repeat and phenotypic variability of spinocerebellar ataxia type 1.* Ann Neurol, 1996. **39**(4): p. 500-6.
132. Zuhlke, C., et al., *Spinocerebellar ataxia type 1 (SCA1): phenotype-genotype correlation studies in intermediate alleles.* Eur J Hum Genet, 2002. **10**(3): p. 204-9.
133. Zoghbi, H.Y., et al., *Spinocerebellar ataxia: variable age of onset and linkage to human leukocyte antigen in a large kindred.* Ann Neurol, 1988. **23**(6): p. 580-4.
134. Matsuyama, Z., et al., *The effect of CAT trinucleotide interruptions on the age at onset of spinocerebellar ataxia type 1 (SCA1).* J Med Genet, 1999. **36**(7): p. 546-8.
135. Cummings, C.J., et al., *Mutation of the E6-AP ubiquitin ligase reduces nuclear inclusion frequency while accelerating polyglutamine-induced pathology in SCA1 mice.* Neuron, 1999. **24**(4): p. 879-92.
136. Fernandez-Funez, P., et al., *Identification of genes that modify ataxin-1-induced neurodegeneration.* Nature, 2000. **408**(6808): p. 101-6.
137. Cummings, C.J., et al., *Over-expression of inducible HSP70 chaperone suppresses neuropathology and improves motor function in SCA1 mice.* Hum Mol Genet, 2001. **10**(14): p. 1511-8.
138. Park, Y., et al., *Proteasome function is inhibited by polyglutamine-expanded ataxin-1, the SCA1 gene product.* Mol Cells, 2005. **19**(1): p. 23-30.
139. Emamian, E.S., et al., *Serine 776 of ataxin-1 is critical for polyglutamine-induced disease in SCA1 transgenic mice.* Neuron, 2003. **38**(3): p. 375-87.
140. Saleem, Q., et al., *Molecular analysis of autosomal dominant hereditary ataxias in the Indian population: high frequency of SCA2 and evidence for a common founder mutation.* Hum Genet, 2000. **106**(2): p. 179-87.
141. Laffita-Mesa, J.M., et al., *Unexpanded and intermediate CAG polymorphisms at the SCA2 locus (ATXN2) in the Cuban population: evidence about the origin of expanded SCA2 alleles.* Eur J Hum Genet. **20**(1): p. 41-9.
142. Silveira, I., et al., *Machado-Joseph disease is genetically different from Holguin dominant ataxia (SCA2).* Genomics, 1993. **17**(3): p. 556-9.
143. Hernandez, A., et al., *Genetic mapping of the spinocerebellar ataxia 2 (SCA2) locus on chromosome 12q23-q24.1.* Genomics, 1995. **25**(2): p. 433-5.
144. Burk, K., et al., *Autosomal dominant cerebellar ataxia type I clinical features and MRI in families with SCA1, SCA2 and SCA3.* Brain, 1996. **119 (Pt 5)**: p. 1497-505.
145. Giunti, P., et al., *The role of the SCA2 trinucleotide repeat expansion in 89 autosomal dominant cerebellar ataxia families. Frequency, clinical and genetic correlates.* Brain, 1998. **121 (Pt 3)**: p. 459-67.
146. Geschwind, D.H., et al., *The prevalence and wide clinical spectrum of the spinocerebellar ataxia type 2 trinucleotide repeat in patients with autosomal dominant cerebellar ataxia.* Am J Hum Genet, 1997. **60**(4): p. 842-50.
147. Schols, L., et al., *Spinocerebellar ataxia type 2. Genotype and phenotype in German kindreds.* Arch Neurol, 1997. **54**(9): p. 1073-80.
148. Shan, D.E., et al., *Spinocerebellar ataxia type 2 presenting as familial levodopa-responsive parkinsonism.* Ann Neurol, 2001. **50**(6): p. 812-5.
149. Pulst, S.M., *Spinocerebellar Ataxia Type 2.* 1993.

150. Choudhry, S., et al., *CAG repeat instability at SCA2 locus: anchoring CAA interruptions and linked single nucleotide polymorphisms*. Hum Mol Genet, 2001. **10**(21): p. 2437-46.
151. Pulst, S.M., et al., *Moderate expansion of a normally biallelic trinucleotide repeat in spinocerebellar ataxia type 2*. Nat Genet, 1996. **14**(3): p. 269-76.
152. Charles, P., et al., *Are interrupted SCA2 CAG repeat expansions responsible for parkinsonism?* Neurology, 2007. **69**(21): p. 1970-5.
153. Costanzi-Porrini, S., et al., *An interrupted 34-CAG repeat SCA-2 allele in patients with sporadic spinocerebellar ataxia*. Neurology, 2000. **54**(2): p. 491-3.
154. Huynh, D.P., et al., *Expansion of the polyQ repeat in ataxin-2 alters its Golgi localization, disrupts the Golgi complex and causes cell death*. Hum Mol Genet, 2003. **12**(13): p. 1485-96.
155. Huynh, D.P., et al., *Nuclear localization or inclusion body formation of ataxin-2 are not necessary for SCA2 pathogenesis in mouse or human*. Nat Genet, 2000. **26**(1): p. 44-50.
156. Shibata, H., D.P. Huynh, and S.M. Pulst, *A novel protein with RNA-binding motifs interacts with ataxin-2*. Hum Mol Genet, 2000. **9**(9): p. 1303-13.
157. Kiehl, T.R., et al., *Generation and characterization of Sca2 (ataxin-2) knockout mice*. Biochem Biophys Res Commun, 2006. **339**(1): p. 17-24.
158. Huynh, D.P., et al., *Dissociated fear and spatial learning in mice with deficiency of ataxin-2*. PLoS One, 2009. **4**(7): p. e6235.
159. Elden, A.C., et al., *Ataxin-2 intermediate-length polyglutamine expansions are associated with increased risk for ALS*. Nature, 2010. **466**(7310): p. 1069-75.
160. Orozco, G., et al., *Dominantly inherited olivopontocerebellar atrophy from eastern Cuba. Clinical, neuropathological, and biochemical findings*. J Neurol Sci, 1989. **93**(1): p. 37-50.
161. Rub, U., et al., *Thalamic involvement in a spinocerebellar ataxia type 2 (SCA2) and a spinocerebellar ataxia type 3 (SCA3) patient, and its clinical relevance*. Brain, 2003. **126**(Pt 10): p. 2257-72.
162. Rub, U., et al., *Damage to the reticulotegmental nucleus of the pons in spinocerebellar ataxia type 1, 2, and 3*. Neurology, 2004. **63**(7): p. 1258-63.
163. Rub, U., et al., *Extended pathoanatomical studies point to a consistent affection of the thalamus in spinocerebellar ataxia type 2*. Neuropathol Appl Neurobiol, 2005. **31**(2): p. 127-40.
164. Nakano, K.K., D.M. Dawson, and A. Spence, *Machado disease. A hereditary ataxia in Portuguese emigrants to Massachusetts*. Neurology, 1972. **22**(1): p. 49-55.
165. Paulson, H., *Spinocerebellar Ataxia Type 3*. 1993.
166. D'Abreu, A., et al., *Caring for Machado-Joseph disease: current understanding and how to help patients*. Parkinsonism Relat Disord. **16**(1): p. 2-7.
167. Lima, L. and P. Coutinho, *Clinical criteria for diagnosis of Machado-Joseph disease: report of a non-Azorena Portuguese family*. Neurology, 1980. **30**(3): p. 319-22.
168. C. Franca M, J., et al., *Prospective study of peripheral neuropathy in Machado-Joseph disease*. Muscle Nerve, 2009. **40**(6): p. 1012-8.
169. Tuite, P.J., et al., *Dopa-responsive parkinsonism phenotype of Machado-Joseph disease: confirmation of 14q CAG expansion*. Ann Neurol, 1995. **38**(4): p. 684-7.
170. Schols, L., et al., *Sleep disturbance in spinocerebellar ataxias: is the SCA3 mutation a cause of restless legs syndrome?* Neurology, 1998. **51**(6): p. 1603-7.
171. D'Abreu, A., et al., *Sleep symptoms and their clinical correlates in Machado-Joseph disease*. Acta Neurol Scand, 2009. **119**(4): p. 277-80.

172. Schols, L., et al., *Relations between genotype and phenotype in German patients with the Machado-Joseph disease mutation*. J Neurol Neurosurg Psychiatry, 1996. **61**(5): p. 466-70.
173. Riess, O., et al., *SCA3: neurological features, pathogenesis and animal models*. Cerebellum, 2008. **7**(2): p. 125-37.
174. Jardim, L.B., et al., *Neurologic findings in Machado-Joseph disease: relation with disease duration, subtypes, and (CAG)_n*. Arch Neurol, 2001. **58**(6): p. 899-904.
175. Sasaki, H., et al., *CAG repeat expansion of Machado-Joseph disease in the Japanese: analysis of the repeat instability for parental transmission, and correlation with disease phenotype*. J Neurol Sci, 1995. **133**(1-2): p. 128-33.
176. Sequeiros, J. and P. Coutinho, *Epidemiology and clinical aspects of Machado-Joseph disease*. Adv Neurol, 1993. **61**: p. 139-53.
177. Kieling, C., et al., *Survival estimates for patients with Machado-Joseph disease (SCA3)*. Clin Genet, 2007. **72**(6): p. 543-5.
178. Kawaguchi, Y., et al., *CAG expansions in a novel gene for Machado-Joseph disease at chromosome 14q32.1*. Nat Genet, 1994. **8**(3): p. 221-8.
179. Ichikawa, Y., et al., *The genomic structure and expression of MJD, the Machado-Joseph disease gene*. J Hum Genet, 2001. **46**(7): p. 413-22.
180. Bettencourt, C., et al., *Increased transcript diversity: novel splicing variants of Machado-Joseph disease gene (ATXN3)*. Neurogenetics. **11**(2): p. 193-202.
181. Cancel, G., et al., *Marked phenotypic heterogeneity associated with expansion of a CAG repeat sequence at the spinocerebellar ataxia 3/Machado-Joseph disease locus*. Am J Hum Genet, 1995. **57**(4): p. 809-16.
182. Maciel, P., et al., *Correlation between CAG repeat length and clinical features in Machado-Joseph disease*. Am J Hum Genet, 1995. **57**(1): p. 54-61.
183. Matilla, T., et al., *Molecular and clinical correlations in spinocerebellar ataxia type 3 and Machado-Joseph disease*. Ann Neurol, 1995. **38**(1): p. 68-72.
184. Ranum, L.P., et al., *Spinocerebellar ataxia type 1 and Machado-Joseph disease: incidence of CAG expansions among adult-onset ataxia patients from 311 families with dominant, recessive, or sporadic ataxia*. Am J Hum Genet, 1995. **57**(3): p. 603-8.
185. Takiyama, Y., et al., *Evidence for inter-generational instability in the CAG repeat in the MJD1 gene and for conserved haplotypes at flanking markers amongst Japanese and Caucasian subjects with Machado-Joseph disease*. Hum Mol Genet, 1995. **4**(7): p. 1137-46.
186. Rubinsztein, D.C., et al., *Sequence variation and size ranges of CAG repeats in the Machado-Joseph disease, spinocerebellar ataxia type 1 and androgen receptor genes*. Hum Mol Genet, 1995. **4**(9): p. 1585-90.
187. Limprasert, P., et al., *Analysis of CAG repeat of the Machado-Joseph gene in human, chimpanzee and monkey populations: a variant nucleotide is associated with the number of CAG repeats*. Hum Mol Genet, 1996. **5**(2): p. 207-13.
188. Matsumura, R., et al., *Relationship of (CAG)_nC configuration to repeat instability of the Machado-Joseph disease gene*. Hum Genet, 1996. **98**(6): p. 643-5.
189. Silveira, I., et al., *Frequency of spinocerebellar ataxia type 1, dentatorubropallidolusian atrophy, and Machado-Joseph disease mutations in a large group of spinocerebellar ataxia patients*. Neurology, 1996. **46**(1): p. 214-8.
190. Watanabe, M., et al., *Analysis of CAG trinucleotide expansion associated with Machado-Joseph disease*. J Neurol Sci, 1996. **136**(1-2): p. 101-7.
191. Hashida, H., et al., *Brain regional differences in the expansion of a CAG repeat in the spinocerebellar ataxias: dentatorubral-pallidolusian atrophy, Machado-Joseph disease, and spinocerebellar ataxia type 1*. Ann Neurol, 1997. **41**(4): p. 505-11.

192. Ikeuchi, T., et al., *Non-Mendelian transmission in dentatorubral-pallidoluysian atrophy and Machado-Joseph disease: the mutant allele is preferentially transmitted in male meiosis*. *Am J Hum Genet*, 1996. **58**(4): p. 730-3.
193. Takiyama, Y., et al., *Single sperm analysis of the CAG repeats in the gene for Machado-Joseph disease (MJD1): evidence for non-Mendelian transmission of the MJD1 gene and for the effect of the intragenic CGG/GGG polymorphism on the intergenerational instability*. *Hum Mol Genet*, 1997. **6**(7): p. 1063-8.
194. Paulson, H.L., et al., *Machado-Joseph disease gene product is a cytoplasmic protein widely expressed in brain*. *Ann Neurol*, 1997. **41**(4): p. 453-62.
195. Burnett, B., F. Li, and R.N. Pittman, *The polyglutamine neurodegenerative protein ataxin-3 binds polyubiquitylated proteins and has ubiquitin protease activity*. *Hum Mol Genet*, 2003. **12**(23): p. 3195-205.
196. Donaldson, K.M., et al., *Ubiquitin-mediated sequestration of normal cellular proteins into polyglutamine aggregates*. *Proc Natl Acad Sci U S A*, 2003. **100**(15): p. 8892-7.
197. Doss-Pepe, E.W., et al., *Ataxin-3 interactions with rad23 and valosin-containing protein and its associations with ubiquitin chains and the proteasome are consistent with a role in ubiquitin-mediated proteolysis*. *Mol Cell Biol*, 2003. **23**(18): p. 6469-83.
198. Chai, Y., et al., *Poly-ubiquitin binding by the polyglutamine disease protein ataxin-3 links its normal function to protein surveillance pathways*. *J Biol Chem*, 2004. **279**(5): p. 3605-11.
199. Berke, S.J., et al., *Defining the role of ubiquitin-interacting motifs in the polyglutamine disease protein, ataxin-3*. *J Biol Chem*, 2005. **280**(36): p. 32026-34.
200. Winborn, B.J., et al., *The deubiquitinating enzyme ataxin-3, a polyglutamine disease protein, edits Lys63 linkages in mixed linkage ubiquitin chains*. *J Biol Chem*, 2008. **283**(39): p. 26436-43.
201. Nicastro, G., et al., *The solution structure of the Josephin domain of ataxin-3: structural determinants for molecular recognition*. *Proc Natl Acad Sci U S A*, 2005. **102**(30): p. 10493-8.
202. Hofmann, K. and L. Falquet, *A ubiquitin-interacting motif conserved in components of the proteasomal and lysosomal protein degradation systems*. *Trends Biochem Sci*, 2001. **26**(6): p. 347-50.
203. Takeshita, Y., et al., *Interaction of ataxin-3 with huntingtin-associated protein 1 through Josephin domain*. *Neuroreport*, 2011. **22**(5): p. 232-8.
204. Chow, M.K., et al., *Polyglutamine expansion in ataxin-3 does not affect protein stability: implications for misfolding and disease*. *J Biol Chem*, 2004. **279**(46): p. 47643-51.
205. Chow, M.K., et al., *Structural and functional analysis of the Josephin domain of the polyglutamine protein ataxin-3*. *Biochem Biophys Res Commun*, 2004. **322**(2): p. 387-94.
206. Chow, M.K., H.L. Paulson, and S.P. Bottomley, *Destabilization of a non-pathological variant of ataxin-3 results in fibrillogenesis via a partially folded intermediate: a model for misfolding in polyglutamine disease*. *J Mol Biol*, 2004. **335**(1): p. 333-41.
207. Masino, L., et al., *Characterization of the structure and the amyloidogenic properties of the Josephin domain of the polyglutamine-containing protein ataxin-3*. *J Mol Biol*, 2004. **344**(4): p. 1021-35.
208. Ellisdon, A.M., M.C. Pearce, and S.P. Bottomley, *Mechanisms of ataxin-3 misfolding and fibril formation: kinetic analysis of a disease-associated polyglutamine protein*. *J Mol Biol*, 2007. **368**(2): p. 595-605.
209. Warrick, J.M., et al., *Ataxin-3 suppresses polyglutamine neurodegeneration in Drosophila by a ubiquitin-associated mechanism*. *Mol Cell*, 2005. **18**(1): p. 37-48.

210. Burnett, B.G. and R.N. Pittman, *The polyglutamine neurodegenerative protein ataxin 3 regulates aggregates formation*. Proc Natl Acad Sci U S A, 2005. **102**(12): p. 4330-5.
211. Durcan, T.M., et al., *The Machado-Joseph disease-associated mutant form of ataxin-3 regulates parkin ubiquitination and stability*. Hum Mol Genet. **20**(1): p. 141-54.
212. Williams, A.J. and H.L. Paulson, *Polyglutamine neurodegeneration: protein misfolding revisited*. Trends Neurosci, 2008. **31**(10): p. 521-8.
213. Evert, B.O., et al., *High level expression of expanded full-length ataxin-3 in vitro causes cell death and formation of intranuclear inclusions in neuronal cells*. Hum Mol Genet, 1999. **8**(7): p. 1169-76.
214. Cemal, C.K., et al., *YAC transgenic mice carrying pathological alleles of the MJD1 locus exhibit a mild and slowly progressive cerebellar deficit*. Hum Mol Genet, 2002. **11**(9): p. 1075-94.
215. Evert, B.O., et al., *Neuronal intranuclear inclusions, dysregulation of cytokine expression and cell death in spinocerebellar ataxia type 3*. Clin Neuropathol, 2006. **25**(6): p. 272-81.
216. Bichelmeier, U., et al., *Nuclear localization of ataxin-3 is required for the manifestation of symptoms in SCA3: in vivo evidence*. J Neurosci, 2007. **27**(28): p. 7418-28.
217. Alves, S., et al., *Striatal and nigral pathology in a lentiviral rat model of Machado-Joseph disease*. Hum Mol Genet, 2008. **17**(14): p. 2071-83.
218. Chen, X., et al., *Deranged calcium signaling and neurodegeneration in spinocerebellar ataxia type 3*. J Neurosci, 2008. **28**(48): p. 12713-24.
219. Warrick, J.M., et al., *Expanded polyglutamine protein forms nuclear inclusions and causes neural degeneration in Drosophila*. Cell, 1998. **93**(6): p. 939-49.
220. Seidel, K., et al., *Axonal inclusions in spinocerebellar ataxia type 3*. Acta Neuropathol, 2010.
221. Schmidt, T., et al., *Protein surveillance machinery in brains with spinocerebellar ataxia type 3: redistribution and differential recruitment of 26S proteasome subunits and chaperones to neuronal intranuclear inclusions*. Ann Neurol, 2002. **51**(3): p. 302-10.
222. Chai, Y., et al., *Analysis of the role of heat shock protein (Hsp) molecular chaperones in polyglutamine disease*. J Neurosci, 1999. **19**(23): p. 10338-47.
223. Rub, U., et al., *Spinocerebellar ataxia type 3 (SCA3): thalamic neurodegeneration occurs independently from thalamic ataxin-3 immunopositive neuronal intranuclear inclusions*. Brain Pathol, 2006. **16**(3): p. 218-27.
224. Ikeda, H., et al., *Expanded polyglutamine in the Machado-Joseph disease protein induces cell death in vitro and in vivo*. Nat Genet, 1996. **13**(2): p. 196-202.
225. Jung, J., et al., *Preventing Ataxin-3 protein cleavage mitigates degeneration in a Drosophila model of SCA3*. Hum Mol Genet, 2009. **18**(24): p. 4843-52.
226. Toulouse, A., et al., *Ribosomal frameshifting on MJD-1 transcripts with long CAG tracts*. Hum Mol Genet, 2005. **14**(18): p. 2649-60.
227. Li, L.B., et al., *RNA toxicity is a component of ataxin-3 degeneration in Drosophila*. Nature, 2008. **453**(7198): p. 1107-11.
228. Rubin, G.M. and E.B. Lewis, *A brief history of Drosophila's contributions to genome research*. Science, 2000. **287**(5461): p. 2216-8.
229. Reiter, L.T., et al., *A systematic analysis of human disease-associated gene sequences in Drosophila melanogaster*. Genome Res, 2001. **11**(6): p. 1114-25.
230. Pandey, U.B. and C.D. Nichols, *Human Disease Models in Drosophila melanogaster and the Role of the Fly in Therapeutic Drug Discovery*. Pharmacol Rev, 2011.

231. Brand, A.H. and N. Perrimon, *Targeted gene expression as a means of altering cell fates and generating dominant phenotypes*. *Development*, 1993. **118**(2): p. 401-15.
232. Brand, A.H., A.S. Manoukian, and N. Perrimon, *Ectopic expression in Drosophila*. *Methods Cell Biol*, 1994. **44**: p. 635-54.
233. Phelps, C.B. and A.H. Brand, *Ectopic gene expression in Drosophila using GAL4 system*. *Methods*, 1998. **14**(4): p. 367-79.
234. Kramer, J.M. and B.E. Staveley, *GAL4 causes developmental defects and apoptosis when expressed in the developing eye of Drosophila melanogaster*. *Genet Mol Res*, 2003. **2**(1): p. 43-7.
235. Fire, A., et al., *Potent and specific genetic interference by double-stranded RNA in Caenorhabditis elegans*. *Nature*, 1998. **391**(6669): p. 806-11.
236. Ecker, J.R. and R.W. Davis, *Inhibition of gene expression in plant cells by expression of antisense RNA*. *Proc Natl Acad Sci U S A*, 1986. **83**(15): p. 5372-6.
237. Napoli, C., C. Lemieux, and R. Jorgensen, *Introduction of a Chimeric Chalcone Synthase Gene into Petunia Results in Reversible Co-Suppression of Homologous Genes in trans*. *Plant Cell*, 1990. **2**(4): p. 279-289.
238. Guo, S. and K.J. Kemphues, *par-1, a gene required for establishing polarity in C. elegans embryos, encodes a putative Ser/Thr kinase that is asymmetrically distributed*. *Cell*, 1995. **81**(4): p. 611-20.
239. Pal-Bhadra, M., U. Bhadra, and J.A. Birchler, *Cosuppression in Drosophila: gene silencing of Alcohol dehydrogenase by white-Adh transgenes is Polycomb dependent*. *Cell*, 1997. **90**(3): p. 479-90.
240. Lee, R.C., R.L. Feinbaum, and V. Ambros, *The C. elegans heterochronic gene lin-4 encodes small RNAs with antisense complementarity to lin-14*. *Cell*, 1993. **75**(5): p. 843-54.
241. Carrington, J.C. and V. Ambros, *Role of microRNAs in plant and animal development*. *Science*, 2003. **301**(5631): p. 336-8.
242. Stram, Y. and L. Kuzntzova, *Inhibition of viruses by RNA interference*. *Virus Genes*, 2006. **32**(3): p. 299-306.
243. Elbashir, S.M., W. Lendeckel, and T. Tuschl, *RNA interference is mediated by 21- and 22-nucleotide RNAs*. *Genes Dev*, 2001. **15**(2): p. 188-200.
244. Elbashir, S.M., et al., *Functional anatomy of siRNAs for mediating efficient RNAi in Drosophila melanogaster embryo lysate*. *EMBO J*, 2001. **20**(23): p. 6877-88.
245. Lee, Y.S., et al., *Distinct roles for Drosophila Dicer-1 and Dicer-2 in the siRNA/miRNA silencing pathways*. *Cell*, 2004. **117**(1): p. 69-81.
246. Liu, Q., et al., *R2D2, a bridge between the initiation and effector steps of the Drosophila RNAi pathway*. *Science*, 2003. **301**(5641): p. 1921-5.
247. Tomari, Y., et al., *A protein sensor for siRNA asymmetry*. *Science*, 2004. **306**(5700): p. 1377-80.
248. Rand, T.A., et al., *Argonaute2 cleaves the anti-guide strand of siRNA during RISC activation*. *Cell*, 2005. **123**(4): p. 621-9.
249. Hammond, S.M., et al., *An RNA-directed nuclease mediates post-transcriptional gene silencing in Drosophila cells*. *Nature*, 2000. **404**(6775): p. 293-6.
250. Dietzl, G., et al., *A genome-wide transgenic RNAi library for conditional gene inactivation in Drosophila*. *Nature*, 2007. **448**(7150): p. 151-6.
251. Ready, D.F., T.E. Hanson, and S. Benzer, *Development of the Drosophila retina, a neurocrystalline lattice*. *Dev Biol*, 1976. **53**(2): p. 217-40.
252. Ellis, M.C., E.M. O'Neill, and G.M. Rubin, *Expression of Drosophila glass protein and evidence for negative regulation of its activity in non-neuronal cells by another DNA-binding protein*. *Development*, 1993. **119**(3): p. 855-65.

253. Moses, K. and G.M. Rubin, *Glass encodes a site-specific DNA-binding protein that is regulated in response to positional signals in the developing Drosophila eye*. *Genes Dev*, 1991. **5**(4): p. 583-93.
254. Wolff, T. and D.F. Ready, *Cell death in normal and rough eye mutants of Drosophila*. *Development*, 1991. **113**(3): p. 825-39.
255. Shulman, J.M. and M.B. Feany, *Genetic modifiers of tauopathy in Drosophila*. *Genetics*, 2003. **165**(3): p. 1233-42.
256. Bilen, J. and N.M. Bonini, *Genome-wide screen for modifiers of ataxin-3 neurodegeneration in Drosophila*. *PLoS Genet*, 2007. **3**(10): p. 1950-64.
257. Marsh, J.L., et al., *Expanded polyglutamine peptides alone are intrinsically cytotoxic and cause neurodegeneration in Drosophila*. *Hum Mol Genet*, 2000. **9**(1): p. 13-25.
258. Marsh, J.L., J. Pallos, and L.M. Thompson, *Fly models of Huntington's disease*. *Hum Mol Genet*, 2003. **12 Spec No 2**: p. R187-93.
259. Jackson, G.R., et al., *Polyglutamine-expanded human huntingtin transgenes induce degeneration of Drosophila photoreceptor neurons*. *Neuron*, 1998. **21**(3): p. 633-42.
260. Kaltenbach, L.S., et al., *Huntingtin interacting proteins are genetic modifiers of neurodegeneration*. *PLoS Genet*, 2007. **3**(5): p. e82.
261. Romero, E., et al., *Suppression of neurodegeneration and increased neurotransmission caused by expanded full-length huntingtin accumulating in the cytoplasm*. *Neuron*, 2008. **57**(1): p. 27-40.
262. Pandey, U.B., et al., *HDAC6 at the intersection of autophagy, the ubiquitin-proteasome system and neurodegeneration*. *Autophagy*, 2007. **3**(6): p. 643-5.
263. Bilen, J., et al., *MicroRNA pathways modulate polyglutamine-induced neurodegeneration*. *Mol Cell*, 2006. **24**(1): p. 157-63.
264. Rorth, P., *A modular misexpression screen in Drosophila detecting tissue-specific phenotypes*. *Proc Natl Acad Sci U S A*, 1996. **93**(22): p. 12418-22.
265. Willingham, S., et al., *Yeast genes that enhance the toxicity of a mutant huntingtin fragment or alpha-synuclein*. *Science*, 2003. **302**(5651): p. 1769-72.
266. Doumanis, J., et al., *RNAi screening in Drosophila cells identifies new modifiers of mutant huntingtin aggregation*. *PLoS One*, 2009. **4**(9): p. e7275.
267. Nollen, E.A., et al., *Genome-wide RNA interference screen identifies previously undescribed regulators of polyglutamine aggregation*. *Proc Natl Acad Sci U S A*, 2004. **101**(17): p. 6403-8.
268. Zhang, S., et al., *A genomewide RNA interference screen for modifiers of aggregates formation by mutant Huntingtin in Drosophila*. *Genetics*, 2010. **184**(4): p. 1165-79.
269. *NCBI Gene*. 2011; Available from: <http://www.ncbi.nlm.nih.gov/gene/>.
270. *Genetic nomenclature for Drosophila melanogaster*. 2008; Available from: http://flybase.org/static_pages/docs/nomenclature/nomenclature3.html.
271. Wittmann, C.W., et al., *Tauopathy in Drosophila: neurodegeneration without neurofibrillary tangles*. *Science*, 2001. **293**(5530): p. 711-4.
272. Sullivan, W., Ashburner, M. & Hawley, R.S., ed. *Drosophila Protocols*. 2000, Cold Spring Harbor Press.
273. Scherzinger, E., et al., *Huntingtin-encoded polyglutamine expansions form amyloid-like protein aggregates in vitro and in vivo*. *Cell*, 1997. **90**(3): p. 549-58.
274. Wanker, E.E., et al., *Membrane filter assay for detection of amyloid-like polyglutamine-containing protein aggregates*. *Methods Enzymol*, 1999. **309**: p. 375-86.
275. Ren, P.H., et al., *Cytoplasmic penetration and persistent infection of mammalian cells by polyglutamine aggregates*. *Nat Cell Biol*, 2009. **11**(2): p. 219-25.

276. Wong, S.L., W.M. Chan, and H.Y. Chan, *Sodium dodecyl sulfate-insoluble oligomers are involved in polyglutamine degeneration*. FASEB J, 2008. **22**(9): p. 3348-57.
277. Hsiung, F. and K. Moses, *Retinal development in Drosophila: specifying the first neuron*. Hum Mol Genet, 2002. **11**(10): p. 1207-14.
278. Wolff, T. and D.F. Ready, *The beginning of pattern formation in the Drosophila compound eye: the morphogenetic furrow and the second mitotic wave*. Development, 1991. **113**(3): p. 841-50.
279. Tsai, H.F., H.J. Tsai, and M. Hsieh, *Full-length expanded ataxin-3 enhances mitochondrial-mediated cell death and decreases Bcl-2 expression in human neuroblastoma cells*. Biochem Biophys Res Commun, 2004. **324**(4): p. 1274-82.
280. Chou, A.H., et al., *Polyglutamine-expanded ataxin-3 activates mitochondrial apoptotic pathway by upregulating Bax and downregulating Bcl-xL*. Neurobiol Dis, 2006. **21**(2): p. 333-45.
281. Spreij, T.E., *Cell death during the development of the imaginal discs of Calliphora erythrocephala*. Neth. J. Zool., 1971. **21**: p. 221-264.
282. *Gene Ontology Annotation Database*. Available from: <http://www.ebi.ac.uk/GOA/>.
283. *NCBI HomoloGene Database*. November/December 2011; Available from: <http://www.ncbi.nlm.nih.gov/homologene>.
284. *NCBI BLAST*. November/December 2011; Available from: <http://blast.ncbi.nlm.nih.gov/Blast.cgi>.
285. McGuire, S.E., Z. Mao, and R.L. Davis, *Spatiotemporal gene expression targeting with the TARGET and gene-switch systems in Drosophila*. Sci STKE, 2004. **2004**(220): p. pl6.
286. Bangs, P., N. Franc, and K. White, *Molecular mechanisms of cell death and phagocytosis in Drosophila*. Cell Death Differ, 2000. **7**(11): p. 1027-34.
287. Sokolowski, J.D. and J.W. Mandell, *Phagocytic clearance in neurodegeneration*. Am J Pathol, 2011. **178**(4): p. 1416-28.
288. Jana, N.R., et al., *Co-chaperone CHIP associates with expanded polyglutamine protein and promotes their degradation by proteasomes*. J Biol Chem, 2005. **280**(12): p. 11635-40.
289. Chan, H.Y., et al., *Mechanisms of chaperone suppression of polyglutamine disease: selectivity, synergy and modulation of protein solubility in Drosophila*. Hum Mol Genet, 2000. **9**(19): p. 2811-20.
290. Chang, H.C., et al., *Hsc70 is required for endocytosis and clathrin function in Drosophila*. J Cell Biol, 2002. **159**(3): p. 477-87.
291. Chang, H.C., M. Hull, and I. Mellman, *The J-domain protein Rme-8 interacts with Hsc70 to control clathrin-dependent endocytosis in Drosophila*. J Cell Biol, 2004. **164**(7): p. 1055-64.
292. Holzl, H., et al., *The regulatory complex of Drosophila melanogaster 26S proteasomes. Subunit composition and localization of a deubiquitylating enzyme*. J Cell Biol, 2000. **150**(1): p. 119-30.
293. Pena, A.N., K. Tominaga, and O.M. Pereira-Smith, *MRG15 activates the cdc2 promoter via histone acetylation in human cells*. Exp Cell Res, 2011.
294. Chan, W.M., et al., *Expanded polyglutamine domain possesses nuclear export activity which modulates subcellular localization and toxicity of polyQ disease protein via exportin-1*. Hum Mol Genet, 2011.
295. Perez, M.K., et al., *Recruitment and the role of nuclear localization in polyglutamine-mediated aggregation*. J Cell Biol, 1998. **143**(6): p. 1457-70.
296. Breuer, P., et al., *Nuclear aggregation of polyglutamine-expanded ataxin 3: Fragments escape the cytoplasmic quality control*. J Biol Chem, 2010.

297. Kobayashi, H., et al., *Expansion of intronic GGCCTG hexanucleotide repeat in NOP56 causes SCA36, a type of spinocerebellar ataxia accompanied by motor neuron involvement*. Am J Hum Genet. **89**(1): p. 121-30.
298. Lessing, D. and N.M. Bonini, *Polyglutamine genes interact to modulate the severity and progression of neurodegeneration in Drosophila*. PLoS Biol, 2008. **6**(2): p. e29.
299. Jimenez-Sanchez, M., et al., *Autophagy and polyglutamine diseases*. Prog Neurobiol.
300. Hagen, N., et al., *Sphingosine-1-phosphate links glycosphingolipid metabolism to neurodegeneration via a calpain-mediated mechanism*. Cell Death Differ, 2011.
301. Mao, C. and L.M. Obeid, *Ceramidases: regulators of cellular responses mediated by ceramide, sphingosine, and sphingosine-1-phosphate*. Biochim Biophys Acta, 2008. **1781**(9): p. 424-34.
302. Hicks, D.G., et al., *The expression of TRMT2A, a novel cell cycle regulated protein, identifies a subset of breast cancer patients with HER2 over-expression that are at an increased risk of recurrence*. BMC Cancer, 2010. **10**: p. 108.
303. Liu, Y.L., et al., *HTF9C gene of 22q11.21 region associates with schizophrenia having deficit-sustained attention*. Psychiatr Genet, 2007. **17**(6): p. 333-8.
304. Sengupta, R., et al., *Modified constructs of the tRNA T_{Psi}C domain to probe substrate conformational requirements of m(1)A(58) and m(5)U(54) tRNA methyltransferases*. Nucleic Acids Res, 2000. **28**(6): p. 1374-80.
305. Johansson, M.J. and A.S. Bystrom, *Dual function of the tRNA(m(5)U54)methyltransferase in tRNA maturation*. RNA, 2002. **8**(3): p. 324-35.
306. Gustavsson, M. and H. Ronne, *Evidence that tRNA modifying enzymes are important in vivo targets for 5-fluorouracil in yeast*. RNA, 2008. **14**(4): p. 666-74.
307. Kealey, J.T., X. Gu, and D.V. Santi, *Enzymatic mechanism of tRNA (m5U54)methyltransferase*. Biochimie, 1994. **76**(12): p. 1133-42.

Curriculum Vitae

Name	Hannes Voßfeldt
Date of Birth	16 August 1983
Place of Birth	Zerbst/Anhalt, Germany
Nationality	German

Education

July 1990 – July 1993

Primary School Güterglück

August 1993 – June 1994

Primary School Walternienburg

August 1994 – July 2003

Gymnasium “Francisceum” Zerbst

Course of Studies

October 2003 – August 2006

Enrolment in Bachelor Degree Course “Molecular Medicine”

Georg-August University Göttingen

Bachelor Thesis at Department of Nephrology & Rheumatology

University Medicine, Georg-August University Göttingen:

“The Role of Calreticulin in the Osmotic Stress Resistance of Renal Epithelial Cells”

October 2006 – April 2008

Enrolment in Master Degree Course “Molecular Medicine”

Georg-August University Göttingen

Master Thesis at Department of Neuroanatomy

University Medicine, Georg-August University Göttingen:

“The Role of TGF- β during Eye Development”

December 2008 – December 2011

Enrolment in PhD Programme “Molecular Medicine”

Georg August University Göttingen

PhD Thesis at Department of Neurodegeneration and Restorative Research, University Medicine, Georg August University Göttingen and at Department of Neurology, University Medical Centre, RWTH Aachen University:

“A Genome-Wide Screen for Modifiers of Polyglutamine-Induced Neurotoxicity in *Drosophila*”

Graduation

2003, General Qualification for University Entrance (Abitur)

Gymnasium “Francisceum” Zerbst

2006, Bachelor of Science

Georg August University Göttingen

2008, Master of Science

Georg August University Göttingen

Private Danksagungen

An dieser Stelle möchte ich mich bei den Menschen bedanken, die mir eher unabhängig von Studium und Arbeit in meinem Leben beigestanden haben, die mir auf meinem Weg geholfen haben und ohne die ich nicht die Person wäre, die ich bin. Ich bin unendlich dankbar für die Unterstützung, die Motivation und die Geborgenheit meiner Familie, insbesondere meiner Eltern, die es mir ermöglicht haben, diesen Lebensweg einzuschlagen, ihn durchzuhalten und bei denen ich immer wieder spüren darf was es heißt, zurück nach Hause zu kommen. Gleiches gilt für meine Großeltern und meinen Bruder, auf den ich sehr stolz bin.

Den allermeisten Anteil an der Verwirklichung dieser Arbeit hat Lisa, ohne deren Hilfe, Aufmunterung, Vertrauen und den gelegentlichen entscheidenden Schubser in die richtige Richtung ich schwerlich die Kraft dafür und auch noch alle Sachen nebenbei aufgebracht hätte und bei der ich mich immer unendlich wohlgeföhlt habe.

Natürlich danke ich den Menschen, mit denen ich während der letzten Jahre auch mein Leben abseits des Studiums und der Arbeit teilen durfte, allen voran Malte; ich werde unser WG-Leben und deine Loyalität und Freundschaft nie vergessen. Ich bin sehr glücklich, die „Gruppe Dino“ mit Julia, Nadine, Alexandra, Nils und Malte getroffen zu haben und hoffe noch auf viele Dino-Wochenenden und gemeinsame Zeit mit euch, eure Freundschaft bedeutet mir unendlich viel. Ebenfalls danke ich meinem „Vermieter“ Adrian für die sehr kurzweilige Zeit, gute Gespräche und Versorgung und sein Freundschaft.

Ich danke meinen Jungs aus der Heimat, Dennis, Holger, Martin, Stephan, Daniel und Chris für ihre langjährige Freundschaft und dafür, dass es immer wie früher ist, wenn wir uns treffen. Ich danke Henna und Venita für ihre Freundschaft und die schöne Zeit, die wir miteinander verbracht haben und hoffentlich noch verbringen werden.

Zu guter Letzt danke ich noch einmal meinen Kollegen für die tolle Zeit auch abseits der Arbeit, meinen Kommilitonen und Dr. Erik Meskauskas und Dr. Werner Albig für ihren Einsatz und die gemeinsame Zeit als MolMed in Göttingen.

Appendix

I Additional eye phenotypes



Appendix Figure 1. Additional eye phenotypes referred to in the thesis.

(A) REP induced by GMR-mediated *Tau[R406W]* expression and utilised in rescreening for polyQ specificity of the RNAi effects. **(B)** GMR-mediated overexpression of *UAS-p35* in *SCA3tr-Q78* flies results in amelioration of the polyQ-induced REP. **(C)** A different *SCA3tr-Q78* individual exhibits a worsened REP with *UAS-p35*. **(D)** Co-expression of *SCA3tr-Q78* and shRNA against the *white* gene shows loss of *white*-mediated eye coloration, but no change in degenerative appearance of the compound eye.






All scale bars apply to 200 μ m respectively.










II RNAi lines modifying SCA3tr-Q78-induced REP





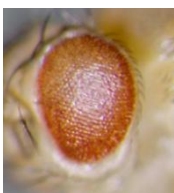




Appendix Table 1. RNAi lines modifying SCA3tr-Q78-induced REP.

Lines marked with **(Tau)** in *REP modification* column exhibited similar result in rescuing with Tau[R406W]-induced REP. Lines listed in red colour show reduced vitality or lethality of progeny following ubiquitous shRNA expression with actin5C-GAL4.


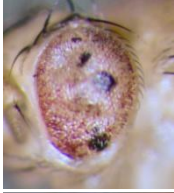
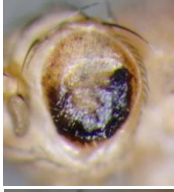
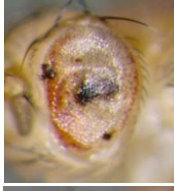



S, suppression of REP; E, enhancement of REP; n.a., not available.





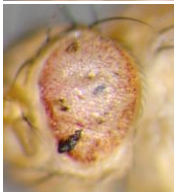



Transformant ID	CG number	Gene name	REP modification	Phenotype
8780	CG17048	CG17048	S	
7903	CG9501	<i>ppk14</i>	S	
23121	CG7123	<i>LanB1</i>	S	n.a.
44362	CG9131	<i>slmo</i>	S	n.a.
37221	CG9153	CG9153	S	
15789	CG8696	<i>LvpH</i>	S	
26465	CG4264	<i>Hsc70-4</i>	S	
50222	CG4264	<i>Hsc70-4</i>	S	








11219	CG3284	<i>Rpl115</i>	S	
3780	CG5799	<i>dve-s</i>	S	
24030	CG9448	<i>trbd</i>	S	
40006	CG15618	CG15618	S	
41530	CG14514	<i>Brd8</i>	S	
23637	CG8863	<i>Droj2</i>	S	
43870	CG7108	<i>DNApol-alpha50</i>	S	
45596	CG8937	<i>Hsc70-1</i>	S	
41696	CG2720	<i>Hop</i>	S (Tau)	

40044	<i>CG16890</i>	<i>CG16890</i>	S	
8070	<i>CG13969</i>	<i>bwa</i>	S	
6282	<i>CG6755</i>	<i>EloA</i>	S	
31257	<i>CG10545</i>	<i>Gbeta13F</i>	S	
19066	<i>CG1658</i>	<i>Doa</i>	S	n.a.
33262	<i>CG5687</i>	<i>CG5687</i>	S	
13005	<i>CG9695</i>	<i>Dab</i>	S	
16182	<i>CG1107</i>	<i>aux</i>	S	
37930	<i>CG14619</i>	<i>CG14619</i>	S	
46473	<i>CG17919</i>	<i>CG17919</i>	S	

43606	<i>CG6758</i>	<i>CG6758</i>	S	
43802	<i>CG6363</i>	<i>MRG15</i>	S (Tau)	
8408	<i>CG3389</i>	<i>Cad88C</i>	S	
34713	<i>CG3808</i>	<i>CG3808</i>	S	
25030	<i>CG31110</i>	<i>5Ptasel</i>	S	
26475	<i>CG4266</i>	<i>CG4266</i>	S	
23843	<i>CG16807</i>	<i>roq</i>	S	
16040	<i>CG10377</i>	<i>Hrb27C</i>	S	
17196	<i>CG13467</i>	<i>CG42247</i>	S	n.a.
22590	<i>CG7855</i>	<i>timeout</i>	E	

24070	<i>CG9601</i>	<i>CG9601</i>	E	
30186	<i>CG15534</i>	<i>CG15534</i>	E	
1326	<i>CG10001</i>	<i>AR-2</i>	E	
47569	<i>CG12935</i>	<i>CG12935</i>	E	
21293	<i>CG31048</i>	<i>CG31048</i>	E	
10942	<i>CG1119</i>	<i>Gnf1</i>	E	n.a.
48062	<i>CG1695</i>	<i>CG1695</i>	E	
28386	<i>CG4881</i>	<i>salr</i>	E	n.a.
36025	<i>CG8781</i>	<i>tsu</i>	E	n.a.
22454	<i>CG6873</i>	<i>CG6873</i>	E (Tau)	
41960	<i>CG3799</i>	<i>Exn</i>	E	n.a.
31777	<i>CG13298</i>	<i>CG13298</i>	E	n.a.

43612	CG14966	CG14966	E	
24885	CG14622	DAAM	E	
40478	CG3869	Marf	E	
29711	CG6115	CG6115	E	n.a.
5684	CG5229	chm	E	
42798	CG6627	Dnz1	E	
49792	CG3678	CG3678	E	n.a.
30717	CG10872	CG33128	E	
23659	CG8954	Smg5	E	
33581	CG2887	CG2887	E (Tau)	n.a.
48692	CG5748	Hsf	E	

35147	CG6930	<i>l(3)neo38</i>	E	
44114	CG11722	CG11722	E	
19450	CG15399	CG15399	E	
24725	CG3225	CG3225	E	n.a.
20536	CG17753	CCS	E	
10020	CG4016	<i>Spt-1</i>	E	n.a.
32370	CG31641	<i>stai</i>	E	n.a.
36153	CG18679	CG34372	E	
20183	CG12345	<i>Cha</i>	E	n.a.
36572	CG7066	<i>Sbp2</i>	E	
33837	CG10524	<i>Pkcdelta</i>	E	

8620	CG4288	CG4288	E
28019	CG7436	<i>Nmt</i>	lethal
22574	CG7843	<i>Ars2</i>	lethal
51209	CG10281	<i>TfIIFalpa</i>	lethal
14874	CG2145	CG2145	lethal
14890	CG15739	CG15739	lethal
22561	CG7275	CG7275	lethal
30179	CG6921	<i>bond</i>	lethal
30214	CG16785	<i>fz3</i>	lethal
21393	CG31687	CG31687	lethal
1385	CG9753	<i>AdoR</i>	lethal
9865	CG7709	<i>Muc91C</i>	lethal
41130	CG7807	<i>AP-2</i>	lethal
46150	CG7085	<i>l(2)s5379</i>	lethal
21985	CG31318	<i>Rpb4</i>	lethal
38471	CG1129	CG1129	lethal
45635	CG6944	<i>Lam</i>	lethal
46072	CG6589	<i>spag4</i>	lethal
26959	CG8431	<i>Aats-cys</i>	lethal
44942	CG31321	CG31321	lethal
40907	CG5404	CG5404	lethal
39402	CG5310	<i>nmdyn-D6</i>	lethal
14210	CG8189	<i>ATPsyn-b</i>	lethal
14194	CG17081	<i>Cep135</i>	lethal



39224	<i>CG18812</i>	<i>CG18812</i>	lethal
39256	<i>CG9742</i>	<i>SmG</i>	lethal
20334	<i>CG16938</i>	<i>Tif-IA</i>	lethal
18107	<i>CG7279</i>	<i>Lip1</i>	lethal
32680	<i>CG1640</i>	<i>CG1640</i>	lethal
44991	<i>CG11136</i>	<i>Lrt</i>	lethal
16506	<i>CG5599</i>	<i>CG5599</i>	lethal
28745	<i>CG12524</i>	<i>CG34356</i>	lethal
34160	<i>CG6340</i>	<i>CG6340</i>	lethal
50706	<i>CG4241</i>	<i>att-ORFA</i>	lethal
13613	<i>CG2917</i>	<i>Orc4</i>	lethal
35065	<i>CG6066</i>	<i>CG6066</i>	lethal
36050	<i>CG8849</i>	<i>mRpL24</i>	lethal
21792	<i>CG4132</i>	<i>pkaap</i>	lethal
40076	<i>CG17419</i>	<i>CG41099</i>	lethal
21793	<i>CG4152</i>	<i>l(2)35Df</i>	lethal
11852	<i>CG9245</i>	<i>Pis</i>	lethal
15602	<i>CG3759</i>	<i>CG3759</i>	lethal
47537	<i>CG11010</i>	<i>Ent3</i>	lethal
49822	<i>CG9958</i>	<i>snapin</i>	lethal

6143	<i>CG4928</i>	<i>CG4928</i>	lethal
40972	<i>CG17681</i>	<i>CG17681</i>	lethal
43998	<i>CG6335</i>	<i>Aats-his</i>	lethal (Tau)
44104	<i>CG10126</i>	<i>CG10126</i>	lethal
39848	<i>CG14905</i>	<i>CG14905</i>	lethal
21308	<i>CG31291</i>	<i>CG31291</i>	lethal
33735	<i>CG31000</i>	<i>heph</i>	lethal
33787	<i>CG31211</i>	<i>CG31211</i>	lethal
25195	<i>CG15143</i>	<i>CG15143</i>	lethal
14869	<i>CG2124</i>	<i>CG2124</i>	lethal
29332	<i>CG9927</i>	<i>Art6</i>	lethal
14861	<i>CG7598</i>	<i>CG7598</i>	lethal
34316	<i>CG5121</i>	<i>MED28</i>	lethal
38269	<i>CG3776</i>	<i>CG3776</i>	lethal
33186	<i>CG4482</i>	<i>mol</i>	lethal
21139	<i>CG3035</i>	<i>cm</i>	lethal
38963	<i>CG7935</i>	<i>msk</i>	lethal
49153	<i>CG13779</i>	<i>CG13779</i>	lethal
24177	<i>CG9998</i>	<i>U2af50</i>	lethal
38491	<i>CG11360</i>	<i>CG11360</i>	lethal
39450	<i>CG31704</i>	<i>CG31704</i>	lethal
34479	<i>CG32253</i>	<i>CG11583</i>	lethal
21999	<i>CG5085</i>	<i>Sirt2</i>	lethal
22068	<i>CG5335</i>	<i>CG5335</i>	lethal
31789	<i>CG13779</i>	<i>CG13779</i>	lethal

33561	CG2708	Tom34	lethal
49879	CG7014	RpS5b	lethal
3245	CG10913	Spn6	lethal
26432	CG4202	Sas10	lethal
6723	CG10693	slo	lethal
30623	CG5553	DNApol- alpha60	lethal
49525	CG33505	U3-55K	lethal
51979	CG10564	Ac78C	lethal
7802	CG8933	exd	lethal
52165	CG13849	Nop56	lethal
7800	CG4035	eIF-4E	lethal
51363	CG16884	CG16884	lethal
4634	CG30048	CG30048	lethal
52094	CG10582	Sin	lethal
46977	CG1989	Yippee	lethal
44976	CG7769	pic	lethal
27610	CG4969	Wnt6	lethal
42915	CG7176	ldh	lethal
21374	CG3158	spn-E	lethal
42716	CG5911	ETHR	lethal
2487	CG17075	CG17075	lethal
8361	CG11278	Syx13	lethal
7787	CG9696	dom	lethal

34145	CG5869	CG5869	lethal
38319	CG10033	<i>for</i>	lethal
41406	CG1882	CG1882	lethal
44562	CG11739	CG11739	lethal
45402	CG12298	<i>sub</i>	lethal
1335	CG11958	<i>Cnx99A</i>	lethal
8907	CG1139	CG1139	lethal
24749	CG3329	<i>Prosbeta2</i>	lethal (Tau)
49245	CG2241	<i>Rpt6R</i>	lethal
7308	CG3305	CG3305	lethal
52486	CG2905	<i>Nipped-A</i>	lethal
9039	CG6827	<i>Nrx-IV</i>	lethal (Tau)
2857	CG7431	CG7431	lethal
18440	CG2918	CG2918	lethal
31522	CG11546	<i>kermit</i>	lethal
44325	CG5651	<i>pix</i>	lethal
44589	CG12275	<i>RpS10a</i>	lethal (Tau)
47116	CG5969	CG5969	lethal
17171	CG13391	<i>Aats-ala</i>	lethal
12482	CG2478	<i>bru</i>	lethal (Tau)
46499	CG1030	<i>Scr</i>	lethal
38154	CG3589	CG3589	lethal
39091	CG31289	<i>Dph5</i>	lethal
22496	CG6509	CG6509	lethal
37250	CG5751	<i>TrpA1</i>	lethal
28341	CG1903	<i>sno</i>	lethal

27152	CG10315	<i>elf2B-delta</i>	lethal
40477	CG3843	<i>RpL10Aa</i>	lethal
13054	CG7162	<i>MED1</i>	lethal
52392	CG4960	<i>CG4960</i>	lethal
47126	CG3849	<i>Lasp</i>	lethal
33135	CG4521	<i>mthl1</i>	lethal
33256	CG3499	<i>CG3499</i>	lethal
25246	CG17293	<i>CG17293</i>	lethal
15877	CG12031	<i>MED14</i>	lethal (Tau)
10639	CG6146	<i>Top1</i>	lethal
25547	CG7757	<i>CG7757</i>	lethal
17302	CG12727	<i>CG32635</i>	lethal
25535	CG7742	<i>CG7742</i>	lethal
42010	CG4843	<i>Tm2</i>	lethal
49800	CG6835	<i>GS</i>	lethal
23689	CG9344	<i>CG9344</i>	lethal
36252	CG12283	<i>kek1</i>	lethal
31726	CG12325	<i>CG12325</i>	lethal
13503	CG8222	<i>Pvr</i>	lethal
30000	CG4357	<i>Ncc69</i>	lethal
41980	CG4180	<i>l(2)35Bg</i>	lethal
36175	CG9961	<i>CG9961</i>	lethal
30462	CG6534	<i>slou</i>	lethal
36121	CG9619	<i>CG9619</i>	lethal

30448	<i>CG5179</i>	<i>Cdk9</i>	lethal
30431	<i>CG7772</i>	<i>CG7772</i>	lethal
34618	<i>CG3431</i>	<i>Uch-L3</i>	lethal
41977	<i>CG4165</i>	<i>CG4165</i>	lethal
41965	<i>CG30000</i>	<i>CG30000</i>	lethal
35200	<i>CG7292</i>	<i>Rrp6</i>	lethal
34845	<i>CG4438</i>	<i>CG4438</i>	lethal
12375	<i>CG12318</i>	<i>CG33121</i>	lethal
13828	<i>CG7636</i>	<i>mRpL2</i>	lethal
14972	<i>CG16812</i>	<i>CG16812</i>	lethal
40789	<i>CG10549</i>	<i>Nipped-A</i>	lethal
4426	<i>CG14511</i>	<i>CG14511</i>	lethal
11765	<i>CG8727</i>	<i>cyc</i>	lethal
15547	<i>CG9271</i>	<i>Vm34Ca</i>	lethal
49979	<i>CG17664</i>	<i>CG17664</i>	lethal
13643	<i>CG10898</i>	<i>CG10898</i>	lethal
44201	<i>CG3876</i>	<i>CG3876</i>	lethal
3579	<i>CG7899</i>	<i>Acph-1</i>	lethal
34377	<i>CG7222</i>	<i>CG7222</i>	lethal
41599	<i>CG1578</i>	<i>CG1578</i>	lethal
17490	<i>CG1433</i>	<i>Atu</i>	lethal
45116	<i>CG11454</i>	<i>CG11454</i>	lethal
42018	<i>CG5018</i>	<i>CG5018</i>	lethal
50797	<i>CG17949</i>	<i>His2B:CG17949</i>	lethal

27498	<i>CG5735</i>	<i>orb2</i>	lethal
15261	<i>CG13926</i>	<i>CG13926</i>	lethal
18567	<i>CG8877</i>	<i>Prp8</i>	lethal (Tau)
25787	<i>CG31657</i>	<i>PNUTS</i>	lethal
31456	<i>CG11201</i>	<i>TLL3B</i>	lethal
49547	<i>CG31201</i>	<i>GluRIIE</i>	lethal
50510	<i>CG33931</i>	<i>Rpp20</i>	lethal
32443	<i>CG31639</i>	<i>Uch-L3</i>	lethal
34995	<i>CG5394</i>	<i>Aats-glupro</i>	lethal
7752	<i>CG5353</i>	<i>Aats-thr</i>	lethal
29589	<i>CG3071</i>	<i>CG3071</i>	lethal
23033	<i>CG8091</i>	<i>Nc</i>	lethal
13044	<i>CG1271</i>	<i>CG1271</i>	lethal
41714	<i>CG7650</i>	<i>CG7650</i>	lethal
26001	<i>CG6852</i>	<i>CG6852</i>	lethal
11693	<i>CG6364</i>	<i>CG6364</i>	lethal (Tau)
26759	<i>CG10726</i>	<i>barr</i>	lethal
5322	<i>CG5582</i>	<i>cln3</i>	lethal
26007	<i>CG7039</i>	<i>CG7039</i>	lethal
7878	<i>CG7234</i>	<i>GluRIIB</i>	lethal
10756	<i>CG10037</i>	<i>vvl</i>	lethal
49844	<i>CG14206</i>	<i>RpS10b</i>	lethal
46284	<i>CG15772</i>	<i>CG15772</i>	lethal

17002	CG10811	<i>eIF4G</i>	lethal
43955	CG1412	<i>RhoGAP19D</i>	lethal
3347	CG13387	<i>emb</i>	lethal
44557	CG6707	CG6707	lethal
28065	CG7788	<i>Ice</i>	lethal
28798	CG9924	<i>rdx</i>	lethal
45530	CG4751	CG4751	lethal
4047	CG12891	<i>CPTI</i>	lethal
44263	CG7480	<i>Pgant35A</i>	lethal
44535	CG4780	<i>membrin</i>	lethal
46445	CG33193	<i>sav</i>	lethal
44570	CG9867	CG9867	lethal
49372	CG11877	CG11877	lethal
12209	CG2901	CG2901	lethal
38481	CG11299	CG11299	lethal
45789	CG8258	CG8258	lethal
12746	CG5163	<i>TfIIA-S</i>	lethal
12645	CG1064	<i>Snr1</i>	lethal
39207	CG9802	<i>Cap</i>	lethal
22480	CG6226	<i>FK506-bp1</i>	lethal
18031	CG10192	<i>eIF4G2</i>	lethal

49655	CG10546	<i>Cralbp</i>	lethal
38399	CG10716	<i>4EHP</i>	lethal
23873	CG13349	CG13349	lethal
44484	CG1616	<i>dpa</i>	lethal
23851	CG1316	CG1316	lethal
44449	CG1718	CG1718	lethal
40336	CG5913	CG5913	lethal
4789	CG10975	<i>Ptp69D</i>	lethal
10843	CG9426	CG9426	lethal
31619	CG11989	<i>Ard1</i>	lethal (Tau)
21010	CG5994	<i>Nelf-E</i>	lethal (Tau)
842	CG14396	<i>Ret</i>	lethal
31444	CG11184	<i>Upf3</i>	lethal
12768	CG5499	<i>His2Av</i>	lethal
21258	CG3058	<i>Dim1</i>	lethal
23625	CG8841	CG8841	lethal
19208	CG3011	CG3011	lethal
32719	CG1676	<i>cactin</i>	lethal
15627	CG10984	CG10984	lethal
43790	CG5405	<i>KrT95D</i>	lethal
43549	CG11899	CG11899	lethal
50643	CG31809	CG31809	lethal
3326	CG10657	CG10657	lethal
34792	CG4090	<i>Mur89F</i>	lethal

6315	CG8384	<i>gro</i>	lethal
20876	CG2503	<i>atms</i>	lethal
865	CG10776	<i>wit</i>	lethal
35272	CG7791	CG7791	lethal
36028	CG8786	CG8786	lethal
26615	CG4735	<i>shu</i>	lethal
12581	CG8151	<i>Tfb1</i>	lethal
12149	CG7623	<i>sll</i>	lethal
49328	CG11907	<i>Ent1</i>	lethal
15453	CG3644	<i>bic</i>	lethal (Tau)
50435	CG32602	<i>Muc12Ea</i>	lethal
30884	CG10374	<i>Lsd-1</i>	lethal
32395	CG16901	<i>sqd</i>	lethal
4180	CG12929	CG12929	lethal
16125	CG10961	<i>Traf6</i>	lethal
49848	CG1740	<i>Ntf-2</i>	lethal
37663	CG5640	<i>Utx</i>	lethal
7748	CG7926	<i>Axn</i>	lethal
15185	CG5186	<i>slim</i>	lethal
22548	CG7257	<i>Rpt4R</i>	lethal
29253	CG13628	<i>Rpb10</i>	lethal
42779	CG3881	<i>GlcAT-S</i>	lethal
16569	CG12951	CG12951	lethal
42776	CG18419	CG33298	lethal
27528	CG5844	CG5844	lethal

26075	<i>CG4599</i>	<i>Tpr2</i>	lethal
14268	<i>CG4086</i>	<i>Su(P)</i>	lethal
1414	<i>CG5677</i>	<i>Spase22-23</i>	lethal
50221	<i>CG2076</i>	<i>CG2076</i>	lethal
23556	<i>CG17935</i>	<i>Mst84Dd</i>	lethal
33516	<i>CG2272</i>	<i>slpr</i>	lethal
27110	<i>CG32179</i>	<i>Krn</i>	lethal
27002	<i>CG9100</i>	<i>Rab30</i>	lethal (Tau)
33423	<i>CG1911</i>	<i>CAP-D2</i>	lethal
30066	<i>CG7398</i>	<i>CG8219</i>	lethal
33507	<i>CG2253</i>	<i>Upf2</i>	lethal
8254	<i>CG7026</i>	<i>CG7026</i>	lethal
3016	<i>CG4001</i>	<i>Pfk</i>	lethal
3166	<i>CG10778</i>	<i>CG10778</i>	lethal
3046	<i>CG11282</i>	<i>caps</i>	lethal
33523	<i>CG2321</i>	<i>CG2321</i>	lethal
39937	<i>CG17083</i>	<i>CG17083</i>	lethal
39976	<i>CG1542</i>	<i>CG1542</i>	lethal
29295	<i>CG9836</i>	<i>CG9836</i>	lethal
48153	<i>CG15804</i>	<i>Dhc62B</i>	lethal
6098	<i>CG18549</i>	<i>CG18549</i>	lethal
4801	<i>CG15744</i>	<i>CG15744</i>	lethal
43944	<i>CG1965</i>	<i>CG1965</i>	lethal
26277	<i>CG3733</i>	<i>Chd1</i>	lethal

42485	<i>CG3297</i>	<i>mnd</i>	lethal
19616	<i>CG15816</i>	NA	lethal
27607	<i>CG4364</i>	<i>CG4364</i>	lethal
35162	<i>CG7034</i>	<i>sec15</i>	lethal
15736	<i>CG6443</i>	<i>CG6443</i>	lethal
32085	<i>CG14034</i>	NA	lethal
28982	<i>CG8887</i>	<i>ash1</i>	lethal
40013	<i>CG15666</i>	<i>CG15666</i>	lethal
40278	<i>CG31551</i>	<i>CG31551</i>	lethal
40218	<i>CG31256</i>	<i>Brf</i>	lethal
21937	<i>CG4738</i>	<i>Nup160</i>	lethal
37329	<i>CG31522</i>	<i>CG31522</i>	lethal
27680	<i>CG6603</i>	<i>Hsc70Cb</i>	lethal
47731	<i>CG5676</i>	<i>CG5676</i>	lethal
31364	<i>CG10837</i>	<i>eIF-4B</i>	lethal
7965	<i>CG8975</i>	<i>RnrS</i>	lethal
37699	<i>CG5748</i>	<i>Hsf</i>	lethal
22019	<i>CG5160</i>	<i>CG5160</i>	lethal
41917	<i>CG3339</i>	<i>CG3339</i>	lethal
16334	<i>CG11870</i>	<i>CG11870</i>	lethal
24992	<i>CG2779</i>	<i>Muc11A</i>	lethal
2912	<i>CG13425</i>	<i>bl</i>	lethal
40932	<i>CG6475</i>	<i>CG6475</i>	lethal
26325	<i>CG32202</i>	<i>CG32202</i>	lethal
29337	<i>CG9938</i>	<i>Ndc80</i>	lethal

34737	CG3923	<i>Exp6</i>	lethal
27486	CG5692	<i>raps</i>	lethal
34331	CG5596	<i>Mlc1</i>	lethal
17463	CG14286	CG14286	lethal
21563	CG5323	CG5323	lethal
35343	CG8108	CG8108	lethal (Tau)
29070	CG9177	<i>eIF5</i>	lethal
39529	CG17743	<i>pho</i>	lethal
36584	CG9973	CG9973	lethal
11210	CG9633	<i>RpA-70</i>	lethal
28895	CG8351	<i>Tcp-1eta</i>	lethal
26275	CG3714	CG3714	lethal
26227	CG3542	CG3542	lethal
49168	CG14210	CG14210	lethal
11205	CG12005	<i>Mms19</i>	lethal
21845	CG4389	CG4389	lethal
27943	CG7293	<i>Klp68D</i>	lethal
16091	CG10920	CG10920	lethal
3909	CG10165	CG10165	lethal
21782	CG4062	<i>Aats-val</i>	lethal
20144	CG12085	<i>pUf68</i>	lethal
11227	CG6349	<i>DNApol- alpha180</i>	lethal
12920	CG7929	<i>ocn</i>	lethal
13566	CG7665	<i>Fsh</i>	lethal
12662	CG6545	<i>lbe</i>	lethal

36308	<i>CG5528</i>	<i>Toll-9</i>	lethal
33650	<i>CG7686</i>	<i>CG7686</i>	lethal
28396	<i>CG5684</i>	<i>Pop2</i>	lethal
41740	<i>CG30390</i>	<i>Sgf29</i>	lethal
41964	<i>CG3820</i>	<i>Nup214</i>	lethal
32025	<i>CG12812</i>	<i>Fancl</i>	lethal
6236	<i>CG1378</i>	<i>tll</i>	lethal
7563	<i>CG14077</i>	<i>CG14077</i>	lethal
51496	<i>CG13077</i>	<i>CG13077</i>	lethal
26309	<i>CG3931</i>	<i>Rrp4</i>	lethal
5150	<i>CG5950</i>	<i>SrpRbeta</i>	lethal
18762	<i>CG12630</i>	<i>tio</i>	lethal
51846	<i>CG1571</i>	<i>CG1571</i>	lethal
29072	<i>CG9198</i>	<i>shtd</i>	lethal
40834	<i>CG13431</i>	<i>Mgat1</i>	lethal
27831	<i>CG7067</i>	<i>NitFhit</i>	lethal
42976	<i>CG12050</i>	<i>CG12050</i>	lethal
30442	<i>CG4079</i>	<i>Taf11</i>	lethal
35452	<i>CG9480</i>	<i>Glycogenin</i>	lethal
23028	<i>CG8086</i>	<i>CG8086</i>	lethal (Tau)
27598	<i>CG6369</i>	<i>Smg6</i>	lethal
27600	<i>CG6375</i>	<i>pit</i>	lethal
38637	<i>CG12238</i>	<i>e(y)3</i>	lethal

16744	CG15749	<i>dmrt11E</i>	lethal
27515	CG5788	<i>UbcD10</i>	lethal
41819	CG3358	CG3358	lethal
28058	CG7516	<i>l(2)34Fd</i>	lethal
35611	CG7052	<i>TepII</i>	lethal
41885	CG32376	CG32376	lethal
34070	CG5374	<i>T-cp1</i>	lethal
27457	CG5546	<i>MED19</i>	lethal
49345	CG9155	<i>Myo61F</i>	lethal
48835	CG7281	<i>CycC</i>	lethal
48793	CG33051	CG33051	lethal
48708	CG10315	<i>eIF2B-delta</i>	lethal
35222	CG7376	CG7376	lethal
27870	CG7128	<i>Taf8</i>	lethal
31320	CG10687	<i>Aats-asn</i>	lethal
31311	CG10645	<i>lama</i>	lethal
31333	CG10719	<i>brat</i>	lethal
35107	CG6620	<i>ial</i>	lethal
6543	CG7398	<i>Trn</i>	lethal
14444	CG6343	<i>ND42</i>	lethal
26585	CG4649	<i>Sodh-2</i>	lethal

41351	<i>CG31015</i>	<i>PH4alphaPV</i>	lethal
40727	<i>CG9004</i>	<i>CG9004</i>	lethal
30673	<i>CG6772</i>	<i>Slob</i>	lethal
44146	<i>CG12752</i>	<i>Nxt1</i>	lethal
8784	<i>CG10808</i>	<i>synaptogyrin</i>	lethal
17701	<i>CG13778</i>	<i>Mnn1</i>	lethal
29462	<i>CG7564</i>	<i>CG7564</i>	lethal
40665	<i>CG9705</i>	<i>CG9705</i>	lethal
14107	<i>CG32374</i>	<i>CG32374</i>	lethal
30140	<i>CG6249</i>	<i>Csl4</i>	lethal
36085	<i>CG9049</i>	<i>hiw</i>	lethal
36086	<i>CG9124</i>	<i>eIF-3p40</i>	lethal
32749	<i>CG16837</i>	<i>CG16837</i>	lethal
36092	<i>CG9200</i>	<i>Atac1</i>	lethal
35165	<i>CG7070</i>	<i>PyK</i>	lethal
46903	<i>CG14230</i>	<i>CG14230</i>	lethal
49030	<i>CG5440</i>	<i>CG5440</i>	lethal
32612	<i>CG15481</i>	<i>Ski6</i>	lethal
51088	<i>CG4602</i>	<i>Srp54</i>	lethal
34388	<i>CG7861</i>	<i>tbce</i>	lethal
22108	<i>CG5383</i>	<i>PSR</i>	lethal
51202	<i>CG9452</i>	<i>CG9452</i>	lethal
31206	<i>CG10230</i>	<i>Rpn9</i>	lethal (Tau)
15872	<i>CG3069</i>	<i>Taf10b</i>	lethal

8573	<i>CG18578</i>	<i>Ugt86Da</i>	lethal
22773	<i>CG11985</i>	<i>CG11985</i>	lethal (Tau)
31216	<i>CG10308</i>	<i>CycJ</i>	lethal (Tau)
20567	<i>CG1789</i>	<i>CG1789</i>	lethal
15791	<i>CG8695</i>	<i>LvpL</i>	lethal
41703	<i>CG2854</i>	<i>CG2854</i>	lethal
50126	<i>CG10098</i>	<i>CG10098</i>	lethal
36205	<i>CG9995</i>	<i>htt</i>	lethal
39920	<i>CG30144</i>	<i>CG33786</i>	lethal
34847	<i>CG4448</i>	<i>wda</i>	lethal
24054	<i>CG9527</i>	<i>CG9527</i>	lethal
50176	<i>CG3022</i>	<i>GABA-B-R3</i>	lethal
32521	<i>CG31809</i>	<i>CG31809</i>	lethal
52549	<i>CG9191</i>	<i>Klp61F</i>	lethal
4659	<i>CG8657</i>	<i>Dgkepsilon</i>	lethal
23037	<i>CG8107</i>	<i>CalpB</i>	lethal
12618	<i>CG6258</i>	<i>Rfc38</i>	lethal
6053	<i>CG14709</i>	<i>CG14709</i>	lethal
50021	<i>CG11276</i>	<i>RpS4</i>	lethal
40497	<i>CG4005</i>	<i>yki</i>	lethal
28172	<i>CG7989</i>	<i>wcd</i>	lethal
6832	<i>CG4907</i>	<i>CG4907</i>	lethal
25967	<i>CG4247</i>	<i>mRpS10</i>	lethal

24835	CG1404	<i>ran</i>	lethal
36428	CG5742	CG5742	lethal
5985	CG14690	<i>tomboy20</i>	lethal
49325	CG32708	CG32708	lethal
31271	CG10578	<i>DnaJ-1</i>	lethal
46584	CG9899	CG9899	lethal
16313	CG11804	<i>ced-6</i>	lethal
16806	CG16804	<i>spt4</i>	lethal
34498	CG3229	CG33123	lethal
12392	CG5367	CG5367	lethal
40276	CG31531	CG31531	lethal
36440	CG5021	CG5021	lethal
39134	CG31155	<i>Rpb7</i>	lethal
34395	CG7860	CG7860	lethal
16696	CG11395	CG11395	lethal
22123	CG5429	<i>Atg6</i>	lethal
26299	CG10797	<i>dnc</i>	lethal
51472	CG6582	<i>Aac11</i>	lethal
36557	CG6701	CG6701	lethal
17946	CG12959	CG34365	lethal
14900	CG1627	NA	lethal
47248	CG15776	CG42265	lethal
49950	CG17835	<i>inv</i>	lethal
46191	CG9288	CG9288	lethal
27503	CG5753	<i>stau</i>	lethal
33705	CG30327	CG42257	lethal
30537	CG11641	<i>pdm3</i>	lethal
5094	CG12139	<i>Megalin</i>	lethal

31318	<i>CG10662</i>	<i>sick</i>	lethal
51705	<i>CG11105</i>	<i>CG42683</i>	lethal
16331	<i>CG11861</i>	<i>Cul-3</i>	lethal
32482	<i>CG2578</i>	<i>Ten-a</i>	lethal
28628	<i>CG7826</i>	<i>mnb</i>	lethal
12616	<i>CG9207</i>	<i>Gas41</i>	lethal

III Fly lines used for verification of RNAi

Appendix Table 2. Essential *Drosophila* genes exhibiting lethality/semilethality upon Actin5C-induced ubiquitous RNAi.

Gene	Gene Symbol	Transformant ID	
<i>CG1030</i>	<i>Scr</i>	46499 (enhancer) 3033 (enhancer)	semilethal (2/15, 13 %) lethal
<i>CG1064</i>	<i>Snr1</i>	12645 (enhancer)	lethal
<i>CG1378</i>	<i>tll</i>	6236 (enhancer)	semilethal (13/82, 16 %)
<i>CG1433</i>	<i>Atu</i>	17490 (enhancer)	lethal
<i>CG1616</i>	<i>dpa</i>	44484 (enhancer)	lethal
<i>CG1903</i>	<i>sno</i>	28341 (enhancer)	n.a.
<i>CG2503</i>	<i>atms</i>	20876 (enhancer)	lethal
<i>CG2708</i>	<i>Tom34</i>	33561 (enhancer)	lethal
<i>CG3035</i>	<i>cm</i>	21139 (enhancer)	lethal
<i>CG3158</i>	<i>spn-E</i>	21374 (enhancer)	semilethal (8/57, 14 %)
<i>CG3297</i>	<i>mnd</i>	42485 (enhancer)	semilethal (2/28, 7 %)
<i>CG3329</i>	<i>Prosbeta2</i>	24749 (enhancer)	lethal
<i>CG3431</i>	<i>Uch-L3</i>	34618 (enhancer)	lethal
<i>CG3644</i>	<i>bic</i>	15453 (enhancer)	lethal
<i>CG3820</i>	<i>Nup214</i>	41964 (enhancer)	n.a.
<i>CG3923</i>	<i>Exp6</i>	34737 (enhancer)	n.a.
<i>CG4001</i>	<i>Pfk</i>	3016 (enhancer)	semilethal (7/42, 17 %)
<i>CG4035</i>	<i>eIF-4E</i>	7800 (enhancer)	lethal
<i>CG4062</i>	<i>Aats-val</i>	21782 (enhancer)	lethal
<i>CG4152</i>	<i>l(2)35Df</i>	21793 (enhancer)	n.a.
<i>CG4180</i>	<i>l(2)35Bg</i>	41980 (enhancer)	n.a.
<i>CG4482</i>	<i>mol</i>	33186 (enhancer)	lethal
<i>CG4843</i>	<i>Tm2</i>	42010 (enhancer)	lethal
<i>CG5163</i>	<i>TfIIA-S</i>	12746 (enhancer)	lethal
<i>CG5429</i>	<i>Atg6</i>	22123 (enhancer)	lethal
<i>CG5499</i>	<i>His2Av</i>	12768 (enhancer)	lethal
<i>CG5553</i>	<i>DNApol-alpha60</i>	30623 (enhancer)	lethal

<i>CG5748</i>	<i>Hsf</i>	37699 (enhancer) 48692 (enhancer)	lethal semilethal (23/83, 28 %)
<i>CG5753</i>	<i>stau</i>	27503 (enhancer)	lethal
<i>CG6146</i>	<i>Top1</i>	10639 (enhancer)	lethal
<i>CG6603</i>	<i>Hsc70Cb</i>	27680 (enhancer)	n.a.
<i>CG6827</i>	<i>Nrx-IV</i>	9039 (enhancer)	lethal
<i>CG6944</i>	<i>Lam</i>	45635 (enhancer)	lethal
<i>CG7085</i>	<i>l(2)s5379</i>	46150 (enhancer)	lethal
<i>CG7128</i>	<i>Taf8</i>	27870 (enhancer)	lethal
<i>CG7176</i>	<i>Idh</i>	42915 (enhancer)	semilethal (12/74, 16 %)
<i>CG7436</i>	<i>Nmt</i>	28019 (enhancer)	n.a.
<i>CG7480</i>	<i>Pgant35A</i>	44263 (enhancer)	semilethal (10/83, 12 %)
<i>CG7516</i>	<i>l(2)34Fd</i>	28058 (enhancer)	lethal
<i>CG7769</i>	<i>pic</i>	44976 (enhancer)	n.a.
<i>CG7807</i>	<i>AP-2</i>	41130 (enhancer)	lethal
<i>CG8151</i>	<i>Tfb1</i>	12581 (enhancer)	lethal
<i>CG8384</i>	<i>gro</i>	6315 (enhancer)	lethal
<i>CG8887</i>	<i>ash1</i>	28982 (enhancer)	semilethal (20/86, 23 %)
<i>CG8933</i>	<i>exd</i>	7802 (enhancer)	lethal
<i>CG9191</i>	<i>Klp61F</i>	52549 (enhancer)	lethal
<i>CG9998</i>	<i>U2af50</i>	24177 (enhancer)	n.a.
<i>CG10033</i>	<i>for</i>	38319 (enhancer)	n.a.
<i>CG10037</i>	<i>vvl</i>	10756 (enhancer) 47182 (no effect)	lethal lethal
<i>CG10687</i>	<i>Aats-asn</i>	31320 (enhancer)	lethal
<i>CG10719</i>	<i>brat</i>	31333 (enhancer)	lethal
<i>CG10726</i>	<i>barr</i>	26759 (enhancer)	lethal
<i>CG10776</i>	<i>wit</i>	42244 (no effect) 856 (enhancer)	lethal lethal
<i>CG10975</i>	<i>Ptp69D</i>	4789 (enhancer) 942 (no effect) 27090 (no effect)	lethal semilethal (2/15, 13 %) semilethal (19/73, 26 %)
<i>CG11278</i>	<i>Syx13</i>	8361 (enhancer)	n.a.
<i>CG11282</i>	<i>caps</i>	3046 (enhancer) 27097 (no effect)	semilethal (8/39, 20 %) n.a.
<i>CG11546</i>	<i>kermi</i>	31522 (enhancer)	lethal
<i>CG11989</i>	<i>vnc</i>	31619 (enhancer)	lethal

<i>CG12238</i>	<i>e(y)3</i>	38637 (enhancer)	lethal
<i>CG12283</i>	<i>kek1</i>	36252 (enhancer) 4761 (no effect) 43521 (no effect)	n.a. semilethal (7/77, 9 %) n.a.
<i>CG12298</i>	<i>sub</i>	45402 (enhancer)	semilethal (11/49, 22 %)
<i>CG14206</i>	<i>RpS10b</i>	49844 (enhancer)	lethal
<i>CG17743</i>	<i>pho</i>	39529 (enhancer)	lethal
<i>CG31000</i>	<i>heph</i>	33735 (enhancer)	lethal

IV List of screened RNAi lines obtained from the VDRC as human orthologue sublibrary

Appendix Table 3.

CG10001	1326	CG10126	44104	CG10250	51311	CG10376	35473	CG10546	31258
CG10002	37063	CG10128	8868	CG10251	9534	CG10377	16040	CG10546	49655
CG10002	49961	CG10130	8785	CG10253	3321	CG10379	16044	CG10549	40789
CG10006	44539	CG10133	18014	CG10254	15992	CG10383	33911	CG10555	16961
CG10009	17954	CG10137	38342	CG10255	18600	CG10384	16045	CG10555	50115
CG10011	45096	CG10142	15246	CG10257	8710	CG10385	9239	CG10564	51979
CG10018	37591	CG10143	51564	CG10260	15993	CG10390	37563	CG10565	38393
CG10021	3774	CG10144	18019	CG10261	2907	CG10392	18611	CG10566	27281
CG10023	17957	CG10145	15194	CG10262	37672	CG10393	11796	CG1057	27284
CG10029	16583	CG10149	18022	CG10272	16001	CG10395	31244	CG10571	49078
CG10030	44480	CG10155	18024	CG10272	47199	CG10399	18617	CG10572	45370
CG10032	51688	CG10157	14004	CG10275	37283	CG10406	23363	CG10573	31266
CG10033	38319	CG10158	47388	CG10275	36246	CG10406	50865	CG10574	39053
CG10034	30525	CG10160	31192	CG10277	7518	CG10413	3882	CG10575	31270
CG10036	15425	CG10162	23362	CG10278	10418	CG10414	47391	CG10576	28761
CG10037	10756	CG10165	3909	CG10280	5733	CG10415	12591	CG10578	31271
CG10037	47182	CG10166	46385	CG10281	51209	CG10417	27259	CG10579	47859
CG1004	51953	CG10166	13731	CG10286	16002	CG10418	50245	CG1058	8549
CG10043	17966	CG10168	1151	CG10289	16006	CG10419	47373	CG10580	51977
CG10047	33317	CG1017	15610	CG10293	13756	CG10420	1753	CG10581	18650
CG10050	30020	CG10170	1141	CG10295	12553	CG10423	12795	CG10581	48315
CG10052	44717	CG10174	31195	CG10298	28706	CG10426	16048	CG10582	52094
CG10053	50811	CG10175	1140	CG1030	46499	CG10435	38384	CG10583	45092
CG10053	17972	CG10178	8064	CG1030	3033	CG10438	23296	CG10584	28681
CG10055	17973	CG10181	9019	CG10302	22837	CG10443	36270	CG10585	31273
CG10060	28150	CG10184	3311	CG10305	16012	CG10444	4722	CG10588	18655
CG10061	17975	CG10185	18135	CG10308	31216	CG10446	27049	CG1059	39711
CG10062	4697	CG10188	18029	CG1031	31220	CG10446	3066	CG10590	5035
CG10064	38322	CG10189	51692	CG10315	27152	CG10447	45660	CG10592	38171
CG10066	23303	CG1019	18593	CG10315	48708	CG10449	7183	CG10593	3324
CG10067	17979	CG10191	38353	CG10318	15451	CG10459	41451	CG10594	51081
CG10068	15948	CG10192	18031	CG10320	8837	CG10463	31248	CG10597	6157
CG10069	6591	CG10198	31198	CG10324	31226	CG10466	23367	CG10600	31276
CG10072	29434	CG10203	31202	CG10325	51900	CG10467	27263	CG10601	50133
CG10073	11133	CG10206	31204	CG10326	5894	CG10470	3897	CG10601	22841
CG10075	50067	CG1021	37336	CG10326	47194	CG10473	16052	CG10602	31280
CG10075	15399	CG10210	38356	CG10327	38377	CG10474	41455	CG10603	31285
CG10076	44092	CG10211	12352	CG10333	18132	CG10479	45098	CG10604	15716
CG10078	48823	CG10212	10711	CG10335	40612	CG10480	38388	CG10605	2931
CG10078	17981	CG10215	12622	CG10336	16019	CG10483	33276	CG10610	31286
CG10079	43268	CG10220	45999	CG10338	3215	CG10484	49423	CG10616	36605
CG10080	46133	CG10221	1163	CG10340	16020	CG10489	13625	CG10619	45859
CG10081	10066	CG10222	18038	CG10341	52092	CG1049	18628	CG10620	5236
CG10082	38326	CG10223	30625	CG10343	38380	CG10491	50358	CG10621	31291
CG10083	38330	CG10225	38363	CG10344	48026	CG10492	12357	CG10622	30889
CG10084	38336	CG10228	38365	CG10346	31228	CG10493	45364	CG10623	31294
CG10089	17991	CG10229	38368	CG10347	16025	CG10495	18631	CG10624	44928
CG1009	35354	CG10230	31206	CG10348	39663	CG10497	13322	CG10626	22845
CG10090	37346	CG10231	18041	CG10353	5550	CG10505	6593	CG10627	31298
CG10096	50765	CG10234	37124	CG10354	27254	CG10510	18635	CG10628	47392
CG10097	6090	CG10236	18873	CG10355	9308	CG10517	44107	CG1063	6484
CG10098	50126	CG10238	15990	CG10361	16034	CG10523	47636	CG10635	35481
CG10103	31174	CG10240	33238	CG10362	8317	CG10524	33837	CG10635	46220
CG10104	13969	CG10242	50169	CG10363	13466	CG10531	16071	CG10637	35482
CG10105	18002	CG10242	4880	CG10365	16036	CG10532	16073	CG10638	31306
CG10106	7934	CG10243	7398	CG10369	3886	CG10535	45366	CG10639	30737
CG10107	18004	CG10243	49532	CG10371	47623	CG10536	16078	CG1064	12645
CG10110	18009	CG10245	3313	CG10372	31238	CG10537	41101	CG10640	30890
CG10117	4871	CG10246	29980	CG10373	6375	CG10539	18126	CG10641	31307
CG10118	3308	CG10246	50262	CG10374	48109	CG10541	31253	CG10642	45372
CG10122	12688	CG10247	3317	CG10374	30884	CG10542	15620	CG10645	31311
CG10123	10635	CG10249	15009	CG10375	16039	CG10545	31257	CG10646	38396

CG1065	27298	CG10798	2947	CG10960	8359	CG11094	11096	CG11221	42947
CG10653	35483	CG10803	27318	CG10961	16125	CG11095	37910	CG11228	7823
CG10655	2985	CG10805	17000	CG10962	30850	CG11096	38444	CG11233	45386
CG10657	3326	CG10806	33149	CG10966	3024	CG11098	7625	CG11236	38460
CG1066	46889	CG10808	8784	CG10967	16133	CG11099	9272	CG11237	38462
CG10662	31318	CG10809	38408	CG10971	16138	CG11102	13478	CG11242	38463
CG10663	27299	CG10811	17002	CG10973	41463	CG11103	5562	CG11246	11203
CG10664	3923	CG10814	27319	CG10975	4789	CG11105	51705	CG11250	35501
CG10667	46522	CG1082	45102	CG10975	942	CG11107	44119	CG11251	38467
CG10670	47601	CG10823	1783	CG10975	27090	CG11109	17528	CG11253	31473
CG10671	44435	CG10824	16588	CG10977	37238	CG11110	3801	CG11254	18198
CG10672	18661	CG10825	31360	CG10979	16144	CG11111	6226	CG11255	17534
CG10673	27301	CG10827	30823	CG1098	27346	CG11115	49942	CG11257	31475
CG10674	11366	CG10830	31362	CG10981	16149	CG1112	42942	CG11258	23376
CG10679	28445	CG10833	7870	CG10984	15627	CG11121	8950	CG11259	17537
CG10681	27305	CG10837	31364	CG10986	31390	CG11123	18142	CG1126	18200
CG10682	27306	CG10838	28289	CG10988	2983	CG11124	13911	CG11262	16912
CG10685	17847	CG1084	40613	CG1099	16158	CG11125	18143	CG11263	31112
CG10686	31319	CG10840	31365	CG10990	16162	CG11128	45587	CG11265	41097
CG10687	31320	CG10846	8057	CG10992	45345	CG11130	18145	CG11266	12945
CG10688	39715	CG10847	15291	CG10993	16165	CG11133	18150	CG11267	47087
CG10689	31324	CG10849	7480	CG10996	16168	CG11136	44991	CG11268	5240
CG10691	12358	CG10850	18847	CG10997	28303	CG11136	4758	CG11270	8322
CG10692	37816	CG10859	27322	CG10999	16171	CG11137	48241	CG11274	6439
CG10693	6723	CG1086	13326	CG1100	18676	CG11137	8464	CG11276	35718
CG10694	13649	CG10862	31373	CG11001	45015	CG11138	18154	CG11276	50021
CG10695	27307	CG10863	48619	CG11006	31394	CG11139	17530	CG11278	8361
CG10697	3329	CG10866	3234	CG11007	40833	CG11140	37726	CG1128	6420
CG10698	44309	CG10868	45009	CG11009	16173	CG11141	18157	CG11280	5242
CG10699	45231	CG10869	27326	CG1101	12031	CG11143	5616	CG11281	5247
CG10701	37917	CG10872	30717	CG11010	47537	CG11144	1793	CG11282	3046
CG10702	3691	CG10873	38235	CG11015	30892	CG11146	50598	CG11284	31482
CG10703	35486	CG10877	45750	CG1102	18970	CG11148	18159	CG1129	38471
CG10706	28155	CG10881	35495	CG11024	46489	CG11149	7882	CG11290	37527
CG1071	45743	CG10882	37543	CG11025	45497	CG11151	18129	CG11294	10497
CG10711	16846	CG10887	16082	CG11027	12931	CG11153	19022	CG11295	31484
CG10716	38399	CG10889	27329	CG11029	44228	CG11154	37812	CG11299	38481
CG10718	31329	CG1089	27332	CG11030	43530	CG11156	31432	CG1130	41070
CG10719	31333	CG10890	50554	CG11033	31402	CG11162	8326	CG11301	15344
CG1072	46755	CG10895	44981	CG11034	37941	CG11163	13311	CG11305	18043
CG1072	9830	CG10897	38413	CG11035	8478	CG11164	3180	CG11306	8448
CG10721	33098	CG10898	13643	CG11041	45061	CG11165	18166	CG11308	31487
CG10722	44128	CG10899	16084	CG11043	23370	CG11166	31435	CG11309	7513
CG10724	22850	CG1090	26783	CG11044	16178	CG11168	18170	CG1131	18048
CG10726	26759	CG10903	27334	CG11048	31407	CG11170	41302	CG11312	31488
CG10728	50141	CG10907	16085	CG1105	28305	CG11172	30566	CG11315	38273
CG10732	18664	CG10908	44211	CG11050	12371	CG11173	18172	CG11315	46906
CG10739	31337	CG10909	17522	CG11052	23373	CG11176	18175	CG11318	3395
CG10742	10140	CG1091	16088	CG11055	18686	CG11177	45975	CG11319	7621
CG10743	16850	CG10910	46896	CG11058	31409	CG11178	18178	CG1132	30553
CG10747	38403	CG10913	3245	CG11059	36348	CG11180	31438	CG11320	18054
CG10749	27311	CG10914	38419	CG11059	37291	CG11181	18179	CG11321	18055
CG10750	27313	CG10915	31377	CG1106	37867	CG11182	15318	CG11323	18057
CG10751	22761	CG10918	23190	CG11061	38441	CG11183	31442	CG11324	18061
CG10753	31343	CG10920	16091	CG11062	12174	CG11184	31444	CG11325	9546
CG10754	31347	CG10922	2989	CG11063	38442	CG11186	15919	CG11326	7535
CG10756	44466	CG10923	52105	CG11064	6878	CG11188	18182	CG11329	18065
CG10757	45494	CG10924	13929	CG11069	51367	CG1119	10942	CG1133	51292
CG1076	40807	CG10927	16094	CG1107	16182	CG11190	14821	CG11333	44110
CG10760	13996	CG1093	27335	CG11070	31413	CG11194	30561	CG11334	38485
CG10761	5474	CG10931	52107	CG11077	42671	CG11196	36497	CG11335	17259
CG10772	22853	CG10932	16099	CG11079	23374	CG11197	41368	CG11337	16420
CG10776	42244	CG10938	16104	CG1108	16184	CG11198	8105	CG11339	45390
CG10776	865	CG10939	16958	CG11081	27238	CG11199	51707	CG1134	7481
CG10777	46933	CG10947	16117	CG11081	4740	CG1120	18184	CG11342	38488
CG10778	3166	CG10948	31388	CG11082	45349	CG11200	4725	CG11348	39421
CG1078	27317	CG10950	41462	CG11084	11099	CG11201	31456	CG11348	33824
CG10791	18140	CG10951	16120	CG11085	10493	CG11202	37656	CG1135	15613
CG10792	15444	CG10952	9127	CG11086	18690	CG11206	42943	CG11356	33812
CG10793	31351	CG10954	45013	CG1109	16186	CG11208	4720	CG11357	5027
CG10795	8833	CG10955	27341	CG11092	16188	CG11210	7363	CG11360	38491
CG10797	26299	CG10958	26763	CG11093	15478	CG11217	28762	CG11367	40900

CG11367	40900	CG11546	31522	CG11755	17555	CG11909	14735	CG12082	17568
CG11374	15561	CG11547	31525	CG11757	16296	CG11913	16366	CG12083	7434
CG11376	40673	CG11551	48368	CG11759	16298	CG11922	13721	CG12084	31646
CG11386	38493	CG11556	52439	CG11760	11925	CG11926	38600	CG12085	20144
CG11386	49657	CG11561	9542	CG11761	9963	CG1193	31598	CG12090	16390
CG11386	49657	CG11567	44232	CG11763	45981	CG11935	15472	CG12091	13985
CG11386	38493	CG11568	30060	CG11765	18708	CG11936	37927	CG12092	35514
CG11387	5687	CG11569	8706	CG11770	16801	CG11940	16369	CG12093	41293
CG11388	3604	CG11573	52126	CG11771	18946	CG11943	38608	CG12099	18734
CG1139	8907	CG11576	7577	CG11778	7374	CG11949	9787	CG1210	18736
CG11392	42959	CG11577	14334	CG11779	16309	CG11951	16532	CG12101	18739
CG11393	33839	CG11579	7767	CG11780	42092	CG11951	48791	CG12106	16400
CG11393	47725	CG1158	9455	CG11781	49584	CG11956	3335	CG12107	8731
CG11395	16696	CG11582	35379	CG11783	10958	CG11958	1335	CG12108	5499
CG11396	18073	CG11586	31531	CG11788	47245	CG11963	20097	CG12109	20151
CG11397	10937	CG11588	8348	CG1179	14123	CG11963	50300	CG12110	38626
CG11399	31489	CG11590	19867	CG1179	49832	CG11964	35511	CG12111	16513
CG11401	16768	CG11591	22770	CG11793	31551	CG11968	20130	CG12113	18742
CG11408	45394	CG11592	2495	CG11796	31563	CG11975	26799	CG12116	6498
CG1141	18081	CG11593	16227	CG11799	45697	CG11981	31608	CG12117	17018
CG11412	49370	CG11594	28311	CG1180	13842	CG11982	38623	CG12118	13340
CG11416	40674	CG11596	35505	CG11801	30042	CG11984	31615	CG1212	41479
CG11417	18087	CG11597	38541	CG11802	31570	CG11985	22773	CG12125	5492
CG11418	31497	CG11598	49831	CG11804	16313	CG11986	20136	CG12127	3295
CG11419	20027	CG11600	42964	CG11807	38564	CG11987	10735	CG12128	42979
CG11423	38500	CG11601	42737	CG11811	30917	CG11988	10662	CG12129	17065
CG11426	42600	CG11601	50814	CG11814	38567	CG11989	31619	CG1213	6487
CG11427	38504	CG11606	44093	CG11819	31571	CG11990	28318	CG12130	7388
CG11428	38508	CG11607	15876	CG11820	39724	CG11992	49413	CG12131	45744
CG11430	12221	CG11608	19932	CG11821	26796	CG11994	18719	CG12132	31651
CG11440	42592	CG1161	44964	CG11821	46858	CG11999	16423	CG12134	31654
CG11444	31501	CG11611	39157	CG11823	12044	CG1200	50007	CG12135	17032
CG11444	50278	CG11614	3004	CG11824	23381	CG12000	16381	CG12136	5520
CG11446	26839	CG11617	30533	CG11825	33917	CG12001	16383	CG12139	27242
CG11446	43370	CG11621	16240	CG11825	49834	CG12002	15277	CG12139	5094
CG11447	16199	CG11622	16244	CG11833	4417	CG12004	10287	CG12140	15508
CG11448	16202	CG11639	23285	CG11836	38570	CG12005	11205	CG12149	17035
CG11449	31503	CG11641	30537	CG11837	38574	CG12006	39481	CG12151	31661
CG11450	41069	CG11642	50359	CG11838	31575	CG12007	20137	CG12152	17037
CG11454	45116	CG11648	12024	CG11839	31576	CG12008	37075	CG12153	13690
CG11455	12838	CG1165	13886	CG11840	7247	CG12010	6463	CG12154	51480
CG11459	16573	CG11652	38549	CG11844	17245	CG12012	33097	CG12156	31666
CG11459	48053	CG11654	16251	CG11847	38578	CG12014	13990	CG12157	13177
CG11465	28457	CG11655	9131	CG11848	18717	CG12016	22871	CG1216	17043
CG11466	38045	CG11658	16255	CG11849	37753	CG12018	13621	CG12161	31669
CG1147	9605	CG11659	16260	CG11851	3419	CG12019	47776	CG12162	20156
CG11474	31507	CG11660	18526	CG11856	38581	CG12020	18727	CG12163	46406
CG11482	12685	CG11661	50393	CG11857	23203	CG12021	31620	CG12163	12787
CG11486	51713	CG11661	12778	CG11858	49586	CG12024	20143	CG12163	15366
CG11488	31508	CG11665	7314	CG11858	31579	CG12025	4098	CG12165	17044
CG11489	47544	CG11669	15794	CG11859	47401	CG12026	43385	CG12169	38630
CG11490	20040	CG1167	6225	CG11861	16331	CG12026	42480	CG12170	31672
CG11495	6459	CG11671	41146	CG11866	31582	CG12029	26980	CG12171	47411
CG11502	37087	CG11678	17242	CG11870	16334	CG12030	16385	CG12173	31674
CG11505	15286	CG11679	14834	CG11873	16337	CG12031	15877	CG12175	48909
CG11508	38519	CG1168	30816	CG11874	4418	CG12038	51178	CG12175	32503
CG11511	38526	CG11680	19691	CG11875	16342	CG12042	31623	CG12176	12627
CG11513	16206	CG11685	16267	CG11877	49372	CG12050	42976	CG12178	7245
CG11514	13705	CG11687	46097	CG11880	22867	CG12051	12456	CG1218	31685
CG11518	19692	CG11699	15861	CG11881	16352	CG12052	12574	CG1218	46777
CG1152	38041	CG11709	5594	CG11883	38590	CG12054	45986	CG12186	17068
CG11522	51715	CG11716	16283	CG11886	42970	CG12055	31631	CG12189	13617
CG11523	46794	CG1172	44113	CG11887	17560	CG12058	31635	CG12190	52138
CG11523	16210	CG11722	44114	CG11888	44134	CG12068	16388	CG12192	41484
CG11525	13654	CG11726	17545	CG11895	51379	CG12068	50111	CG12194	7846
CG11526	16211	CG11727	17549	CG11896	38596	CG12070	51129	CG12194	46796
CG11529	37098	CG11734	45302	CG11897	28259	CG12071	49512	CG12200	31688
CG11533	45120	CG11737	5807	CG11898	4430	CG12072	9928	CG12200	50229
CG11534	16216	CG11738	16289	CG11899	43549	CG12077	4125	CG12201	42648
CG11537	4118	CG11739	44562	CG11900	6430	CG12078	15288	CG12202	17571
CG11539	49580	CG11750	45978	CG11901	31589	CG12079	13856	CG12203	42983
CG11539	31518	CG11753	33829	CG11907	49328	CG12081	31642	CG12207	18747

CG12208	20157	CG12345x	40918	CG12605	20250	CG12877	20265	CG13178	44816
CG12210	30605	CG12346	48112	CG12608	24629	CG12879	4407	CG13190	43001
CG12211	38634	CG12346	20185	CG12608	49840	CG12891	4047	CG13192	32157
CG12212	3788	CG12352	31741	CG1263	17262	CG12892	20270	CG13197	36422
CG12214	31689	CG12355	47109	CG12630	48656	CG12895	49607	CG1320	18101
CG12215	8754	CG12357	50433	CG12630	18762	CG12895	18093	CG1320	52257
CG12217	31690	CG12358	46299	CG1264	2990	CG12896	32111	CG13201	2976
CG12218	31693	CG12359	31744	CG12646	17267	CG12904	10268	CG13202	28290
CG12220	23040	CG1236	17789	CG12647	22781	CG12909	32114	CG13213	43004
CG12223	41029	CG12360	41487	CG12648	23518	CG1291	32116	CG1322	42856
CG12225	31701	CG12361	10513	CG1265	44951	CG12913	44296	CG13221	32164
CG12230	4548	CG12362	31747	CG12653	12668	CG12915	38737	CG13223	1684
CG12231	31705	CG12363	31749	CG12657	29843	CG12918	38082	CG13232	28772
CG12233	50829	CG12366	44045	CG12659	31757	CG12919	45252	CG13251	17127
CG12233	41191	CG12367	31920	CG12661	47422	CG12921	20271	CG13252	33301
CG12234	31706	CG12369	35524	CG1268	9174	CG12924	20280	CG13263	17129
CG12235	31711	CG12370	43314	CG12698	18256	CG12929	4180	CG1327	31086
CG12238	38637	CG12373	24521	CG12701	38706	CG12935	47569	CG13277	23862
CG12240	6655	CG12374	13919	CG12702	24588	CG12936	38750	CG13281	12648
CG12244	20166	CG12375	45309	CG1271	13044	CG12938	50331	CG13287	36601
CG12245	2961	CG12376	22879	CG12713	17296	CG12938	38754	CG13293	39797
CG12245	2961	CG12384	36388	CG12723	41389	CG12948	41492	CG13295	32171
CG1225	31716	CG1239	17100	CG12727	17302	CG12951	46921	CG13298	31777
CG12252	38640	CG12390	38682	CG12728	24592	CG12951	16569	CG13306	44960
CG12253	31719	CG12395	17101	CG12728	52287	CG12954	18765	CG13308	13862
CG12254	47922	CG12396	31927	CG12733	24601	CG12956	13014	CG13309	14133
CG12259	38646	CG12397	47517	CG12734	32008	CG12959	17946	CG13310	43960
CG12261	17060	CG12398	11540	CG12737	24604	CG12975	18098	CG13311	51574
CG12262	15053	CG12399	12635	CG1274	43254	CG12993	20304	CG13312	14060
CG12263	10060	CG12400	37462	CG12740	49123	CG12995	13346	CG1332	32175
CG12265	43112	CG12403	46397	CG12740	18090	CG12997	33914	CG13320	23866
CG12267	43528	CG12404	1463	CG12746	33313	CG13001	42347	CG13322	32178
CG12268	1166	CG12405	24522	CG12749	51759	CG13016	37428	CG13326	18784
CG1227	38648	CG12405	50772	CG1275	4103	CG13018	33859	CG1333	51169
CG12272	18749	CG12410	9727	CG12750	17304	CG13019	31769	CG13334	15005
CG12273	42919	CG1242	7716	CG12752	52631	CG13020	17116	CG13343	17137
CG12275	44589	CG12424	25222	CG12752	44146	CG13029	8502	CG13344	17141
CG12276	18528	CG1245	13697	CG12753	1617	CG1303	41494	CG13345	17145
CG12278	29484	CG12455	3849	CG12756	31761	CG1303	50742	CG13348	36555
CG12279	44123	CG12467	46883	CG12759	17306	CG13030	17117	CG13349	23873
CG1228	38652	CG12467	41377	CG1276	17917	CG13032	29454	CG13350	44474
CG12283	36252	CG12477	31942	CG12765	17307	CG13035	14247	CG13364	28464
CG12283	4761	CG12478	35526	CG12766	50403	CG13037	32138	CG13364	48265
CG12286	37348	CG12489	20239	CG12770	31894	CG13072	49484	CG13366	29606
CG12287	52272	CG1249	31947	CG12772	46140	CG13072	18099	CG13367	17157
CG12289	31724	CG12497	24549	CG12773	9899	CG13076	45906	CG13369	17161
CG12297	7926	CG12498	17793	CG12782	31857	CG13077	51496	CG13375	2944
CG12298	45402	CG12499	24550	CG12785	31830	CG13078	3917	CG13379	17167
CG12301	51733	CG1250	24552	CG12787	7854	CG1308	44503	CG13383	23886
CG12304	38654	CG12505	31122	CG12788	49610	CG13089	2810	CG13383	50566
CG12306	20177	CG12505	48131	CG12788	23044	CG1309	37227	CG13384	44246
CG12311	5583	CG12506	19879	CG12789	33153	CG13090	43558	CG13387	3347
CG12313	4075	CG12506	50327	CG12792	41489	CG13091	11729	CG13388	5647
CG12314	48764	CG12511	12451	CG12795	32019	CG13095	15541	CG13389	17168
CG12317	45191	CG1252	4566	CG12797	32021	CG13096	41499	CG13390	17169
CG12318	12375	CG12524	28745	CG12799	20260	CG13098	38015	CG13391	17171
CG12321	17077	CG12529	3337	CG12812	32025	CG1311	39695	CG13393	33164
CG12323	38658	CG12531	6203	CG12813	31094	CG13124	29648	CG13396	30760
CG12324	49105	CG12532	7720	CG12816	17314	CG13125	17123	CG13398	38669
CG12324	17785	CG12533	11670	CG12817	40655	CG13137	41500	CG13399	31781
CG12325	31726	CG12533	11670	CG12818	31898	CG13139	32146	CG13399	50778
CG12327	8372	CG12539	38689	CG12818	46248	CG13142	24511	CG1340	32192
CG12333	23091	CG12542	51748	CG12822	32031	CG13151	39782	CG13400	29954
CG12334	17079	CG12544	31961	CG12833	32038	CG1316	23851	CG13401	43572
CG12339	17081	CG12548	31964	CG12836	24614	CG13160	4629	CG13402	30051
CG1234	17084	CG12560	29725	CG12846	52561	CG13162	32148	CG13404	30255
CG12340	22878	CG1257	31974	CG12848	31900	CG13163	39785	CG13409	47577
CG12341	7391	CG12582	15028	CG12855	5639	CG13167	18770	CG1341	17176
CG12342	31736	CG12598	7763	CG12858	1688	CG13168	18776	CG13410	13443
CG12343	31737	CG12600	31993	CG12859	8787	CG1317	4106	CG13415	49138
CG12345	20183	CG12602	6121	CG1287	12127	CG13175	50775	CG13415	17178
CG12345	20183	CG12605	49556	CG12876	32047	CG13176	24643	CG13418	39049

CG13423	45404	CG13745	24655	CG13985	51447	CG14198	51785	CG14476	48375
CG13424	10514	CG13746	41403	CG1399	24826	CG14199	40884	CG14477	28731
CG13425	2912	CG13748	43985	CG13993	18210	CG1420	32100	CG14480	32270
CG13426	8821	CG1375	39808	CG13994	48622	CG14201	37047	CG14480	46974
CG13430	49662	CG13752	877	CG13994	31791	CG14206	49844	CG14482	33849
CG13431	40834	CG13756	29592	CG13996	46532	CG14208	50572	CG1449	13305
CG13442	4736	CG13758	42724	CG13999	7889	CG14208	37420	CG14490	17660
CG1345	17187	CG13771	31868	CG14001	45028	CG14209	49642	CG14505	17683
CG13458	17193	CG13772	44236	CG1401	52176	CG14210	31803	CG14507	35712
CG13466	3152	CG13773	43011	CG14013	17343	CG14210	49168	CG1451	51468
CG13467	17196	CG13775	44814	CG14015	45891	CG14211	3146	CG14511	4426
CG1347	24515	CG13777	41507	CG14016	28329	CG14212	17429	CG14512	47661
CG13470	17198	CG13778	17701	CG14016	49613	CG14213	32104	CG14512	41527
CG13472	32193	CG13779	49153	CG1402	39251	CG14214	11989	CG14513	26806
CG13473	32195	CG13779	31789	CG14020	44221	CG14214	46474	CG14514	41530
CG13475	12608	CG1378	6236	CG14022	31796	CG14217	17432	CG14514	49989
CG1349	17214	CG13780	7629	CG14022	48332	CG1422	44510	CG14515	51637
CG13502	32203	CG13784	8042	CG14023	36480	CG14221	32106	CG14517	42693
CG13510	28433	CG1379	41030	CG14024	13402	CG14222	18213	CG14522	32275
CG13521	42241	CG1380	44934	CG14025	13998	CG14224	47449	CG1453	41534
CG13521	4329	CG13801	45925	CG14028	13403	CG14228	7161	CG14536	11725
CG13521	42578	CG13807	47439	CG14028	33841	CG14230	46903	CG14542	24869
CG13526	32206	CG13809	24793	CG14029	5650	CG14232	47897	CG14543	4563
CG13531	17230	CG1381	24797	CG1403	17344	CG14234	30309	CG14544	32279
CG13533	6633	CG13822	38068	CG14030	24833	CG14238	2673	CG14547	14767
CG13551	31786	CG13827	24481	CG14031	48920	CG14255	39397	CG14549	43588
CG13559	6644	CG13829	28321	CG14033	23052	CG14256	35615	CG1455	32283
CG13567	43344	CG13830	44583	CG14034	32085	CG14268	14535	CG1455	49987
CG13570	23895	CG13832	24802	CG14036	28475	CG1427	17457	CG14550	50317
CG1358	13313	CG13833	6845	CG1404	24835	CG14283	37802	CG14550	4369
CG13585	13323	CG13842	17714	CG14040	13399	CG14283	50292	CG14551	24625
CG13585	50392	CG13844	29689	CG14041	39821	CG14286	17463	CG14562	32286
CG13588	45755	CG13849	52165	CG14043	17351	CG1429	15549	CG14575	43325
CG13597	32225	CG13852	17716	CG14048	39648	CG14290	15858	CG14575	13384
CG13598	32230	CG13855	17717	CG1405	31908	CG14291	16897	CG14577	9117
CG13601	19953	CG13859	48179	CG14057	48963	CG14296	24617	CG1458	4439
CG13602	32235	CG13859	17718	CG14057	22718	CG14299	17469	CG1458	33925
CG13603	6778	CG1386	13188	CG1406	17358	CG1430	17473	CG14591	9945
CG13604	32239	CG13867	24806	CG14066	24841	CG14303	17474	CG14593	1658
CG13605	1170	CG13875	44819	CG1407	50031	CG14305	17477	CG14611	31811
CG13608	22713	CG13876	39817	CG14073	39823	CG14322	30026	CG14615	24872
CG13609	17326	CG13880	24809	CG14077	7563	CG14325	17485	CG14617	24874
CG13610	48870	CG13886	17730	CG14079	14337	CG1433	17490	CG14618	50597
CG13610	1176	CG13887	23207	CG14080	45415	CG14339	17493	CG14619	37930
CG13611	45793	CG13889	17732	CG14084	8420	CG1434	30996	CG1462	6862
CG13617	32247	CG1389	1016	CG14085	45757	CG14353	24860	CG14620	24881
CG13623	17334	CG1389	36280	CG1409	30988	CG14366	17505	CG14621	8661
CG13624	32250	CG1389	4298	CG1410	24845	CG14394	39307	CG14622	24885
CG13626	1209	CG13892	44823	CG1410	50568	CG14396	12292	CG1463	31877
CG13628	29253	CG13893	32077	CG14100	46739	CG14396	29907	CG14630	24894
CG13633	14398	CG13898	23905	CG14105	17388	CG14396	842	CG1464	42845
CG13645	32255	CG13900	18955	CG1411	15320	CG1440	24622	CG14641	38790
CG13646	1421	CG13906	12584	CG1412	43955	CG14407	43020	CG14647	18297
CG13651	11515	CG1391	17740	CG14122	51782	CG1441	4034	CG14648	23918
CG13654	13550	CG13916	51569	CG14130	31911	CG14411	17579	CG14650	45458
CG13661	14730	CG13917	32082	CG14133	23322	CG14413	22740	CG1467	8644
CG13663	6731	CG13919	4086	CG1414	12630	CG14414	48176	CG14670	32301
CG13667	36578	CG13920	46993	CG14142	17410	CG1442	17580	CG14671	51803
CG13671	52026	CG13922	41516	CG14149	24851	CG14428	9730	CG14680	32304
CG13686	31867	CG13926	15261	CG1416	41548	CG14428	39362	CG14683	52664
CG13688	43824	CG13927	4084	CG14163	5201	CG14429	11683	CG14685	24905
CG13690	24648	CG13929	17752	CG14164	48825	CG1443	1333	CG14688	39840
CG13691	32058	CG13930	17753	CG14164	17863	CG14435	17600	CG14689	24907
CG13693	46527	CG13937	3375	CG14168	17414	CG14437	17602	CG14690	5985
CG13702	50000	CG13941	3464	CG1417	18561	CG1444	40949	CG14693	18332
CG1371	13276	CG13946	17858	CG1418	37728	CG14440	23916	CG14694	5994
CG1372	36346	CG1395	17760	CG14181	42548	CG14440	48156	CG14701	28517
CG13722	46470	CG13956	17766	CG14182	5370	CG14444	17621	CG14704	13159
CG13722	30939	CG13957	31840	CG14184	35613	CG14446	10274	CG14709	6053
CG1374	16892	CG13969	8070	CG14185	32097	CG14463	44552	CG1471	30189
CG13743	40974	CG13972	47444	CG14192	35684	CG1447	19831	CG14712	18347
CG13744	44796	CG13978	47488	CG14194	6181	CG14472	17648	CG14715	12829

CG14717	38813	CG14909	9082	CG1511	27236	CG15340	39973	CG15602	40001
CG14718	32311	CG1492	8320	CG15110	37185	CG15341	43660	CG15609	43406
CG1472	44460	CG14921	32331	CG15112	43056	CG15342	19428	CG15610	25074
CG14721	18354	CG14933	33920	CG15113	46485	CG15343	29569	CG15618	40006
CG14721	50259	CG14933	7683	CG15113	9558	CG15358	13372	CG15619	40007
CG14722	23919	CG14934	15833	CG15116	30877	CG1536	32579	CG15624	7858
CG14724	44490	CG14936	6123	CG15117	47527	CG15362	38282	CG15625	29368
CG1474	42996	CG14938	7779	CG15118	16854	CG15365	47648	CG15626	7844
CG14740	32318	CG14939	32334	CG1512	19298	CG15368	32583	CG15629	49077
CG14743	4142	CG14940	31038	CG15120	32374	CG15372	13184	CG15629	7839
CG14744	40829	CG14941	5690	CG15120	46222	CG15373	19439	CG15635	46490
CG14745	52289	CG14945	13459	CG1513	48600	CG15378	22908	CG15636	13072
CG14745	6444	CG14946	38306	CG1513	39148	CG15385	51859	CG15637	44029
CG14746	50792	CG14956	3254	CG15130	43491	CG15387	35759	CG15644	41587
CG14746	43201	CG14962	39855	CG15133	8059	CG15388	32599	CG15645	52291
CG14749	24917	CG14965	31848	CG15134	19305	CG15388	32599	CG15645	20206
CG1475	24921	CG14966	43612	CG1514	5467	CG15389	52199	CG15651	37206
CG14757	38293	CG14966	47189	CG15141	19307	CG15389	52199	CG15653	8827
CG14763	8737	CG14967	44431	CG15142	19309	CG1539	32601	CG15655	6586
CG14767	50355	CG14969	8913	CG15143	25195	CG15390	25112	CG15661	16904
CG14771	45498	CG14971	39479	CG15144	19315	CG15395	39929	CG15663	15445
CG14777	9737	CG14977	18233	CG15145	19316	CG15398	8873	CG15666	40013
CG14778	44970	CG14980	18479	CG15148	19323	CG15399	19450	CG15667	19150
CG14783	18226	CG14983	32341	CG1515	19329	CG15400	7261	CG15669	19536
CG14788	18379	CG14985	32342	CG15150	19332	CG15403	29945	CG15671	2938
CG14789	41361	CG14991	46494	CG15154	51821	CG15405	52652	CG15676	20121
CG14792	38823	CG14992	39857	CG1516	41576	CG1542	39976	CG1569	19152
CG14792	50129	CG14993	43032	CG15160	44601	CG15427	27046	CG15693	32383
CG14793	3195	CG14994	32344	CG15161	25198	CG15427	3064	CG15694	40018
CG14801	38826	CG14995	12725	CG15168	12248	CG15429	19462	CG15696	16979
CG14802	28264	CG14996	5654	CG15168	48614	CG1543	51667	CG15697	32511
CG14802	48491	CG14997	47016	CG1517	3306	CG15432	19466	CG15701	19541
CG14803	18395	CG14998	18491	CG1518	12250	CG15432	49216	CG15706	4907
CG14804	18396	CG14999	37756	CG1518	48653	CG15433	19470	CG1571	51846
CG14805	32325	CG1500	39575	CG15187	30628	CG15434	29236	CG15715	28563
CG14806	45107	CG15000	6273	CG1519	46544	CG15438	7303	CG15723	28566
CG14808	8305	CG15000	6273	CG15191	48720	CG15439	19490	CG1573	22915
CG14812	31815	CG15001	24943	CG15191	16751	CG15440	19494	CG15730	19582
CG14813	41549	CG15011	51517	CG1520	13757	CG15441	29123	CG15735	33813
CG14814	41553	CG15012	9176	CG15208	19368	CG15442	49184	CG15736	23926
CG14816	51655	CG15014	43615	CG15211	35704	CG15442	49184	CG15737	19584
CG14817	26894	CG15015	18492	CG15216	32541	CG15444	8880	CG15738	47929
CG14818	40700	CG15016	38842	CG15218	36216	CG15445	29158	CG15739	14890
CG14820	15456	CG15019	28438	CG1522	5551	CG15448	30894	CG15743	42685
CG14824	45594	CG1502	14894	CG15220	15380	CG15450	8645	CG15744	1095
CG14825	41554	CG15021	52038	CG15224	32378	CG15455	30539	CG15744	4801
CG1484	39528	CG15027	24627	CG1523	25199	CG15456	23106	CG15749	16744
CG14853	39734	CG1503	32349	CG1524	39870	CG15467	41584	CG1575	19153
CG14861	47458	CG15035	32352	CG15254	15604	CG15468	25116	CG15751	19594
CG14865	28532	CG15037	37789	CG15255	12412	CG1548	31012	CG15752	43686
CG14866	18419	CG1506	33217	CG15257	3837	CG15481	32612	CG15759	41597
CG14868	51810	CG15069	44611	CG15262	25100	CG15483	30763	CG15762	29871
CG14869	33347	CG1507	12765	CG15266	51827	CG15498	19508	CG1577	23356
CG1487	41559	CG1507	48249	CG15270	3829	CG15509	6212	CG15771	43689
CG14870	46307	CG15072	39866	CG1528	25101	CG15523	47481	CG15772	46284
CG14881	31821	CG15077	18524	CG15283	28550	CG15525	48660	CG15775	39358
CG14882	38838	CG15078	10061	CG15287	19379	CG15525	39993	CG15775	28570
CG14883	8028	CG15081	32361	CG15288	3141	CG15526	19518	CG15776	47248
CG14885	46916	CG15087	32527	CG15297	29623	CG15527	39323	CG15776	19611
CG14887	48256	CG15093	5655	CG15298	38884	CG15528	14865	CG1578	41599
CG1489	24936	CG15094	5002	CG15299	43501	CG15529	14867	CG15792	7819
CG1489	46803	CG15096	39463	CG1530	45166	CG15529	50227	CG15793	40025
CG14893	43598	CG15097	25188	CG15300	25140	CG1553	52179	CG15797	41603
CG14895	39843	CG15099	20126	CG15304	11317	CG15532	39877	CG15803	43635
CG14898	18229	CG15100	25193	CG15305	29622	CG15533	42520	CG15804	48544
CG14898	49177	CG15101	13749	CG15309	19388	CG15534	30186	CG15804	48153
CG1490	18231	CG15102	30909	CG15318	32382	CG15547	32621	CG15811	19696
CG14902	43028	CG15104	10642	CG15319	3787	CG1555	11322	CG15814	30429
CG14903	40658	CG15105	19290	CG1532	19398	CG15552	45961	CG15816	19616
CG14903	49107	CG15106	5008	CG15329	32564	CG15556	1791	CG15817	41605
CG14905	39848	CG1511	4771	CG15331	39285	CG15561	41582	CG15818	15537
CG14906	31851	CG1511	6545	CG1534	43097	CG1560	29619	CG15819	32385

CG1582	19617	CG1671	32697	CG16912	20327	CG17124	19078	CG17320	49013
CG15820	43874	CG16716	40042	CG1692	20329	CG17134	18110	CG17324	6379
CG1583	8928	CG16717	29199	CG16928	30476	CG17136	21083	CG17326	32878
CG1583	50353	CG16718	37472	CG1693	43841	CG17137	39107	CG17327	41654
CG15835	32652	CG16719	39934	CG16932	19165	CG17141	50241	CG17329	19171
CG1584	10677	CG16721	25201	CG16933	35558	CG17143	46676	CG17331	19079
CG15862	39437	CG1673	25204	CG16938	20334	CG17146	25214	CG17332	19173
CG15865	19157	CG16732	1148	CG16940	51853	CG17149	25218	CG17335	46117
CG1587	19061	CG16733	47020	CG16941	20338	CG1715	52253	CG17336	37408
CG15871	43691	CG16738	15749	CG16944	48582	CG17150	35624	CG17342	32885
CG15877	40031	CG16740	7210	CG16944	11968	CG1716	30707	CG17348	3047
CG15879	46754	CG16742	23832	CG1695	48062	CG17161	12680	CG17348	27053
CG15879	38899	CG16749	46390	CG1695	20340	CG17166	20388	CG17349	32887
CG15881	32390	CG16749	7555	CG16952	19166	CG17168	41625	CG17358	12654
CG15890	11538	CG1675	32712	CG1696	12939	CG17170	32868	CG1736	32889
CG15897	41618	CG16751	19069	CG16965	32782	CG17173	8370	CG17360	40070
CG15898	41114	CG16756	45655	CG16975	52247	CG1718	44449	CG17367	32892
CG15898	33897	CG16757	19658	CG16979	51594	CG17180	29141	CG17369	46553
CG15902	8577	CG16758	32714	CG16982	32399	CG17181	20396	CG17378	47367
CG15907	40762	CG1676	32719	CG16983	46605	CG17183	32459	CG1738	32464
CG15908	19623	CG16764	26976	CG16983	32790	CG17184	20401	CG17386	5701
CG1591	38908	CG16766	51387	CG16985	32401	CG17187	40051	CG17387	32902
CG15910	38910	CG1677	50195	CG16986	39129	CG17195	1435	CG1739	32904
CG15912	32654	CG16771	6386	CG16988	32798	CG17196	6743	CG17396	10833
CG15914	41571	CG16779	40824	CG16989	32802	CG17198	1432	CG1740	49848
CG15916	19627	CG16781	7018	CG16995	23078	CG17200	6024	CG17419	40076
CG15923	37373	CG16783	32724	CG17002	39883	CG17202	41628	CG1742	44445
CG15925	8982	CG16784	48045	CG17003	32804	CG17203	45360	CG1743	32929
CG15929	26830	CG16785	30214	CG17004	11471	CG17204	32872	CG17437	38925
CG1594	40037	CG16787	19661	CG17018	32810	CG17204	32872	CG17441	13444
CG1597	37383	CG16787	48685	CG17019	48749	CG17207	46640	CG17446	47221
CG1598	32391	CG16788	51851	CG1702	48635	CG17209	30512	CG17446	20453
CG1599	13317	CG16789	32729	CG17024	50187	CG1721	52336	CG17450	50795
CG1607	13793	CG16790	19160	CG17026	49199	CG17219	41635	CG17461	43639
CG1609	32664	CG16799	35709	CG17026	32813	CG17221	25229	CG17462	19801
CG1615	40953	CG16804	16806	CG17027	50076	CG17223	2608	CG1747	32932
CG1616	44484	CG16807	23843	CG17027	32817	CG17224	41177	CG1748	32933
CG1617	23822	CG1681	43041	CG17028	32819	CG17227	13330	CG1749	32937
CG1618	46483	CG16812	14972	CG17029	49565	CG17230	20409	CG17492	40078
CG1620	12682	CG16817	15309	CG17029	32822	CG17233	25231	CG17494	8199
CG1622	38915	CG16827	37172	CG17030	32827	CG1724	30315	CG17498	25264
CG1624	41623	CG1683	45174	CG17031	32829	CG17245	8383	CG17508	1487
CG1625	32668	CG16833	32741	CG17033	32830	CG17245	46687	CG17509	36527
CG1627	14900	CG16837	32749	CG17034	8136	CG17245	27220	CG1751	51149
CG1628	47475	CG16838	32754	CG17035	44443	CG17248	44011	CG17514	47269
CG1634	27202	CG16840	20305	CG17036	2869	CG17248	49202	CG17521	19084
CG1635	32672	CG16857	4806	CG17043	8777	CG17249	19170	CG17523	32945
CG1638	32676	CG16857	36224	CG17048	8780	CG1725	41136	CG17525	20472
CG1638	46275	CG16858	16986	CG17051	25209	CG17251	48024	CG1753	32946
CG1639	23825	CG16863	20312	CG17054	40047	CG17252	20410	CG1754	8651
CG1640	32680	CG16865	19162	CG17059	23535	CG17255	48633	CG17540	32948
CG1646	32682	CG16868	8209	CG17060	28758	CG17256	40052	CG17544	47934
CG1650	12568	CG16873	15758	CG17064	32841	CG17257	2611	CG17556	49518
CG1652	38104	CG16879	32759	CG17065	32845	CG17258	44372	CG17556	20483
CG1656	35555	CG16882	52426	CG17068	32850	CG17262	2614	CG17559	27057
CG1657	19649	CG16884	51363	CG1707	26832	CG17265	36479	CG17559	8002
CG1658	19066	CG16885	48049	CG17075	2487	CG17266	25243	CG17559	6547
CG1658	19066	CG16886	38026	CG17077	7170	CG17268	46876	CG1756	37517
CG1658	19066	CG16889	32766	CG17081	14194	CG17268	40056	CG17560	52002
CG1659	19653	CG16890	40044	CG17083	39937	CG17272	32874	CG17562	37365
CG1660	28801	CG16892	23844	CG1709	22925	CG1728	28805	CG17564	47273
CG1662	50409	CG16894	10067	CG17090	32855	CG17280	12965	CG17565	32951
CG1662	12197	CG16896	20316	CG17097	41244	CG17284	2558	CG17566	25271
CG1664	32690	CG16899	15732	CG17098	46309	CG17286	36623	CG17569	41657
CG1665	9958	CG16901	32395	CG1710	46998	CG17287	49415	CG17574	45729
CG1666	32693	CG16902	37067	CG17100	42821	CG17291	49672	CG17577	4664
CG1666	50144	CG16903	37572	CG17109	32858	CG17293	25246	CG1759	49563
CG1667	4031	CG16905	12130	CG17109	50820	CG17294	39105	CG1759	3361
CG1669	52246	CG16905	48663	CG17117	12764	CG17301	25252	CG17592	30452
CG16700	6145	CG16908	32767	CG17118	37624	CG17302	32875	CG17593	13029
CG16705	30972	CG1691	20321	CG17119	51127	CG17309	32877	CG17595	29228
CG16708	43413	CG16910	7723	CG17122	25212	CG1732	13359	CG17596	5702

CG17597	49204	CG1785	52467	CG18174	19272	CG1848	25343	CG18769	9501
CG17597	25276	CG17856	33016	CG18176	20604	CG18480	1072	CG1877	42445
CG17598	32956	CG1787	5503	CG18177	40844	CG18480	3821	CG18780	52484
CG17599	14682	CG17870	48724	CG18182	40134	CG1849	3025	CG18787	20697
CG1760	32961	CG17888	37769	CG18208	10215	CG18493	18930	CG18787	49686
CG17603	41099	CG1789	20567	CG1821	24977	CG18495	49680	CG18789	49689
CG17604	32962	CG17894	37673	CG18214	40138	CG18495	43705	CG18789	20699
CG17608	51162	CG17903	33019	CG1824	5554	CG18497	48846	CG18799	5528
CG17610	4331	CG17904	41660	CG18241	47967	CG18497	49543	CG18801	37110
CG17610	3121	CG17907	3968	CG18247	25304	CG18497	20637	CG18802	5838
CG17610	36251	CG17912	40107	CG18251	40143	CG18505	28285	CG18803	43082
CG17617	32965	CG17919	38204	CG18258	20621	CG18508	52071	CG18809	20702
CG17618	32403	CG17919	46473	CG18259	50094	CG18516	46403	CG18810	40825
CG1762	42234	CG17921	12773	CG1826	33049	CG1852	8309	CG18811	14011
CG1762	893	CG17922	6599	CG1827	46039	CG18528	40149	CG18812	39224
CG1762	40895	CG17923	3976	CG18278	22936	CG18530	6109	CG18814	5283
CG17633	47634	CG17927	7164	CG18278	50084	CG18530	47205	CG18815	33414
CG17636	8675	CG1793	51476	CG1828	10916	CG18549	6098	CG18818	20705
CG1764	20507	CG17934	19093	CG18281	50086	CG1855	40150	CG1882	41406
CG17642	51611	CG17935	23556	CG18284	49221	CG18558	33366	CG18820	20706
CG17642	30719	CG17941	36219	CG18284	31030	CG1856	10855	CG18826	13336
CG17645	41658	CG17941	4312	CG18287	36660	CG18572	33375	CG18827	9894
CG1765	37059	CG17945	42407	CG18296	18866	CG18578	8573	CG18828	23572
CG17657	40088	CG17945	23558	CG1830	33054	CG18582	46044	CG18829	33415
CG17660	2684	CG17946	23560	CG18301	31023	CG18585	19917	CG1883	20711
CG17664	49979	CG17947	19182	CG18313	49211	CG18591	23569	CG18831	13007
CG17669	36538	CG17949	33025	CG18313	44735	CG18594	20650	CG18833	39189
CG1768	20518	CG17949	50797	CG18315	19101	CG18596	41675	CG18833	39352
CG17680	45211	CG1795	37738	CG18315	48613	CG18599	25363	CG18838	12187
CG17681	40972	CG17950	19026	CG18317	44203	CG18600	32470	CG1884	12571
CG17683	19180	CG17952	39468	CG18319	9413	CG18605	33377	CG18842	6932
CG17691	40686	CG1796	44862	CG18324	33234	CG18609	4994	CG18843	24340
CG17697	43077	CG17964	3014	CG18331	48500	CG1861	14872	CG18844	39335
CG1770	20522	CG17970	16988	CG18332	12821	CG18619	19110	CG18844	28816
CG1771	5671	CG17973	20571	CG18335	52470	CG18620	40811	CG18845	14934
CG17712	32987	CG17985	7355	CG18340	33128	CG18624	29883	CG18846	29892
CG17716	6561	CG1799	40116	CG18341	52475	CG18624	33893	CG18848	45684
CG17716	42237	CG17998	1835	CG18345	35571	CG18627	33386	CG18849	42391
CG17723	7461	CG1800	40118	CG1836	30498	CG18630	25366	CG18851	20721
CG17725	20529	CG18000	48333	CG18362	52606	CG18631	47215	CG18858	50800
CG17726	32991	CG18005	25290	CG1837	15660	CG18635	8993	CG1886	8315
CG17734	13791	CG18009	10443	CG18374	52478	CG1864	2971	CG1890	39894
CG17734	49497	CG18012	20580	CG18375	25332	CG18642	7266	CG1891	46350
CG17735	50189	CG18013	33041	CG18378	25333	CG18647	9409	CG1891	42456
CG17737	29215	CG1803	39945	CG1838	33132	CG18654	38239	CG1894	41574
CG17739	36542	CG18039	40929	CG18380	20634	CG18660	51459	CG1897	7791
CG1774	16622	CG18041	46031	CG18381	25335	CG18662	26833	CG1898	33420
CG17743	39529	CG18048	19184	CG18389	13075	CG18667	25371	CG1900	29259
CG17746	40102	CG18065	15361	CG1839	15476	CG18668	20673	CG1903	28341
CG1775	19689	CG18065	49677	CG18398	43647	CG18671	33394	CG1905	48768
CG17753	20536	CG18069	47280	CG18402	991	CG18675	33397	CG1906	32476
CG17754	47274	CG18085	49924	CG18405	36147	CG18678	23225	CG1909	20745
CG17757	35772	CG1809	43231	CG18405	4743	CG18679	3128	CG1911	33423
CG17759	19088	CG18096	30873	CG18408	19054	CG18679	36153	CG1912	43711
CG17765	32405	CG18102	3798	CG18412	50027	CG1868	25379	CG1913	52346
CG17766	14531	CG18104	47186	CG18412	50024	CG1869	42877	CG1913	33427
CG17768	49674	CG18104	14933	CG18414	10679	CG1871	39287	CG1915	47301
CG17769	20544	CG18110	1349	CG18418	9008	CG1873	52343	CG1916	38079
CG17779	45670	CG18112	43415	CG18419	42776	CG1873	40156	CG1919	15265
CG17785	1181	CG1812	15491	CG18428	35638	CG18730	50098	CG1921	6948
CG17800	36233	CG18128	40127	CG18432	25336	CG18730	30745	CG1922	10663
CG17800	3115	CG18130	20599	CG18436	16523	CG18732	35641	CG1924	52348
CG17809	39572	CG18136	13128	CG18437	1310	CG18734	1020	CG1924	42397
CG17818	19089	CG1814	19096	CG1844	23268	CG18735	30914	CG1925	24472
CG17821	4997	CG18144	23306	CG18445	4039	CG1874	41680	CG1935	52670
CG17828	39887	CG18146	36261	CG1845	30436	CG18740	6969	CG1937	6870
CG17829	41659	CG18146	3705	CG1846	41672	CG18741	3391	CG1938	41686
CG1783	33007	CG18146	3120	CG18466	5705	CG18745	20686	CG1939	44765
CG17835	49950	CG18155	42446	CG18467	47282	CG18746	33399	CG1942	7942
CG17838	33012	CG1817	8010	CG1847	43701	CG18747	41252	CG1942	48583
CG17840	45037	CG18171	25299	CG18472	40148	CG18766	20694	CG1945	2955
CG17841	5530	CG18173	4092	CG18473	25341	CG18767	38251	CG1945	30679

CG1946	33428	CG2095	45032	CG2248	49247	CG2702	33557	CG2931	20946
CG1946	48259	CG2096	2964	CG2249	40977	CG2708	33561	CG2934	20950
CG1951	33430	CG2097	33469	CG2252	51305	CG2713	5587	CG2937	30087
CG1954	33434	CG2098	20804	CG2253	33507	CG2714	6308	CG2938	7035
CG1956	33437	CG2099	39895	CG2254	5470	CG2715	32413	CG2939	37658
CG1957	29575	CG2100	38037	CG2256	40170	CG2716	8307	CG2943	8477
CG1960	28342	CG2101	33473	CG2257	33510	CG2718	40174	CG2944	8688
CG1961	40161	CG2102	2929	CG2259	33512	CG2720	41696	CG2945	19280
CG1962	33444	CG2103	33264	CG2260	25154	CG2727	12232	CG2947	43725
CG1963	48872	CG2104	30016	CG2262	14609	CG2747	33566	CG2948	33593
CG1963	19117	CG2105	39535	CG2263	33514	CG2759	30033	CG2956	37091
CG1964	28347	CG2108	13145	CG2272	33516	CG2765	43721	CG2957	25462
CG1965	43944	CG2109	45000	CG2286	52049	CG2766	33888	CG2958	45294
CG1966	33446	CG2112	25405	CG2292	51933	CG2766	28819	CG2960	25466
CG1967	12196	CG2118	25406	CG2304	4448	CG2772	15577	CG2962	50422
CG1968	20767	CG2121	3386	CG2309	33522	CG2779	24992	CG2962	5526
CG1970	38224	CG2124	14869	CG2316	12170	CG2781	48139	CG2964	42293
CG1972	33450	CG2125	51479	CG2321	33523	CG2789	2507	CG2969	42751
CG1973	19275	CG2126	47598	CG2330	46555	CG2790	20903	CG2970	48124
CG1975	20771	CG2128	20814	CG2331	24354	CG2791	42622	CG2970	43497
CG1977	25387	CG2128	50213	CG2358	9055	CG2803	25160	CG2971	14637
CG1981	13657	CG2136	33486	CG2371	15483	CG2807	25161	CG2972	48771
CG1982	47191	CG2137	41235	CG2380	14918	CG2812	52485	CG2974	32484
CG1982	3761	CG2140	43065	CG2381	24989	CG2816	29700	CG2975	2601
CG1983	24980	CG2143	20819	CG2397	4019	CG2818	25441	CG2976	20962
CG1986	51669	CG2144	3996	CG2412	1494	CG2826	46588	CG2980	25470
CG1989	46977	CG2145	14874	CG2453	20872	CG2827	25444	CG2984	33599
CG1989	39898	CG2146	44292	CG2471	39140	CG2829	20905	CG2986	28822
CG1994	13479	CG2151	47307	CG2478	12482	CG2830	29339	CG2987	7182
CG1998	37395	CG2152	19121	CG2488	10461	CG2835	24959	CG2988	9419
CG2005	27208	CG2155	3349	CG2493	3929	CG2839	17952	CG2988	48649
CG2005	6705	CG2158	20824	CG2503	20876	CG2843	52326	CG2989	46286
CG2005	8009	CG2160	33490	CG2505	20879	CG2843	38933	CG2991	2604
CG2009	48037	CG2161	20826	CG2508	52280	CG2845	20909	CG2993	33605
CG2013	46927	CG2162	33493	CG2520	12732	CG2848	33571	CG2994	8176
CG2013	23229	CG2163	33499	CG2522	14877	CG2849	43623	CG2995	25473
CG2014	50731	CG2165	30203	CG2525	15880	CG2852	15069	CG2996	14613
CG2014	40165	CG2168	50311	CG2528	33532	CG2854	41703	CG2998	42419
CG2017	20780	CG2168	43627	CG2534	7769	CG2855	16820	CG2998	35783
CG2019	10004	CG2173	36516	CG2540	33536	CG2856	10970	CG2999	33609
CG2022	9049	CG2174	37530	CG2543	25417	CG2857	7417	CG3000	25553
CG2025	25392	CG2177	51084	CG2551	29635	CG2859	15334	CG30000	41965
CG2028	13664	CG2179	20829	CG2574	40173	CG2861	20918	CG30005	25555
CG2031	20783	CG2182	20834	CG2578	32482	CG2863	33573	CG3001	21054
CG2033	50635	CG2183	13762	CG2595	43717	CG2864	23962	CG30010	48606
CG2033	19198	CG2184	51201	CG2608	20886	CG2867	20926	CG30010	33660
CG2038	40690	CG2185	29477	CG2614	32407	CG2872	39221	CG30011	43070
CG2048	9241	CG2187	7575	CG2615	49365	CG2872	3399	CG30012	21057
CG2051	33459	CG2189	7782	CG2616	11052	CG2872	48496	CG30013	41415
CG2053	13546	CG2189	50110	CG2617	3931	CG2875	33575	CG30014	25557
CG2060	49044	CG2194	19279	CG2621	7005	CG2887	33581	CG30016	40488
CG2060	9953	CG2198	22944	CG2637	22348	CG2890	25446	CG30019	32429
CG2061	44186	CG2201	33502	CG2641	25422	CG2899	45041	CG30021	29965
CG2062	4018	CG2204	19124	CG2647	5709	CG2901	12209	CG30022	30880
CG2063	33462	CG2205	43630	CG2655	30564	CG2902	37333	CG30035	52360
CG2064	8728	CG2210	33198	CG2656	25423	CG2903	20933	CG30038	21068
CG2065	19119	CG2212	5469	CG2662	33544	CG2905	52486	CG3004	46557
CG2069	43382	CG2216	49537	CG2666	42611	CG2906	25449	CG30043	11708
CG2070	20793	CG2216	12925	CG2669	47309	CG2910	20942	CG30046	13947
CG2072	43714	CG2218	32517	CG2670	11499	CG2911	25452	CG30047	4623
CG2075	13673	CG2221	1054	CG2671	51249	CG2913	7028	CG30048	4634
CG2076	50221	CG2221	27247	CG2674	7167	CG2914	51225	CG30051	43066
CG2076	5537	CG2221	39505	CG2675	10149	CG2916	25456	CG30051	49256
CG2078	25402	CG2222	20849	CG2677	25427	CG2917	13613	CG30059	13010
CG2079	20796	CG2224	20852	CG2679	37435	CG2918	18440	CG30059	50732
CG2083	20798	CG2239	43044	CG2681	33549	CG2919	25457	CG3006	38148
CG2086	27084	CG2241	49245	CG2682	44783	CG2921	33585	CG30062	15433
CG2086	4830	CG2241	25412	CG2684	13308	CG2922	25166	CG30063	48780
CG2087	16427	CG2244	20855	CG2685	20887	CG2925	20943	CG30075	25563
CG2091	20799	CG2245	25415	CG2694	33551	CG2926	33589	CG30077	25568
CG2092	33465	CG2246	48877	CG2699	33556	CG2929	25458	CG30078	30610
CG2093	29971	CG2246	24987	CG2701	25433	CG2930	7031	CG3008	43731

CG30084	36564	CG30354	23575	CG3093	33733	CG31183	36323	CG31447	25761
CG30085	33672	CG30359	43151	CG3095	14524	CG31187	43739	CG31447	50997
CG3009	12216	CG3036	42755	CG3099	25636	CG31188	15364	CG31450	26319
CG30093	17893	CG30360	47951	CG3100	14526	CG31192	42318	CG31452	27194
CG30097	8977	CG30368	13913	CG31000	33735	CG31194	45433	CG31452	3744
CG30100	43236	CG30372	19287	CG31002	22960	CG31201	49547	CG31453	21350
CG30100	48945	CG30373	4013	CG31002	48225	CG31202	43522	CG31460	33323
CG30101	15514	CG30378	21153	CG31004	40940	CG3121	25712	CG31467	40268
CG30102	33677	CG30387	3468	CG31007	33739	CG31211	33787	CG31469	23396
CG30103	4949	CG30387	48313	CG31009	27216	CG31212	40214	CG31477	42108
CG30104	10050	CG30388	41735	CG31009	3739	CG31223	43426	CG31482	45931
CG30105	19204	CG30389	19002	CG31009	3733	CG31229	9660	CG3149	47560
CG30106	1678	CG30390	41740	CG3101	21275	CG31232	13090	CG31501	25773
CG30109	50925	CG30392	12862	CG31012	38854	CG31234	30389	CG3151	33939
CG3011	19208	CG30394	3470	CG31014	30975	CG31237	23308	CG31522	37329
CG30112	42444	CG30398	21166	CG31015	41351	CG31241	29503	CG31523	9807
CG30113	41562	CG3040	19219	CG3102	33744	CG31243	14385	CG31527	43255
CG30115	39952	CG30404	29385	CG31022	2464	CG31256	40218	CG31528	30811
CG30123	25571	CG3041	47602	CG31027	25644	CG31259	46362	CG31531	40276
CG30124	4998	CG30410	40176	CG31033	25651	CG3126	21306	CG31534	21366
CG30131	52556	CG30418	38152	CG31038	25655	CG3127	33797	CG31536	25049
CG30144	39920	CG3042	25620	CG3104	21289	CG31274	40222	CG31546	13140
CG30147	25580	CG30420	7414	CG31040	39926	CG31278	38938	CG31547	8551
CG30149	21109	CG30421	33726	CG31042	9704	CG31289	39091	CG31548	13144
CG30152	38848	CG30423	10600	CG31046	9701	CG3129	40228	CG31550	25779
CG3016	7090	CG30426	21173	CG31048	21293	CG31290	38860	CG31551	40278
CG30163	39687	CG30427	7423	CG31049	21294	CG31291	21308	CG3156	12182
CG30164	3633	CG30429	21175	CG3105	25662	CG31299	45442	CG3157	47163
CG30165	19709	CG30438	37106	CG31050	48824	CG3130	40229	CG3158	21374
CG3017	21110	CG30440	21178	CG31053	33750	CG31301	40232	CG3160	7070
CG30170	25590	CG30441	50583	CG31057	25023	CG31302	40235	CG31601	21378
CG30171	29412	CG3045	25621	CG31063	45246	CG31304	45035	CG31605	2789
CG30173	35794	CG30460	40624	CG31064	33756	CG31306	40236	CG3161	44487
CG30174	45060	CG30462	10046	CG31069	25026	CG3131	2593	CG3161	49291
CG30175	24378	CG30463	4923	CG31072	1251	CG31311	23079	CG3161	49291
CG30176	25593	CG30467	21203	CG31075	25676	CG31314	44406	CG3161	44487
CG30178	21111	CG3047	21206	CG31076	28776	CG31318	21985	CG31613	33972
CG30179	26836	CG30476	23495	CG3108	25680	CG31319	40238	CG31617	33975
CG30183	25594	CG3048	21214	CG31089	12449	CG3132	16779	CG31618	25782
CG3019	25597	CG30481	13320	CG3109	14529	CG31320	25742	CG31619	33102
CG30193	39474	CG30483	21216	CG31091	33085	CG31321	44942	CG3162	21380
CG30194	50234	CG30489	49271	CG31092	25684	CG31325	45139	CG31623	21383
CG30194	3527	CG30489	21235	CG31095	14756	CG31332	49701	CG31624	33976
CG30197	9586	CG30491	12817	CG31106	3415	CG31332	16813	CG31624	50803
CG30203	33913	CG30493	43131	CG31110	25030	CG31342	51330	CG31628	46295
CG3021	25603	CG30495	21241	CG31111	40198	CG31345	24656	CG31629	37935
CG3022	50176	CG30496	21244	CG31115	25693	CG31346	45943	CG31632	21386
CG3024	30985	CG30497	41745	CG31120	3402	CG31349	38863	CG31634	2650
CG30259	19211	CG30498	13457	CG31123	25034	CG3135	14803	CG31634	2650
CG3026	33688	CG30499	25016	CG31126	23395	CG31352	49112	CG31637	7614
CG30268	42703	CG30502	21253	CG31126	49277	CG31352	25750	CG31638	33981
CG3027	25610	CG30503	9036	CG31136	33112	CG31357	40248	CG31639	48790
CG30271	32436	CG3051	1827	CG31137	13365	CG3136	36504	CG31639	32443
CG30271	50158	CG3052	13724	CG31138	29541	CG31363	25044	CG31640	3498
CG30275	25612	CG3054	13555	CG3114	4559	CG31367	37625	CG31641	32370
CG3028	25615	CG3057	47965	CG31140	38936	CG31373	21726	CG31648	44225
CG30280	34743	CG3058	21258	CG31141	29537	CG31381	14720	CG31649	50192
CG30284	21118	CG3059	7265	CG31145	25036	CG31385	3704	CG3165	25785
CG3029	25014	CG3060	2993	CG31146	42616	CG31385	8394	CG31650	30690
CG30290	49962	CG3061	5868	CG31148	14698	CG31385	27178	CG31651	2629
CG30290	41564	CG3064	6972	CG31151	51341	CG3139	8875	CG31652	33993
CG30291	21120	CG3069	15872	CG31152	14480	CG31390	11504	CG31653	25786
CG30295	47790	CG3071	29589	CG31155	39134	CG31391	33801	CG31654	15565
CG30327	33705	CG3073	25627	CG31156	44478	CG31391	49286	CG31655	45883
CG3033	7086	CG3074	6617	CG31158	42321	CG3140	25046	CG31657	25787
CG30336	21134	CG3075	41034	CG31159	46144	CG31408	41420	CG31660	7852
CG30338	29188	CG3077	25631	CG31163	25701	CG3141	7074	CG31663	2533
CG30342	21136	CG3078	51390	CG31168	43222	CG31414	21336	CG31665	8021
CG30345	42868	CG3083	25020	CG31169	25706	CG31421	25760	CG3167	11149
CG30346	45429	CG3085	43421	CG31170	25707	CG31426	21340	CG31671	25793
CG30349	39959	CG3086	3170	CG31175	19230	CG3143	30556	CG31673	25797
CG3035	21139	CG3090	10856	CG31183	4773	CG31445	51642	CG31678	1473

CG31679	21392	CG31832	47633	CG3204	45230	CG3220	23511	CG32446	23058
CG3168	48010	CG31837	23407	CG32041	43632	CG32202	26325	CG32447	5417
CG31682	7257	CG3184	25880	CG32045	40308	CG32210	41865	CG32448	9120
CG31683	6400	CG31842	21429	CG32048	19251	CG32211	34452	CG32451	22975
CG31684	29130	CG31843	43198	CG32051	21435	CG32217	34458	CG32454	26141
CG31687	21393	CG31849	2876	CG32052	21437	CG3222	34459	CG32463	7254
CG31688	50139	CG31851	3754	CG32062	34046	CG32220	23280	CG32464	12781
CG31689	2584	CG31852	25179	CG32063	15207	CG32225	5383	CG32465	5783
CG3169	10818	CG31855	34295	CG32064	34051	CG32226	34464	CG32473	8281
CG31690	43813	CG31858	3367	CG32066	44825	CG32227	43928	CG32478	24740
CG31692	21396	CG3186	25129	CG32067	13066	CG3223	30003	CG32479	37859
CG31693	37131	CG31860	7688	CG32068	23412	CG32230	9804	CG3248	26055
CG31694	21398	CG31864	28079	CG32069	9202	CG32238	29424	CG32483	22977
CG31702	25807	CG31864	50051	CG32072	9206	CG3224	29561	CG32484	41905
CG31703	32493	CG31865	25897	CG32075	19255	CG32245	14017	CG32485	34565
CG31704	39450	CG31865	50589	CG32076	52402	CG3225	24725	CG32486	41908
CG31708	38261	CG31866	25899	CG3208	41779	CG32250	7491	CG32487	26154
CG3171	7219	CG3187	40295	CG32082	21438	CG32251	34477	CG32488	46571
CG31711	25814	CG31871	51241	CG32085	34053	CG32253	34479	CG3249	48005
CG31712	21402	CG31872	31028	CG32086	19261	CG3226	47034	CG32490	21477
CG31713	39150	CG31873	36375	CG32087	47238	CG32262	44923	CG32495	49719
CG31715	21505	CG31874	41766	CG32087	8345	CG32263	33272	CG32500	49724
CG31716	10850	CG3189	34017	CG32089	8340	CG32276	49568	CG3251	34574
CG31717	7662	CG31908	51924	CG3209	10281	CG32276	15911	CG32516	48377
CG31719	41758	CG31911	7618	CG32090	7495	CG3228	37079	CG3253	26159
CG3172	25817	CG31913	3376	CG32092	41785	CG32280	15908	CG32531	47915
CG31721	21405	CG31915	37944	CG32094	21442	CG32281	41873	CG3254	26162
CG31725	7836	CG31917	25909	CG32095	13833	CG3229	34498	CG32579	48384
CG31726	25823	CG31919	52494	CG32099	43650	CG32296	34502	CG3258	29041
CG31729	7697	CG3192	30413	CG3210	44156	CG32297	34506	CG32581	49727
CG3173	25825	CG31922	36386	CG32103	29439	CG32300	7442	CG32584	48387
CG31730	21407	CG31924	36469	CG32104	41790	CG3231	34515	CG3259	46163
CG31731	11082	CG31928	12276	CG32105	51269	CG32315	45459	CG3260	11521
CG31738	998	CG3193	25919	CG32108	21454	CG32316	34087	CG32602	50435
CG31738	29906	CG31935	25922	CG32110	34062	CG32319	24728	CG32616	49729
CG31739	21410	CG31937	3449	CG32113	41792	CG32333	26118	CG3263	26328
CG3174	42829	CG31938	40306	CG32120	11690	CG32335	44172	CG3264	43250
CG31740	33850	CG3194	7333	CG32130	34408	CG3234	2886	CG3265	24451
CG31741	7930	CG3195	32450	CG32131	23279	CG32343	15741	CG32656	46776
CG31743	7538	CG31950	34751	CG32134	949	CG32344	21675	CG32669	47916
CG31746	35727	CG31953	49301	CG32134	27108	CG32346	46645	CG3267	13259
CG31751	21414	CG31954	13028	CG32135	21665	CG32350	24732	CG32675	46667
CG31756	25833	CG31956	46910	CG32137	37872	CG32351	46784	CG32679	47158
CG31758	23522	CG31956	7284	CG32138	34412	CG32351	41881	CG32688	47804
CG31759	47321	CG31957	25926	CG32139	41098	CG32369	45129	CG3269	34766
CG31760	7686	CG31960	50102	CG3214	34079	CG32371	24735	CG32698	50316
CG31761	46014	CG31961	29359	CG32145	5263	CG32374	14107	CG3270	41196
CG31762	41568	CG31964	25929	CG32146	10299	CG32376	41885	CG32708	49325
CG31762	48237	CG31965	44154	CG32147	34419	CG3238	34533	CG3271	3983
CG3178	19819	CG31967	25933	CG32149	41861	CG32380	39482	CG32727	48271
CG31783	3875	CG31968	25934	CG3215	12723	CG32381	41835	CG3274	34581
CG31787	6372	CG31988	50935	CG32155	5279	CG32384	42302	CG32750	52403
CG31790	46057	CG31988	25939	CG32158	45641	CG32386	26126	CG32754	46509
CG31792	50152	CG31989	9402	CG3216	29915	CG32387	1003	CG32754	50591
CG31793	8069	CG31990	34752	CG3216	6115	CG32387	36287	CG32756	49853
CG31794	25853	CG31990	34752	CG32163	14259	CG32392	34537	CG32778	48869
CG31795	7560	CG31991	6367	CG32164	34423	CG3240	12677	CG32782	46425
CG3180	45959	CG31992	45773	CG32164	49304	CG32407	26131	CG32789	49744
CG31800	28162	CG31999	29155	CG32165	26112	CG32409	34543	CG3279	45726
CG31802	18562	CG3200	14125	CG32168	34429	CG3241	29356	CG32791	48926
CG31803	45277	CG32000	29174	CG32169	29799	CG32412	38277	CG32792	47047
CG31807	25863	CG32008	25945	CG32171	34081	CG32413	5043	CG3280	42556
CG31809	50643	CG3201	31160	CG32174	21468	CG32417	34547	CG3282	47599
CG31809	32521	CG32016	34755	CG32176	30015	CG32418	34549	CG32823	50763
CG3181	29354	CG32018	21610	CG32178	8413	CG32423	37863	CG32832	47810
CG31810	49296	CG32019	46253	CG32179	6119	CG32427	27252	CG3284	11219
CG31810	6757	CG32022	10105	CG32179	27110	CG32434	36625	CG32847	48422
CG31811	37521	CG32024	52031	CG32180	45900	CG32435	26051	CG32854	50338
CG31812	23403	CG32026	34032	CG32183	38208	CG32438	38969	CG3289	41913
CG31812	50487	CG3203	41778	CG3219	48576	CG32441	13134	CG3290	52378
CG3182	3606	CG32031	34036	CG32190	5319	CG32442	6481	CG3290	6622
CG31823	43145	CG32039	38867	CG32191	14294	CG32444	41899	CG3291	21677

CG3292	19989	CG3353	41920	CG3460	46165	CG3634	16720	CG3762	34389
CG3294	26110	CG3353	41921	CG3461	6975	CG3638	6914	CG3763	33173
CG3295	24709	CG33533	51100	CG3466	30218	CG3639	34671	CG3764	34707
CG3297	42485	CG33544	48807	CG3469	24759	CG3640	15241	CG3766	34709
CG32971	49456	CG3355	13037	CG3473	26201	CG3641	40314	CG3769	40469
CG3298	43751	CG33558	46456	CG3474	43956	CG3642	26261	CG3770	4064
CG3299	34585	CG3356	34601	CG3476	2734	CG3644	15453	CG3772	7238
CG33002	46440	CG3358	41819	CG3479	3010	CG3647	47973	CG3773	26281
CG3301	43225	CG3359	37889	CG3480	26205	CG3648	10156	CG3774	30238
CG33012	48408	CG3360	8287	CG3483	41939	CG3652	35574	CG3776	38269
CG3303	9916	CG3362	26171	CG3488	7534	CG3653	27227	CG3780	40471
CG3304	7280	CG3363	26176	CG3491	34631	CG3653	3111	CG3781	7113
CG3305	7308	CG33635	48813	CG3493	40450	CG3653	6695	CG3782	41949
CG33051	48793	CG33649	49765	CG3494	24760	CG3654	21700	CG3788	21715
CG33052	48410	CG33650	49769	CG3495	26208	CG3656	12190	CG3791	41954
CG33054	48413	CG33665	51606	CG3496	43768	CG3658	41084	CG3792	48233
CG33057	49458	CG33670	51016	CG3499	33256	CG3661	23416	CG3792	7862
CG3306	34588	CG33671	49772	CG3500	19703	CG3663	12879	CG3793	40475
CG3307	34589	CG33672	49774	CG3501	26025	CG3665	8392	CG3794	20117
CG3308	43756	CG33694	49776	CG3504	26211	CG3665	36351	CG3796	7756
CG3309	15415	CG33695	49777	CG3506	9271	CG3668	37637	CG3798	28365
CG33104	49750	CG33713	49611	CG3508	34632	CG3671	44000	CG3799	41960
CG3312	24742	CG33714	51020	CG3510	43771	CG3675	26057	CG3803	3596
CG3313	43758	CG33718	49781	CG3511	21733	CG3678	26267	CG3806	34711
CG3314	43760	CG33722	49646	CG3520	40455	CG3678	49792	CG3808	34713
CG3315	42858	CG3376	12226	CG3522	4053	CG3680	34675	CG3809	43780
CG33172	49462	CG33785	50678	CG3523	29349	CG3682	47027	CG3810	6922
CG33178	49464	CG3380	39469	CG3524	4290	CG3683	46799	CG3811	22984
CG33182	46444	CG3385	3618	CG3525	34286	CG3688	26269	CG3812	44418
CG3319	10442	CG3388	9277	CG3526	26214	CG3689	45280	CG3814	4671
CG33193	46445	CG3389	36164	CG3527	24762	CG3692	45939	CG3817	21716
CG33198	46214	CG3389	8408	CG3530	26216	CG3694	26872	CG3820	41964
CG3321	46764	CG33931	50510	CG3532	26221	CG3695	28361	CG3821	7750
CG33217	47818	CG33932	50690	CG3534	41276	CG3696	46685	CG3822	40985
CG3322	42559	CG33933	50694	CG3536	11816	CG3696	10762	CG3825	15238
CG33230	48803	CG3394	3621	CG3539	26223	CG3697	12670	CG3830	16896
CG33237	49758	CG3397	34604	CG3542	26227	CG3699	5667	CG3832	52052
CG3324	34595	CG3399	34278	CG3544	21684	CG3702	7296	CG3835	30979
CG33242	49760	CG3400	25959	CG3552	30952	CG3703	34679	CG3837	44576
CG33246	49762	CG3401	34607	CG3560	34090	CG3704	34684	CG3839	12704
CG3325	30490	CG3402	21483	CG3561	43773	CG3705	23179	CG3839	47122
CG33250	46450	CG3403	40442	CG3564	7039	CG3707	34686	CG3842	7117
CG3326	24746	CG3408	36306	CG3570	48219	CG3708	26272	CG3843	40477
CG33260	47820	CG3409	37141	CG3571	43778	CG3709	34687	CG3845	34719
CG33276	48363	CG3410	37836	CG3572	21686	CG3710	22979	CG3848	10749
CG33277	47828	CG3412	34274	CG3573	34649	CG3711	11166	CG3849	47126
CG33288	51189	CG3412	34273	CG3587	37902	CG3712	42412	CG3850	21719
CG33289	48289	CG3415	34613	CG3589	38154	CG3712	36406	CG3857	44734
CG3329	24749	CG3416	26183	CG3590	6343	CG3714	26275	CG3858	51221
CG33300	46768	CG3419	3626	CG3593	21688	CG3715	40464	CG3861	26301
CG3331	45689	CG3420	39052	CG3595	7916	CG3717	45284	CG3862	34721
CG3332	3451	CG3421	41934	CG3597	21693	CG3719	21495	CG3869	40478
CG3333	46279	CG3422	26187	CG3599	16665	CG3723	41947	CG3871	30456
CG3333	34597	CG3422	48735	CG3603	51663	CG3725	4474	CG3874	47543
CG33331	50209	CG3424	44536	CG3604	48507	CG3727	37525	CG3876	44201
CG3337	29169	CG3425	26190	CG3605	26252	CG3730	34291	CG3878	34179
CG3337	29170	CG3425	48882	CG3609	52600	CG3733	26277	CG3879	42514
CG3338	21678	CG3427	43445	CG3612	34663	CG3734	12899	CG3880	34725
CG3339	41917	CG3427	50372	CG3613	26332	CG3736	30470	CG3881	42779
CG3340	40873	CG3428	41938	CG3615	10045	CG3737	45133	CG3885	35806
CG3342	40324	CG3430	40444	CG3618	6977	CG3739	29508	CG3886	30586
CG3344	15212	CG3431	34618	CG3619	27187	CG3740	13525	CG3889	34727
CG33466	46260	CG3433	19045	CG3619	3720	CG3743	30455	CG3891	11270
CG33466	46260	CG3434	45130	CG3619	37288	CG3744	34695	CG3893	40479
CG33474	51188	CG3437	34221	CG3620	21490	CG3751	34699	CG3894	21721
CG33479	48461	CG3443	10133	CG3625	40855	CG3752	21707	CG3896	4913
CG33489	48465	CG3445	26196	CG3626	34667	CG3753	34701	CG3903	37115
CG3350	11259	CG3446	42696	CG3629	11529	CG3756	15675	CG3905	50368
CG33503	50506	CG3450	26871	CG3630	21697	CG3759	15602	CG3905	43869
CG33505	49525	CG3454	34620	CG3631	13770	CG3760	43437	CG3909	12758
CG3351	21480	CG3455	49574	CG3632	26254	CG3760	46862	CG3911	21738
CG3352	9396	CG3455	34624	CG3633	34670	CG3761	40468	CG3915	40484

CG3917	34731	CG4039	13661	CG4163	51493	CG4299	21827	CG4485	12498
CG3918	47144	CG4040	26372	CG4164	22996	CG4300	26500	CG4494	34113
CG3918	34734	CG4040	48694	CG4165	41977	CG4301	6125	CG4495	49350
CG3921	52608	CG4041	34780	CG4166	45775	CG4302	37207	CG4498	10330
CG3922	25964	CG4042	26377	CG4167	21806	CG4303	12673	CG4498	39411
CG3923	34737	CG4043	21776	CG4169	26404	CG4307	12794	CG4500	34852
CG3924	30454	CG4045	34784	CG4170	26408	CG4311	26504	CG4501	34853
CG3925	40486	CG4046	21516	CG4173	26412	CG4314	40875	CG4502	34858
CG3926	34738	CG4049	6981	CG4179	7054	CG4316	1613	CG4510	26544
CG3929	7795	CG4050	33248	CG4180	41980	CG4317	14163	CG4511	34861
CG3931	26309	CG4051	21779	CG4183	6983	CG4320	13112	CG4520	34862
CG3935	4542	CG4057	21780	CG4184	21809	CG4321	21615	CG4521	33135
CG3936	1112	CG4058	16668	CG4185	3161	CG4322	1800	CG4523	21860
CG3936	27228	CG4059	2959	CG4186	35814	CG4324	37211	CG4525	34864
CG3938	47941	CG4061	40498	CG4187	7226	CG4328	30516	CG4527	43784
CG3939	21513	CG4062	21782	CG4192	6354	CG4330	11078	CG4532	21861
CG3940	13806	CG4063	40862	CG4193	21811	CG4332	37392	CG4533	40531
CG3943	21745	CG4064	26382	CG4195	43120	CG4334	49330	CG4535	21862
CG3944	21749	CG4065	3614	CG4196	11926	CG4335	26514	CG4536	7128
CG3947	40886	CG4067	26385	CG4199	26424	CG4337	23299	CG4537	48669
CG3948	34768	CG4068	34786	CG4200	7173	CG4341	29341	CG4537	28832
CG3949	21755	CG4069	21783	CG4201	26427	CG4342	21519	CG4538	16432
CG3953	16416	CG4070	12259	CG4202	26432	CG4346	37389	CG4539	21865
CG3954	21756	CG4071	47653	CG4202	49946	CG4347	21832	CG4542	7132
CG3956	50003	CG4074	26070	CG4204	12952	CG4349	40505	CG4545	11346
CG3956	6232	CG4076	21784	CG4205	24497	CG4350	38988	CG4546	34868
CG3959	34770	CG4078	37607	CG4206	51217	CG4351	26517	CG4547	21870
CG3960	34098	CG4079	30442	CG4207	46688	CG4353	47507	CG4548	10618
CG3961	37305	CG4080	9026	CG4207	26439	CG4354	10709	CG4550	44179
CG3964	38981	CG4082	13639	CG4208	30505	CG4356	33123	CG4551	40534
CG3967	26338	CG4083	34789	CG4209	21611	CG4357	30000	CG4552	40537
CG3969	26065	CG4086	14268	CG4210	49494	CG4364	27607	CG4553	14743
CG3971	47519	CG4087	12944	CG4211	26441	CG4365	6261	CG4554	21620
CG3973	34772	CG4088	33197	CG4212	45774	CG4370	4341	CG4555	41990
CG3977	46757	CG4090	34792	CG4214	3857	CG4372	36431	CG4556	40540
CG3978	6224	CG4091	34102	CG4215	10374	CG4376	7760	CG4557	51263
CG3979	9981	CG4094	34797	CG4217	37819	CG4380	16893	CG4560	26548
CG3980	34773	CG4095	47685	CG4220	42813	CG4386	41291	CG4561	40541
CG3981	40495	CG4095	26074	CG4221	34810	CG4389	21845	CG4562	6770
CG3985	35813	CG4097	34801	CG4222	48009	CG4394	34835	CG4565	5665
CG3985	46482	CG4098	14265	CG4225	37356	CG4395	7223	CG4567	34874
CG3986	13875	CG4101	9089	CG4226	51438	CG4396	48891	CG4568	1405
CG3988	26346	CG4103	26390	CG4233	26452	CG4400	21618	CG4569	21871
CG3989	2901	CG4105	47499	CG4236	26455	CG4402	33252	CG4572	16428
CG3991	26348	CG4107	21786	CG4237	26459	CG4405	48531	CG4573	21874
CG3997	23578	CG4108	21788	CG4238	41982	CG4407	34228	CG4574	26557
CG3999	26354	CG4109	42561	CG4239	11857	CG4410	26536	CG4579	21878
CG4001	3016	CG4111	38950	CG4241	50706	CG4412	35385	CG4583	39562
CG4005	40497	CG4114	22994	CG4244	21813	CG4420	40512	CG4584	21883
CG4006	2902	CG4119	26395	CG4247	25967	CG4422	26537	CG4586	21886
CG4007	36282	CG4120	34806	CG4252	11251	CG4426	7143	CG4587	3840
CG4007	841	CG4123	8493	CG4257	43867	CG4427	15555	CG4589	6662
CG4007	9653	CG4124	35580	CG4260	4267	CG4429	34301	CG4591	42643
CG4008	21772	CG4125	27225	CG4261	30495	CG4433	29468	CG4592	6255
CG4009	19942	CG4125	951	CG4262	37915	CG4434	21521	CG4593	21888
CG4012	28367	CG4128	8890	CG4264	26465	CG4435	40519	CG4594	13284
CG4013	14915	CG4129	21789	CG4264	50222	CG4438	34845	CG4598	34879
CG4015	26356	CG4132	21792	CG4265	26469	CG4438	50033	CG4599	26075
CG4016	10020	CG4140	26396	CG4266	26475	CG4439	41232	CG4600	26562
CG4019	46880	CG4141	38986	CG4268	45127	CG4443	34109	CG4602	51088
CG4019	6650	CG4143	12751	CG4270	34105	CG4445	42864	CG4603	21893
CG4020	3290	CG4145	28369	CG4272	26479	CG4447	38195	CG4604	15389
CG4023	43781	CG4147	14882	CG4274	44834	CG4448	34847	CG4606	42652
CG4025	6924	CG4152	21793	CG4276	26482	CG4450	42770	CG4608	5732
CG4027	7139	CG4153	9416	CG4278	26487	CG4451	42658	CG4609	21895
CG4029	12610	CG4153	48911	CG4279	28793	CG4452	40525	CG4610	34881
CG4030	26368	CG4154	21797	CG4279	50653	CG4453	47155	CG4611	21898
CG4032	2897	CG4157	21799	CG4288	8620	CG4466	40530	CG4613	14089
CG4033	37581	CG4158	6248	CG4289	42591	CG4481	42891	CG4617	26568
CG4035	7800	CG4159	26397	CG4290	26496	CG4482	33186	CG4618	41993
CG4036	26370	CG4161	26400	CG4291	21819	CG4483	5176	CG4619	2755
CG4038	21775	CG4162	21805	CG4293	6885	CG4484	5174	CG4621	21903

CG4622	21904	CG4767	21946	CG4911	45141	CG5030	31092	CG5179	30448
CG4623	21624	CG4768	21541	CG4912	26658	CG5032	46172	CG5183	9235
CG4624	34303	CG4769	9180	CG4913	15671	CG5033	30551	CG5184	23249
CG4625	1429	CG4770	6783	CG4916	49379	CG5037	42786	CG5186	15185
CG4627	4681	CG4774	6742	CG4917	42665	CG5038	52421	CG5187	37634
CG4629	26573	CG4775	42499	CG4918	31005	CG5041	12559	CG5188	34320
CG4630	4687	CG4779	21544	CG4920	37001	CG5044	40570	CG5189	40318
CG4633	21905	CG4780	44535	CG4921	24672	CG5045	26687	CG5190	28282
CG4634	3200	CG4785	21948	CG4924	43786	CG5047	26692	CG5192	1836
CG4636	21908	CG4789	26626	CG4924	50123	CG5048	34120	CG5195	31044
CG4637	1402	CG4792	24667	CG4925	45142	CG5053	42019	CG5196	6096
CG4638	34885	CG4795	13086	CG4926	935	CG5055	2914	CG5197	22028
CG4643	26578	CG4798	26627	CG4926	29930	CG5057	12755	CG5198	27370
CG4645	10164	CG4799	34265	CG4928	6143	CG5059	9847	CG5201	42840
CG4646	21461	CG4800	26632	CG4931	34907	CG5063	49383	CG5202	27373
CG4648	21914	CG4802	42001	CG4933	24674	CG5064	27351	CG5202	49982
CG4649	46701	CG4803	34898	CG4934	45457	CG5065	4921	CG5203	34125
CG4649	26585	CG4805	44412	CG4935	12563	CG5067	40867	CG5205	34128
CG4654	12722	CG4806	26633	CG4937	24679	CG5068	27352	CG5206	44284
CG4656	21916	CG4807	41005	CG4938	23004	CG5069	43858	CG5208	27378
CG4660	50362	CG4810	26637	CG4942	42888	CG5070	6150	CG5214	34966
CG4662	41260	CG4813	21950	CG4943	24680	CG5072	40576	CG5215	34969
CG4663	39544	CG4816	21951	CG4945	24683	CG5073	46549	CG5216	23201
CG4666	36293	CG4817	44343	CG4946	21550	CG5075	34927	CG5219	45542
CG4670	7984	CG4821	45232	CG4947	41644	CG5076	45198	CG5220	34972
CG4672	8380	CG4822	42730	CG4952	2942	CG5077	6766	CG5222	27380
CG4673	21917	CG4824	42004	CG4953	41214	CG5078	8085	CG5226	37181
CG4675	3664	CG4825	5391	CG4954	26664	CG5081	5413	CG5227	9437
CG4676	4689	CG4827	49359	CG4956	24487	CG5085	21999	CG5229	5684
CG4677	28376	CG4832	44526	CG4957	40565	CG5091	2782	CG5232	22040
CG4679	38111	CG4836	41431	CG4960	2732	CG5093	30550	CG5235	16705
CG4681	40552	CG4840	21959	CG4960	52392	CG5094	22002	CG5237	45780
CG4683	22173	CG4841	26645	CG4963	12342	CG5098	27356	CG5241	34976
CG4684	44282	CG4842	50516	CG4965	46064	CG5099	11784	CG5242	17830
CG4685	14751	CG4842	37490	CG4966	24687	CG5102	51300	CG5242	48166
CG4686	46370	CG4843	42010	CG4968	21978	CG5103	46604	CG5245	27381
CG4690	45740	CG4845	21960	CG4969	27610	CG5104	13787	CG5247	16758
CG4692	13324	CG4847	3230	CG4972	2777	CG5105	22003	CG5248	9248
CG4696	40554	CG4848	40559	CG4973	42015	CG5108	34934	CG5249	34978
CG4697	34308	CG4849	21962	CG4974	14136	CG5109	22004	CG5249	50171
CG4698	38011	CG4852	9014	CG4975	26673	CG5110	34935	CG5252	27383
CG4700	15810	CG4853	19877	CG4976	10836	CG5111	28642	CG5254	6887
CG4703	26601	CG4858	26649	CG4980	26676	CG5112	14747	CG5258	35729
CG4704	21921	CG4860	34899	CG4984	10055	CG5116	16476	CG5261	48939
CG4706	34888	CG4863	23420	CG4991	30264	CG5119	22007	CG5263	22044
CG4709	21923	CG4863	46265	CG4993	45863	CG5121	34316	CG5264	30465
CG4713	21928	CG4866	34116	CG4994	8366	CG5122	27358	CG5264	50658
CG4719	21932	CG4867	30360	CG4996	34913	CG5124	22010	CG5265	34323
CG4720	34892	CG4871	47955	CG4998	16453	CG5125	27359	CG5266	29686
CG4722	46675	CG4875	1830	CG4999	37252	CG5127	47030	CG5268	13796
CG4722	8892	CG4875	47226	CG5000	21982	CG5131	42025	CG5270	27390
CG4729	48592	CG4877	21966	CG5002	10058	CG5133	16747	CG5271	34325
CG4729	5284	CG4878	26651	CG5003	26680	CG5140	22013	CG5274	22046
CG4733	34893	CG4879	13363	CG5004	26683	CG5142	22015	CG5275	47621
CG4735	26615	CG4881	28386	CG5005	13725	CG5144	30946	CG5277	34979
CG4738	21937	CG4882	15718	CG5009	21991	CG5149	34944	CG5280	22050
CG4739	6019	CG4884	23421	CG5012	26684	CG5150	15298	CG5281	6049
CG4742	21534	CG4887	21970	CG5012	50149	CG5155	27364	CG5282	5387
CG4743	9487	CG4889	13351	CG5013	38992	CG5157	34947	CG5284	6465
CG4746	21629	CG4893	22358	CG5013	48108	CG5160	22019	CG5285	10376
CG4749	21941	CG4894	52644	CG5014	30404	CG5161	34951	CG5287	51882
CG4750	41998	CG4896	26652	CG5017	21582	CG5162	14661	CG5288	24440
CG4751	45530	CG4896	48197	CG5018	42018	CG5163	12746	CG5289	22052
CG4752	40557	CG4897	21973	CG5021	36440	CG5164	40582	CG5290	22057
CG4753	1730	CG4898	34119	CG5022	8262	CG5165	34953	CG5295	37880
CG4753	46850	CG4899	46766	CG5023	34914	CG5166	34955	CG5300	34983
CG4755	34895	CG4899	6470	CG5025	26685	CG5167	6092	CG5310	39402
CG4756	13683	CG4901	34905	CG5026	34915	CG5168	22021	CG5313	37762
CG4757	38052	CG4904	26653	CG5027	12106	CG5169	22024	CG5315	40936
CG4758	8895	CG4907	6832	CG5029	39418	CG5170	37583	CG5316	25953
CG4759	21943	CG4908	44845	CG5029	29733	CG5174	29752	CG5317	46572
CG4760	21536	CG4909	26657	CG5029	33803	CG5178	9780	CG5319	34986

CG5320	22059	CG5442	40590	CG5560	14814	CG5695	37535	CG5840	22214
CG5321	22061	CG5443	46573	CG5561	47055	CG5703	22194	CG5841	27526
CG5322	34989	CG5443x	47331	CG5561	27461	CG5704	42044	CG5842	5261
CG5323	21563	CG5444	12600	CG5565	27463	CG5705	19854	CG5844	27528
CG5325	22064	CG5447	21566	CG5567	44319	CG5706	42046	CG5847	3162
CG5327	25972	CG5450	42114	CG5569	21568	CG5707	22195	CG5850	1456
CG5330	27392	CG5451	42035	CG5571	22160	CG5708	23425	CG5851	42051
CG5333	22066	CG5452	39137	CG5577	22163	CG5714	28398	CG5855	37722
CG5335	22068	CG5454	22132	CG5580	41845	CG5715	14710	CG5857	3408
CG5336	10455	CG5455	35011	CG5582	5322	CG5718	34239	CG5859	45677
CG5337	22069	CG5458	27420	CG5583	10932	CG5720	27487	CG5861	6360
CG5338	22074	CG5461	19679	CG5585	22166	CG5721	27488	CG5861	47665
CG5339	22075	CG5462	27424	CG5586	22169	CG5723	51173	CG5862	45155
CG5341	22077	CG5462	27424	CG5589	44322	CG5725	44157	CG5863	14366
CG5342	44404	CG5462	27424	CG5590	42039	CG5728	24696	CG5864	12913
CG5342	50058	CG5463	22135	CG5591	22170	CG5729	27490	CG5869	34145
CG5343	10468	CG5465	14916	CG5594	10278	CG5730	27493	CG5870	42053
CG5344	22082	CG5467	45556	CG5595	27465	CG5731	15543	CG5871	41822
CG5347	22088	CG5469	39000	CG5596	34331	CG5733	27495	CG5874	43211
CG5348	1698	CG5473	21567	CG5599	16506	CG5734	43798	CG5877	39004
CG5352	40587	CG5474	12101	CG5602	51315	CG5735	27498	CG5880	1264
CG5353	7752	CG5475	52277	CG5603	15340	CG5737	41048	CG5882	27532
CG5354	22095	CG5475	34238	CG5604	27467	CG5741	5158	CG5884	19730
CG5355	40588	CG5479	22138	CG5605	45027	CG5742	36428	CG5884	19731
CG5358	15645	CG5481	11823	CG5608	45569	CG5744	23428	CG5886	22216
CG5359	21565	CG5482	4991	CG5610	1189	CG5745	35034	CG5887	47142
CG5362	27399	CG5483	22139	CG5610	48159	CG5748	37699	CG5887	33338
CG5363	41838	CG5484	2679	CG5613	24694	CG5748	48692	CG5889	27535
CG5364	2781	CG5485	5341	CG5621	47549	CG5751	37250	CG5890	23431
CG5366	12067	CG5486	26027	CG5626	27469	CG5753	27503	CG5892	6807
CG5367	12392	CG5488	11570	CG5627	35019	CG5757	28654	CG5893	49549
CG5370	46616	CG5489	45558	CG5629	40601	CG5760	44002	CG5893	2940
CG5370	46616	CG5491	27433	CG5632	39087	CG5771	22198	CG5894	27538
CG5371	15683	CG5492	11901	CG5634	1106	CG5772	6750	CG5898	23432
CG5372	6646	CG5493	50637	CG5634	27199	CG5776	27507	CG5899	15679
CG5374	34070	CG5493	26082	CG5634	8016	CG5783	23429	CG5902	6274
CG5375	22099	CG5495	27436	CG5637	22693	CG5784	49386	CG5903	31098
CG5377	34392	CG5497	41800	CG5638	1748	CG5786	39001	CG5904	35048
CG5378	22104	CG5498	27440	CG5639	1305	CG5788	48146	CG5905	7108
CG5379	14461	CG5499	12768	CG5640	37663	CG5788	27515	CG5906	5227
CG5380	11228	CG5500	15376	CG5641	48200	CG5789	1204	CG5907	49870
CG5383	22108	CG5505	11152	CG5641	42043	CG5790	45044	CG5907	23433
CG5384	27405	CG5508	1316	CG5642	46592	CG5792	34143	CG5911	42716
CG5387	34990	CG5510	28393	CG5645	9289	CG5793	35044	CG5912	4819
CG5389	22112	CG5514	27445	CG5650	35025	CG5793	47883	CG5912	36286
CG5392	52427	CG5515	27447	CG5651	44325	CG5794	27517	CG5913	40336
CG5394	34995	CG5516	51402	CG5653	14064	CG5796	40607	CG5915	40338
CG5395	34999	CG5517	15957	CG5654	27472	CG5798	8931	CG5917	8347
CG5403	51314	CG5521	22150	CG5656	18119	CG5799	3780	CG5919	28402
CG5404	40907	CG5522	40595	CG5657	51526	CG5800	27519	CG5920	20963
CG5405	43790	CG5523	5038	CG5658	40605	CG5802	6801	CG5921	37875
CG5406	27406	CG5524	13650	CG5659	35029	CG5803	3091	CG5926	24996
CG5407	27411	CG5525	22155	CG5660	29445	CG5803	42229	CG5927	17853
CG5408	22113	CG5526	27450	CG5661	1052	CG5804	23587	CG5930	41011
CG5411	25976	CG5528	924	CG5661	9428	CG5805	35592	CG5931	43962
CG5412	27413	CG5528	36308	CG5662	35030	CG5807	6726	CG5933	20968
CG5412	50266	CG5529	19834	CG5663	27475	CG5808	22199	CG5934	20970
CG5413	14356	CG5532	30346	CG5669	45300	CG5809	43148	CG5935	25477
CG5414	35001	CG5535	42584	CG5670	12330	CG5810	44988	CG5938	32418
CG5417	23422	CG5537	22157	CG5671	35731	CG5813	28401	CG5939	33615
CG5422	28649	CG5543	27454	CG5675	27479	CG5814	22201	CG5940	32421
CG5423	44702	CG5545	13056	CG5675	28652	CG5815	22203	CG5941	48773
CG5424	33200	CG5546	27457	CG5676	47731	CG5818	40608	CG5942	37721
CG5428	43796	CG5547	27459	CG5677	1414	CG5821	37850	CG5946	5226
CG5429	22123	CG5548	24714	CG5680	34139	CG5823	8301	CG5949	41028
CG5430	44712	CG5549	8222	CG5684	28396	CG5826	27521	CG5950	5150
CG5432	27417	CG5550	31000	CG5685	42660	CG5827	23590	CG5952	17849
CG5433	22125	CG5553	30623	CG5686	7777	CG5828	27522	CG5954	13994
CG5434	21641	CG5554	20101	CG5687	33262	CG5830	40611	CG5955	15836
CG5435	35005	CG5555	35013	CG5688	27482	CG5832	16755	CG5958	20982
CG5439	27418	CG5558	39560	CG5690	28651	CG5837	22207	CG5960	20983
CG5440	49030	CG5558	46814	CG5692	27486	CG5838	22210	CG5962	20989

CG5965	20994	CG6094	27564	CG6213	25986	CG6369	27598	CG6513	34173
CG5966	13164	CG6096	37691	CG6218	35069	CG6372	52508	CG6514	27649
CG5969	47116	CG6096	47124	CG6220	40350	CG6375	27600	CG6515	13392
CG5970	20998	CG6098	27566	CG6222	10854	CG6376	15887	CG6516	27654
CG5973	24998	CG6106	30120	CG6223	15419	CG6378	16677	CG6517	39622
CG5974	2889	CG6110	22221	CG6224	22476	CG6379	29611	CG6518	2894
CG5977	33110	CG6113	31021	CG6225	8276	CG6380	29950	CG6519	13860
CG5978	21000	CG6114	22225	CG6226	22480	CG6383	39177	CG6521	22497
CG5980	21003	CG6115	29711	CG6227	40351	CG6385	27601	CG6522	22500
CG5986	25479	CG6120	3422	CG6230	8897	CG6386	48980	CG6523	34174
CG5987	21005	CG6121	22233	CG6232	31020	CG6390	4385	CG6524	33286
CG5989	5149	CG6122	22235	CG6233	24700	CG6391	25995	CG6533	19870
CG5991	25483	CG6126	7326	CG6235	34340	CG6392	35081	CG6534	30462
CG5992	16456	CG6128	50641	CG6238	30136	CG6393	40376	CG6535	22502
CG5992	50426	CG6129	22237	CG6246	6217	CG6395	47208	CG6538	12602
CG5994	21010	CG6133	37601	CG6249	30140	CG6395	34168	CG6539	49505
CG5996	9337	CG6136	22239	CG6251	44808	CG6396	35082	CG6539	7154
CG5998	25484	CG6137	30125	CG6253	44629	CG6396	35082	CG6543	27658
CG6000	23436	CG6139	4856	CG6255	40355	CG6396	35082	CG6544	34066
CG6004	25489	CG6140	50305	CG6258	12618	CG6401	39552	CG6545	12662
CG6005	25492	CG6141	22244	CG6259	25990	CG6405	35087	CG6546	24703
CG6007	21012	CG6142	19930	CG6262	25993	CG6407	32257	CG6547	46065
CG6008	5717	CG6143	22245	CG6264	5963	CG6410	24701	CG6550	4947
CG6009	33623	CG6144	41847	CG6267	30079	CG6412	44327	CG6554	40388
CG6009	46891	CG6145	48698	CG6267	42260	CG6413	35090	CG6562	46070
CG6011	13760	CG6146	10639	CG6269	10825	CG6414	44328	CG6565	39006
CG6013	33625	CG6147	22252	CG6271	50744	CG6415	51541	CG6567	27667
CG6014	31067	CG6148	22253	CG6272	34156	CG6418	40379	CG6570	52323
CG6015	41708	CG6149	40847	CG6275	3053	CG6420	42060	CG6570	30461
CG6016	7988	CG6151	39596	CG6275	845	CG6422	27614	CG6571	35105
CG6017	8487	CG6152	41825	CG6278	23598	CG6424	27619	CG6574	40902
CG6018	33629	CG6153	22257	CG6279	37267	CG6428	27622	CG6576	26695
CG6019	47606	CG6154	23008	CG6281	15372	CG6432	43451	CG6577	12588
CG6020	13130	CG6155	34151	CG6284	22483	CG6434	36424	CG6578	6170
CG6022	45020	CG6156	22258	CG6287	40358	CG6437	45275	CG6582	51472
CG6025	17826	CG6167	22268	CG6292	37562	CG6438	37023	CG6584	25999
CG6027	43633	CG6168	28405	CG6293	33220	CG6439	14443	CG6589	46072
CG6028	52314	CG6169	22272	CG6299	46105	CG6443	15736	CG6593	27673
CG6030	21018	CG6171	30128	CG6302	28794	CG6444	27626	CG6597	28237
CG6034	33631	CG6171	49472	CG6303	48309	CG6449	5208	CG6603	27680
CG6036	21023	CG6172	13062	CG6304	48212	CG6450	40382	CG6604	28416
CG6042	49491	CG6173	14703	CG6308	30273	CG6451	27630	CG6604	50849
CG6042	25168	CG6176	30131	CG6311	30149	CG6453	37991	CG6605	27683
CG6045	48191	CG6177	22280	CG6312	10416	CG6454	36655	CG6607	27688
CG6045	21032	CG6178	1172	CG6318	10759	CG6455	11938	CG6608	6005
CG6046	15710	CG6179	40341	CG6320	27581	CG6459	15520	CG6612	42064
CG6049	25497	CG6180	47677	CG6321	47682	CG6461	18545	CG6613	42065
CG6050	48982	CG6181	37945	CG6321	27584	CG6463	34171	CG6614	26700
CG6051	25500	CG6182	14705	CG6322	34242	CG6464	3029	CG6615	27691
CG6052	5311	CG6184	40920	CG6323	4391	CG6465	27632	CG6618	8052
CG6053	35052	CG6186	14666	CG6325	35072	CG6472	22495	CG6619	15622
CG6054	35055	CG6187	34152	CG6327	43988	CG6475	40932	CG6620	35107
CG6056	34148	CG6188	25983	CG6330	44326	CG6476	33834	CG6621	27695
CG6057	6532	CG6189	22287	CG6331	6782	CG6476	39377	CG6622	27699
CG6058	27542	CG6190	45876	CG6331	47132	CG6477	27639	CG6623	40390
CG6058	47667	CG6191	27133	CG6332	43799	CG6479	45648	CG6625	22379
CG6059	35056	CG6192	24719	CG6335	43998	CG6480	23449	CG6627	42798
CG6061	35061	CG6193	22290	CG6338	12632	CG6484	4954	CG6630	26701
CG6064	27545	CG6194	22294	CG6339	15879	CG6485	14281	CG6632	52510
CG6066	35065	CG6196	47140	CG6340	34160	CG6486	43804	CG6633	6016
CG6070	1262	CG6197	46312	CG6341	22488	CG6492	6162	CG6634	30519
CG6072	27546	CG6198	22300	CG6342	30153	CG6493	25090	CG6637	21658
CG6073	17256	CG6199	45484	CG6343	14444	CG6495	42796	CG6643	28418
CG6074	31148	CG6201	13245	CG6345	27588	CG6498	35100	CG6649	7320
CG6081	7868	CG6202	5883	CG6347	16837	CG6500	2916	CG6650	8363
CG6083	27549	CG6203	8933	CG6349	11227	CG6502	27645	CG6652	26706
CG6084	27551	CG6204	30135	CG6350	50009	CG6504	6940	CG6653	8574
CG6089	27554	CG6205	47864	CG6352	51289	CG6506	34349	CG6656	1630
CG6090	22218	CG6205	9149	CG6353	40363	CG6508	28413	CG6657	8144
CG6091	27558	CG6206	49352	CG6358	40368	CG6509	46234	CG6658	8569
CG6092	44165	CG6208	40348	CG6363	43802	CG6509	22496	CG6659	8038
CG6094	48721	CG6210	5215	CG6364	11693	CG6512	8515	CG6660	6835

CG6662	26713	CG6782	50714	CG6914	35139	CG7041	26097	CG7168	27894
CG6664	12780	CG6784	39312	CG6915	35141	CG7042	23452	CG7172	27898
CG6665	8202	CG6788	48054	CG6919	47896	CG7044	27811	CG7176	42915
CG6666	6031	CG6788	42912	CG6920	13310	CG7047	15203	CG7177	35194
CG6667	45998	CG6789	27747	CG6921	30179	CG7048	29811	CG7178	34196
CG6668	6719	CG6790	12134	CG6923	26096	CG7049	15846	CG7180	34368
CG6673	41806	CG6792	35118	CG6928	5231	CG7050	4306	CG7183	40429
CG6674	26716	CG6794	30578	CG6930	35147	CG7050	36328	CG7184	34373
CG6677	7141	CG6796	6494	CG6931	22468	CG7051	22340	CG7186	27904
CG6678	26719	CG6798	1199	CG6937	22315	CG7052	35611	CG7187	28610
CG6682	26721	CG6800	40397	CG6938	37271	CG7053	27815	CG7188	37108
CG6684	52603	CG6811	34250	CG6939	22317	CG7054	40416	CG7190	31070
CG6686	21573	CG6812	8534	CG6944	45635	CG7055	37684	CG7192	52526
CG6690	14439	CG6814	22442	CG6946	27752	CG7056	15719	CG7193	40434
CG6691	3951	CG6815	39675	CG6948	22318	CG7057	27820	CG7194	24723
CG6692	13959	CG6816	5601	CG6949	40405	CG7059	21651	CG7195	39303
CG6693	27717	CG6817	10102	CG6950	22321	CG7060	42883	CG7195	28160
CG6695	36656	CG6818	49479	CG6951	27756	CG7061	27823	CG7197	19736
CG6696	28426	CG6818	26723	CG6953	1530	CG7062	34190	CG7199	48979
CG6696	49114	CG6819	47693	CG6954	27759	CG7066	36572	CG7199	37072
CG6697	27720	CG6822	5142	CG6961	35150	CG7067	27831	CG7200	27913
CG6699	42071	CG6824	12663	CG6963	26003	CG7069	27834	CG7206	22530
CG6700	39007	CG6827	9039	CG6964	13687	CG7070	49533	CG7207	27914
CG6701	36557	CG6831	40399	CG6966	22326	CG7070	35165	CG7211	35386
CG6702	41812	CG6835	49800	CG6967	27769	CG7071	46823	CG7212	40436
CG6703	34185	CG6838	35123	CG6971	35153	CG7073	34191	CG7215	49802
CG6704	46856	CG6840	23290	CG6971	48986	CG7075	3666	CG7215	27916
CG6706	1784	CG6841	34253	CG6972	27772	CG7076	28740	CG7217	49806
CG6707	44557	CG6842	35126	CG6975	6314	CG7077	33835	CG7217	35196
CG6711	37548	CG6844	1194	CG6976	37532	CG7081	5136	CG7218	5908
CG6712	39012	CG6847	22451	CG6978	7041	CG7082	2554	CG7220	34198
CG6713	27722	CG6850	16467	CG6980	29148	CG7083	22342	CG7221	22536
CG6716	6221	CG6851	44306	CG6983	35158	CG7085	46150	CG7222	34377
CG6717	18961	CG6852	26001	CG6987	27775	CG7090	14610	CG7223	6692
CG6719	27727	CG6854	12762	CG6988	23358	CG7092	27837	CG7224	36437
CG6721	23016	CG6856	34354	CG6990	50520	CG7097	35166	CG7225	13863
CG6723	13769	CG6857	7231	CG6990	27782	CG7098	46320	CG7228	33155
CG6724	27730	CG6859	12426	CG6993	10715	CG7099	27848	CG7230	15900
CG6725	37361	CG6860	7306	CG6998	43116	CG7103	6175	CG7231	2783
CG6726	34247	CG6863	2656	CG6999	41829	CG7103	46875	CG7234	7878
CG6733	50172	CG6866	22453	CG7000	42496	CG7106	45634	CG7235	22539
CG6737	46197	CG6867	37416	CG7002	37005	CG7107	27853	CG7238	34382
CG6738	48918	CG6868	1216	CG7004	27785	CG7108	43870	CG7241	5851
CG6738	27736	CG6869	5271	CG7005	9797	CG7109	41924	CG7245	22541
CG6741	16826	CG6870	52570	CG7006	29512	CG7111	27858	CG7245	22541
CG6742	27738	CG6871	6283	CG7007	33342	CG7112	35174	CG7246	34256
CG6743	22407	CG6873	22454	CG7007	47187	CG7113	37083	CG7250	27103
CG6744	48329	CG6875	2910	CG7009	27790	CG7115	9404	CG7250	927
CG6745	46746	CG6877	22455	CG7009	27789	CG7121	44705	CG7250	7995
CG6746	46513	CG6878	9224	CG7010	40410	CG7121	17903	CG7254	27928
CG6747	28431	CG6881	1815	CG7011	46860	CG7121	839	CG7255	8373
CG6750	9408	CG6884	27750	CG7013	12834	CG7123	23121	CG7257	22548
CG6751	12577	CG6888	26094	CG7014	49879	CG7125	22344	CG7259	5273
CG6752	43605	CG6890	9430	CG7014	27792	CG7127	27867	CG7260	43909
CG6753	16600	CG6890	13549	CG7015	49498	CG7128	27870	CG7261	27931
CG6754	28215	CG6890	27099	CG7015	41858	CG7129	52571	CG7262	22552
CG6755	6282	CG6891	50055	CG7018	15355	CG7131	52520	CG7263	2544
CG6756	18112	CG6892	30552	CG7020	27796	CG7134	27881	CG7264	22554
CG6757	22412	CG6894	9154	CG7023	27799	CG7137	27884	CG7265	27932
CG6758	43606	CG6897	35134	CG7024	27803	CG7139	35177	CG7266	26009
CG6759	52667	CG6898	37358	CG7025	43187	CG7140	27888	CG7266	48992
CG6760	27743	CG6899	1012	CG7026	8254	CG7143	44721	CG7268	24453
CG6762	35734	CG6899	4297	CG7026	48830	CG7145	40422	CG7269	22556
CG6763	18940	CG6900	49629	CG7028	27808	CG7146	40427	CG7272	8374
CG6766	38035	CG6900	23602	CG7033	41190	CG7149	43821	CG7274	40440
CG6767	35112	CG6903	3285	CG7034	35162	CG7152	27893	CG7275	22561
CG6768	13645	CG6904	35136	CG7035	22331	CG7154	37669	CG7277	30691
CG6770	35825	CG6905	13492	CG7036	13070	CG7156	26036	CG7279	18107
CG6772	30673	CG6906	8357	CG7037	22335	CG7158	35179	CG7280	18550
CG6778	44603	CG6907	22460	CG7038	47159	CG7161	35186	CG7281	27937
CG6779	37742	CG6910	22464	CG7038	40413	CG7162	13054	CG7281	48835
CG6781	34227	CG6913	46690	CG7039	26007	CG7163	38247	CG7282	50406

CG7282	27941	CG7424	44630	CG7568	45783	CG7727	42673	CG7851	33157
CG7283	52411	CG7425	26011	CG7571	37295	CG7728	21048	CG7852	7178
CG7283	23458	CG7427	28006	CG7573	8337	CG7729	37010	CG7855	22590
CG7285	13560	CG7429	28008	CG7577	36659	CG7734	3226	CG7860	34395
CG7288	47663	CG7430	28011	CG7578	33634	CG7735	43508	CG7861	34388
CG7289	34281	CG7431	2857	CG7580	28839	CG7736	1501	CG7864	46613
CG7291	30725	CG7432	31091	CG7581	21037	CG7737	49437	CG7865	15782
CG7292	35200	CG7433	28014	CG7582	1353	CG7739	51521	CG7867	28069
CG7293	27943	CG7436	28019	CG7590	25506	CG7740	51956	CG7870	2802
CG7301	39384	CG7437	28023	CG7595	9265	CG7741	33655	CG7872	9134
CG7307	18553	CG7438	12558	CG7597	25510	CG7742	25535	CG7873	26019
CG7317	28694	CG7439	49473	CG7598	14861	CG7744	33247	CG7875	1365
CG7319	27949	CG7441	28027	CG7600	47473	CG7747	44854	CG7878	35288
CG7322	9258	CG7446	5329	CG7601	4456	CG7749	5098	CG7879	15260
CG7323	15631	CG7449	40898	CG7602	37594	CG7749	3749	CG7882	8103
CG7324	31064	CG7449	27065	CG7605	43730	CG7749	27113	CG7883	40321
CG7328	27951	CG7449	9471	CG7609	21041	CG7757	25547	CG7885	14000
CG7329	48340	CG7452	36595	CG7610	16539	CG7758	12823	CG7886	22610
CG7331	27955	CG7457	46671	CG7611	25511	CG7760	37611	CG7887	1374
CG7332	27959	CG7457	26740	CG7614	12575	CG7761	8692	CG7887	43329
CG7334	13375	CG7459	5805	CG7615	47312	CG7762	25549	CG7888	37264
CG7335	27962	CG7460	13115	CG7616	41408	CG7764	12596	CG7891	26085
CG7337	35204	CG7461	28028	CG7620	30391	CG7765	44337	CG7892	3002
CG7338	27963	CG7462	40638	CG7621	48032	CG7766	52573	CG7893	6241
CG7339	13629	CG7464	10558	CG7622	39914	CG7768	35266	CG7894	3060
CG7340	3174	CG7466	42462	CG7623	12149	CG7769	44976	CG7894	869
CG7343	35206	CG7467	7810	CG7625	30382	CG7770	34203	CG7894	42251
CG7343	35206	CG7469	28033	CG7626	19793	CG7771	26888	CG7895	12656
CG7343	35206	CG7470	38955	CG7627	2807	CG7772	30431	CG7896	907
CG7345	10813	CG7471	46930	CG7628	49973	CG7773	35267	CG7896	36340
CG7349	51481	CG7471	30599	CG7628	19713	CG7776	35268	CG7896	3813
CG7351	27966	CG7473	39151	CG7632	45675	CG7777	8124	CG7899	3579
CG7352	40636	CG7480	44263	CG7633	6178	CG7779	29046	CG7900	43157
CG7354	14305	CG7484	13358	CG7635	9160	CG7785	36650	CG7904	37279
CG7356	26100	CG7485	26876	CG7636	13828	CG7787	45715	CG7904	848
CG7359	9888	CG7486	28041	CG7637	42402	CG7788	28065	CG7908	2733
CG7360	40773	CG7487	10614	CG7637	23669	CG7791	35272	CG7910	51546
CG7362	7556	CG7490	28618	CG7638	8235	CG7793	42848	CG7911	23075
CG7364	7706	CG7494	48961	CG7639	33641	CG7804	49886	CG7912	1377
CG7365	14318	CG7494	28042	CG7640	23671	CG7804	28067	CG7913	22614
CG7367	43822	CG7497	9374	CG7642	25172	CG7806	2804	CG7914	22619
CG7368	27978	CG7499	9179	CG7646	35742	CG7807	41130	CG7915	22620
CG7371	27984	CG7504	28050	CG7650	41714	CG7808	35278	CG7917	22623
CG7371	48711	CG7507	28053	CG7654	47988	CG7809	22564	CG7919	5117
CG7375	35220	CG7508	48674	CG7655	12429	CG7810	22565	CG7921	1381
CG7376	35222	CG7508	2924	CG7656	26881	CG7811	2890	CG7923	7492
CG7378	35226	CG7509	51585	CG7659	12639	CG7813	22566	CG7925	52533
CG7378	47855	CG7510	8532	CG7659	46805	CG7814	35279	CG7926	7748
CG7379	27988	CG7511	52654	CG7662	46962	CG7815	22567	CG7927	22627
CG7382	47494	CG7512	13829	CG7662	43094	CG7818	13541	CG7929	12920
CG7387	27993	CG7513	35250	CG7664	26885	CG7818	48559	CG7931	21578
CG7391	42834	CG7514	37233	CG7665	13566	CG7820	26015	CG7931	50524
CG7392	35232	CG7515	35251	CG7669	29200	CG7821	40641	CG7935	38963
CG7394	9210	CG7516	28058	CG7670	44595	CG7823	46154	CG7940	22633
CG7395	9379	CG7518	26745	CG7671	33645	CG7825	44723	CG7943	28632
CG7397	13429	CG7519	21653	CG7678	11649	CG7826	28628	CG7945	35296
CG7398	30066	CG7520	15927	CG7686	33650	CG7828	7728	CG7946	35298
CG7398	4769	CG7530	5872	CG7694	25520	CG7830	4253	CG7948	14021
CG7398	6543	CG7532	12405	CG7698	39557	CG7831	22570	CG7949	21657
CG7399	35240	CG7536	11576	CG7700	12152	CG7832	49339	CG7950	22635
CG7400	48719	CG7538	10967	CG7704	45957	CG7833	44030	CG7951	46696
CG7400	9406	CG7542	47336	CG7706	25524	CG7834	36661	CG7954	52538
CG7402	37302	CG7546	35253	CG7708	30301	CG7837	22573	CG7955	40838
CG7405	10398	CG7550	35254	CG7709	9865	CG7839	12691	CG7956	22638
CG7408	8415	CG7555	13121	CG7712	50214	CG7840	47495	CG7957	44027
CG7413	10696	CG7556	28621	CG7716	25526	CG7842	46334	CG7960	13679
CG7414	18804	CG7560	28063	CG7717	25528	CG7842	14279	CG7961	35306
CG7415	35242	CG7562	30441	CG7718	25532	CG7843	22574	CG7962	5121
CG7417	37555	CG7564	29462	CG7719	21046	CG7845	22578	CG7964	50645
CG7420	46316	CG7565	36291	CG7722	25534	CG7847	9921	CG7966	22639
CG7421	27995	CG7565	8396	CG7724	43927	CG7849	22588	CG7970	8857
CG7423	28003	CG7565	3707	CG7726	45427	CG7850	3018	CG7971	34262

CG7972	28072	CG8111	29391	CG8254	13716	CG8372	8043	CG8494	42609
CG7974	28074	CG8112	37345	CG8257	35865	CG8376	37791	CG8495	28849
CG7975	40645	CG8114	35349	CG8257	50371	CG8378	40705	CG8497	24111
CG7978	51974	CG8116	45735	CG8258	45789	CG8379	35911	CG8498	35388
CG7979	5126	CG8117	23254	CG8261	28844	CG8380	12082	CG8500	28795
CG7980	28169	CG8117	47174	CG8266	35867	CG8383	35915	CG8506	24114
CG7986	22646	CG8127	44851	CG8267	35870	CG8384	6315	CG8507	42640
CG7988	46277	CG8128	47740	CG8268	23678	CG8385	23082	CG8509	28915
CG7988	22651	CG8129	46959	CG8269	23728	CG8386	35919	CG8520	36546
CG7989	28172	CG8129	24201	CG8270	23755	CG8390	46229	CG8522	37640
CG7990	46157	CG8132	17254	CG8271	4607	CG8392	35923	CG8523	51165
CG7993	35314	CG8134	24204	CG8272	24262	CG8394	45917	CG8525	28916
CG7995	22652	CG8135	42635	CG8273	28887	CG8395	24305	CG8527	39580
CG7997	16840	CG8138	24208	CG8274	24265	CG8396	47383	CG8529	44360
CG7998	22654	CG8142	10881	CG8276	28888	CG8400	35419	CG8531	24122
CG7999	15878	CG8144	24214	CG8277	24267	CG8401	45237	CG8532	35949
CG8001	35317	CG8146	48210	CG8280	49890	CG8402	24308	CG8534	49893
CG8003	22659	CG8146	23126	CG8280	24270	CG8403	42478	CG8536	4867
CG8005	22664	CG8147	2892	CG8282	24275	CG8404	45482	CG8538	35952
CG8007	11462	CG8149	24215	CG8284	35872	CG8405	11127	CG8542	24125
CG8008	4158	CG8151	12581	CG8285	4365	CG8407	23504	CG8545	35954
CG8009	41105	CG8152	13978	CG8286	14154	CG8408	12432	CG8546	5110
CG8009	48955	CG8153	15695	CG8287	28092	CG8409	31995	CG8548	28920
CG8013	42423	CG8155	24218	CG8288	24278	CG8411	28897	CG8549	28924
CG8014	22671	CG8161	35843	CG8289	24279	CG8412	5934	CG8552	35957
CG8019	41022	CG8166	8137	CG8290	12739	CG8415	50956	CG8553	35959
CG8020	44076	CG8167	44761	CG8293	2972	CG8415	35421	CG8556	28926
CG8021	23675	CG8169	39193	CG8297	8972	CG8416	12734	CG8556	50349
CG8023	34210	CG8171	23131	CG8297	46760	CG8417	49508	CG8557	28927
CG8025	26039	CG8173	35845	CG8298	43541	CG8418	35929	CG8561	44361
CG8026	4163	CG8174	26933	CG8300	24291	CG8419	24097	CG8566	23464
CG8029	48016	CG8177	39492	CG8302	51943	CG8421	52589	CG8566	47171
CG8031	35326	CG8184	26935	CG8303	4917	CG8425	44049	CG8567	39592
CG8032	28175	CG8186	49888	CG8306	23134	CG8426	37545	CG8568	18534
CG8036	35330	CG8187	24230	CG8308	24297	CG8427	35934	CG8569	35962
CG8038	28179	CG8189	14210	CG8311	8985	CG8428	3229	CG8571	35967
CG8042	35331	CG8190	43917	CG8314	1691	CG8431	26959	CG8577	51237
CG8043	28181	CG8194	13018	CG8315	28892	CG8432	28866	CG8578	35969
CG8048	46563	CG8197	42125	CG8318	35877	CG8433	49808	CG8580	24130
CG8049	22675	CG8199	24231	CG8320	8797	CG8433	4902	CG8581	16923
CG8053	26022	CG8200	42130	CG8321	8765	CG8434	43898	CG8581	24475
CG8058	13314	CG8202	35410	CG8322	30280	CG8434	42570	CG8581	29909
CG8060	46991	CG8203	35855	CG8323	4861	CG8434	4319	CG8582	35970
CG8060	22684	CG8207	24236	CG8325	35881	CG8435	28900	CG8583	33282
CG8064	28182	CG8208	9261	CG8326	23760	CG8440	6216	CG8584	26988
CG8064	49076	CG8209	35858	CG8327	35883	CG8442	44439	CG8587	26989
CG8067	47871	CG8211	24239	CG8330	23763	CG8443	42136	CG8589	24180
CG8067	22687	CG8211	24237	CG8331	35377	CG8444	5830	CG8590	35975
CG8068	30709	CG8212	44731	CG8332	35415	CG8445	47743	CG8591	30713
CG8069	28189	CG8213	7372	CG8333	10950	CG8446	23141	CG8593	47001
CG8070	35333	CG8214	24240	CG8334	18982	CG8448	39126	CG8594	4642
CG8073	23020	CG8219	24244	CG8335	15506	CG8449	24102	CG8595	6541
CG8075	7376	CG8222	13503	CG8336	23729	CG8453	4615	CG8595	39176
CG8079	23023	CG8222	43459	CG8338	28240	CG8454	23769	CG8596	5089
CG8085	28192	CG8223	35861	CG8339	5070	CG8455	47953	CG8598	35982
CG8086	23028	CG8224	3825	CG8340	35890	CG8461	24103	CG8601	28932
CG8090	30341	CG8224	853	CG8343	7735	CG8464	24104	CG8603	47148
CG8091	23033	CG8226	8747	CG8344	15692	CG8465	24107	CG8603	26992
CG8092	28196	CG8230	37160	CG8349	48682	CG8468	6452	CG8604	9264
CG8093	19561	CG8231	23751	CG8351	28895	CG8470	40712	CG8605	29435
CG8094	35337	CG8233	24248	CG8353	35896	CG8472	28243	CG8609	14032
CG8095	4891	CG8234	40980	CG8354	28848	CG8474	51285	CG8610	35986
CG8097	28199	CG8237	9324	CG8355	20210	CG8475	2800	CG8611	28936
CG8098	6455	CG8239	24253	CG8356	7317	CG8481	28906	CG8612	15199
CG8102	16898	CG8240	28877	CG8357	30485	CG8481	49470	CG8614	42146
CG8103	10766	CG8241	47782	CG8360	41643	CG8483	41263	CG8615	42152
CG8104	29788	CG8243	26952	CG8361	16753	CG8485	35940	CG8616	38249
CG8105	8037	CG8244	33842	CG8362	35901	CG8486	2796	CG8624	26995
CG8107	46241	CG8244	30642	CG8363	35904	CG8487	42140	CG8625	6208
CG8107	23037	CG8250	11446	CG8365	37685	CG8491	23142	CG8627	23680
CG8108	35343	CG8251	24257	CG8368	45259	CG8492	14929	CG8628	35392
CG8110	35345	CG8253	35411	CG8370	42509	CG8493	24109	CG8629	39155

CG8630	33340	CG8768	36022	CG8893	23645	CG9012	23666	CG9139	46329
CG8630	50290	CG8772	7192	CG8895	7866	CG9013	4964	CG9140	43184
CG8631	2998	CG8773	10203	CG8895	33919	CG9014	36084	CG9143	46330
CG8632	4654	CG8774	5862	CG8896	965	CG9018	40732	CG9144	48207
CG8635	24131	CG8776	7909	CG8896	36305	CG9019	33909	CG9144	27006
CG8636	28937	CG8776	40803	CG8896	44386	CG9022	45173	CG9147	29050
CG8637	35988	CG8778	23621	CG8900	23083	CG9023	51936	CG9148	45224
CG8639	29968	CG8779	979	CG8902	23650	CG9025	44428	CG9150	16877
CG8641	35993	CG8779	30073	CG8905	42162	CG9027	37794	CG9151	47881
CG8641	52260	CG8779	37282	CG8907	28987	CG9031	42189	CG9151	9827
CG8642	35997	CG8781	36025	CG8909	29900	CG9032	23685	CG9153	37221
CG8645	35431	CG8782	28950	CG8912	28989	CG9032	50958	CG9154	29054
CG8648	15698	CG8783	40721	CG8914	26915	CG9033	44287	CG9154	49534
CG8649	47514	CG8784	15989	CG8915	28857	CG9035	8759	CG9155	49345
CG8649	6276	CG8785	4650	CG8916	9138	CG9038	29012	CG9156	29057
CG8651	37715	CG8786	36028	CG8918	28994	CG9041	28163	CG9159	7893
CG8652	46514	CG8789	26910	CG8919	28996	CG9042	29013	CG9160	43503
CG8654	4715	CG8793	36033	CG8920	28998	CG9044	42193	CG9160	39232
CG8655	40715	CG8795	1768	CG8922	36060	CG9045	37711	CG9163	45927
CG8656	24184	CG8798	36035	CG8923	36063	CG9046	13230	CG9163	30075
CG8657	4659	CG8799	39539	CG8928	23480	CG9047	23153	CG9166	28109
CG8660	35432	CG8800	42117	CG8930	29931	CG9049	36085	CG9169	27008
CG8663	44486	CG8803	4174	CG8930	905	CG9054	29019	CG9170	29066
CG8664	47568	CG8804	51091	CG8930	4753	CG9056	29021	CG9171	13451
CG8665	35999	CG8804	6446	CG8933	7802	CG9057	40734	CG9171	50541
CG8667	44470	CG8805	4176	CG8936	47207	CG9060	12665	CG9172	23255
CG8669	2935	CG8806	40723	CG8937	45596	CG9062	3810	CG9176	40964
CG8675	26997	CG8808	37966	CG8938	50140	CG9063	40738	CG9177	29070
CG8676	37694	CG8809	39076	CG8938	23084	CG9064	2647	CG9181	37437
CG8677	23608	CG8811	29774	CG8942	9976	CG9065	33879	CG9184	10283
CG8678	36002	CG8814	2606	CG8942	40747	CG9065	29838	CG9187	44366
CG8679	30778	CG8815	10808	CG8946	37974	CG9066	45185	CG9191	52549
CG8680	23467	CG8816	50135	CG8947	14218	CG9067	35744	CG9195	9130
CG8681	1479	CG8816	36045	CG8948	42165	CG9071	4062	CG9198	29072
CG8690	15798	CG8817	13081	CG8949	48307	CG9075	42201	CG9200	36092
CG8693	7947	CG8819	49637	CG8950	36069	CG9081	38218	CG9201	29073
CG8694	28292	CG8821	37660	CG8954	23659	CG9084	45609	CG9203	29075
CG8695	15791	CG8823	30821	CG8956	3343	CG9086	28961	CG9204	28111
CG8696	15789	CG8825	46268	CG8958	42169	CG9088	42203	CG9206	3785
CG8705	11791	CG8825	28958	CG8959	14837	CG9089	40966	CG9207	12616
CG8706	8397	CG8827	41219	CG8962	29003	CG9090	44297	CG9209	44638
CG8706	39215	CG8830	28960	CG8963	42110	CG9092	51445	CG9210	11547
CG8706	3710	CG8831	42153	CG8967	30834	CG9095	23159	CG9211	29898
CG8707	36003	CG8833	36408	CG8967	42565	CG9096	29023	CG9211	42577
CG8708	45194	CG8839	4620	CG8968	48894	CG9098	27001	CG9212	28116
CG8709	36007	CG8841	48253	CG8968	26923	CG9099	28106	CG9214	42209
CG8711	44829	CG8841	23625	CG8969	30483	CG9099	49895	CG9218	28119
CG8714	9951	CG8843	28873	CG8972	45845	CG9100	27002	CG9219	35750
CG8717	8739	CG8844	35437	CG8974	5572	CG9102	8943	CG9220	29085
CG8719	50531	CG8846	35439	CG8975	7965	CG9102	49042	CG9224	37407
CG8719	39121	CG8849	36050	CG8976	7394	CG9104	10472	CG9227	40858
CG8721	30038	CG8853	51322	CG8977	36071	CG9108	30030	CG9231	9101
CG8722	40717	CG8855	19050	CG8978	42171	CG9109	16982	CG9232	29087
CG8725	28942	CG8857	23475	CG8979	28860	CG9111	39183	CG9236	39161
CG8726	40719	CG8858	23634	CG8980	42175	CG9113	3275	CG9238	24149
CG8727	11765	CG8860	8768	CG8981	28098	CG9115	29032	CG9240	14833
CG8728	48677	CG8862	38085	CG8983	51675	CG9116	50537	CG9242	24152
CG8728	23617	CG8863	23637	CG8987	3133	CG9116	38139	CG9243	37422
CG8729	15533	CG8865	23639	CG8988	4601	CG9117	52545	CG9244	12455
CG8730	23772	CG8873	45618	CG8989	12771	CG9118	49813	CG9245	11852
CG8732	3222	CG8874	36053	CG8993	41126	CG9118	14931	CG9246	24136
CG8733	51921	CG8877	18567	CG8995	23665	CG9119	46326	CG9247	52612
CG8734	7949	CG8881	28975	CG8996	44378	CG9120	49896	CG9248	41226
CG8735	4025	CG8882	28976	CG8998	28102	CG9124	36086	CG9249	47643
CG8739	47750	CG8884	35445	CG9000	37179	CG9126	47073	CG9250	48548
CG8743	45989	CG8886	46702	CG9001	4931	CG9126	47074	CG9250	36095
CG8757	13110	CG8887	28982	CG9002	49812	CG9127	47972	CG9257	6406
CG8759	36017	CG8888	30336	CG9003	23481	CG9128	37216	CG9258	46542
CG8760	28945	CG8890	24148	CG9004	40727	CG9131	44362	CG9265	46577
CG8764	35829	CG8891	36055	CG9005	36079	CG9134	48756	CG9267	2879
CG8766	4658	CG8892	28985	CG9009	12016	CG9135	36091	CG9270	29961
CG8767	36533	CG8893	50351	CG9010	40728	CG9138	1047	CG9271	15547

CG9272	41018	CG9414	30479	CG9540	14807	CG9699	7742	CG9879	29311
CG9283	15223	CG9415	15347	CG9542	45620	CG9701	3358	CG9881	28141
CG9286	23735	CG9416	10064	CG9548	35453	CG9702	6859	CG9882	29312
CG9288	46191	CG9418	37665	CG9550	43996	CG9703	6137	CG9886	48079
CG9290	14349	CG9422	30171	CG9554	43911	CG9705	40665	CG9886	29320
CG9291	15302	CG9423	36103	CG9556	48044	CG9706	49347	CG9890	23062
CG9294	29092	CG9426	10843	CG9564	45717	CG9709	29119	CG9895	41035
CG9296	29096	CG9427	15375	CG9565	37803	CG9712	23944	CG9899	46584
CG9300	24139	CG9428	3986	CG9569	1820	CG9717	42669	CG9900	24171
CG9302	15544	CG9429	51272	CG9569	1820	CG9722	6679	CG9901	29944
CG9304	11142	CG9430	7339	CG9571	10480	CG9723	37412	CG9903	42690
CG9305	30523	CG9433	41021	CG9573	49820	CG9725	23945	CG9904	45478
CG9306	23088	CG9438	37148	CG9576	47261	CG9726	41347	CG9906	5597
CG9307	23163	CG9441	33923	CG9577	24064	CG9727	30575	CG9907	6131
CG9308	6606	CG9443	5843	CG9578	45082	CG9728	42895	CG9908	7001
CG9310	12692	CG9444	43275	CG9580	50546	CG9730	36139	CG9910	24175
CG9311	14173	CG9448	24030	CG9581	48220	CG9732	27035	CG9910	24175
CG9313	29099	CG9450	24031	CG9581	39208	CG9734	23483	CG9911	46585
CG9314	44647	CG9451	14344	CG9582	2845	CG9735	23951	CG9913	36459
CG9320	24141	CG9452	51202	CG9586	28250	CG9738	26928	CG9914	29322
CG9322	29100	CG9453	47262	CG9588	47763	CG9739	44390	CG9916	41015
CG9323	44984	CG9455	13263	CG9590	29482	CG9741	51061	CG9920	29326
CG9325	29101	CG9456	37955	CG9591	44696	CG9742	39256	CG9921	14921
CG9326	24157	CG9458	48700	CG9593	24165	CG9747	1394	CG9922	35465
CG9328	28125	CG9459	48905	CG9594	13636	CG9748	6299	CG9924	28798
CG9331	44653	CG9459	5948	CG9595	24068	CG9749	36142	CG9925	29328
CG9333	52551	CG9460	24036	CG9596	27025	CG9750	19021	CG9927	29332
CG9334	49899	CG9461	24039	CG9597	36117	CG9752	50282	CG9930	47793
CG9334	30774	CG9463	48063	CG9598	15975	CG9752	28138	CG9931	7743
CG9342	15775	CG9463	15587	CG9601	24070	CG9753	1385	CG9938	29337
CG9343	41095	CG9465	52269	CG9602	29498	CG9755	45815	CG9940	40756
CG9344	23689	CG9466	46288	CG9603	37496	CG9761	23171	CG9941	29902
CG9345	16643	CG9466	13040	CG9606	44699	CG9762	11381	CG9941	29596
CG9346	27013	CG9467	45806	CG9610	48121	CG9764	28674	CG9943	48887
CG9347	29108	CG9468	15590	CG9611	36120	CG9770	43462	CG9943	5081
CG9350	30619	CG9469	15469	CG9613	5801	CG9772	15636	CG9945	23742
CG9351	24143	CG9472	8424	CG9615	24072	CG9774	3793	CG9946	7799
CG9353	35447	CG9473	15339	CG9619	36121	CG9776	29266	CG9949	50178
CG9354	49902	CG9474	48033	CG9620	42623	CG9778	11037	CG9951	36172
CG9357	44656	CG9480	35452	CG9621	16641	CG9779	29275	CG9951	29457
CG9359	24144	CG9484	44676	CG9623	5600	CG9783	29276	CG9952	29903
CG9360	13189	CG9485	45809	CG9629	44700	CG9784	30098	CG9953	9024
CG9361	8564	CG9488	29720	CG9630	31081	CG9786	11775	CG9954	12712
CG9362	24012	CG9490	23316	CG9633	11210	CG9790	23702	CG9958	49822
CG9363	37012	CG9491	27015	CG9636	28133	CG9796	36452	CG9958	28145
CG9364	30730	CG9493	40743	CG9637	9073	CG9802	39207	CG9961	36175
CG9373	44658	CG9494	44877	CG9638	24076	CG9804	46579	CG9968	36185
CG9376	9457	CG9495	3795	CG9643	24081	CG9805	28140	CG9968	29693
CG9377	42837	CG9496	2824	CG9646	14982	CG9811	30103	CG9973	36187
CG9378	28130	CG9499	7900	CG9648	15351	CG9818	29285	CG9973	36584
CG9379	22824	CG9501	7903	CG9650	23170	CG9819	30105	CG9976	38002
CG9381	44662	CG9508	24052	CG9655	37309	CG9828	29289	CG9977	49573
CG9383	23737	CG9510	44683	CG9657	43922	CG9834	29290	CG9977	36193
CG9384	14169	CG9512	14809	CG9660	24083	CG9836	29295	CG9981	11566
CG9386	47755	CG9514	37403	CG9662	7278	CG9839	36455	CG9983	29523
CG9388	24017	CG9517	24162	CG9662	7278	CG9847	12863	CG9984	42217
CG9389	44663	CG9518	8328	CG9666	45658	CG9849	12850	CG9985	6229
CG9391	23723	CG9519	16501	CG9667	36127	CG9852	48717	CG9986	46113
CG9393	44400	CG9519	47195	CG9668	46919	CG9854	42283	CG9987	36198
CG9394	13879	CG9520	2826	CG9670	24086	CG9855	33309	CG9987	36494
CG9398	29110	CG9521	16497	CG9674	24089	CG9862	29302	CG9994	36201
CG9399	13788	CG9521	47136	CG9677	27032	CG9865	40701	CG9994	43486
CG9400	43296	CG9522	19861	CG9678	23342	CG9867	44570	CG9995	29531
CG9401	28132	CG9526	51451	CG9680	36131	CG9868	45506	CG9995	36205
CG9406	48893	CG9527	24054	CG9682	16549	CG9870	44215	CG9996	36207
CG9406	29765	CG9528	44687	CG9683	22830	CG9873	29760	CG9998	24177
CG9410	44669	CG9533	5569	CG9688	43887	CG9876	10481	CG9999	30568
CG9412	29113	CG9536	7907	CG9695	13005	CG9878	23705		
CG9413	45180	CG9537	29374	CG9696	7787	CG9878	50446		